IAEA-TECDOC-263

NUCLEAR DATA FOR RADIATION DAMAGE ASSESSMENT AND RELATED SAFETY ASPECTS

PROCEEDINGS OF THE ADVISORY GROUP MEETING ON
NUCLEAR DATA FOR RADIATION DAMAGE ASSESSMENT
AND RELATED SAFETY ASPECTS
ORGANIZED BY THE
INTERNATIONAL ATOMIC ENERGY AGENCY
AND HELD IN
VIENNA, 12–16 OCTOBER 1981

A TECHNICAL DOCUMENT ISSUED BY THE
INTERNATIONAL ATOMIC ENERGY AGENCY, VIENNA, 1982

NUCLEAR DATA FOR RADIATION DAMAGE ASSESSMENT
AND RELATED SAFETY ASPECTS, IAEA, VIENNA, 1982

Printed by the IAEA in Austria
April 1982

PLEASE BE AWARE THAT
ALL OF THE MISSING PAGES IN THIS DOCUMENT
WERE ORIGINALLY BLANK

The IAEA does not maintain stocks of reports in this series. However, microfiche copies of these reports can be obtained from

INIS Microfiche Clearinghouse
International Atomic Energy Agency
Wagramerstrasse 5
P.O. Box 100
A-1400 Vienna, Austria

on prepayment of Austrian Schillings 40.00 or against one IAEA microfiche service coupon.

SUMMARY OF THE MEETING

The Advisory Group Meeting on Nuclear Data for Radiation Damage Assessment and Related Safety Aspects was convened by the IAEA Nuclear Data Section at the IAEA Headquarters in Vienna from 12-16 October 1981. The meeting was attended by 34 participants from 15 countries and 2 international organizations.

The main objectives of the meeting were to review the requirements for and the status of nuclear data needed for radiation damage estimates in reactor structural materials and related reactor safety aspects, and to develop recommendations to the Nuclear Data Section of the IAEA for its future activities in this field.

The proposed publication will contain the texts of all the papers prepared especially for this meeting including the conclusions and recommendations worked out during the meeting.

TABLE OF CONTENTS

OPENING OF THE MEETING

SESSION 1:

Nuclear data required for the characterization of the radiation environment in fission and fusion reactors by means of activation and damage detector techniques. Uncertainties in the required data, status of covariance information.

---

* Not presented during the meeting

SESSION 4:

Status of data required for calculations of gas production and transmutation. Uncertainties in the required data, status of covariance information.

SESSION 5:

Correlations between the results of microscopic damage calculations and macroscopic property changes in irradiated materials. Uncertainties involved and their effect on life-time prediction of reactor structural components including pressure vessels.

SESSION 6:

Discussion of first results of the international project REAL-80 for the intercomparison of radiation damage (displacements per atom) estimates.

OPENING REMARKS

M. ZIFFERERO
Deputy Director General,
Department of Research and Isotopes,
International Atomic Energy Agency,
Vienna

It gives me great pleasure to welcome you on behalf of the Director General to the Agency's Advisory Group Meeting on Nuclear Data for Radiation Damage Assessment and Related Safety Aspects.

This meeting is convened by the Nuclear Data Section of my Department in response to several recommendations made at IAEA meetings to compile and maintain special nuclear data libraries for use in material radiation damage calculations. It was also recommended to coordinate and sponsor activities on reviewing the status of such data and to premote work on eliminating existing discrepancies in these data.

Here, inside the Agency, the Scientific Advisory Committee has put a high priority to matters connected with reactor safety. There are about three hundred nuclear power and research reactors operating throughout the world today. This number is steadily increasing and will continue to do so in the future.

This means that the number of reactor service years is growing rapidly. There are reactors which operate already for about 30 years and are approaching the end of their service-life due to accumulation of radiation damage in their construction components.

In fact even in advanced laboratories in developed countries we often cannot find out with the needed reliability how far radiation-induced changes in construction materials have actually gone and for how long these components can still be kept in operation.

The experimental and theoretical data on this subject are still not accurate enough to make decisions on duration of safe service life of reactor components without introducing uneconomically large margins.

Moreover the number of power and research reactors in developing countries is also growing. To deal with these problems a certain effort on international level and scope is needed today.

During the seventies the Nuclear Data Section has pursued a programme dealing with nuclear data for reactor dosimetry. This activity has lead to the creation of an internationally accepted reactor dosimetry file containing

RADIATION DAMAGE IN FISSION AND FUSION REACTORS

Related safety, design and economic aspects

R. DIERCKX,
Joint Research Centre,
Ispra (Italy)

ABSTRACT

Radiation damage is seen differently by the physicists and the technologists. The physicist wants to understand all physical processes from the first interaction of the irradiating particle with the material leading to the mechanical failure. For technological use it is important to correlate (theoretical, empirical, semi-empirical) the mechanical failure with the irradiation source. The basic damage mechanisms are discussed. Radiation damage is directly related to the safety, economy, and design of reactors, either fission or fusion. High energy neutron sources are necessary to study materials and their behaviour for fusion applications. At present exists still the problem how damage data obtained in fission reactors can be correlated to useful data for fusion reactor applications. This requires a good dosimetry for the development of correlations. All this radiation damage experiments, their analysis, application and monitoring make use of nuclear data.

INTRODUCTION

Damage, due to radiation by neutrons or charged particles, has to be taken into consideration whenever a material is used as part of a radioactive plant. (fission or fusion reactor, accelerator and s.o.). It is necessary to be able to estimate this damage from the point of view of economics, end of life and safety. The economy of an energy-producing plant is very important. Such a plant must be able to produce energy at a low cost, for a long time and in safe conditions. In case of research installations, the economic aspect is less important, more its lifetime and still more a safe operation.

Therefore knowledge has to be gained about the damage producing mechanisms and damage correlations with the radiation source parameters (energy-spectrum, flux and fluence). Nuclear data form the basis for this knowledge. Cross-sections for processes and reactions leading to damage as well as cross-sections used to characterize, experimentally and theoretically, the radiation field have to be known. It is the scope of this meeting to define the state of the art of the nuclear data base, which nuclear data are still lacking and have to be measured or calculated and with which priority.

RADIATION DAMAGE PHENOMENA

The physics of radiation damage is very complex. Although a lot of the basic physics phenomena and their interaction with material characteristics are known, we are far from understanding Radiation Damage Physics in its totality.[1]

The importance of Radiation Damage was recognized when the first operating fission reactors suffered from breakdowns due to a change in the materials behaviour under irradiation. Since that time studies of Radiation Damage in many different metals and alloys became of increasing interest all over the world. A broad knowledge in the field of Radiation Damage Physics is available nowadays. Nevertheless it is still not possible starting from the knowledge of these physical phenomena to predict the lifetime and end of life properties of the construction materials. Data banks for material damages under irradiation have been created to serve the construction engineers. In the last years a big effort has been put into the development of correlations and intercorrelations using this data bank.

In Fig.1 we have tried to present a schematic view of radiation damage phenomena and their interaction with material parameters. The projectile-particle (neutron or charged particle) interact with the target nucleus, displaces atoms and produces primary knock-on atoms with a certain energy distribution.[2-4] Whether this primary recoil spectrum has an influence on the final damage structure is still an open question. Recent views attribute it less and less importance, especially at higher irradiation temperature. The primary knock-on atoms create basically two primary

damage states : vacancies and interstitials, and some higher order defects as divacancies, clusters and cascades.

These primary defects diffuse, recombine, anneal out or disappear in the sinks. Vacancy and interstitial-loops are formed. The concentration of these defects, responsible for the observed structural changes, depends on the irradiation temperature, dislocation density, impurities and sinks for defects. The final result is a number of voids, dislocation loops, microstructural and microchemical changes, especially under influence of solid transmutation products. These radiation induced structural changes give rise to swelling and changes in the mechanical behaviour of a material, which leads finally to its failure [5-7].

The damage structures depend on the energy and type of the high energy particle. In order to reduce the trouble for future fission and fusion reactors, radiation damage effects have to be studied by irradiation in adequate sources. As not always the adequate source (f.e. 14 MeV neutrons in case of fusion) is available with enough intensity and irradiation space, simulation experiments with charged particles are performed. The lack of these adequate sources obliges us to search for correlations and intercorrelations which will enable us to predict with a certain precision radiation damage effects. Correlations of experimental results in different neutron spectra have to be developed. Further, intercorrelations between charged particle damage and neutron damage have to be investigated [4,8-12]. These correlations or intercorrelations can be either fully empirical (without any theoretical input) semi-empirical or theoretical (based on the known theoretical formulas with some adapted parameters).
In addition to the study of the physical phenomena, the study of correlations and intercorrelations has to be undertaken. For these studies we need a data base.

CONSEQUENCES OF RADIATION DAMAGE

Radiation damage has a direct influence on the economy, design and safety of nuclear power plants.
An economic power station, based on fission or fusion reactions needs to have a long lifetime. The high investment costs do not permit a break down of the installation. Repairs and regular replacement of parts must be reduced to a minimum.

The economic aspects interact strongly with the design. The design has to be such to guaranty a long life time. Most exposed parts must be easily replaceable or have protective layers (as f.e. in the case of the first wall of fusion reactors).

Finally the safety of a nuclear power plant depends on the knowledge of the damage from which critical parts in the plants suffer and the consequences. Most of the troubles encountered in the first and actual fission reactors could have been avoided if a more detailed knowledge of the Radiation Damage effects on the structural materials and fuel had been available in the past.

RADIATION DAMAGE EFFECTS IN FISSION REACTORS

Radiation damage effects in fission reactors are extensively studied and some problems are solved. Nevertheless there are still large programmes going on because actual solutions to radiation damage problems are not fully satisfactory.

Examples of the damage effects are : the swelling of the nuclear fuel leading to cladding failure, crack development in the supporting structure, and the pressure vessel embrittlement.

The pressure vessel embrittlement, is a relative new problem. A lot of the first built reactors, reach now their end of life due to this radiation damage effect. A good knowledge of the pressure-vessel ebrittlment as function of radiation dose will permit to determine with more precision the end of live of the early built reactors and the life time of new plants.

Pressure vessel embrittlement [13,14,15] is now under study and is the subject of an international research project with the participation of Europe, the USA and other countries. A pressure vessel Bench Mark is built at the ORR Reactor at Oak Ridge and an intensive campaign of calculations and measurements in existing reactors is under way. Recently designed reactors are foreseen with a set of metallurgical samples and monitors to follow as function of time the state of the pressure vessel.

For fission reactors enough neutron sources with similar irradiation environments, sufficient space, and high fluxes are available.Beside the study of the physics of radiation damage, correlation measurements

in fission spectra are widely executed. The use of damage cross sections is common. A good monitoring of the irradiation source becomes a routine and will hopefully permit to correlate and utilize radiation damage experiments in fission reactors for fusion environments.

RADIATION DAMAGE EFFECT IN FUSION REACTORS[22]

For future fusion plants the situation is completely different. The main problems will rise during the operation of the first fusion reactors. Present efforts are concentrated on the first wall. The first wall of a fusion reactor is bombarded with high energy neutrons (14 MeV) and with charged particles leaking from the plasma.

The neutrons create damage in the bulk material, whereas the charged particles interact only in a small layer of the order of 10 to 100 micron. In this thin layer they deposit their energy as heat and create a localized damage at the end of their range. The local heating gives rise to tension forces and high localized temperatures.

Transmutation product, solids and the gaseous helium and hydrogen are a special problem in fusion reactors.

The high energy neutrons react with the material atoms according to a series of different reactions (n, α), (n,p), (n,nα), (n,np) (n,x), (n,nx)) leading to reaction products different from the original material.

The first wall material undergoes a changement in composition due to the irradiation source. Besides the classical radiation damage effects, the plasma disruptions occurring at each end of a burning cycle deposits such a heat on the first wall that a thin layer will melt with each disruption, decreasing the stability of the first wall.

It is doubtful that before the plasma disruptions will be under control, any fusion reactor will be able to operate.

The first wall of a fusion reactor is important, however we may not forget radiation damage in the other parts of a fusion reactor as magnets, neutral beam injection and coolant.

All the above mentioned effects have to be studied before the large investment for building a fusion reactor can be justified.

It is clear that extrapolation from radiation damage measurements will not give a full guarantee that the first fusion reactor will work. A part of the finally needed data can only be obtained in working fusion reactors itself, but the risks due to radiation damage breakdown can be reduced, starting early with radiation damage studies.

The damage problems related to laser fusion are even worser [16].

The radiation damage phenomena caused by charged particles are since a long time studied with accelerators. Surface damage due to charged particles as sputtering and blistering are well known effects [17,18].

In absence of high energy neutron sources, light ion irradiation is used to try to simulate neutron damage. Creep measurements are common experiments. But it has still to be shown how far these experiments are valid for neutron radiation damage. The effect of the missing gaseous transmutation products as helium and hydrogen and of the missing solid transmutation products is an unknown factor especially near end of life conditions.

The trials to introduce helium by preinjection has some drawbacks and does not really solve the problem.

In the HFIR irradiations two successive reactions on Ni produce helium. The first reaction in Ni is mainly proportional to the thermal neutron fluence. The resulting transmutation product is transformed via (n-α) reactions by the fast neutron flux. The resulting He production becomes such a non linear function of the fast fluence. Recent dual beam experiments at Argonne N.L. (simultaneous irradiation by self-ions and helium injection) have demonstrated that the damage effects are different from those in pre-injected samples [19].

The plasma disruption effects can only be studied in the fusion devices themselves and as already said have to be reduced to a minimum if a fusion reactor will work at all.

The conclusion is that we need high intensity high energy neutron sources to select materials for fusion applications [20]. The type of possible sources are :

1) 14 MeV sources based on the D.T. reaction, as RTNS II at L.L.L. Livermore with a flux of 10^{13} n/cm^2 s or the projected but not continued INS (Tritons impinging on a supersonic gaseous deuterium target) with a blanket to create the non - 14 MeV energy tail present in the first wall neutron spectrum [21].

2) D-Li sources, which have a broad spectrum, peaking at 14 MeV but with a tail up to 40 MeV neutrons. The FMIT project at HEDL is of this type.

3) spallation neutron sources in light target materials (f.e. Copper) which have an evaporation spectrum peaking at 4 MeV and an high energy tail up to 100 MeV.

Except the 14 MeV sources all others are simulations and damage results have to be correlated with real fusion spectra.

NUCLEAR DATA NEEDS

The nuclear data needed to interprete all radiation damage experiments and to correlate and intercorrelate them are of two types : those data needed to characterize theoretically and experimentally the environment and those data needed to interprete the damage phenomena. The matter may be subdivided in data necessary for the analysis of the damage itself and the data needed in the study of the gaseous and solids transmutation products. For fission-reactor applications data up to a neutron energy of 10 MeV are sufficient and practically available, except for some new detectors and special applications. For D.T. fusion the data have to be known up to 15 MeV. Using D-Li sources and spallation sources, cross section data up to about 40 MeV are required. These data are in most cases not available, especially measured data. Cross sections up to 40 MeV are calculated with nuclear models, but should be verified by experiments. Charged particle data are quite well known and are not of immediate concern here.
The characterization of the environment (flux, fluence, energy spectra, dpa) is very important. Damage obtained in one environment needs to be expressed as function of the source characteristics in order to be able to utilize or extrapolate the data to other environments. To interprete damage data, damage cross sections and damage functions have to be developed either theoretically or experimentally. These damage functions are based on the cross sections of the structural materials. A last point is the calculation of the transmutation products which need nuclear data.
The scope of this meeting is to elaborate a precision and priority list of existing and required nuclear data.

I hope that the result of this meeting will be a clear view of the required needs and a firm recommendation on what is necessary.

REFERENCES

1. H.ULLMAYER, W.SCHILLING
   Radiation damage in metallic reactor materials
   IAEA-SMR-46/105

2. D.PARKIN and A.GOLAND
   A computational method for the evaluation of radiation effects produced by CTR related neutron spectra
   BNL 50434 (1974)

3. A.GOLAND
   Experimental evaluation of the primary damage proces
   Neutron energy effects BNL-25807

4. R.DIERCKX, C.R.EMIGH
   Characterization for fusion first wall damage studies of using tailored D-T neutron fields
   3° ASTM Euratom Symposium on Reactor Dosimetry
   Ispra, Oct.1979 EUR 6813 vol.I p.230

5. Fundamental mechanisms of radiation induced creep and growth
   Chalk River, May 1980

6. Measurement of irradiation enhanced creep in nuclear materials
   Petten, May 1976

7. Effects of radiation on structural materials
   ASTM-STP 683 (1978)

8. D.G.DORAN et al.
   Damage analysis and fundamental studies (DAFS)
   Task group of the office of fusion energy (OFE)
   private communication

9. G.R.ODETTE, D.G.DORAN
   Radiation damage analysis as applied to fusion reactor first wall
   Tech. of Controlled nuclear fusion CONF 760935
   p.1485 (1976)

10. R.DIERCKX, C.R.EMIGH
    Application of the INS facility as a high flux Bench Mark for neutron dosimetry and for radiation damage studies in D-T fusion spectra
    2° ASTM EURATOM Symposium on reactor dosimetry Oct.1977
    Palo Alto

11. R.GOLD et al.
    Radiation damage function analysis in effects of radiation on structural materials
    ASTM STP 683, p.380 (1978)

12. J.P.GENTHON
    Dosimetrie et applications metallurgiques
    3° ASTM-EURATOM Symposium on reactor dosimetry
    Ispra Sept.1979, EUR 6813 vol.I, p.33

13. IAEA specialist meeting on irradiation embrittlement, thermal annealing and surveillance of reactor vessels
    Vienna 26-28 Febr.1979
    Proceedings to be published

14. Workshop on "LWR pressure vessel surveillance in practice and irradiation experiments
3° ASTM Euratom symposium on reactor dosimetry
Ispra Oct.1979 EUR 6813, vol.I p.397-521

15. Caprice 79
Correlation accuracy in pressure vessel steel as reactor component investigations of charge of materials properties with exposure data
Jül-CONF-37 Mai 1980 (ISSN 0344-5798)

16. G.L.KULCINSKI
Unique materials requirements for laser fusion reactors
3° topical meeting on the technology of controlled nuclear fusion , Santa Fe, May 1978, Transactions p.197

17. D.L.SMITH
Physical sputtering model for fusion first wall materials
J. of Nucl.Materials 75(1) July 1978

18. 3° Int.Conf. on plasma surface interactions in controlled nuclear fusion devices
Culham April 1978

19. F.V.NOLFI Jr. Argonne Nat.Lab.
personal communication

20. R.DIERCKX
Neutron sources for the fusion materials radiation programme
3° ASTM Euratom symposium on reactor dosimetry
Ispra 1979 EUR 6813 Vol I p.53

21. M.E.BATTAT, R.DIERCKX and C.R.EMIGH
Feasibility study to produce fast wall fusion reactor spectra around a 14 MeV neutron point source
Nucl.Techn. vol.43 May 1979 p.338

22. R.E.GOLD et al.
Materials technology for fusion. Current status and future requirements. Overview.
Nucl.Tech. Fusion Vol.1, n.1, p.169, April 1981

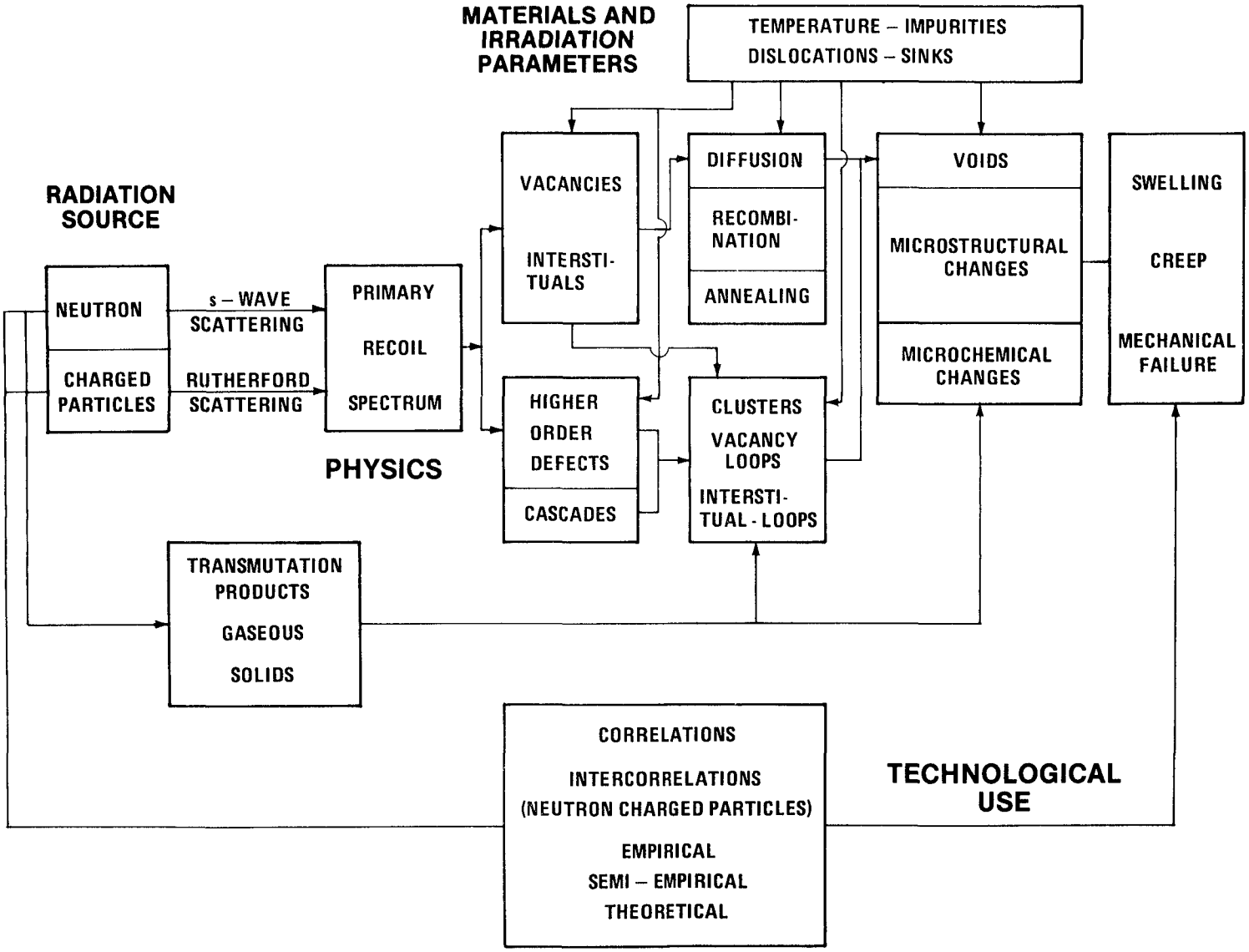

Fig . 1 Schematic View of Radiation Damage Phenomena

ASTM STANDARD RECOMMENDED GUIDE ON APPLICATION OF ENDF/A CROSS SECTION AND UNCERTAINTY FILE
Establishment of the file

E.P. LIPPINCOTT, W.N. McELROY
Westinghouse Hanford Company,
Hanford Engineering Development Laboratory,
Richland, Washington,
United States of America

A b s t r a c t

A new ASTM standard recommended guide is in preparation for application of an ENDF/A cross section and uncertainty file for a dosimetry and damage analysis. The file will consist of a standardized, self-consistent set of cross sections, validated using measurements in benchmark spectra, and cross sections and uncertainties will be in a convenient format for use with adjustment codes.

A new ASTM Standard Recommended Guide on "Application of ENDF/A Cross Section and Uncertainty File" is in preparation by ASTM Committee E10 on Nuclear Technology and Applications. This ASTM Standard is being prepared in support of the standardization of physics-dosimetry procedures and data needed for Light Water Reactor (LWR) power plant pressure vessel and support structure materials surveillance and test reactor development programs. The main subject of this paper is the establishment of the "ENDF/A Cross Section and Uncertainty File".

The development of evaluated cross section files such as the "evaluated nuclear data file," ENDF/B, has occurred mainly to meet the needs of physics calculators. These files are tested by calculations of well-measured benchmark problems such as reactivity or critical mass measurements. Data in the files have then been re-evaluated where disagreements with the benchmark measurements indicate data to be deficient.

For cross sections of reactions used for dosimetry measurements it was found that a more specialized file was needed in order to contain the specific dosimetry reactions. For example, instead of an iron (n,p) cross section, the $^{54}Fe(n,p)^{54}Mn$ cross section is needed. Until the creation of the dosimetry file,[1] and later the ENDF gas production file,[2] the cross sections for many dosimetry reactions which are unimportant for neutron transport calculations, did not receive the proper attention by the evaluators.[3 5]

Furthermore, in neutron dosimetry and damage analysis work, standardized techniques and data must be established to characterize a diversity of irradiation environments.[6] The techniques must be implemented in such a manner that fuels and materials data from the different environments can be intercompared, and the environments are sufficiently characterized so that the fuels and materials data can be properly correlated, and then interpolated and extrapolated to different reactor design conditions. The need of such standardization is clear when the high cost of the replacement of fuels, materials, and components (including surveillance and irradiation tests) for light water reactor (LWR), fast breeder reactor (FBR), or magnetic fusion reactor (MFR) nuclear power systems are considered. Derived irradiation effects data, therefore, must have as much general applicability as possible to effect the highest benefit to cost ratio. For U. S. reactor programs key test irradiation facilities, adequately characterized and labeled as "benchmarks", are being utilized for the validation and calibration of

dosimetry, damage analysis, and the associated reactor analysis procedures and data. A provisional list of such benchmarks is given in Reference 6 as well as a discussion of goal accuracies. More recent information for LWRs is given in References 7, 8, and 9.

The need for a standardized approach is accentuated by the variety of dosimetry monitors and techniques used for the various applications. Consistency from one set of measurement conditions to another must obviously start with a consistent cross section file. To meet this need for LWR pressure vessel surveillance dosimetry, an ENDF/A cross section and uncertainty file is being established together with an ASTM Standard recommended guide for application of the file.[10] The file will be issued as ENDF/A because it may contain cross sections inconsistent with those on ENDF/B. (ENDF/B files are evaluated files officially approved by the Cross Section Evaluation Working Group (CSEWG) after suitable review and testing.) In addition, the ASTM ENDF/A file will contain damage cross sections [e.g. displacements per atom (dpa)] for steel, graphite, silicon, sapphire, quartz, etc. for which reaction mechanisms are only known theoretically and differential cross section measurements do not exist.

Differences with the ENDF/B dosimetry file may be created by the need for a standardized, self-consistent cross section set. At present, evaluations and testing of many dosimetry reactions have reduced discrepancies between evaluations and integral data. Thus only a few cross sections may need significant adjustment from the ENDF/B file to achieve self-consistency with benchmark integral data. In general, these cross sections are ones for which present differential measurements are inadequate and theoretical calculations have only partly filled the gap. A prime example is the $^{58}Fe(n,\gamma)$ reaction. Table 1 shows the present status of cross sections measured in the ^{235}U thermal neutron induced fission spectrum compared with calculated values using the 620 point ENDF/B-V dosimetry file cross sections. It is seen that most reactions agree within about the quoted experimental error but discrepancies still exist with the reactions $^{47}Ti(n,p)$, $^{27}Al(n,p)$, $^{127}I(n,2n)$, and $^{55}Mn(n,2n)$.

Limiting the present ASTM ENDF/A file to LWR pressure vessel dosimetry and damage analysis applications may create an adjusted file not suitable for other applications. Thus caution must be observed when extending its use beyond the limits within which the file has been tested. This is caused by the fact that the adjustments may be caused by effects not explicitly considered. For example, in an environment containing thermal or low energy neutrons, the measured value for the $^{63}Cu(n,\alpha)^{60}Co$ reaction may be affected by ^{59}Co impurity in the copper used as the dosimeter. As little as 1 ppm ^{59}Co may cause a 20% effect. Thus an effective copper cross section might contain a low energy part due to $^{59}Co(n,\gamma)^{60}Co$ that is specific for the source of the copper used. Other effects that could cause similar problems are photofission and burn-in, burn-out effects.[11]

An integral part of the ENDF/A file will be an uncertainty file which can be used by least squares adjustment codes such as FERRET[12] or STAYSL[13] to properly weight data used in neutron flux and spectrum determinations and provide a statistical evaluation of uncertainty in processed quantities such as fluence or dpa.[14,15] The use of a validated uncertainty file will provide the needed confidence to justify usage of the derived uncertainties for defining neutron induced materials property change exposure limits.[9]

In order to make the ENDF/A file easily usable by the adjustment codes,[14] it will be issued in a multigroup format with sufficient groups for most applications. Groups can be condensed for input to the codes. The uncertainties will be specified in the form of a covariance matrix and correlations between cross sections will be specified, either in the file or in the file documentation. Codes exist for collapsing or expanding covariance file data into any desired group structure.

It is expected that the use of the ENDF/A file will result in standardized analysis of LWR dosimetry and the subsequent derivation of exposure parameter values. It should therefore, find wide application to define uncertainties on a rigorous statistical basis, thereby enabling materials property exposure limits to be established in a consistent, scientifically justified manner. The use of such data files for international intercomparisons, such as REAL-80, can be expected to play an important part in meeting this goal.

REFERENCES

1. B. A. Magurno and O. Ozer, "ENDF/B file for Dosimetry Applications," Nucl. Technol., 25, 376 (1975).

2. L. Stewart, et al., "Status of the ENDF/B Special Applications Files," Proceedings of the Second ASTM-EURATOM Symposium on Reactor Dosimetry, NUREG/CP-0004, pp. 843-853, 1978.

3. W. N. McElroy and L. S. Kellogg, Fuels and Materials Fast-Reactor Dosimetry Data Development and Testing, Nuclear Technology, 25, p. 180-223, February 1975.

4. A. Fabry, et al., "Review of Microscopic Integral Cross Section Data in Fundamental Reactor Dosimetry Benchmark Neutron Fields", Neutron Cross Sections for Reactor Dosimetry, IAEA-208, Vol I, p. 233 (1978).

5. W. N. McElroy, et al., "Spectral Characterization of Combining Neutron Spectroscopy, Analytical Calculations, and Integral Measurements," Neutron Cross Sections for Reactor Dosimetry, IAEA-208, Vol I, p. 147 (1978).

6. W. N. McElroy, et al., "Standardization of Dosimetry and Damage Analysis Work for U. S. LWR, FBR, and MFR Development Programs," Proc. of the Second ASTM EURATOM Symposium on Reactor Dosimetry - Dosimetry Methods for Fuels, Cladding and Structural Materials, NUREG/CP-0004, Vol I, p. 17 (1978) and HEDL SA-1374, January 1978.

7. ASTM E706-81, "Standard Master Matrix for Light-Water Reactor Pressure Vessel Surveillance Standards," American Society for Testing and Materials, 1916 Race St., Philadelphia, PA 19103, 1981.

8. W. N. McElroy, et al., "LWR Pressure Vessel Surveillance Dosimetry Improvement Program: PCA Experiments and Blind Test," NUREG/CR-1861, HEDL-TME 80-87, Hanford Engineering Development Laboratory, Richland, WA., July 1981.

9. W. N. McElroy, et al., "Surveillance Dosimetry of Operating Power Plants," HEDL-SA 2546, Hanford Engineering Development Laboratory, Richland, WA., October 1981.

10. ASTM E706-81, "Standard Master Matrix for Light-Water Reactor Pressure Vessel Surveillance Standards, Section 5.3.2, Application of ENDF/A Cross Section and Uncertainty Files-IIB(E10.05)," American Society for Testing and Materials, 1916 Race St., Philadelphia, PA 19103, 1981.

11. ASTM E706-81, "Standard Master Matrix for Light-Water Reactor Pressure Vessel Surveillance Standards, Section 5.3.3, Sensor Set Design and Irradiation for Reactor Surveillance-IIC(E10.05)", American Society for Testing and Materials, 1916 Race St., Philadelphia, PA 19103, 1981.

12. F. A. Schmittroth, "FERRET Data Analysis Code," HEDL-TME 79-40, Hanford Engineering Development Laboratory, Richland, WA., 1979.

13. F. G. Perey, "Least-Squares Dosimetry Unfolding: The Program STAYSL," Oak Ridge National Laboratory, ORNL/TM-6062, 1977.

14. ASTM E706-81, "Standard Master Matrix for Light-Water Reactor Pressure Vessel Surveillance Standards, Section 5.3.1, Application of Neutron Spectrum Adjustment Methods-IIA(E10.05)," American Soceity for Testing and Materials, 1916 Race St., Philadelphia, PA 19103, 1981.

15. J. J. Wagschal, R. E. Maerker, and B. L. Broadhead, "LWR-PV Damage Estimate Methodology," Transactions of the ANS Topical Meeting, 1980 Advances in Reactor Physics and Shielding, Sun Valley, ID., September 14-17, 1980.

TABLE 1

COMPARISON OF MEASURED AND CALCULATED CROSS SECTIONS
IN THE U-235 FISSION NEUTRON SPECTRUM

Reaction	Effective Threshold (MeV)	Measured Value (mb)[a]	Quoted Error in Measured Value %[a]	Calculated Value (mb)[b]	Calculated/ Measured
$^{115}In(n,\gamma)^{116m}In$		134.5	4.5	124.7	0.93
$^{197}Au(n,\gamma)^{198}Au$		83.5	6.0	78.3	0.94
$^{63}Cu(n,\gamma)^{64}Cu$		9.30	15.1	9.87	1.06
$^{235}U(n,f)$		1203	2.5	1236	1.03
$^{239}Pu(n,f)$		1811	3.3	1791	0.99
$^{237}Np(n,f)$	0.6	1312	3.8	1347	1.03
$^{115}In(n,n')^{115m}In$	1.2	189	4.2	179	0.95
$^{232}Th(n,f)$	1.4	81	6.7	75.0	0.93
$^{238}U(n,f)$	1.5	305	3.3	305	1.00
$^{47}Ti(n,p)^{47}Sc$	2.2	19.0	7.4	22.5	1.18
$^{58}Ni(n,p)^{58}Co$	2.8	108.5	5.0	105.0	0.97
$^{32}S(n,p)^{32}P$	2.9	66.8	5.5	70.5	1.06
$^{54}Fe(n,p)^{54}Mn$	3.1	79.7	6.1	81.0	1.02
$^{46}Ti(n,p)^{46}Sc$	3.9	11.8	6.4	11.2	0.95
$^{27}Al(n,p)^{27}Mg$	4.4	3.86	6.5	4.26	1.10
$^{56}Fe(n,p)^{56}Mn$	6.0	1.035	7.2	1.036	1.00
$^{59}Co(n,\alpha)^{56}Mn$	6.8	0.143	7.0	0.150	1.05
$^{63}Cu(n,\alpha)^{60}Co$	6.8	0.500	11.2	0.558	1.12
$^{27}Al(n,\alpha)^{24}Na$	7.2	0.705	5.7	0.719	1.02
$^{48}Ti(n,p)^{48}Sc$	7.6	0.300	6.0	0.282	0.94
$^{127}I(n,2n)^{126}I$	10.5	1.05	6.2	1.21	1.15
$^{55}Mn(n,2n)^{54}Mn$	11.6	0.244	6.1	0.201	0.82

(a) Taken from Reference 2, 1σ values.
(b) Using ENDF/B-V dosimetry file 620 point cross sections and the ENDF/B-V Watt form for the ^{235}U fission spectrum.

CHARACTERIZATION OF THE RADIATION ENVIRONMENT IN FISSION REACTORS BY THE ACTIVATION TECHNIQUE AND OPTIMIZATION OF THE SET OF NUCLEAR REACTIONS OF POSSIBLE USE*

A. CESANA, G. SANDRELLI, V. SANGIUST, M. TERRANI
CESNEF, Politecnico di Milano

ENEL – CRTN,
Milan,
Italy

SUMMARY

In the hostile environment of power reactors the multiple foil activation is the only possible technique to be used to evaluate neutron fluxes. Through the use of adjustment algoritms (e.g. SAND II or STAY'SL) an input spectrum, required by the indetermination of the problem, is modified and pulled toward the spectrum implied by the measured reaction rates. In the paper special reference is made to the measurement of a fast neutron spectrum, created by the B_4C filtering of a thermal reactor spectrum. Attention is given to the number of energy groups used to represent the neutron spectrum and to the different informations obtained when different sets of detectors are used. Fission detectors like ^{237}Np, ^{241}Am and possibly ^{238}Pu, are shown to be of utility since their cross section in the subthreshold fission region is such to add information to that given by the commonly employed (n,γ) detectors.
Estimate of uncertainties and evaluation of the convenience of particular detectors are made through the code STAY'SL.

INTRODUCTION.

The characterization of the neutron field in power reactor environments, usually at first performed by calculations, may be convalidated experimentally by the MFA (multiple foil activation) technique (1).

As it is well known the indetermination of the problem requires the use of an input spectrum, which is modified and moved toward the "true" spectrum implied by the measured reaction rates; it is then clear that the whole procedure is actually an adjustment of the calculated spectrum, obtained combining together computations and experimental informations and taking into account their respective uncertainties (2,3).

*This work is part of a research program supported by ENEL.

Many good adjustment codes,SPECTRA (4),CRYSTALL BALL (5) and SAND II (6), may be used,but STAY'SL (2) has the major advantage of allowing a clear and correct assessment of the uncertainties propagated to the derived flux starting from the uncertainties of reaction rates,cross sections and input flux. Conclusions may then be drawn about nuclear data needs nec essary to improve our knowledge of the radiation environment under study.

In this work the measurement of the neutron spectrum,created by B_4C filtering (7) of the core neutrons of the L54 reactor at Cesnef,is described and discussed,with attention to the uncertainties and their propagation.

FLUX COMPUTATION AND MEASUREMENTS IN THE B_4C FILTER

A neutron filter made of sintered B_4C, was placed against the reactor core, with the aim of realizing a neutron field,physically well defined,with spectrum definition,useful for validation experiments.

The neutron space and energy distribution in the irradiation cavity inside the filter,have been calculated using the DOT 3.5 E code (8,9,10); the flux shape obtained is shown in fig. 1; an integral flux of $1.2\ 10^{11}\ n/cm^2 \cdot s$ is reached. The list of reactions employed in the measurement is given below and is seen to include (n,γ),(n,n'),(n,p),(n,α),thermal and threshold fission reactions,in order to achieve a reasonably good coverage of the whole energy range.

List of the 22 reactions employed

$^{23}Na(n,\gamma)$ $^{24}Mg(n,p)$ $^{27}Al(n,p)$ $^{27}Al(n,\alpha)$ $^{47}Ti(n,p)$ $^{48}Ti(n,p)$ $^{54}Fe(n,p)$
$^{55}Mn(n,\gamma)$ $^{58}Ni(n,p)$ $^{58}Fe(n,\gamma)$ $^{63}Cu(n,\gamma)$ $^{103}Rh(n,n')$ $^{115}In(n,n')$
$^{115}In(n,\gamma)$ $^{197}Au(n,\gamma)$ $^{233}U(n,f)$ $^{235}U(n,f)$ $^{237}Np(n,f)$ $^{238/40/41}Pu(n,f)$
$^{241}Am(n,f)$

The actual results of the measurements are counting rates obtained with a Ge-Li detector.To derive the reaction rates per atom a number of error causes must be accounted for:counting statistics, γ -efficiency, γ- branchings and fission yields,mass and isotope fraction of the target,half-life,dead-time and background corrections,positioning of targets and normalizations of different irradiations.

The final result of the reaction rate evaluation is A,a vector of 22 values, and M_A ,a variance covariance matrix (22 x 22),which is obtained considering all the possible correlation of errors for all the reactions.For example for the reactions $^{23}Na(n,\gamma)$,$^{24}Mg(n,p)$ and $^{27}Al(n,\alpha)$ the same γ's of ^{24}Na are counted and a full correlation exists for γ -branchings and γ -efficiency. Clear examples of how to perform these computations were given in ref. 11,12.

ADJUSTMENT PROCEDURE AND RESULTS.

A version of STAY'SL with 40 energy groups between 10^{-10} and 18 MeV was used. STAY'SL requires, after A and M_A, the vector of the input flux ϕ (40 values) and the corresponding matrix M_ϕ (40 x 40), together with the cross section library Σ (40 x 22 values) and the corresponding matrix M_Σ $(40 \times 22)^2$ values. It is clear that a not too high group number is practically necessary for a convenient use of STAY'SL (13); our choice of 40 groups is the result of an investigation (14) about the possible systematics errors introduced in the library by a coarse group structure and propagated to the derived flux. As for the M_σ cov. matrice we adopted a gaussian shape around the diagonal, allowing for errors higher at the very low or the very high energy side and lower in the central groups. In this preliminary evaluation we imposed an arbitrary small error on all the cross sections and no correlation between different reactions. Only some features of the results of the adjustment will be here reported; an improvement factor, defined as the ratio of old to new errors in ϕ, is shown in fig. 2 and shows where the experimental information is good.

CONCLUSIONS

The relative merit of particular reactions may be estimated performing the adjustment with and without them and considering the variation in the improvement factor; $^{241}Am(n,f)$ and $^{237}Np(n,f)$ are shown in this way to be of utility. At contrary $^{238}Pu(n,f)$ and $^{63}Cu(n,\gamma)$ are of scarce merit if the fission yield of the former and the γ-branchings of the latter are not given with better precision. An improvement of the decay data quality of commonly employed detectors is still necessary; on the other side since the use of standard spectra (15) partially eliminates these errors some effort should also be devoted to the validation of spectra of this type.

\+ + + + +

REFERENCES

1) W.N.McElroy, S.Berg, T.Crockett, R.G.Hawkins: AWRL-TR-67-41 (1967)

2) F.G.Perey: ORNL/TM-6062, ENDF-254 (1967)

3) M.Petilli: ORNL/RSIC-40, 79 (1976)

4) C.R.Greer, J.A.Halbleib, J.W.Walker: SC-RR-67-746 (1967)

5) F.Kam, F.Stallman-ORNL-TM-4601 (1974)

6) F.G.Perey: Proceedings 2nd ASTM-Euratom Symposium, Palo Alto, (1977)

7) P.Barbucci, A.Cesana, G.Sandrelli, V.Sangiust, M.Terrani, S.Terrani: Energia Nucleare 26, n° 11, 542, (1979)

8) DOT-3.5 Two -Dimensional Discrete Ordinates Radiation Transport Code RSIC-ORNL (1976)

9) P.Barbucci, F.Di Pasquantonio: NEA Newsletter n.22 (1977)

10) P.Barbucci,F. Di Pasquantonio:5th Int.Conf. on Reactor Shielding Knoxville,Tenn. (1977)

11) M.Petilli: CNEN-RT/FI (80) 18

12) J.J.Wagschal,R.Maerker,D.M.Gilliam:3rd ASTM-Euratom Symposium ISPRA (1979)

13) H.C.Rieffe:ECN-92-Petten (1981)

14) A.Cesana,G.Sandrelli,V.Sangiust,M.Terrani: to be published

15) R.Dierckx:EUR-2532e (1965)

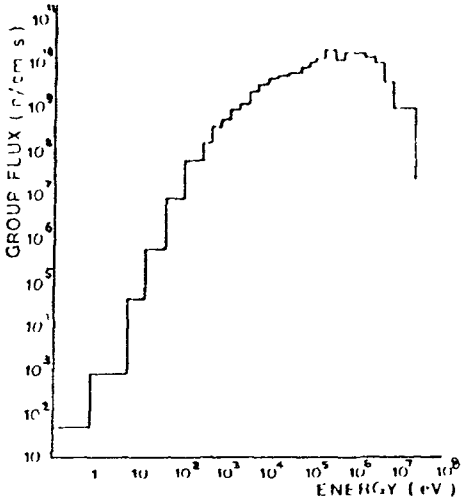

FIG. 1

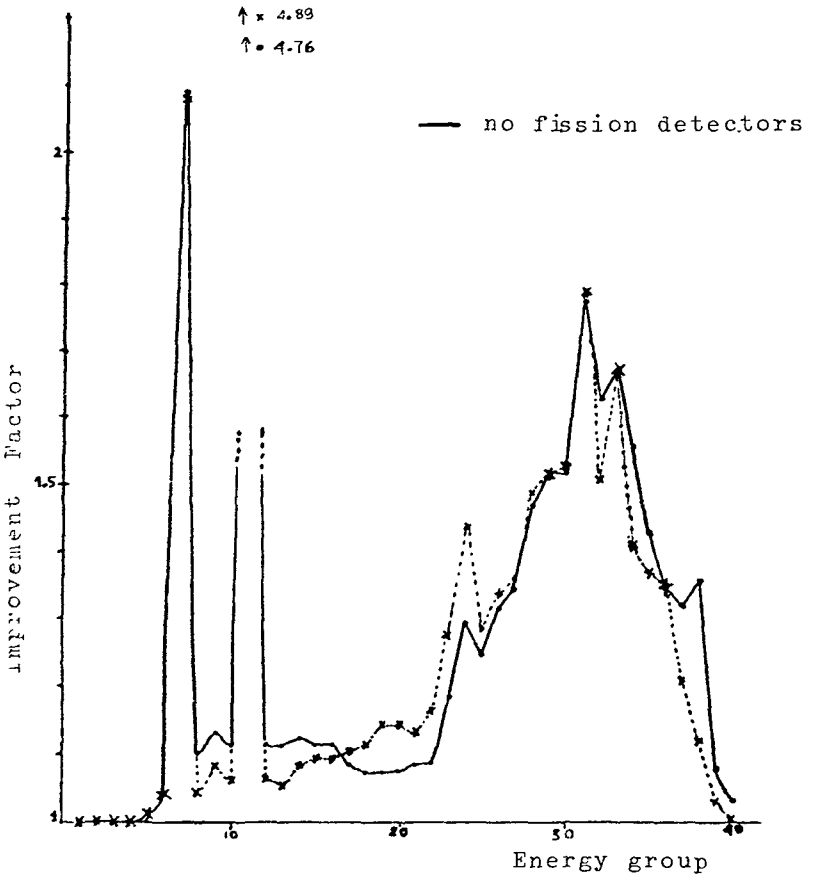

FIG. 2

REQUIREMENTS FOR REFERENCING REACTOR PRESSURE VESSEL SURVEILLANCE DOSIMETRY TO BENCHMARK NEUTRON FIELDS

E.D. McGARRY
National Bureau of Standards,
Gaithersburg, Maryland,
United States of America

SUMMARY

The objective of neutron benchmark field referencing is to guarantee measurement accuracy of neutron dosimetry methods for LWR-PV Dosimetry Surveillance by carrying out various types of calibration irradiations in well-characterized neutron fields. Such referencing is necessary both to establish absolute and defendable levels of accuracy of neutron measurements and to verify the accuracy of dosimetry and physics procedures in certain of 19 ASTM standards for the LWR-Pressure Vessel Surveillance Dosimetry Improvement Program. The participation of the National Bureau of Standards in particular phases of benchmarking is discussed and the status of activities is given. Notable applications to date are the PCA Blind Test Experiment; referencing of in-cavity measurements at a Arkansas Power and Light PWR; standard field irradiation comparisons of HEDL SSTR's with the NBS fission chamber; and production, distribution and evaluation of over 40 neutron fluence standards which were prepared by irradiation of nickel, aluminum, indium and iron in the NBS standard ^{252}Cf and ^{235}U fission neutron fields.

INTRODUCTION

The object of this program is to "improve, standardize and maintain dosimetry, damage correlation and associated reactor analysis procedures used to predict the integrated effects of neutron exposures to light water reactors (LWR) pressure vessels (PV) and support structures." Important program tasks are to validate neutron field measurements and measurement methods and to substantiate the adequacy of physics and analytical procedures in those ASTM standards (under revision or development) which will serve as regulatory guidelines for the U.S. Nuclear Regulatory Commission.

The foundation of the validation effort is benchmark referencing to standard neutron fields. Because NBS is the principal developer and caretaker of standard neutron fields in the United States, the Bureau has primary responsibility for seeing that validation is carried out for the program.

THE ISSUES

The safety issue[1] is that surveillance capsule metallurgy and dosimetry results are necessary to adjust the current end-of-life projections of the reactor's Final Safety Analysis Report (FSAR) to accurately account for changes in the fracture toughness of the steel in the pressure vessel. A relatively accurate measurement of the total accumulated neutron fluence is mandatory, therefore, to permit proper regulatory control of safe operation throughout plant (PV) lifetime. Accurate neutron transport calculations are also needed since neutron flux measurements must be extrapolated from the surveillance (measurement) position into the PV steel.

The benchmarking issue is how to provide the least controversial means for establishing the validity of fast neutron flux measurements and calculational methods? The usefulness of permanent, well-characterized, standard neutron fields to delineate such means is well known.[2,3] Questions arise when the path by which the basis of validity is traced is either not well defined or contains controversial elements. In general, the fewer elements along the path, the less the chance for controversy. It is within this framework that this paper will discuss requirements for referring pressure vessel surveillance dosimetry to standard neutron fields.

The requirements issue is a dual issue. It is necessary to ascertain the level of accuracy required for surveillance dosimetry; it is also necessary to define what must (and can) be done. There would be little more than rhetoric in defining unattainable goals. Therefore, it is necessary to define, and accomplish, provisional goals to satisfy realistic requirements. The first order of business is to discuss the requirements. Consideration is then given to what can be done, what is proposed, and what has already been accomplished. The issue of accuracy level needs is addressed as it comes up naturally in consideration of the requirements.

REQUIREMENTS FOR BENCHMARK FIELD REFERENCING

1. Benchmark Referencing of Vendors, Utilities and Service Laboratories Who Perform Surveillance Dosimetry

At present, in the U.S., there are four nuclear reactor vendors and two radiometric analysis service laboratories involved in the NRC PV Surveillance Dosimetry Improvement Program.[4,5] In addition, the National Dosimetry Center at HEDL and isolated contractors to EPRI (e.g., the University of Arkansas) perform a considerable amount of radiometric analysis. There are three rather separate and distinct approaches to benchmark referencing surveillance capsule dosimetr. They are all aimed at insuring that measurements are made in a consistent and accurate manner. They include gathering of data to establish the obtained levels of accuracy.

First, a program objective[5] is to reference all measurements (fission chambers, solid state track recorders (SSTR), radiometric (RM) foils and emulsions, and helium accumulation fluence monitors (HAFM)) to the standard fission fields at NBS or CEN/SCK. Consistency will, in part, be assured by the development of suitable ASTM standards. Benchmark field referencing is an integral part of validating the procedures to which these standards refer.

Second, an ultimate program goal is to establish certain generic power reactor benchmarks. Here in real-life environment is where dosimetry, metallurgy and calculation are brought together to deal with problems not easily simulated in standard neutron fields or even in specially designed test environments. It is mandatory that the validation established for the various components which will be used to characterize the power reactor benchmarks be carried through to their documentation.

Third, the program must require some periodic surveillance to insure continued quality assurance.

1.1 Nickel Fluence Standards: The first attempt at round-robin benchmarking included the above mentioned laboratories as well as an equal number in Europe and the UK. This involved a distribution of 29 nickel foils in early 1979 that had been irradiated in the NBS ^{235}U Cavity Fission Source. The $^{58}Ni(n,p)^{58}Co$ reaction was induced in a series of six 35-hour irradiations. A 76 percent response of participants was finally achieved but the final NBS evaluation was hampered by a need for re-evaluation of the fluence certification because of the possible influence of local flux perturbations in the cavity during several of the irradiations. This activity has been completed and results are summarized in Table I. A final report nears completion. Because of the flux perturbation problem, uncertainties are larger than the desired ($\pm$ 2%). Consequently, additional irradiations have been done and a radioactive nickel foil, together with the report of the results presented in Table I, will be sent to each participant. To avoid further delays, the certified ^{235}U fluence results for each of the new foils will accompany this November distribution.

1.2 Iron Fluence Standards: The next certified fluence standards to be issued will be iron foils with 312-day ^{54}Mn activity. Two attempts to produce suitable standards have failed; one because of insufficient activity (unscheduled reactor shutdown) and one because of interfering activities from impurities. Approximately ten iron standards should be available by the end of the calendar year. These can be circulated among many laboratories to effectively increase their number. Again, certified values of fluences will be sent with the foils.

1.3 The Principal Standard Neutron Fluxes at NBS: To obtain the neutron flux in a driven field (e.g., ^{235}U fission disks "driven" by thermal neutron fission...see Fig. 2), a method must be used to transfer the absolute flux

from a more primary standard field. In the U.S., a Ra-Be photo-neutron source (NBS-1) is the primary standard neutron source used to establish standard flux intensities.[6] Because of its low neutron emission rate ($\sim 10^6$ n/s), its high gamma emission rate, and because its spectrum is not well known, this source is not used to produce standard neutron fluxes. Instead, secondary standard sources such as ^{252}Cf are used for flux calibrations.[7] The neutron source strengths for these small, nearly-point sources are determined relative to NBS-1 by measurements in a manganous sulphate bath.[8] In addition to the small physical size, advantages of ^{252}Cf sources include respectable source strengths ($\sim 5 \times 10^9$ n/s) and a well-studied neutron spectrum.[9]

1.4 The NBS Cavity Fission Source and Requirements for Flux Transfer: The counting standards are prepared by irradiation in the NBS Cavity Fission Source, depicted in Figure 1. The arrangement shown in the figure was developed specifically for the LWR-PV Dosimetry Program. In such an irradiation facility, the flux is established by means of indium-foil flux monitors which are calibrated by irradiation in the NBS ^{252}Cf fission spectrum.

Table II demonstrates achievable accuracy and identifies the various elements which must be known to guarantee the flux transfer process. The data in Table II are the germanium-lithium Ge(Li), radioactivity-counter calibration-factors associated with flux measurements in the nickel foil irradiations discussed in Sect. 1.1.

To date, the NBS Cavity ^{235}U Fission Source which has a flux intensity range 2×10^{10} to approximately 10^{11}, depending upon the spacing between the ^{235}U sources, is the most intense standard neutron field. The problems of gradients within the field become increasingly significant as the sources are brought closer together. The spacing used for almost all work thus far is 0.950 cm. Figure 3 shows gradients and reproducibility of results if the power level of the NBS reactor is carefully monitored during the nominal 35-hour irradiations.

Obviously the physical size of specimens which can be placed into a standard neutron field is limited as well as the available flux and fluence. Consequently, an immediate (and continuing) program task is to find and develop other reference benchmark neutron fields, either through production and characterization, or when possible through characterization alone...such as the class of generic power reactor benchmarks.[10]

2. Neutronic Characterization of Special Benchmark Fields Developed in Support of the Reactor Vessel Surveillance Dosimetry Program

The necessity for pressure vessel mock-up facilities for dosimetry investigations and for irradiation of metallurgical specimens was recognized early in the formation of the NRC program. Experimental studies associated

with high- and low-flux versions of a PWR pressure vessel mock-up are in progress. The low-flux version is known as the Poolside Critical Assembly (PCA)[11] and the high-flux version is known as the Pool Side Facility (PSF).[12] Both are located at ORNL. As specialized benchmarks, these facilities provide well-characterized neutron environments where active and passive neutron dosimetry, various types of LWR-PV neutron field calculations, and temperature-controlled metallurgical damage exposures are brought together.

2.1 PCA Neutronics Characterization and Calculational Blind Tests: For the most part, PCA characterization and Blind Test evaluations are complete[1/] and reported.[13] In this paper, the subject is mentioned for completeness and for emphasis of the amount of benchmark referencing to standard neutron fields that was necessary to successfully accomplish the subject tasks.

2.1.1 ^{235}U Cavity Fission Spectrum Referencing: Since the in-field measurements at PCA were joint efforts of CEN/SCK, NBS and HEDL, the ^{235}U spectrum was the medium of intercomparison and calibration validation. Both the ^{235}U cavity fission sources at NBS and at Mol[14] were utilized. Initial radiometric calibrations were previously carried out at the Mol facility. An additional 14 irradiations of the $^{115m}In(n,n')$ reaction, the $^{58}Ni(n,p)$ reaction and the $^{27}Al(n,\alpha)$ reaction were carried out in the NBS ^{235}U (or ^{252}Cf) fields to validate the Mol calibrations. Many of these results also served to equilibrate HEDL measured reaction rates, which were absolutely calibrated against NBS gamma sources, to the benchmarked Mol results.

Furthermore, all ^{238}U fission chamber measurements in PCA made by Mol and by NBS, and all ^{237}Np fission chamber measurements made by NBS, were referenced to the standard fission spectra.

2.1.2 Absolute PCA Core Power Standardization: To provide an accurate description of the neutron source distribution in the PCA core for the "Blind Test" calculations, a profile of the ^{235}U fission rate was obtained by CEN/SCK and ORNL personnel[15] using a minature fission chamber. The mass of the chamber was experimentally determined to $\pm$ 2% at NBS.[16] The efforts were essential for absolute comparison of calculations and measurements of leakage fluxes throughout the mockup facility. The reference "standard" herein is not a field but the NBS set of reference and working fissionable deposits,[17] with their long history of redundant and interrelated mass assays. These deposits are also used in the NBS double-fission chamber[17] to provide certified fission rates (e.g., during start-up physics tests in the U. S. Fast Flux Test

1/ Some additional measurements in which the PCA is serving as a gamma-spectrometry proof testing facility are being undertaken now (fall 1981) and HEDL is performing the gamma-spectrum characterization. Also, to-date reports deal with the 8/7 and 12/13 configurations; characterization results for the 4/12 configuration will be reported in September 1982.

Reactor Facility, Richland, Washington[18]), ^{235}U fission equivalent fluxes (e.g., neutronic characterization in the PCA), benchmark referenced spectral index measurements (e.g., PCA characterization tests), and both fast and thermal flux transfer measurements.

2.2 Standard Dosimetry Measurement Facility (SDMF): This facility, which will utilize hardware from the ORR-PSF high-power pressure vessel mockup experiment, will serve as a primary calibration facility[1/] to validate or certify the accuracy of fluxes derived from PV surveillance dosimetry in operating power plants. Since it is to be a comprehensive dosimetry qualification facility which will incorporate surveillance capsule perturbation effects into the testing and calibration procedures, the initial neutronics characterization has been accomplished in a first simulated PWR-surveillance capsule perturbation experiment in 1980. This experiment was performed using the standard PSF-PV geometry but with the inclusion of a 1 x 1 x 12-inch simulated surveillance capsule at the "accelerated position" (which is located on the side of the thermal shield that faces the PV) and another, identical surveillance capsule at the inside surface of the PV wall. These two capsules each contained an extensive set of neutron flux detectors. Most were "threshold detectors" for the neutrons having energies greater than 1 MeV. Results for six U.S. radioactivity counting laboratories and five European laboratories will serve to demonstrate the amount of consistency in this methodology and provide a consensus set of data for this initial characterization.[10,19] Efforts to benchmark reference these results to standard neutron fields is discussed in Section 5. Furthermore, all dosimetry characterization measurements in late 1982 and 1983 must be benchmarked. Since many of the 1982 measurements will be made with SSTR's, benchmark referencing of the HEDL track recorder technique is discussed in Section 6.

3. Requirement to Experimentally Validate Neutron Transport Calculations Used in a Reactor Vessel Surveillance Program

The newly proposed ASTM Standard E706(II-D) "Neutron Transport Methods for Reactor Vessel Surveillance" explicitly calls for validation of methods by comparison of the calculations with dosimetry measurements in a suitable reactor benchmark experiment. Since some neutronics modeling details will undoubted differ from the benchmark configuration to the power reactor

[1/] The SDMF is an in-situ surveillance-capsule-dosimetry validation or calibration facility to be operational in late 1982 in the PSF of the Oak Ridge Research Reactor at Oak Ridge National Laboratory.
The purpose of the PSF-SDMF is to investigate results of current surveillance capsules, so that dosimetry methods applied by vendors and service laboratories can be:

a) validated and certified;
b) improved by development of supplementary experimental data; and
c) evaluated in terms of actual uncertainties. (See Section 4.)

configuration it is necessary that comparative dosimetry measurements -- which in themselves were validated against an established benchmark neutron field -- be in existence for both the benchmark and the reactor regions of interest.

Conceptually, the requirements for this benchmark must satisfy the following:
(1) have sufficient information available to permit accurate determination of the neutron source distribution in the associated reactor core;
(2) fission equivalent fluxes, or reaction rates established relative to neutron fluence standards, must be reported for $^{237}Np(n,f)$, $^{238}U(n,f)$, and $^{58}Ni(n,p)$ or $^{54}Fe(n,p)$ for each specified location;
(3) dosimetry measurements, as mentioned above, must be documented for at least two ex-core locations, well separated by steel and coolant.

Validation is achieved when it has been demonstrated that differences between measurements and calculations are less than some representative, predetermined quantity. The actual differences provide estimates of the minimum uncertainties that can then be assigned to calculated exposure parameters, which should include, at least, flux greater than 1 MeV and dpa.

4. Surveillance Dosimetry Accuracy Requirements

This issue is discussed in considerably more detail in Ref. (5). However, the most stringent U.S. requirement appears to be that associated with the present operating, and regulatory requirements for accuracy on fracture toughness and ductility. That is to say, the uncertainty associated with the determination of fracture toughness must be considered in order to ascertain the level of accuracy required for surveillance capsule exposure parameters. The example below shows that plant safety demands a sufficiently high level of accuracy for the exposure parameters such that fluence (for E>0.1 and E>1.0 MeV) and dpa can be the controlling factors, at least for the older plants.[1/] This comes about as follows:
(1) Based upon PCA/PSF studies, the best presently attainable limits on measured and calculated values of exposure parameters are $\pm$20% (2σ). These hold only for benchmarked results, however; otherwise factors at least three times this large are evident (5).
(2) Considering that these 2σ limits are representative of upper and lower bounds, a typical plant-specific controlling trend curve is shown as the

[1/] Since it is not considered possible to reduce the uncertainty on the RT_{NDT} variable (at a fixed position in the PV wall, such as the surface or 1/4T locations) below approximately $\pm$30°F (2σ). This value is for a typical, older plant weld metal with a RT_{NDT} value of 80°F after approximately 5 EFPY of plant operation with a PV inner surface fluence (E>1.0 MeV) of $3.8 \times 10^{18} n/cm^2$. This example considers a weld material with 0.15% Cu and 0.12% P content and an initial RT_{NDT} of 0°F.

dashed curve in Fig. 4. The intersection of this curve with the Reg. Guide 1.99.1 (1) upper limit band on RT_{NDT} for a nominal operating temperature of 550°F for LWR power plants, is at 5.7 x 10^{18} n/cm^2, at the inner PV surface. (3) If instead of the ±20% fluence uncertainty limits, a more representative, current value (observed in recent surveillance capsule studies) of ±60% (2σ) limit were used, the plant specific (dashed curve would shift even further to the left), resulting in an intersection at a fluence of 2.8 x 10^{18} n/cm^2. (4) Consequently, if the reported fluence value (exposure parameter) had been uncertain to ±60% (2σ), corrective action, such as costly annealing the vessel, would have to be considered approximately one effective full-power year earlier!

(5) The horizontal (fluence) range that is involved with the ±30°F error bars on the metallurgical property in Fig. 5 is 1.5 x 10^{18} n/cm^2, associated with the -30°F limit, and 7.2 x 10^{18} n/cm^2, associated with the +30°F limit. Does this mean that the controlling value on fluence is this uncertainty of ±30°F on the property change and knowing the fluence value to within a factor of 5 should be considered accurate? Absolutely not! The issue is that of the 95 percent confidence limits to be employed to establish currently safe and end-of-life (EOL) fluence operational limits. The reason fluence is used as the extrapolating (independent) variable is that it is obviously determined more accurately, at this time, than the associated metallurgical variable.

(6) For a given uncertainty in fluence, the point of intersection was dictated by the limiting ±30% (2σ) on the RT_{NDT} variable. Therefore, to gain in useable vessel lifetime it is crucial to invest in reduction of uncertainties in the exposure parameters, because they are the "clocks" by which vessel "time" is measured.

5. Benchmark Referencing of Fissionable Radiometric Sensors

The ^{137}Cs isotope with its thirty-year half life is a fission product of particular interest for reactor vessel surveillance. It is presently the fission product most assayed in surveillance capsules. The $^{235}U(n,f)^{137}Cs$ reaction is also a favorable candidate to replace the $^{59}Co(n,\gamma)^{60}Co$ (5.27 years) reaction as the thermal and epithermal fluence monitor for long term exposures. Therefore an urgent need exists to benchmark reference ^{137}Cs production in a fission reaction. This, however, presents certain problems:

^{137}Cs analyses of aliquots: Frequently, the fissionable isotope is dissolved and an aliquot taken before radioactivity analyses. Typically, samples (aliquots) are several milligrams with specific ^{137}Cs activities of 10^7 dps/g for ^{237}Np monitors and 10^6 dps/g for ^{238}U monitors.[1/] Ideally, the benchmark

[1/] These are only crude estimates because the magnitude will vary drastically depending upon length of irradiation and plant-specific power level (i.e., depend on fluence); they were obtained, however, from an actual measurement of a surveillance capsule.

experiment should produce similar fission densities in one of the two mentioned isotopes and the validation exercise should include dissolution to check all steps in the procedure. However, irradiation in the NBS Cavity ^{235}U Fission Field with possible flux levels from 2×10^{10} to 8×10^{10} would require 25 to 100 days. This is prohibative.

Flux Perturbations: An alternate approach is to irradiate ^{235}U in a thermal neutron field. This gains a factor of 600 in cross section magnitude and a factor of 50 to 100 in flux level. However, serious flux perturbation issues attend thermal flux irradiations of "thick" ^{235}U foils. One can choose to fission the ^{235}U in a natural uranium foil which produces far less flux perturbation but also provides fewer ^{235}U atoms. Still the latter appears to be more promising and appears to be feasible in an irradiation of only several days duration. It is not yet clear, however, whether this is best done as a "certified fluence" irradiation or as an irradiation together with the NBS fission chamber to produce a certified number of fissions.

Limited capability to mass produce: In any of the discussed procedures, production will be limited to at most several standards. Of course with a thirty year half life, these may be passed from laboratory to laboratory to achieve availability. Because this will significantly lengthen the time for intercomparison, it is recommended that the certified quanity be supplied with the standard. This has the disadvantage of not being a blind test procedure.

6. Use of Recognized Benchmark Fields to Calibrate New, State-of-the-Art Sensors and Validate the Associated Methodology

As new sensor technology is developed, it is necessary to perform definitative and, easily interpretable experiments in benchmark fields with representative sensor elements. Where possible, these should be performed in the standard benchmark fields and/or with direct reference to other types of previously tested sensors. Because of the stringently controlled geometry and inherent flux limitations in standard neutron fields, other referenced benchmark facilities must sometimes be used (e.g., PCA, PSF, the SDMF or eventually perhaps, generic, benchmarked power reactors).

6.1 Benchmark Referencing of HEDL-SSTR Technology: Two phases of benchmark referencing are in progress. The first, nearing completion, compares total fissions in eight separate ^{252}Cf irradiations as predicted by NBS fission chambers and by HEDL-SSTR's. The fissionable isotopes involved were ^{235}U and ^{240}Pu. A disinterested referee at Argonne National Laboratories has been chosen to accept each laboratory's results.

The second phase, which should be completed in 1982 will address SSTR measurements with ^{238}U, ^{237}Np, and perhaps ^{232}Th. The uranium and neptunium isotopes are of particular interest because of their past use in the PCA characterization measurements, prior to their being benchmarked. The thorium may possibly be useful in conjunction with ^{238}U to further investigate photofission in PWR environments.

6.2 Benchmark Referencing of HAFM's: Plans have been discussed with B. Oliver and H. Farrar (Rockwell International) to irradiate Helium-Accumulation Fluence Monitors (HAFM's) in the NBS Intermediate-Energy Standard Neutron Field (ISNF) and provide a simultaneous fission monitor count to begin the benchmark referencing of HAFM's.

In addition, plans are underway to provide an evaluation of the existing experimental $^{10}B(n,\alpha)$ cross section data (with emphasis on integral experiments), addressing the question of the adequacy of that data for establishment of $^{10}B(n,\alpha)$ as a cross section standard for neutron energy greater than 100 keV.

6.3 Benchmark Referencing of Niobium: Because of the long fourteen-year half life of ^{93m}Nb which results from the $^{93}Nb(n,n')^{93m}Nb$ reaction, there is pressure from primarily the European community to attempt meaningful benchmark irradiations. This is a very difficult experiment to carry out because of the length of exposure time in any field, such as ^{252}Cf or ^{235}U, sufficiently well known to yield cross section information. A provisional experiment is to study the Nb dosimeters from the PSF irradiations and correlate the information with routine "spectral dosimetry" via conventional radiometric foils.

H. Tourwe, at CEN/SCK, is independently pursuing a niobium dosimetry program with HEDL which involves an intercomparison of results from niobium from BR2 and EBR-II. The LWR PV Dosimetry Program remains alert to this endeavor through the ASTM E10.05 Subcommittee on Nuclear Radiation Metrology on which H. Tourwe is the EURATOM representative.

CONCLUSIONS

The principal objective of benchmark field referencing is to guarantee measurement accuracy of dosimetry methods for the LWR-PV Surveillance Dosimetry Improvement Program. This task involves calibration of neutron sensors, validation of procedures to analyze them, and validation of calculations necessary to apply the results to the required surveillance programs. The task also requires referencing, to standard neutron fields, those neutronic characterizations of other environments developed to further meet the needs of higher fluences and realistic representations of operating power reactors. The tasks are not easy ones but substantial progress has been made and documented. One problem, which is extremely important to this author, is the need for more emphasis (support) on the continued development of standard fields and their related basic integral measurements so that they may better serve the needs of applied technologies.

REFERENCES

1. "Licensing of Production and Utilization Facilities," Title 10 Code of Federal Regulations, Part 50: Appendix G, "Fracture Toughness Requirements;" Appendix H, "Reactor Vessel Material Surveillance Program Requirements." Published by the Office of Federal Register, Washington, D.C. (1978)..
2. J. Grundl and C. Eisenhauer, "Fission Rate Measurements for Materials Neutron Dosimetry in Reactor Environments," ASTM-EURATOM Symposium on Reactor Dosimetry, American Society for Testing and Materials (September 1975).
3. E. D. McGarry and A. Fabry, "Dosimetry Characterization of a Reactor Pressure Vessel Simulator by Fission Chamber and Foil Activation Measurements," Proc. of Third ASTM-EURATOM Symposium on Reactor Dosimetry, Ispra, Italy (October 1-5, 1979).
4. C. Z. Serpan, "Standardization of Dosimetry Related Procedures for the Prediction and Verification of Changes in LWR Pressure Vessel Steel Fracture Toughness During Reactor Service Life: Status and Recommendations," Proc. of Third ASTM-EURATOM Symposium on Reactor Dosimetry, Ispra, Italy (October 1-5, 1979).
5. W. N. McElroy, et al., "LWR Pressure Vessel Surveillance Dosimetry Improvement Program 1979 Annual Report," NUREG/CR-1291, HEDL-SA 1949, Hanford Engineering Development Laboratory, Richland, WA (February 1980).*
6. J. A. DeJuren, D. W. Padgett and L. F. Curtiss, Journal of Research, National Bureau of Standards, Vol. 55, No. 2, 63 (August 1955).
7. J. Grundl and C. Eisenhauer, "Fission Spectrum Neutrons for Cross Section Validation and Neutron Flux Transfer; Proc. Conf. Nuclear Cross Sections and Technology, Washington, D. C. 1975. Special Publications 425, Vol. I, p. 250, National Bureau of Standards (October 1975).
8. J. A. DeJuren and J. Chin, Journal of Research, National Bureau of Standards, Vol. 55, No. 6, 311 (December 1955).
9. J. A. Grundl, V. Spiegel, C. Eisenhauer, H. T. Heaton II, D. M. Gilliam, (NBS) and J. Bigelow (ORNL), "A Californium-252 Fission Spectrum Irradiation Facility for Neutron Reaction Rate Measurements," Nucl. Tech. Vol. 32, 315 (March 1977).
10. W. N. McElroy, et al., "Surveillance Dosimetry of Operating Nuclear Power Plants," NRC 9th Water Reactor Safety Information Meeting, October 26-30, 1981, National Bureau of Standards, Washington, D.C.: HEDL-SA-2546 (September 1981).*

*Available for purchase from the NRC/GPO Sales Program, U.S. Nuclear Regulatory Commission, Washington, D.C. 20555 or the National Technical Information Service, Springfield, VA 22161.

11. "LWR Pressure Vessel Surveillance Dosimetry Improvement Program: PCA Experiments and Blind Test," NUREG/CR-1861, HEDL-TME 8087, May 1981, Hanford Engineering Development Laboratory, Richland, WA (July 1981).*
12. A. Fabry, "Results and Implications of the Initial Neutronic Characterization of Two Heavy Section Steel Technology (HSST) Irradiation Capsules and of the PSF-Simulated LWR Pressure Vessel Irradiation Facility," NRC 8th Water Reactor Safety Research Information Meeting, October 27-31, 1981, National Bureau of Standards, Washington, D. C. (1981).
13. F. W. Stallmann and F. B. K. Kan, et al., "Reactor Calculation Benchmarks: PCA Blind Test Results," NUREG/CR-1872, ORNL/NUREG/TM-428, Oak Ridge National Laboratory, Oak Ridge, TN (January 1981) and reference No. 11 above.
14. A. Fabry, J. A. Grundl and C. Eisenhauer, "Fundamental Integral Cross-Section Ratio Measurements in the Thermal-Neutron-Induced ^{235}U Fission Spectrum," NBS Special Publication 425, Vol. 2, p. 254, National Bureau of Standards, Washington, D. C. 20234 (October 1975).
15. F. B. K. Kam, A. Fabry, F. W. Stallmann, G. Minsart, E. D. McGarry, L. F. Miller, J. H. Swankis and W. N. McElroy, "The Core Power of the Pool Critical Assembly Light Water Reactor Pressure Vessel Benchmark," Proc. of the Third ASTM-EURATOM Symposium on Reactor Dosimetry, Ispra, Italy (October 1-5, 1979).
16. E. D. McGarry, "Determination of the Effective Mass of ^{235}U in the Fission Chamber Used for Absolute Core Power Measurements in the PCA," NUREG/CR-1241, Vol. II, HEDL-TME 80-5, Hanford Engineering Development Laboratory, Richland WA (1981).*
17. J. A. Grundl, D. M. Gilliam, N. D. Dudey and R. J. Popek, "Measurements of Absolute Fission Rates," Nucl. Tech., Vol. 25, p. 237 (1975).
18. J. L. Fuller, D. M. Gilliam, and J. A. Grundl, "A Double Fission Chamber for Absolute Fission Rates in Power Reactor Environments," Hanford Engineering Development Laboratory Document HEDL-SA-1939, also, Proceedings of the Third ASTM/EURATOM Symposium, Ispra, Italy (October 1979).
19. NRC Annual Report (1980).

Table I-A. Comparison of Interlaboratory Consistency in Measuring Nickel Fluence Standards[a]

Nickel Foil I.D.	^{235}U Fission Spectrum Fluence in Units of 10^{15} n/cm^2 Reported Value	NBS Value[d]	Ratio of Reported to NBS Value
AP	1.48 ± 5.5 %	1.51 ± 2.5%	0.98
AR	1.479 ± 0.84%	1.47 ± 2.7%	1.01
AS	1.491 ± 1.2 %	1.49 ± 2.7%	1.00
AU	1.672 ± 2.8 %	1.58 ± 3.6%	1.06
BK	2.74 ± 2.6 %	2.74 ± 2.4%	1.00
BL	2.85 ± 4.0 %	2.66 ± 2.5%	1.07
BM	2.60 ± 2.26%	2.65 ± 2.7%	0.98
BN	2.388 ± 0.07%	2.74 ± 2.8%	0.87
BV	2.479 ± ---	2.36 ± 2.8%	1.05
BW	2.25 ± 2.0 %	2.23 ± 3.0%	1.01
BY	2.17 ± 4.0 %	2.23 ± 3.2%	0.97
BX(1)[b]	2.286 ± 3.1 %	2.20 ± 3.2%	1.04
BX(2)	2.232 ± 1.2 %	(2.20 ± 3.2%)	1.01
CA	1.964 ± ---	2.10 ± 3.2%	0.94
CD(1)[c]	2.08 ± (1.8 %)	2.12 ± 3.5%	0.98
CD(2)	2.10 ± (1.7 %)	(2.12 ± 3.5%)	0.99
CD(3)	2.13 ± (1.7 %)	(2.12 ± 3.5%)	1.00
CG	1.61 ± 3.0 %	1.66 ± 2.9%	0.97
CI	1.96 ± 1.6 %	1.73 ± 3.2%	1.13
CJ	2.14 ± ---	2.30 ± 2.7%	0.93
CL	2.26 ± 3.3 %	2.23 ± 2.9%	1.01

Footnotes:

[a]Prepared by activation of the $^{58}Ni(n,p)^{58}Co$ reaction in the NBS Cavity ^{235}U Fission Spectrum.

[b]Two values reported by one laboratory: one for Ge(Li) and one for NaI counting.

[c]Three different groups counted this foil but did not report fluence but specific activity on 29 January 1979: Group 1 reported 8164 ± 1.7% dps; Group 2 reported 8257 ± 1.8% dps; Group 3 reported 8373 ± 1.8% dps. Fluence values were derived using a cross section of 102 mb.

[d]Accuracies differ within various sets because of positioning uncertainties in foil stacks and flux gradients. They differ for various irradiations (see Table I-B) as explained in the text.

Table I-B. Logistics of the Certified Fluence Irradiations of Nickel Foils in the NBS Cavity Fission (U-235) Spectrum

NICKEL FOIL IDENTIFICATION	DATES AND TIMES OF IRRADIATION		TIME DURATION (seconds)
	START	END	
BV, BW, BX, By	7/17/78 17:19 EDST	7/18/78 23:27 EDST	108480
CA, CB, CC, CD	8/1/78 17:35 EDST	8/2/78 23:10 EDST	106500
AP, AR, AS, AT, AU	8/21/78 20:51 EDST	8/22/78 17:53 EDST	75720
CF, CG, CH, CI	9/15/78 11:36 EDST	9/16/78 09:50 EDST	80040
CJ, CK, CL, CM	9/22/78 15:24 EDST	9/23/78 22:37 EDST	112380
BK, BL, BM, BN	1/13/79 14:55 EST	1/14/79 23:03 EST	115680

The foils were distributed to participants between 27 November 1978 and 3 February 1979. The percentage returned as a function of time after February 1979 is as follows:

ELAPSED TIME (months)	DATE	PERCENT RESPONSE
6	August 1979	41%
12	February 1980	69%
18	August 1980	76%

Table II

Reproducibility of flux-to-response ratios, ϕ^{252}/R^{252} for the 4.5 hour $^{115}In(n,n')^{115}In^*$ reaction activated in the NBS ^{252}Cf standard neutron field.

Time and date of the end of irradiation	NBS ^{252}Cf source and strength	Average source to foil distance (cm)	$\frac{S}{4\pi \langle r \rangle^2}$	ϕ^{252} Cf-252 flux over foil	Foil pair results for 4.5hr indium flux monitors (counts/s·g)		Irradiation time (sec.)	4.5hr indium saturation factor for irradiation	Counter used for 4.5hr indium activity	R^{252}_{In} counter response to 4.5hr indium activity	Observed ratio ϕ^{252}/R^{252}_{In}	ϕ^{252}/R^{252}_{In} adjusted for counter efficiency differences
					Individual	Average						
09:34:00 EST 5/1/78	NS-92 4.238×10^9 ±1.1%	4.781 ±0.85%	1.476×10^7 ±1.45%	1.463×10^7 ±1.5%	87.00 88.38	88.06 ±1.1%	9.000×10^4	0.9790	75 ml. Ge(Li)	89.95 ±1.1%	1.626×10^5 ±1.9%	1.626×10^5 ±1.9%
06:12:50 EST 5/7/78	NS-92 4.217×10^9 ±1.1%	4.655 ±0.85%	1.548×10^7 ±1.45%	1.533×10^7 ±1.5%	93.68 95.17	94.87 ±0.7%	2.186×10^5	0.9999	75 ml. Ge(Li)	94.88 ±0.60%	1.616×10^5 ±1.6%	1.616×10^5 ±1.6%
22:10:00 EDST 7/19/78	NS- 4.003×10^9 ±1.1%	4.590 ±0.85%	1.512×10^7 ±1.45%	1.498×10^7 ±1.5%	91.92 92.79	92.36 ±1.0%	1.214×10^5	0.9945	75 ml. Ge(Li)	92.87 ±1.0%	1.613×10^5 ±1.8%	1.613×10^5 ±1.8%
22:45:00 EDST 8/2/78	NS-92 3.962×10^9 ±1.1%	3.013 ±1.3%	3.472×10^7 ±1.8%	3.397×10^7 ±1.8%	207.12 212.32	209.7 ±1.2%	1.159×10^5	0.9931	75 ml. Ge(Li)	211.2 ±1.2%	1.608×10^5 ±2.1%	1.608×10^5 ±2.1%
20:23:00 EDST 8/19/78	NS-92 3.910×10^9 ±1.1%	3.005 ±1.3%	3.445×10^7 ±1.8%	3.370×10^7 ±1.8%	206.02 209.44	207.7 ±0.3%	1.720×10^5	0.9994	75 ml. Ge(Li)	207.8 ±0.3%	1.621×10^5 ±1.8%	1.621×10^5 ±1.8%
08:53:00 EST 11/14/78	NS-92 3.677×10^9 ±1.1%	3.014 ±1.3%	3.222×10^7 ±1.8%	3.152×10^7 ±1.8%	114.06 112.46	113.3 ±0.35%	5.700×10^4	0.9134	60 ml. Ge(Li)	124.0 ±0.4%	2.542×10^5 ±1.8%	1.608×10^5 ±1.8%
09:26:00 EST 12/18/78	NS-92 3.589×10^9 ±1.1%	2.999 ±1.3%	3.175×10^7 ±1.8%	3.106×10^7 ±1.8%	119.46 121.13	120.3 ±1.3%	1.234×10^5	0.9950	60 ml. Ge(Li)	120.9 ±1.3%	2.569×10^5 ±2.2%	1.625×10^5 ±2.2%
09:03:00 EST 1/15/79	NS-92 3.518×10^9 ±1.1%	3.001 ±1.3%	3.109×10^7 ±1.8%	3.042×10^7 ±1.8%	120.46 118.14	119.3 ±0.5%	1.548×10^5	0.9987	60 ml. Ge(Li)	119.5 ±0.45%	2.545×10^5 ±1.9%	1.610×10^5 ±1.9%

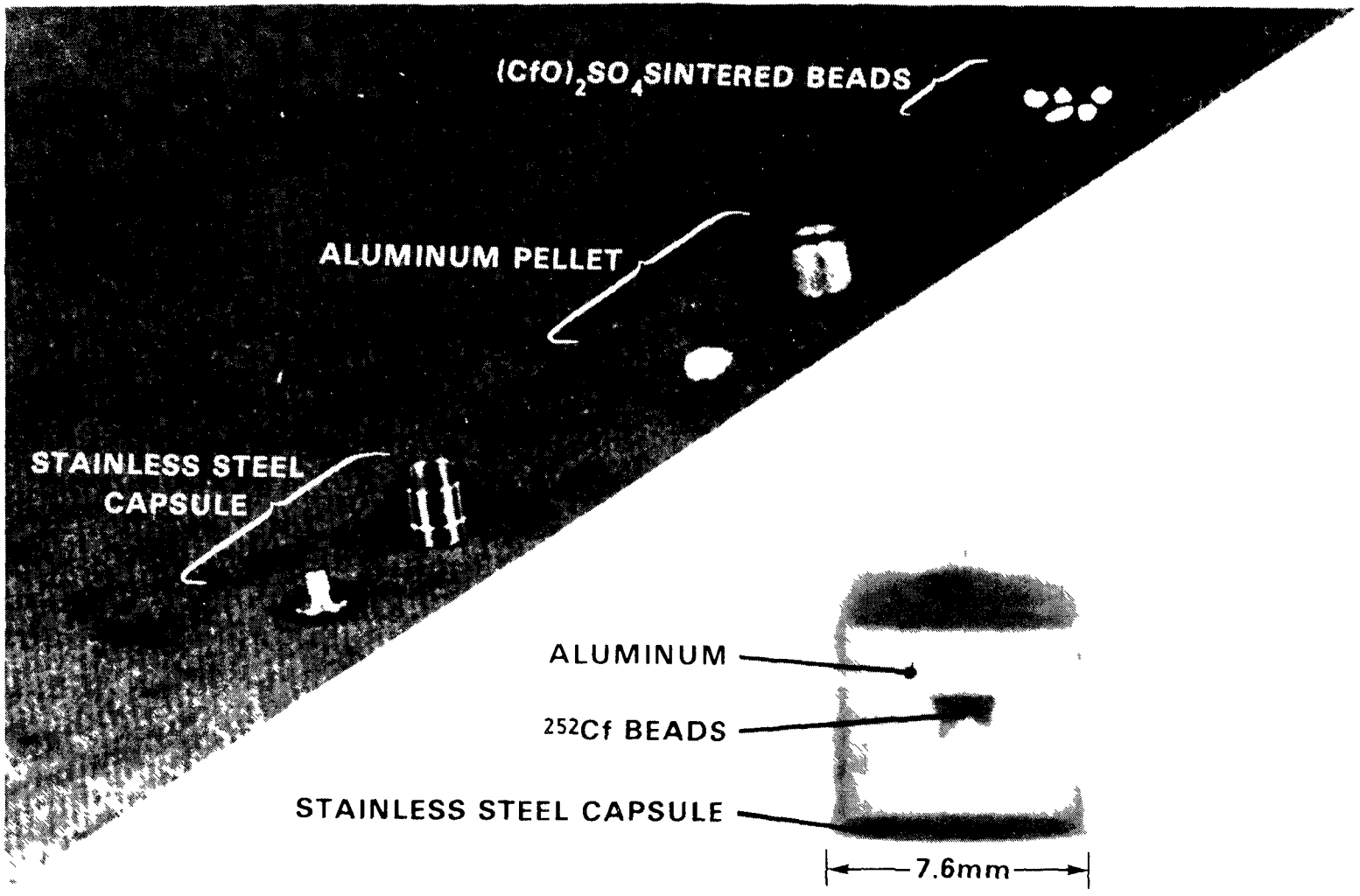

Figure 1. Californium-252 source assembly *components and x ray of* assembled 3-mg source.

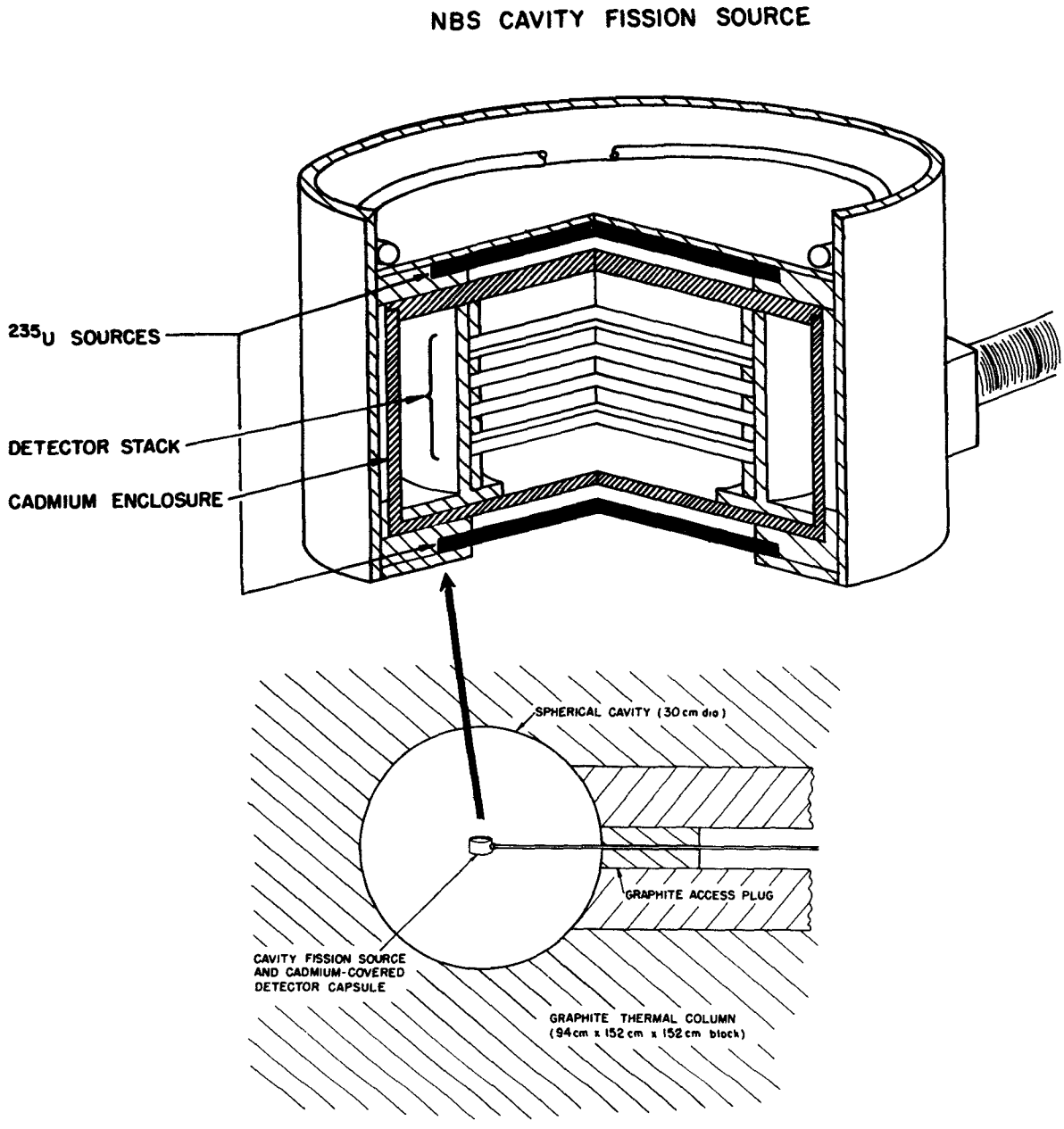

Figure 2. Details of method of exposing the uranium source disks to the required thermal neutron flux.

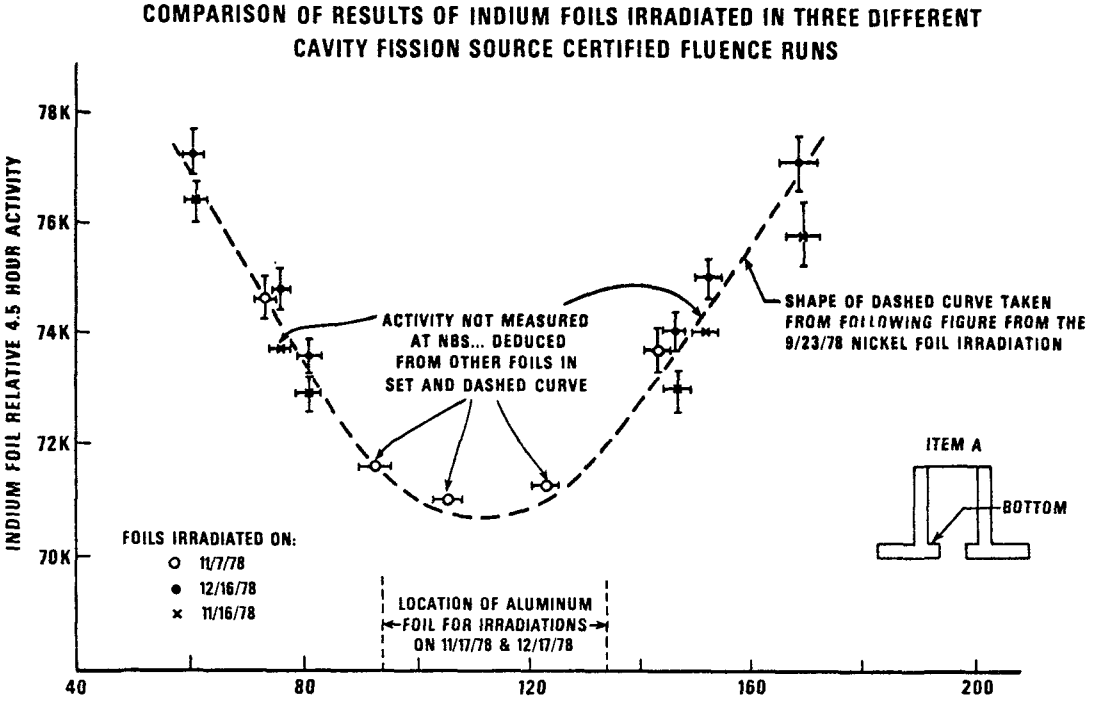

Figure 3. DISTANCE IN MILS FROM THE BOTTOM OF THE ALUMINUM FOIL HOLDER FOR THE CAVITY FISSION SOURCE (SEE ITEM A). THE OBSERVED ACTIVITY IS PLOTTED AT THE CENTER THICKNESS OF THE FOIL.

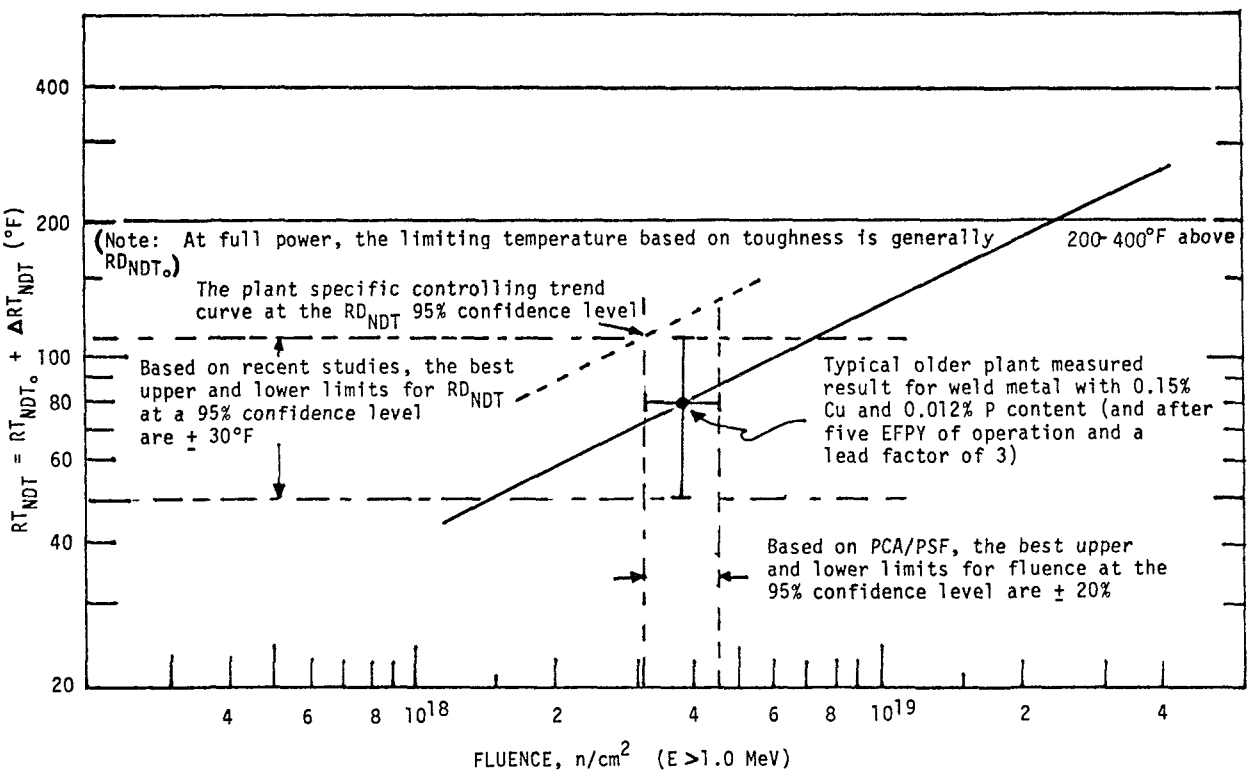

Figure 4. Correlation of limiting accuracy values for fluence (E>1.0 MeV) with those for RT_{NDT} from surveillance capsule results at the inner surface of the PV wall after 5 EFPY of operation of a typical PWR type plant with the older, radiation sensitive steel.

STATUS AND FURTHER NEEDS OF CROSS SECTION COVARIANCE FILES

W. MANNHART
Physikalisch-Technische Bundesanstalt,
Braunschweig,
Federal Republic of Germany

Abstract

The present status of neutron cross section covariance files is shown in the light of the example of the covariance file of the ENDF/B-V Dosimetry File. The special influence of relative cross section measurements on future evaluations is discussed. Proposals are made to improve the applicability of Special Purpose Files by slight modifications in their covariance files. Finally the rules for transforming covariances to another group structure are briefly reviewed.

1. Introduction

Version V of the "Evaluated Nuclear Data File" (ENDF/B-V) was released at the end of 1979 /1/. In contrast to earlier versions, ENDF/B-V contains an essentially new kind of information in the form of covariance files. Two types of covariance files exist for neutron cross sections: "File 32" describing the uncertainty of resonance parameters and "File 33" for the uncertainty of energy-dependent cross section data. For those cross sections which include resonance contributions, File 32 gives the uncertainties and short-range correlations due to specific resonances, whereas all further long-range correlations are contained in File 33. For non-resonant cross sections the information is given in its entirety in File 33.

The formats chosen to represent the data of File 33 are of large flexibility; on the one hand to allow an easy inclusion of different sources of uncertainty and on the other hand to avoid unnecessary repetition of redundant information. The formats are described in detail elsewhere /2/. For the sake of easier understanding here, only a few facts will be reported. A section of File 33 represents the uncertainty data for a specific material MAT and reaction type MT. Each section may contain several subsections with covariance data relating to the same or other material and reaction type. Thus a subsection represents either the correlations between data of the same reaction at different neutron energies or correlations between different reactions. The information belonging to a subsection is given in the form of one or more sub-subsections which have to be combined to obtain a specific covariance matrix. NI-type sub-subsections contain individual components of a covariance matrix, whereas NC-type sub-subsections refer to components which are placed in other portions of File 33 in the form of NI sub-subsections. Each NI segment is identified by an LB index whose numerical value (between 0 and 5) indicates whether the covariance matrix

is an absolute or relative one. Most of the data in File 33 are relative covariance matrices, as the index LB=0, the only one indicating absolute covariances, is not very often used.

2. File 33 of the ENDF Dosimetry File

Tape 531 (Dosimetry File) of ENDF/B-V is the tape which is mainly used for reactor dosimetry purposes. We will therefore restrict ourselves in the following to this tape. The first version of Tape 531 contained several misprints, especially in File 33. Meanwhile a second modified version eliminating these inconsistencies is in preparation. This version will soon be issued /3/.

2.1 Combination of File 33 segments

In the example of the reaction $^{27}Al(n,\alpha)$, Table 1 shows the various NI segments of File 33 which compose the final relative covariance matrix. In this example we have three segments. The first segment with LB=1 contains short-range correlations over the total energy range in the form of diagonal elements only. The second segment (LB=2) contains long-range correlations in the energy range between 3.25 MeV and 12 MeV. All relative variances given are fully correlated. A third segment with LB=1 adds additional short-range correlations above 12 MeV to the final matrix. Each of these partial matrices shows its own energy grid dependent on the details of information. The combination of these partial matrices for the final covariance matrix is straightforward. After the construction of a common energy grid which must contain each segment grid, all partial matrices must be transformed to this common grid; then they can simply be added. The choice of the energy grids for various reactions in File 33 strongly depends on the details of the data uncertainties available. A coarse grid indicates the availability of less uncertainty information and vice versa, a fine grid the contrary.

2.2 Special Rule of NC segments

On inspecting File 33 in more detail, one finds that for Tape 531 only two reactions, $^{238}U(n,\gamma)$ and $^{239}Pu(n,f)$, show NC segments referring to partial covariances given in other parts of the file. For $^{238}U(n,\gamma)$ a portion of the covariance matrix comes from the $^{10}B(n,\alpha)$ reaction in the energy interval between 4 keV and 20 keV, and for $^{239}Pu(n,f)$ the same applies for the reaction $^{235}U(n,f)$ between 0.2 MeV and 15 MeV. The fact of covariances being common to two reactions automatically implies correlations between these reactions. Before discussing this point we shall make a few additional comments on the reference system of NC segments. The NC segments of Tape 531 mentioned both refer to Tape 511 (Standard File), to MAT=1305; MT=107 ($^{10}B(n,\alpha)$) and to MAT=1395; MT=18 ($^{235}U(n,f)$), respectively. Normally, users of Tape 531 will not always have access to other tapes. On the other hand, it was found that MAT=1395; MT=18 can be completely replaced by MAT=6395; MT=18 and MAT=1305; MT=107 can be replaced in good approximation by MAT=6425; MT=207 with both second (MAT,

MT) pairs belonging to the Dosimetry Tape. The author believes that in Special Purpose Files, it would be of advantage to replace the (MAT,MT) numbers referring to other tapes by (MAT,MT) numbers of the same file, and where no (MAT,MT) numbers corresponding to Standard Files exist, to replace the NC segments by (reduced) NI segments which must only contain the relevant portion of information.

2.3 Impact of Cross Section Ratio Measurements

To understand how correlations between different neutron reactions become established, we look at Table 2. We assume that two independent evaluations of the $^{27}Al(n,\alpha)$ and of the $^{65}Cu(n,2n)$ cross section exist which are both based on absolute cross section data only. Looking at Table 2, one recognizes that correlations exist between various data of the same cross section but there are none between the two different cross sections. The extension of the evaluation to additional data in the form of ratios requires a simultaneous evaluation of both cross sections as these data influence both components of the evaluation. In addition, such cross section ratios introduce correlations between the components of the evaluation, as can be seen from Table 2. The example shown is taken from ref. /4/ where more details can also be found.

It is obvious that it would be unrealistic to expect a file as newly established as the covariance file to supply all details which influence the evaluation of nuclear cross section data in its first version. Complex quantities (as indirectly measured ratios are) can therefore only be included step by step in future evaluations. To emphasize the influence of ratios on the cross section data base, we have investigated the existing data base of an arbitrary ENDF/B-V evaluation; here, the evaluation of the $^{48}Ti(n,p)$ reaction /5/. The result is shown in Table 3. The table shows the energy range each experiment covers (the detailed references can be found elsewhere /6/), states if the measurement was an absolute or relative one and quotes the number of data points belonging to an experiment. Experiments based on a neutron flux density determination with a proton recoil detector are quoted as absolute data. In principle, they may also be interpreted as relative ones, namely relative to the elastic hydrogen cross section. The total data base of 89 data points is composed of 28 data determined absolutely and 61 data measured relatively to a reference cross section. The dominant number of relative data reflects the problem of measuring neutron flux densities absolutely. It also shows that relative data must play an essential part in forthcoming evaluations. While in the past, cross section evaluations were mainly carried out for a single reaction without regard to other evaluations, in future the consistent treatment of existing data correlations requires simultaneous evaluations of all cross sections which are interconnected by ratio measurements. The principle of such evaluations has been shown by Perey and co-workers /7/. Simultaneous evaluation of a large number of cross sections makes the work of evaluation more difficult, of course. But the dimension of such an evaluation can probably

be reduced, because only a few reference cross sections play an essential part while the others remain of minor importance.

3. Comments on the Transformation of Covariance Matrices

In this context it should be stressed that the concept of covariance files automatically implies that the cross sections are processed into group cross sections. Of course, covariance files can also be applied to microscopic data. In this case the correlations must be regarded as constant within the given energy intervals (or groups). The transformation of covariance files from the original ENDF/B-V group structure to another specific group structure does not involve principal difficulties provided that the uncertainty propagation rules are correctly handled. Table 4 shows the principles of the transformation of a relative covariance matrix from the group structure i to another group structure m. Knowledge of the group constants of the initial structure, σ_i and ϕ_i, alone is assumed. The uncertainty propagation is governed by the rule that the integral $\int \sigma(E)\ \phi(E)dE$ (with $\phi(E)$ being the spectral neutron flux density) must be conserved independent of the group structure. The elements of the transformation matrix T are shown in very simple examples which cover all possible cases. The energy delimiters of the initial structure are indicated by E_i and that of the final structure by F_m. A little care is necessary if the E_i and F_m do not coincide as shown in case C. The application of a covariance matrix transformation is shown in Table 5. The covariance matrix of the reaction $^{58}Ni(n,p)$ has been transformed from the original ENDF/B-V structure (11 groups) to a 15-group structure used by Zijp and co-workers /8/. Three cases are shown: In the first of these, the group data were generated for a 1/E neutron spectrum. Group cross sections and group fluxes were processed from the data of File 3, corresponding to the group structure of the covariance file. A 1/E spectrum allows a direct analytical integration of the "smooth" data of File 3 with respect to their interpolation rules. Based on these group data and analogous to the procedures shown in Table 4, the covariance matrix was transformed to the new structure. In the second case, the same was done but with a constant neutron spectrum. The comparison between both results shows that the somewhat arbitrary choice of the neutron spectrum in the group compression procedure has only a slight influence on the final covariance matrix. The third result given for comprehensiveness was also calculated for a 1/E spectrum with the additional assumption that all group cross sections are equal, i.e. $\sigma(E)$=const. over the total energy range. This result is identical with that obtained by Zijp and co-workers in ref. /8/. It must be stressed, however, that the third of the three results is the only one which violates the conservation law that the energy integral of the cross section over a certain neutron spectrum must be independent of a specific group structure.

4. Conclusions

With regard to the difficulties inherent in obtaining sufficient information on the uncertainties of neutron cross sections, the ENDF/B-V covariance files mark an essential step towards gaining more realistic estimates of the uncertainties of any nuclear parameters dependent on cross section data. The linking of different cross sections established for the most part as a result of the multitude of relative cross section measurements will make further covariance evaluations more complex but must nevertheless be taken into account in future. It is recommended that possibilities of improving the covariance files in the case of Special Purpose Files be considered with the aim of making the full capacity of the covariance file available to the Special Purpose Files, too.

References

/1/ R. Kinsey: "Data Formats and Procedures of the Evaluated Nuclear Data File, ENDF", BNL-NCS-50496 (ENDF-102) 2nd.Ed.(ENDF/B-V), Oct. 1979

/2/ F.G. Perey: "The Data Covariance Files for ENDF/B-V", ORNL/TM-5938 (ENDF-249), July 1977

/3/ B.A. Magurno: Priv. comm. (August 1981)

/4/ W. Mannhart: "A Small Guide to Generating Covariances of Experimental Data", Report PTB-FMRB-84, June 1981

/5/ C. Philis, O. Bersillon, D. Smith, A. Smith: " Evaluated (n;p) Cross Sections of ^{46}Ti, ^{47}Ti and ^{48}Ti", ANL-NDM-27, January 1977

/6/ CINDA-A and CINDA-81: "An Index to the Literature on Microscopic Neutron Data", IAEA, Vienna 1979 and 1981

/7/ C.Y. Fu, D.M. Hetrick, F.G. Perey: "Simultaneous Evaluation of ^{32}S(n,p), ^{56}Fe(n,p), ^{65}Cu(n,2n) Cross Sections", NBS Spec.Publ.594,63(1980)

/8/ N.J.C.M. van der Borg, H.J. Nolthenius, W.L. Zijp: "Covariances of the data of the ENDF/B-V dosimetry file", Report ECN-80-091, May 1980

Table 1: Final Covariance Matrix and Segments of $^{27}Al(n,\alpha)$

$^{27}Al(n,\alpha)$

MAT = 6313 MT = 107

NEUTRON ENERGY RANGE (IN EV)		REL.STD.DEV. OF SIGMA(E) (IN %)	CORRELATION MATRIX : (LOWER TRIANGLE ONLY) ELEMENTS MULTIPLIED BY 100												
1.00E-5	3.25E+6	0.0	100												
3.25E+6	3.50E+6	50.0	0	100											
3.50E+6	4.00E+6	44.7	0	72	100										
4.00E+6	4.50E+6	24.5	0	65	73	100									
4.50E+6	5.00E+6	21.9	0	73	82	75	100								
5.00E+6	5.50E+6	11.4	0	56	63	58	64	100							
5.50E+6	6.00E+6	9.9	0	64	72	66	73	57	100						
6.00E+6	7.00E+6	7.8	0	61	69	63	70	54	62	100					
7.00E+6	8.00E+6	7.2	0	67	74	68	76	59	67	64	100				
8.00E+6	9.00E+6	6.7	0	72	80	73	82	63	72	69	74	100			
9.00E+6	1.00E+7	5.8	0	69	77	70	78	60	69	66	71	77	100		
1.00E+7	1.20E+7	5.6	0	72	80	73	82	63	72	69	75	8.	77	100	
1.20E+7	1.50E+7	5.0	0	0	0	0	0	0	0	0	0	0	0	0	100
1.50E+7	2.00E+7	5.0	0	0	0	0	0	0	0	0	0	0	0	0	100

MAT = 6313 MT = 107 LB = 1 NI Segment 1

1.00E-5	3.25E+6	0.0	100												
3.25E+6	3.50E+6	30.0	0	100											
3.50E+6	4.00E+6	20.0	0	0	100										
4.00E+6	4.50E+6	14.1	0	0	0	100									
4.50E+6	5.00E+6	8.9	0	0	0	0	100								
5.00E+6	5.50E+6	8.1	0	0	0	0	0	100							
5.50E+6	6.00E+6	5.9	0	0	0	0	0	0	100						
6.00E+6	7.00E+6	5.0	0	0	0	0	0	0	0	100					
7.00E+6	8.00E+6	4.0	0	0	0	0	0	0	0	0	10				
8.00E+6	9.00E+6	3.0	0	0	0	0	0	0	0	0	0	100			
9.00E+6	1.00E+7	3.0	0	0	0	0	0	0	0	0	0	0	100		
1.00E+7	1.20E+7	2.4	0	0	0	0	0	0	0	0	0	0	0	100	
1.20E+7	1.50E+7	3.0	0	0	0	0	0	0	0	0	0	0	0	0	100
1.50E+7	2.00E+7	3.5	0	0	0	0	0	0	0	0	0	0	0	0	100

MAT = 6313 MT = 107 LB = 2 NI Segment 2

1.00E-5	3.25E+6	0.0	100												
3.25E+6	4.00E+6	40.0	0	100											
4.00E+6	5.00E+6	20.0	0	100	100										
5.00E+6	6.00E+6	8.0	0	100	100	100									
6.00E+6	9.00E+6	6.0	0	100	100	100	100								
9.00E+6	1.20E+7	5.0	0	100	100	100	100	100							
1.20E+7	2.00E+7	0.0	0	0	0	0	0	0	100						

MAT = 6313 MT = 107 LB = 1 NI Segment 3

1.00E-5	1.20E+7	0.0	100		
1.20E+7	1.50E+7	4.0	0	100	
1.50E+7	2.00E+7	3.6	0	0	100

Table 2

Fictive Simultaneaus Evaluation

of $^{27}Al(n,\alpha)$ and $^{65}Cu(n,2n)$ Cross Sections

A: Previous Evaluation

Reaction	E_n (MeV)	$\sigma(E)$ (mb)	Rel. Std.Dev. (%)	Correlation Matrix
$^{27}Al(n,\alpha)$	13.6	123.3	4.2	100
	14.0	120.6	5.0	83 100
	14.6	114.0	4.8	90 73 100
$^{65}Cu(n,2n)$	13.6	832.0	5.5	0 0 0 100
	14.0	891.9	6.3	0 0 0 72 100
	14.6	959.6	5.8	0 0 0 85 88 100

B: New Data Set of Ratios

Reaction-Ratio	E_n (MeV)	$\sigma(E)$-Ratio	Rel. Std.Dev. (%)	Correlation Matrix
$^{65}Cu(n,2n)/^{27}Al(n,\alpha)$	13.6	6.753	1.9	100
	14.0	7.426	1.9	41 100
	14.6	8.447	1.7	47 47 100

C: Subsequent Evaluation

Reaction	E_n (MeV)	$\sigma(E)$ (mb)	Rel. Std.Dev. (%)	Correlation Matrix
$^{27}Al(n,\alpha)$	13.6	123.2	3.4	100
	14.0	120.5	3.9	82 100
	14.6	113.9	3.7	89 79 100
$^{65}Cu(n,2n)$	13.6	832.3	3.5	87 72 80 100
	14.0	894.4	4.0	76 90 75 76 100
	14.6	961.6	3.8	83 76 90 82 82 100

Table 3

Cross Section Data Base of $^{48}Ti(n,p)$

Neutron Energy (MeV)		Reference	ENDF/B-V Eval.[a]	Measurement (No. of data)									
				Absolute[b]	Relative to								
from	to				^{27}Al (n,p)	^{27}Al (n,α)	^{47}Ti (n,p)	^{48}Ti[c] (n,p)	^{54}Fe (n,p)	^{56}Fe (n,p)	^{58}Ni (n,p)	^{63}Cu (n,2n)	^{65}Cu (n,2n)	^{238}U (n,f)
THR	4.7		Theory											
4.7	10.0	Smith75	+											(19)
6.1	-	Ghorai71	-		(1)									
6.2	7.0	Lukic71	+			(2)				(1)	(2)			
10.0	12.5		Theory											
12.5	19.6	Bormann65	+	(9)PR										
12.7	17.0	Gabbard62	+	(17)AP										
13.6	14.7	Mannhart75	+			(12)								
13.6	14.6	Vonach68	-			(1)		(11)						
13.9	19.5	Pai66	+			(5)								
14.0	-	Allan61	-						(1)					
14.0?	-	Levkovskij57	N				(1)							
14.5	-	Hillman62	+			(1)								
14.5	-	Cross63	+			(1)								
14.5	-	Paul53	N	(1)AP										
14.7	-	Crumpton69	-	(1)AP										
14.8	-	Prasad71	N							(1)				
14.8	-	Levkovskij70	+										(1)	
14.8		Poularikas59	+									(1)		
Total				(28)	(61)									

a): + Accepted
- Rejected
N Not used

b): PR Proton Recoil
AP Assoc . Part.

c): Rel.excit.fct.

Table 4

TRANSFORMATION OF REL. COVARIANCE MATRICES FROM GROUP STRUCTURE i TO GROUP STRUCTURE m.

GROUP CONSTANTS OF THE INITIAL STRUCTURE i :

$$\sigma_i = \int_{E_i}^{E_{i+1}} \sigma(E)\ \varphi(E)\, dE / \varphi_i$$

$$\varphi_i = \int_{E_i}^{E_{i+1}} \varphi(E)\, dE$$

CONSERVATION LAW :

$\int \sigma(E)\ \varphi(E)\, dE$ must be independent on the structure

TRANSFORMATION RULE :

$$C_m = T^+ C_i\ T \qquad T = (T_{im})$$

C_i Rel. Cov. Matrix of σ_i

T Transformation Matrix

EXAMPLES :

A) COMPRESSION (energy limits conserved)

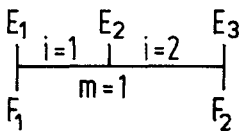

$$T_{11} = \frac{\sigma_1\ \varphi_1}{\sigma_1\ \varphi_1 + \sigma_2\ \varphi_2} \qquad T_{21} = \frac{\sigma_2\ \varphi_2}{\sigma_1\ \varphi_1 + \sigma_2\ \varphi_2}$$

B) EXPANSION (energy limits conserved)

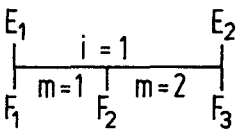

$$T_{11} = T_{12} = 1$$

C) ENERGY LIMITS NOT CONSERVED

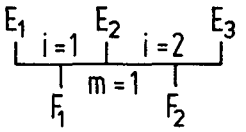

$$T_{11} = \frac{\sigma_1\ \varphi_1'}{\sigma_1\ \varphi_1' + \sigma_2\ \varphi_2'} \qquad T_{21} = \frac{\sigma_2\ \varphi_2'}{\sigma_1\ \varphi_1' + \sigma_2\ \varphi_2'}$$

with $\varphi_1' = \int_{F_1}^{E_2} \varphi(E)\, dE$ and $\varphi_2' = \int_{E_2}^{F_2} \varphi(E)\, dE$

Table 5

Transformation of the Covariance Matrix of ^{58}Ni(n,p) from ENDF/B-V Group Structure to Another Group Structure

Case A: Weighted with $\phi(E) = 1/E$

Energy Range (eV)		Rel. Std.Dev.(%)	Correlation Matrix														
1.0 E-5	4.0 E-1	0.0	100														
4.0 E-1	1.0 E+1	0.0	0	100													
1.0 E+1	1.0 E+4	0.0	0	0	100												
1.0 E+4	1.0 E+5	0.0	0	0	0	100											
1.0 E+5	6.0 E+5	18.0	0	0	0	0	100										
6.0 E+5	1.4 E+6	14.0	0	0	0	0	42	100									
1.4 E+6	2.2 E+6	8.7	0	0	0	0	14	35	100								
2.2 E+6	3.0 E+6	10.3	0	0	0	0	0	0	94	100							
3.0 E+6	4.0 E+6	10.3	0	0	0	0	0	0	94	100	100						
4.0 E+6	5.0 E+6	7.1	0	0	0	0	0	0	32	34	34	100					
5.0 E+6	6.0 E+6	7.1	0	0	0	0	0	0	32	34	34	100	100				
6.0 E+6	8.0 E+6	7.1	0	0	0	0	0	0	32	34	34	50	50	100			
8.0 E+6	1.1 E+7	6.8	0	0	0	0	0	0	34	36	36	52	52	52	100		
1.1 E+7	1.3 E+7	10.1	0	0	0	0	0	0	23	24	24	35	35	35	59	100	
1.3 E+7	2.0 E+7	14.1	0	0	0	0	0	0	0	0	0	0	0	0	0	36	100

Case B: Weighted with $\phi(E) = \text{const}$

1.0 E-5	4.0 E-1	0.0	100														
4.0 E-1	1.0 E+1	0.0	0	100													
1.0 E+1	1.0 E+4	0.0	0	0	100												
1.0 E+4	1.0 E+5	0.0	0	0	0	100											
1.0 E+5	6.0 E+5	17.8	0	0	0	0	100										
6.0 E+5	1.4 E+6	14.0	0	0	0	0	41	100									
1.4 E+6	2.2 E+6	8.8	0	0	0	0	12	30	100								
2.2 E+6	3.0 E+6	10.3	0	0	0	0	0	0	96	100							
3.0 E+6	4.0 E+6	10.3	0	0	0	0	0	0	96	100	100						
4.0 E+6	5.0 E+6	7.1	0	0	0	0	0	0	33	34	34	100					
5.0 E+6	6.0 E+6	7.1	0	0	0	0	0	0	33	34	34	100	100				
6.0 E+6	8.0 E+6	7.1	0	0	0	0	0	0	33	34	34	50	50	100			
8.0 E+6	1.1 E+7	6.8	0	0	0	0	0	0	34	35	35	52	52	52	100		
1.1 E+7	1.3 E+7	10.2	0	0	0	0	0	0	23	24	24	35	35	35	60	100	
1.3 E+7	2.0 E+7	14.0	0	0	0	0	0	0	0	0	0	0	0	0	0	34	100

Case C: Weighted with $\phi(E) = 1/E$; all σ_i are equal

1.0 E-5	4.0 E-1	0.0	100														
4.0 E-1	1.0 E+1	0.0	0	100													
1.0 E+1	1.0 E+4	0.0	0	0	100												
1.0 E+4	1.0 E+5	0.0	0	0	0	100											
1.0 E+5	6.0 E+5	1.8	0	0	0	0	100										
6.0 E+5	1.4 E+6	14.1	0	0	0	0	93	100									
1.4 E+6	2.2 E+6	11.4	0	0	0	0	39	69	100								
2.2 E+6	3.0 E+6	10.3	0	0	0	0	0	0	19	100							
3.0 E+6	4.0 E+6	10.3	0	0	0	0	0	0	19	100	100						
4.0 E+6	5.0 E+6	7.1	0	0	0	0	0	0	7	34	34	100					
5.0 E+6	6.0 E+6	7.1	0	0	0	0	0	0	7	34	34	100	100				
6.0 E+6	8.0 E+6	7.1	0	0	0	0	0	0	7	34	34	50	50	100			
8.0 E+6	1.1 E+7	6.8	0	0	0	0	0	0	7	36	36	52	52	52	100		
1.1 E+7	1.3 E+7	10.2	0	0	0	0	0	0	5	24	24	35	35	35	59	100	
1.3 E+7	2.0 E+7	14.1	0	0	0	0	0	0	0	0	0	0	0	0	0	25	100

TASHI RESULTS FOR DOSIMETRY MULTIGROUP CROSS SECTIONS AND THEIR UNCERTAINTIES

M. Petilli
Comitato Nazionale per l'Energia Nucleare,
Centro Studi Nucleari della Casaccia,
Rome,
Italy

Abstract

The code TASHI has been developped in order to evaluate multigroup cross sections and their variance-covariance matrix for isotopes used as detectors in reactor dosimetry.

The code can elaborate directly data in the format as contained in ENDF dosimetry file, starting by File 3 and File 33.

The average cross section value for each group is calculated by assuming a 1/E spectrum and weighting on it the point energy cross sections.

The configurations with 16 and 100 groups have been considered and the group cross sections, the associated errors of evaluation and the correlation matrix obtained by TASHI are predented for different isotopes.

This work is part of the development of a chain of programs able to handle variance-covariance matrices, which have been written for the analysis of dosimetry experiments.

In particular the TASHI calculates multigroup cross sections starting by data files containing information about uncertainties.

The results presented are obtained from file 3 and file 33 of ENDF/B-5 dosimetry file.

The equations solved by TASHI are, for the average cross section value:

$$\bar{\sigma}_i = \frac{\int_{E_i}^{E_{i+1}} \sigma(E) \cdot \phi(E) dE}{\int_{E_i}^{E_{i+1}} \phi(E) dE} \qquad (1)$$

The E_i and E_{i+1} are respectively lower and upper limits of energy group "i" in the given group structure.

The variance-covariance matrix $N_{\bar{\sigma}} = < \delta\bar{\sigma}_i, \delta\bar{\sigma}_R >$ of the vector of average group cross sections is given by:

$$N_{\bar{\sigma}} = N_{\sigma} \cdot S \cdot N_{\sigma}^{T} \qquad (2)$$

The $N_{\sigma} = < \delta\sigma_j, \delta\sigma_e >$ is the covariance matrix in the input data file, and $S \equiv \{ \delta\bar{\sigma}_i / \delta\sigma_j \}$ is the sensitivity matrix of average group cross sections with respect to the energy point cross sections. The TASHI calculates analitically the integral of Eq. 1.

The solution expression is depending on the particular interpolation law given by the data file and on the particular weighting function $\phi(E)$.

In the first version of TASHI the flux $\phi(E)$ has been taken constant in each group.

The results obtained ENDF/B /1/ dosimetry files have been compared, for 100 energy groups, with calculations performed by D.E. CULLEN /2/ and a satisfactory agreement has been found. Instead some difference has been observed, for 15 energy groups, with respect to results obtained by W.L. ZIJP and al. using their code COVSIG /3/.

The difference was attributed to the different weighting function $\phi(E)$, because the COVSIG used a spectrum 1/E. Therefore a second version of TASHI has been done with group cross section averaged on 1/E spectrum. This is actually considered the definitive version.

The last results obtained, compared with those from the COVSIG /3/, shown differencies still remain for some reactions, both in the errors and in the correlation coefficient values. This seems to give value to the hypotesis there is some difference in the data available in the two laboratories.

REFERENCES

/1/ F.G. PEREY - "The data covariance files for ENDF/B-V" - ORNL-TM-5938 (ENDF-249)

/2/ D.E. CULLEN - private communication - Oct. 1980

/3/ N.J.C.M. VAN DER BORG, H.J. NOLTHENIUS, W.L. ZIJP - "Covaraiances of the data of ENDF/B-V dosimetry file" - Restricted distribution. ECN-80-091.

TASHI RESULTS : $\varphi = 1/E$ (15 groups)

Limits of energy groups (MeV)

1.0E-10 4.0E-7 1.0E-5 0.01 0.1 0.6 1.4 2.2 3. 4. 5. 6. 8. 11. 13. 20.

1) Na23 (n,γ) 6311-102

Group	σ (%)	Correlation matrix (%)														
1	2.0	100														
2	2.0	100	100													
3	2.6	39	39	100												
4	0.0	0	0	0	100											
5	20.0	0	0	0	0	100										
6	20.0	0	0	0	0	100	100									
7	20.0	0	0	0	0	100	100	100								
8	20.0	0	0	0	0	100	100	100	100							
9	20.0	0	0	0	0	100	100	100	100	100						
10	16.4	0	0	0	0	93	93	93	93	93	100					
11	25.0	0	0	0	0	0	0	0	0	0	36	100				
12	25.0	0	0	0	0	0	0	0	0	0	36	100	100			
13	25.0	0	0	0	0	0	0	0	0	0	36	100	100	100		
14	25.0	0	0	0	0	0	0	0	0	0	36	100	100	100	100	
15	25.0	0	0	0	0	0	0	0	0	0	36	100	100	100	100	100

2) Al27 (n,α) 6313-107

9	38.3	100						
10	36.1	75	100					
11	23.4	0	17	100				
12	24.7	0	0	22	100			
13	18.1	0	0	7	32	100		
14	8.9	0	0	0	0	88	100	
15	3.6	0	0	0	0	0	20	100

3) In115 (n,γ) 5437-102

1	6.0	100													
2	6.0	100	100												
3	5.5	90	90	100											
4	8.7	0	0	1	100										
5	5.0	0	0	0	2	100									
6	4.3	0	0	0	1	57	100								
7	7.0	0	0	0	0	0	82	100							
8	7.0	0	0	0	0	0	82	100	100						
9	5.2	0	0	0	0	0	65	80	80	100					
10	13.0	0	0	0	0	0	0	0	0	61	100				
11	13.0	0	0	0	0	0	0	0	0	61	100	100			
12	13.0	0	0	0	0	0	0	0	0	61	100	100	100		
13	13.0	0	0	0	0	0	0	0	0	61	100	100	100	100	
14	13.0	0	0	0	0	0	0	0	0	61	100	100	100	100	100
15	13.0	0	0	0	0	0	0	0	0	61	100	100	100	100	100	100

4) Th232 (n,f) 6390-18

Group	σ (%)	Correlation matrix (%)										
5	32.2	100										
6	5.7	11	100									
7	6.2	8	48	100								
8	6.9	7	41	98	100							
9	5.4	9	52	48	45	100						
10	7.2	7	39	36	32	52	100					
11	7.0	7	40	37	33	53	100	100				
12	10.8	5	26	24	21	28	21	28	100			
13	10.8	5	26	24	21	28	21	28	100	100		
14	10.8	5	26	24	21	28	21	28	100	100	100	
15	10.8	5	26	24	21	28	21	28	100	100	100	100

5) U238 (n,f) 6398-18

1	25.0	100													
2	25.0	100	100												
3	30.0	0	0	100											
4	30.0	0	0	100	100										
5	9.9	0	0	40	40	100									
6	7.3	0	0	0	0	3	100								
7	1.8	0	0	0	0	0	77	100							
8	1.7	0	0	0	0	0	0	18	100						
9	2.2	0	0	0	0	0	0	0	16	100					
10	1.9	0	0	0	0	0	0	0	0	14	100				
11	2.2	0	0	0	0	0	0	0	0	0	27	100			
12	3.4	0	0	0	0	0	0	0	0	0	0	46	100		
13	2.2	0	0	0	0	0	0	0	0	0	0	0	9	100	
14	2.5	0	0	0	0	0	0	0	0	0	0	0	0	27	100
15	5.7	0	0	0	0	0	0	0	0	0	0	0	0	0	6	100

6) Ni58 (n,p) 6433-103

1	18.0	100													
2	18.0	100	100												
3	18.0	100	100	100											
4	18.0	100	100	100	100										
5	13.8	45	45	45	45	100									
6	14.1	39	39	39	39	39	100								
7	8.7	13	13	13	13	33	33	100							
8	10.3	0	0	0	0	0	0	95	100						
9	8.2	0	0	0	0	0	0	92	97	100					
10	7.1	0	0	0	0	0	0	32	34	56	100				
11	6.4	0	0	0	0	0	0	36	38	59	97	100			
12	6.7	0	0	0	0	0	0	34	36	46	53	72	100		
13	7.0	0	0	0	0	0	0	33	35	44	51	56	57	100	
14	10.8	0	0	0	0	0	0	19	20	25	29	33	31	50	100
15	14.0	0	0	0	0	0	0	0	0	0	0	0	0	0	47	100

7) Ni58 (n,2n) 6433-16

14	14.1	100	
15	12.2	60	100

8) Ti46 (n,p) 6427-103

Group	σ (%)	Correlation matrix (%)								
7	12.8	100								
8	12.8	100	100							
9	12.8	100	100	100						
10	12.8	100	100	100	100					
11	12.8	100	100	100	100	100				
12	12.8	100	100	100	100	100	100			
13	11.9	87	87	87	87	87	87	100		
14	14.1	55	55	55	55	55	55	89	100	
15	14.1	55	55	55	55	55	55	89	100	100

9) Ti47 (n,p) 6428-103

1	11.3	100													
2	11.3	100	100												
3	11.3	100	100	100											
4	11.3	100	100	100	100										
5	11.3	100	100	100	100	100									
6	11.3	100	100	100	100	100	100								
7	11.3	100	100	100	100	100	100	100							
8	11.3	100	100	100	100	100	100	100	100						
9	11.3	100	100	100	100	100	100	100	100	100					
10	11.3	100	100	100	100	100	100	100	100	100	100				
11	11.3	100	100	100	100	100	100	100	100	100	100	100			
12	11.3	100	100	100	100	100	100	100	100	100	100	100	100		
13	10.2	84	84	84	84	84	84	84	84	84	84	84	84	100	
14	12.8	44	44	44	44	44	44	44	44	44	44	44	44	86	100	
15	12.8	44	44	44	44	44	44	44	44	44	44	44	44	86	100	100

10) Ti48 (n,p) 6429-103

9	11.3	100						
10	11.3	100	100					
11	11.3	100	100	100				
12	11.3	100	100	100	100			
13	10.6	74	74	74	74	100		
14	12.8	44	44	44	44	93	100	
15	12.8	44	44	44	44	93	100	100

11) Al27 (n,p) 6313-103

7	56.5	100								
8	33.0	0	100							
9	29.4	0	13	100						
10	22.5	0	0	43	100					
11	12.5	0	0	0	76	100				
12	8.3	0	0	0	0	29	100			
13	13.3	0	0	0	0	0	9	100		
14	12.5	0	0	0	0	0	7	80	100	
15	7.9	0	0	0	0	0	0	0	7	100

RESULTS OF NEUTRON FLUENCE MONITORS AT THE PSF SIMULATED PRESSURE VESSEL IRRADIATION FACILITY

W. MANNHART
Physikalisch-Technische Bundesanstalt,
Braunschweig,
Federal Republic of Germany

Abstract

Partial results of an interlaboratory comparison of neutron fluence detectors are presented. The detectors were irradiated in a high-power run in the 4/12 configuation of the ORNL simulated pressure vessel facility at the positions SSC, 1/4 T, 1/2 T and 3/4 T. Fairly consistent results have been obtained.

1. Introduction

In recent years, within the framework of LWR Pressure Vessel Surveillance Programmes, much effort has been concentrated on establishing more accurate interrelationships between dosimetry, metallurgy and fracture mechanics with the objective of defining precise life-time conditions of pressure vessel steels which are relevant to safety as well as being of economic importance /1,2/. The present work is part of an interlaboratory comparison of fluence neutron dosimeters aimed at defining the present state-of-the-art of neutron fluence dosimetry. The results presented here are confined to those which came from the analysis of fluence monitors performed at the PTB. A joint paper summarizing the overall result of this interlaboratory comparison will be published in the future /3/.

2. Experimental Conditions

Irradiations were performed at the ORR-PSF facility of the Oak Ridge National Laboratory. They were carried out at a reactor power of 30 MW over a period of 18 days in an engineering mock-up 4/12 configuration. This configuration consisted of a thermal shield, located 4 cm behind the core window, and the pressure vessel simulator located 12 cm behind the thermal shield. The irradiation positions were a simulated surveillance capsule (SSC) attached to the back of the thermal shield and the positions 1/4 T, 1/2 T and 3/4 T inside the pressure vessel simulator. (T is the total thickness of the simulator and the preceding fraction indicates the distance from the front of the simulator relative to the total thickness). In each of these four irradiation positions, the following neutron monitor reactions were used: $^{46}Ti(n,p)$, $^{54}Fe(n,p)$, $^{58}Fe(n,\gamma)$, $^{58}Ni(n,p)$, $^{59}Co(n,\gamma)$, $^{63}Cu(n,\alpha)$ and $^{109}Ag(n,\gamma)$. The program also comprised other reactions such as $^{237}Np(n,f)$, $^{238}U(n,f)$ and others which are not dealt with here. After irradiation, the neutron dosimeters were distributed to six different laboratories for further analysis.

3. Results

3.1 Spectral Indices

The experimentally determined spectral indices of each of the four irradiation positions are shown in Table 1. The first two columns of Table 1 give the indices for "slow" fluence detectors (fluence below 1 MeV neutron energy) while the remaining columns show "fast" fluence detectors (fluence above 1 MeV). The experimental results are compared with the calculated ones. The calculations are based on neutron spectra obtained from transport calculations in a 171-group structure and are shown in Fig. 1. The transport calculations were done at ORNL in a way similar to that described in ref. /4/. The cross sections used in averaging over these neutron spectra were ENDF/B-V data transformed to the 171-group structure already mentioned and were obtained from SCK/CEN, Mol (Belgium) /5/. In addition to this, the ENDF/B-V data of the non-threshold reactions $^{58}Fe(n,\gamma)$ and $^{59}Co(n,\gamma)$ were generated with the RESEND code and collapsed to the group structure mentioned. The ENDF/B-V data of the reaction $^{109}Ag(n,\gamma)$ are subject to the recent restrictions in the data distribution and were therefore not available. Due to the lack of information, no self-shielding corrections were applied in the calculations of the spectral indices of the non-threshold detectors. The divergence between measured and calculated spectral indices for these reactions is therefore not suprising. Starting at the external surface of the pressure vessel simulator, the experimental spectral indices clearly increase with increasing depth into the vessel and become approximately constant at depths more than half the vessel thickness. For the fast fluence monitors, the spectral indices show a fair consistency (within 3 %) between measured and calculated values. The spectral index of $^{63}Cu(n,\alpha)$ is an exception, where the calculated index systematically exceeds the measured value by about 12 % for the ex-vessel and all in-vessel positions. This fact indicates inconsistencies of the ENDF/B-V data of $^{63}Cu(n,\alpha)$. It is confirmed by a recent experiment of the response of this detector in a ^{252}Cf neutron field /6/. The comparison of the experimental result with that calculated from ENDF/B-V data shows that the calculation is between 7 % and 14 % higher than the experiment (depending on the spectral representation). New data of the energy-dependent cross section of $^{63}Cu(n,\alpha)$ /7/ show a 12 % lower response in fission fields compared with ENDF/B-V. In summary: there are clear indications that spectrum-averaged cross sections of $^{63}Cu(n,\alpha)$ based on ENDF/B-V data are overestimated.

3.2 Absolute Fluences

Fluences were derived based on the measured radioactivities of the fluence monitors and on the known irradiation history and with the aim of spectrum-averaged cross sections calculated according the principles stated in the previous section. They are shown in Fig. 2. To avoid misunderstanding it must be stressed that the given fluences are absolute ones and not, as often used, fission-equivalent fluences. The slow fluences of the monitors $^{59}Co(n,\gamma)$ and

$^{58}Fe(n,\gamma)$ reflect the above-mentioned problem of the lack of self-shielding corrections. It can also be seen from Fig. 2 that with increasing depth inside the pressure vessel, the slow fluence approximates the fast fluence. The ENDF/B-V data of $^{58}Fe(n,\gamma)$ have recently been modified /8/. This is not yet taken into account in Fig. 2.

Values of about $6x10^{19}$ cm^{-2} have been obtained for the fast fluence at the position of the surveillance capsule outside the vessel. For each irradiation position the fast fluence values based on the $^{63}Cu(n,\alpha)$ monitor are lower compared with the results of the other monitors. This is due to the above-mentioned overestimation of the ENDF/B-V cross section. The really surprising result of the experiment is that the fluence values of all fast fluence detectors, $^{58}Ni(n,p)$, $^{54}Fe(n,p)$, $^{46}Ti(n,p)$ and $^{63}Cu(n,\alpha)$, agree within 4 % to 7 % for each irradiation position and even within 2 % to 3 % if the $^{63}Cu(n,\alpha)$ detector is not included. The dominant components of the uncertainty of the fluence values are the cross section data and the neutron spectrum. In the first case the relative uncertainties are larger than 5 % and for the second case more than 10 % have to be expected. A more detailed uncertainty analysis will be given in a forthcoming paper at this meeting /9/.

3.3 Fluence Inside the Pressure Vessel Simulator

Fig. 1 shows that the spectral neutron flux density at the first in-vessel position, 1/4 T, is lower than that at the surveillance capsule by about a factor of 12. It decreases further, by about a factor of 2 per quarter vessel thickness, with increasing depth into the vessel. To investigate the slope of the fluence inside of the pressure vessel simulator in detail, the experimentally determined fluences at irradiation positions in the vessel were normalized relative to the fluence at the SSC position. As the irradiation history of each position was not exactly the same due to different insertion and removal times, all data were referred to the same irradiation duration. The result is shown in Fig. 3 where the slope of the fluence is given separately for each fluence detector. The fast fluence detectors, $^{46}Ti(n,p)$, $^{54}Fe(n,p)$ and $^{63}Cu(n,\alpha)$ yield almost identical values and show almost exactly the same slope. The data of the $^{58}Ni(n,p)$ detector are not given in Fig. 2 as no 1/2 T value was available in the present experiment. The remaining 1/4 T and 3/4 T values fit the given picture quite well. Fig. 2 also clearly shows that the slope of the fluence decreases with the increasing depth of the vessel wall. The slow fluence detectors, $^{58}Fe(n,\gamma)$ and $^{59}Co(n,\gamma)$, yield values which show a parallel behaviour to the fluence slope of the fast detectors. Their absolute values are lower, however, as the neglecting of self-shielding effects overestimates the fluence at the surveillance position.

4. Conclusions

The unique features of the Oak Ridge Pressure Vessel Facility allow more accurate interrelationships between neutron fluences at surveillance positions and inside of the vessel to be established. The present experiment shows that fairly

reproducible fluence values can be obtained with various neutron fluence monitors. It has been found that the ENDF/B-V neutron cross section data of the reactions $^{46}Ti(n,p)$, $^{54}Fe(n,p)$ and $^{58}Ni(n,p)$ are consistent to a high degree. However, as also confirmed by other sources, the ENDF/B-V data of $^{63}Cu(n,\alpha)$ tend to overestimate detector responses in neutron fields. The present status of fast neutron fluence dosimetry seems to be well established. It remains to be investigated whether this also applies to slow neutron fluence dosimetry.

Acknowledgement

The author is much obliged to H. Tourwe, SCK/CEN Mol, for his readiness in making the data of group cross sections and neutron spectra available.

References

/1/ A. Fabry, F.B. Kam: "Towards an Adequate Evaluation of LWR Pressure Vessel Steel Irradiation Exposures", Proc. IAEA Technical Committee Meeting, September 24-27, 1979, Jülich FRG, Jül-Conf-37, p. 210, May 1980

/2/ F.W. Stallmann: "PCA-PSF Pressure Vessel Surveillance Program: Accuracy Requirements and Uncertainty Analysis", Jül-Conf-37, p. 131, May 1980

/3/ H. Tourwe, A. Fabry, F. Kam, A. Fudge, W.L. Zijp, H.J. Nolthenius, W. Zimmer, L.S. Kellog, E.P. Lippincott, W. Mannhart: "Interlaboratory comparison of fluence neutron dosimeters in the frame of the PSF start-up measurement programme" (to be presented at 4th ASTM-EURATOM Symposium on Reactor Dosimetry, Washington, March 1982)

/4/ R.E. Maerker, J.J. Wagschal: "Uncertainties and Biases Arising from Methods Approximations", Jül-Conf-37, p. 192, May 1980

/5/ H. Tourwe: Priv. comm. (1980)

/6/ G. Winkler, V. Spiegel, C.M Eisenhauer, D.L. Smith: "Measurement of the Average Activation Cross Section for the Reaction $^{63}Cu(n,\alpha)^{60}Co$ in the Spontaneous Fission Neutron Field of ^{252}Cf", Nucl. Sci. Eng. 78, 415 (1981)

/7/ G. Winkler, D.L. Smith, J.W. Meadows: "Measurement of Cross Sections for the $^{63}Cu(n,\alpha)^{60}Co$ Reaction from Threshold to 10 MeV", Nucl.Sci. Eng. 76, 30 (1980)

/8/ B.A. Magurno: Priv. Comm. (August 1981)

/9/ W. Mannhart: "Sensitivity Coefficients of Neutron Fluence Detectors in the PCA/PSF Neutron Field (this meeting)

Table 1

Spectral Indices
(PCA/PSF 4/12 Configuration)

Position		$^{109}Ag(n,\gamma)/^{58}Fe(n,\gamma)$	$^{59}Co(n,\gamma)/^{58}Fe(n,\gamma)$	$^{58}Ni(n,p)/^{46}Ti(n,p)$	$^{54}Fe(n,p)/^{46}Ti(n,p)$	$^{63}Cu(n,\alpha)/^{46}Ti(n,p)$
SSC	EXP.	27.0	41.9	10.3	7.40	0.0500
	CALC.	-	56.0	10.4	7.70	0.0548
	C/E	-	(1.34)	(1.01)	(1.04)	(1.09)
1/4T	EXP.	40.7	49.4	9.50	6.59	0.0566
	CALC.	-	64.4	9.46	6.98	0.0622
	C/E	-	(1.30)	(1.00)	(1.06)	(1.10)
1/2T	EXP.	52.4	55.5	-	6.84	0.0581
	CALC.	-	64.6	9.77	7.08	0.0649
	C/E	-	(1.16)	-	(1.03)	(1.12)
3/4T	EXP.	49.5	56.0	10.3	6.90	0.0596
	CALC.	-	61.0	10.0	7.11	0.0680
	C/E	-	(1.09)	(0.97)	(1.03)	(1.14)

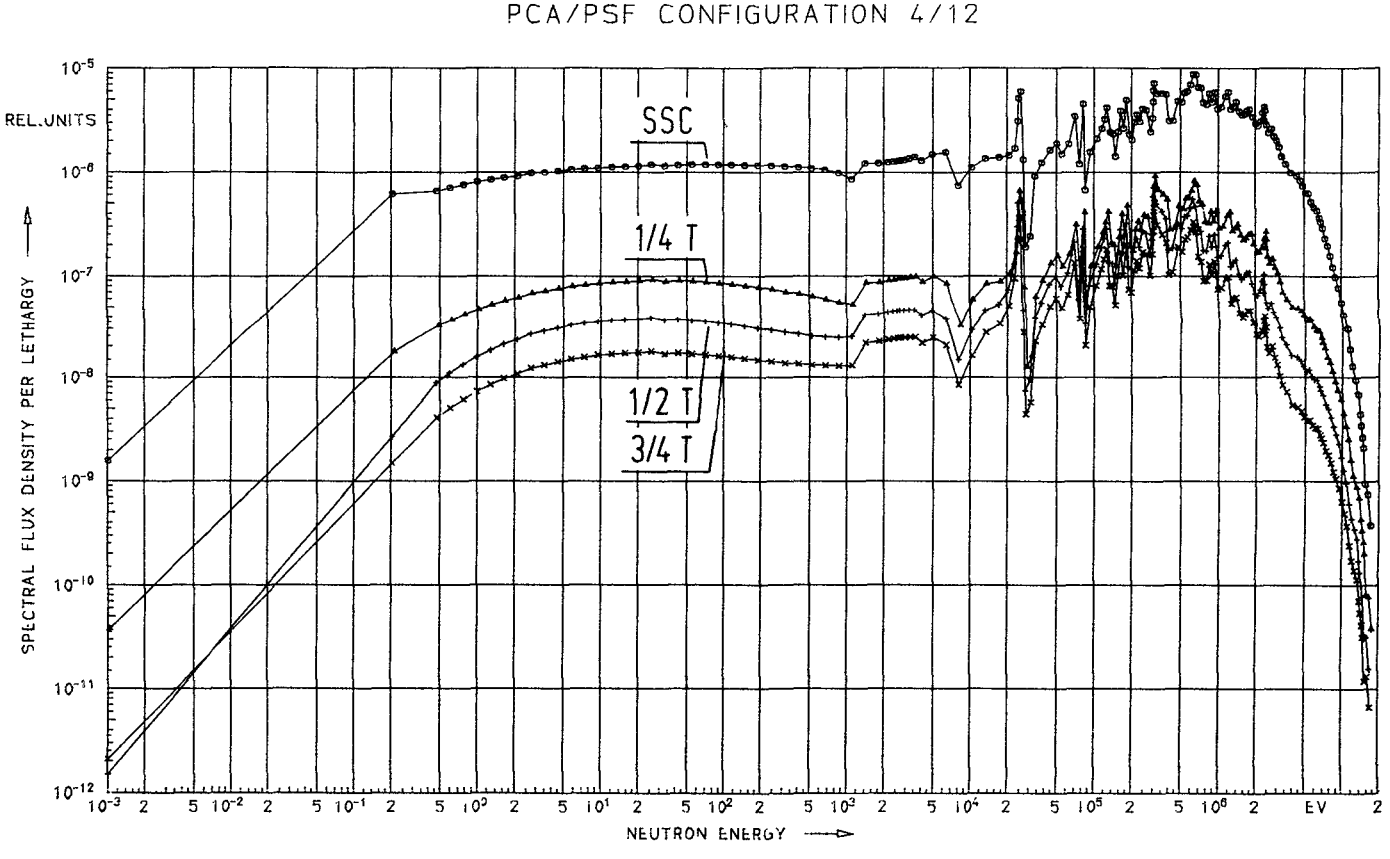

Figure 1: Neutron Spectrum of Various Irradiation Positions at PSF

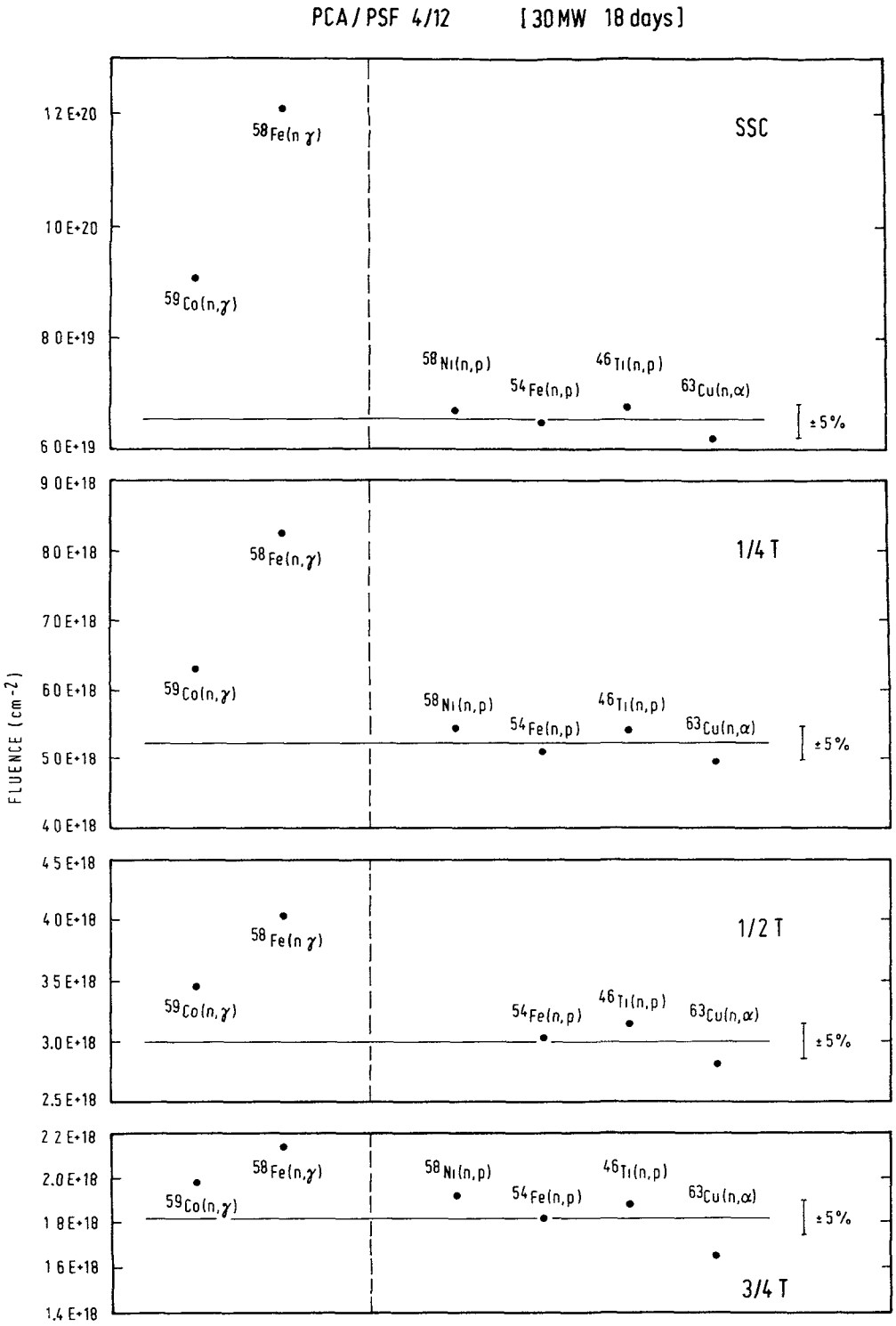

Figure 2: Fluences at PSF 4/12

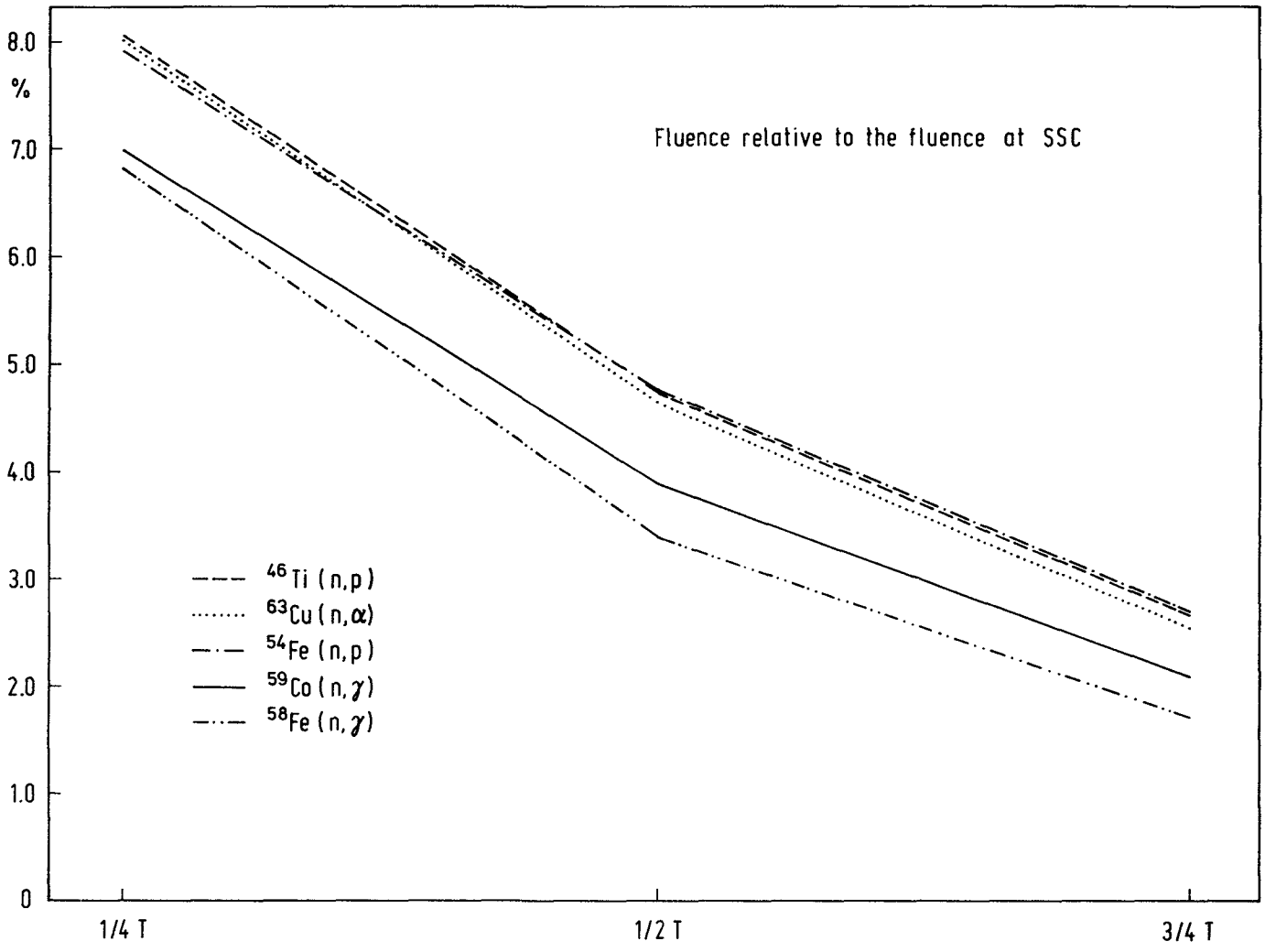

Figure 3: Slope of the Fluence Inside of the Pressure Vessel Simulator

SENSITIVITY COEFFICIENTS OF NEUTRON FLUENCE DETECTORS IN THE PCA/PSF NEUTRON FIELD

W. MANNHART
Physikalisch-Technische Bundesanstalt,
Braunschweig,
Federal Republic of Germany

Abstract

Sensitivity coefficients have been generated with the aim of propagating the covariances of neutron cross section data and neutron spectra to spectrum-averaged cross sections determined in the 4/12 configuration of the simulated pressure vessel neutron field at ORNL in the context of neutron fluence monitoring. The principles of generation are shown and results of application to the covariance file of the ENDF/B-V Dosimetry File are given.

1. Introduction

A variety of nuclear parameters in reactor dosimetry depend on neutron cross section data. In the past, due to lack of information, the influence of the uncertainties of cross section data on derived nuclear parameters has only been roughly estimated or even entirely neglected. This situation was far from satisfactory. In addition, apart from existing inherent limitations in further improving neutron cross section data, it is most meaningful to first investigate to what extent cross section uncertainties influence the quality of relevant "integral" nuclear parameters before starting extensive programs with the aim of improving the quality of nuclear cross section data. The recently released cross section covariance files of ENDF/B-V have to be seen in this context. These data represent the best up-to-date knowledge of the accuracies and their correlations of cross section data. Cross section covariances are quantities which are independent of a specific problem, they represent only the uncertainties of the data themselves. The propagation and application of these uncertainties to a specific problem can be done with sensitivity parameters which establish interrelationships between the data uncertainties and those of derived parameters.

2. Principles

The determination of neutron fluences or flux densities is based on the measured reaction rate per atom of a specific detector in a neutron field and the knowledge of the spectrum-averaged cross section, $\langle\sigma\rangle$, of this detector. The spectrum-averaged cross section given in a group representation is:

$$\langle\sigma\rangle = \sum_i \sigma_i \phi_i \Big/ \sum_i \phi_i \qquad (1)$$

The group cross section is defined as

$$\sigma_i = \int_{E_i}^{E_{i+1}} \sigma(E)\ \phi(E)dE \ /\ \phi_i \qquad (2)$$

with $\phi(E)$ being the spectral neutron flux density, and the group flux density is given by

$$\phi_i = \int_{E_i}^{E_{i+1}} \phi(E)dE \qquad (3)$$

with E_i being the energy delimiters of the groups. The spectrum-averaged cross section depends on the σ_i as well as on the ϕ_i. The influence of a specific σ_i or ϕ_i value on $\langle\sigma\rangle$ is given by the derivatives

$$S_\sigma^i = \frac{\partial \langle\sigma\rangle}{\partial \sigma_i} \quad \text{and} \quad S_\phi^i = \frac{\partial \langle\sigma\rangle}{\partial \phi_i} \qquad (4)$$

The quantities S_σ^i and S_ϕ^i are called sensitivities of $\langle\sigma\rangle$ to the group cross section σ_i or to the group flux ϕ_i, respectively. They represent weighting factors in the uncertainty propagation rule. In propagating relative uncertainties, as most data of the ENDF/B-V covariance file are, it is an advantage to define relative sensitivities (or sensitivity coefficients):

$$P_\sigma^i = \frac{\partial\langle\sigma\rangle/\langle\sigma\rangle}{\partial\ \sigma_i/\sigma_i} \quad \text{and} \quad P_\phi^i = \frac{\partial\langle\sigma\rangle/\langle\sigma\rangle}{\partial\ \phi_i/\phi_i} \qquad (5)$$

With the definition of Eq. (5) the uncertainty propagation is given by

$$\text{Rel.Var}(\langle\sigma\rangle) = P_\sigma^+\ C_\sigma\ P_\sigma \ + \ P_\phi^+\ C_\phi\ P_\phi\ . \qquad (6)$$

C represents the relative covariance matrix of the energy-dependent neutron cross section or of the spectral neutron flux density. P is a column vector with components in the form of Eq. (5) and the superscript($^+$) indicates a transpose. Eq. (6) is valid as long as there are no correlations between cross section data and the neutron spectrum.
A few comments on the sensitivity coefficients of Eq. (5) seem worth making. It can easily be proved that the P_σ^i must be positive and the condition of

$$\sum_i P_\sigma^i = 1 \qquad (7)$$

is valid. In the case of the P_ϕ^i it must be made clear whether or not the neutron spectrum is normalized. In the case of an unnormalized spectrum, as here, one finds

$$\sum_i P_\phi^i = 0, \qquad (8)$$

which indicates that the sensitivity coefficient of the ϕ_i changes its sign within the total energy range. In the case of a normalized spectrum, the P_σ^i

and P_{ϕ}^{i} are equal in the same group structure and are both positive. We then have

$$P_{\phi}^{i} = P_{\sigma}^{i} \quad \text{(only for a normalized spectrum)} \tag{9}$$

There is, however, an essential difference between the covariance matrix of the neutron spectrum in the unnormalized and the normalized case. For the absolute covariance matrix the normalization condition, $\Sigma_i \phi_i = 1$, gives the side condition that the sum of each row and of each column of this matrix must be zero, i.e., the covariance matrix of a normalized neutron spectrum must contain negative off-diagonal elements.

3. Sensitivity Coefficients of PSF Fluence Detectors

For the neutron fluence detectors used in the 4/12 configuration at the ORNL Simulated Pressure Vessel Facility /1/ sensitivity coefficients were calculated in analogy to Eq. (5). The neutron spectrum used was that of the SSC position shown in Fig. 1 of ref. /1/. The neutron cross sections were group data based on the ENDF/B-V Dosimetry File. In Fig. 1 the relative sensitivity of $\langle\sigma\rangle$ with respect to the cross section data is shown for the reactions $^{238}U(n,f)$ and $^{63}Cu(n,\alpha)$. These sensitivity coefficients essentially reflect the shape of the neutron cross sections weighted with the corresponding part of the neutron spectrum. The relative sensitivity of $\langle\sigma\rangle$ with respect to the neutron flux density is shown in Fig. 2 for the example of the reactions $^{58}Ni(n,p)$ and $^{59}Co(n,\gamma)$. The sensitivity coefficients with respect to the neutron spectrum show at least one change of the sign over the total energy range. Both types of sensitivity coefficients allow the neutron cross section as well as the neutron spectrum uncertainties to be propagated to spectrum-averaged cross sections in the PSF neutron field.

4. Uncertainty Contribution to the Fluence

The cross section covariance file of the ENDF/B-V Dosimetry File and the sensitivity coefficients derived here were used, in analogy to Eq. (6), to evaluate the uncertainty component of the fluence due to cross section data. The result is listed in Table 1. The first column of the table lists the fluence detectors used. The second column gives the 90 % energy response ranges. The energies quoted correspond to a response of 5 %, or 95 % of its total value. The next three columns give the dominant uncertainty contributions to the fluences. The uncertainty due to the activity measurement is based on the measurements described in ref. /1/. The fourth column gives the processed covariance data. In the case of the reaction $^{59}Co(n,\gamma)$ the covariance file of ENDF/B-V quotes a relative uncertainty component of 26.5 % between 25.3 meV and 1 MeV. This value is believed to be wrong and has been replaced by a value of 2.7 %. No information on the neutron spectrum uncertainty was available. Regardless therefore, of the P_{ϕ}^{i} values calculated, the second term of Eq. (6) could not be evaluated.

5. Conclusions

The procedure shown here to determine the fluence based on spectrum-averaged cross sections (calculated with absolute neutron cross section data) is an alternative to that of the Pressure Vessel Surveillance Program /2/. In this program the method of benchmark referencing /3/ will be used. This method of interpreting dosimetry measurements in applied neutron fields in terms of similar measurements in well-known benchmark fields eliminates, at least partly, some of the experimental uncertainties such as those associated with energy-dependent neutron cross section data. Nevertheless, a comparison of this procedure with the methods described here seems to be of some advantage in the light of a better understanding of the sources of uncertainty in experimental data.

The present work reflects another principal problem. While cross section covariance files are now available,there are no similar covariance files for neutron spectra. Not until covariance information on neutron cross sections as well as on neutron spectra is available can neutron dosimetry results be consistently interpreted as regards their uncertainties.

References

/1/ W. Mannhart: "Results of Neutron Fluence Monitors at the PSF Simulated Pressure Vessel Irradiation Facility", (this meeting)

/2/ A. Fabry, F.B.K. Kam: "Towards an Adequate Evaluation of LWR Pressure Vessel Steel Irradiation Exposures", Jül-Conf-37, p.210,May 1980

/3/ C.M. Eisenhauer, J.A. Grundl, D.M. Gilliam, E.D. McGarry, V. Spiegel: "Benchmark Referencing of Neutron Dosimetry Measurements", Proc. Third ASTM-EURATOM Symposium on Reactor Dosimetry, EUR 6813, Vol.II, p. 919 (1980)

Table 1

PCA/PSF Fluence Monitors

Reaction	90%-Response Range		Uncertainty (Rel.Std.Dev. in %) due to		
	from	to	Activity Measurement	$\sigma(E)$	$\phi(E)$
$^{59}Co(n,\gamma)$	0.23 eV	164 eV	1.5	2.7[+]	?
$^{58}Fe(n,\gamma)$	0.17 eV	10.8 keV	2.4	3.1	?
$^{237}Np(n,f)$	0.39 MeV	4.07 MeV	-	9.5	?
$^{238}U(n,f)$	1.35 MeV	6.26 MeV	-	1.4	?
$^{58}Ni(n,p)$	1.79 MeV	7.60 MeV	1.5	6.6	?
$^{54}Fe(n,p)$	2.15 MeV	7.70 MeV	1.5	3.6	?
$^{46}Ti(n,p)$	3.78 MeV	9.68 MeV	1.5	12.6	?
$^{63}Cu(n,\alpha)$	4.84 MeV	11.3 MeV	1.5	5.3	?

[+]) (File 33, Original: 26.4 %)

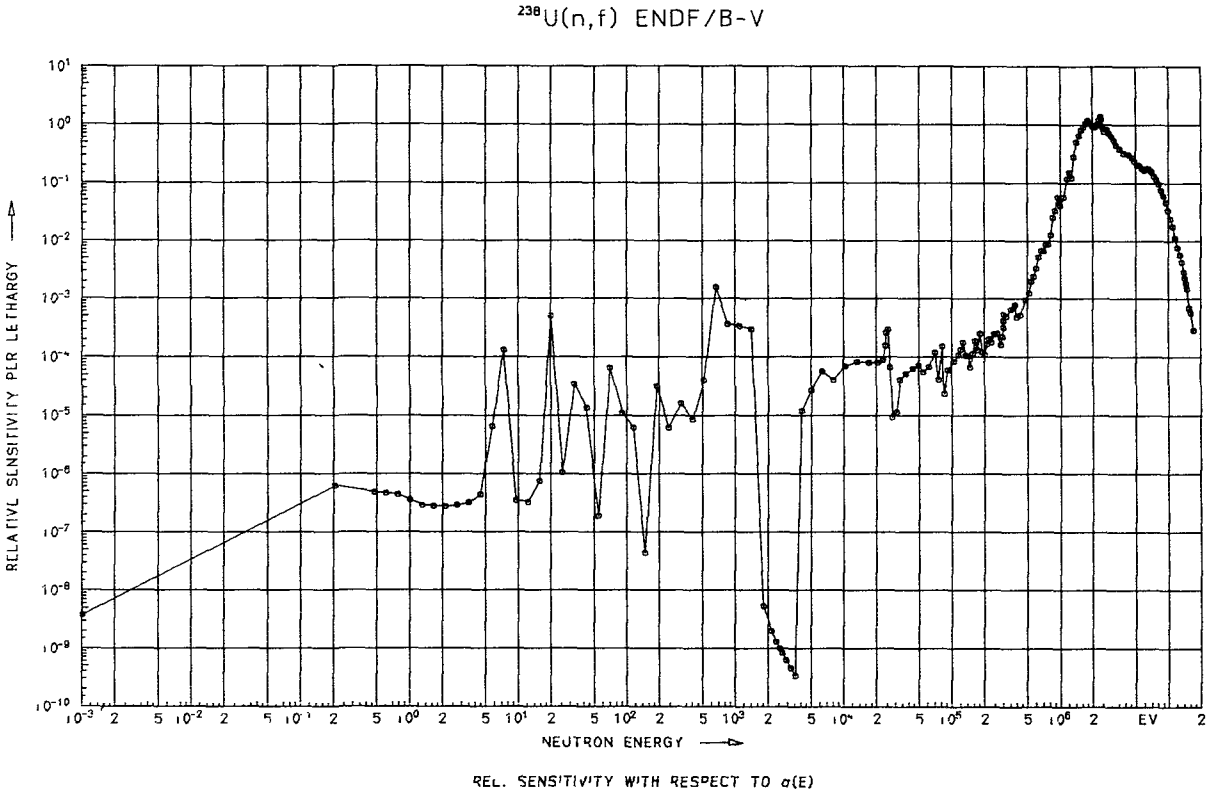

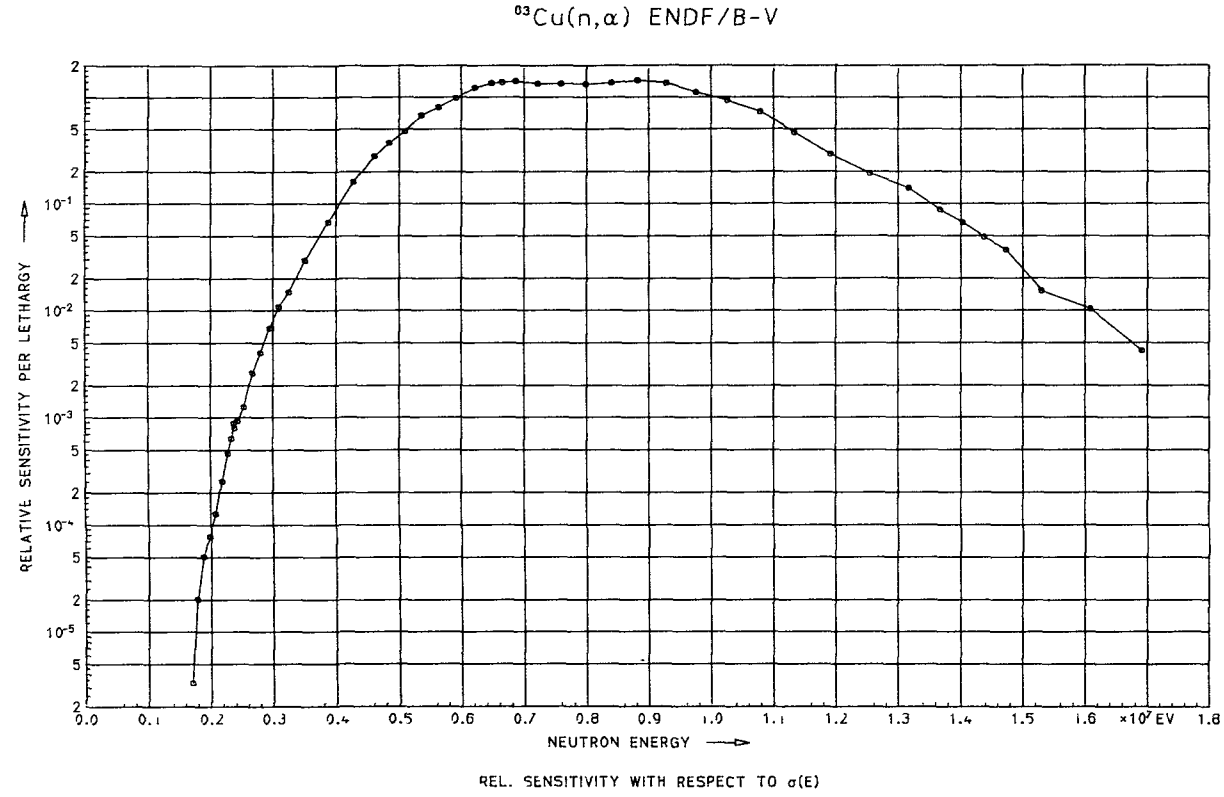

Figure 1: Sensitivity Coefficients with Respect to σ(E)

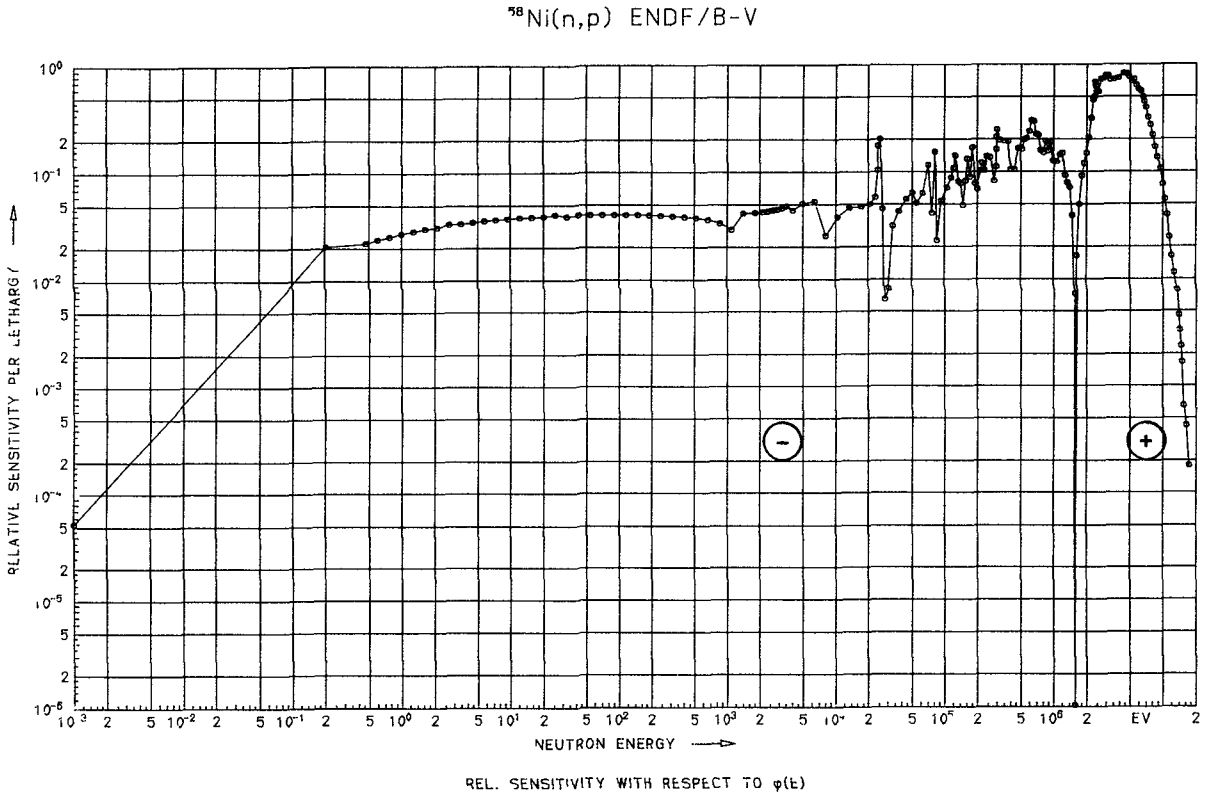

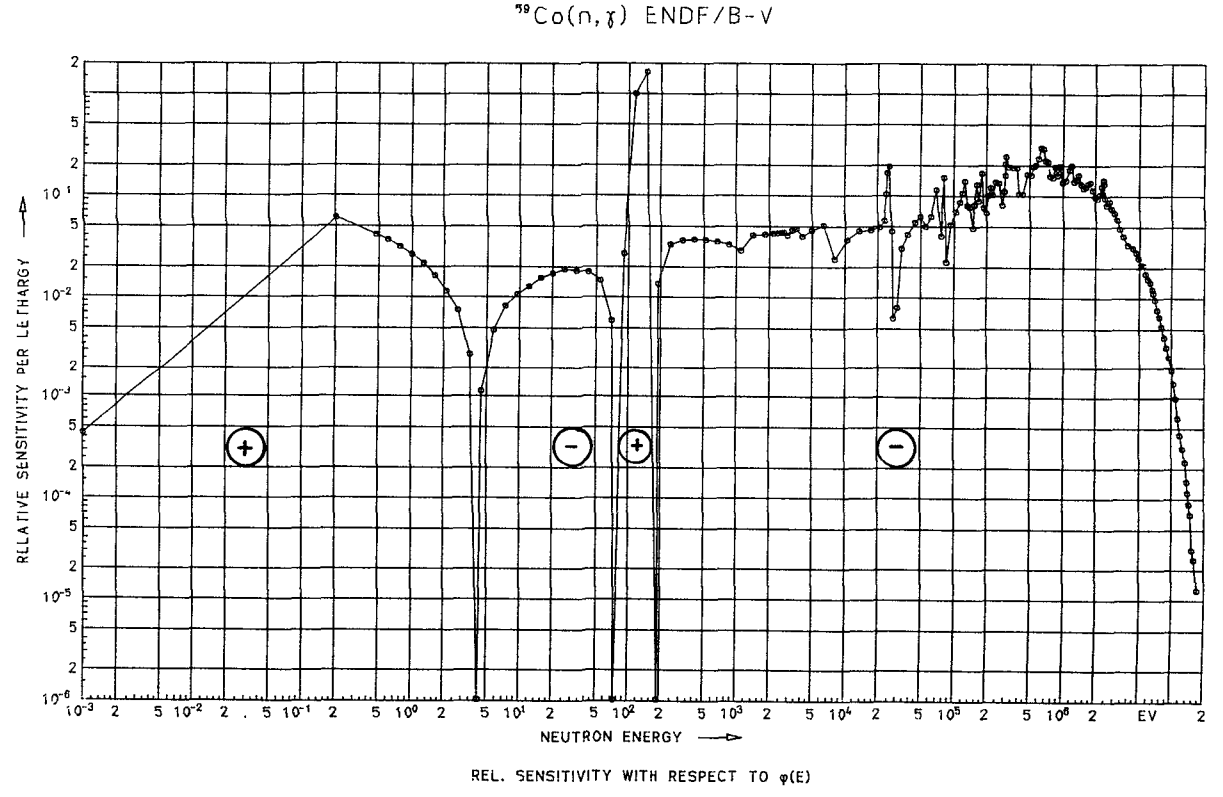

Figure 2: Sensitivity Coefficients with Respect to $\phi(E)$

RELEVANCE OF NONLINEAR EFFECTS OF UNCERTAINTIES IN THE INPUT DATA ON THE CALCULATIONAL RESULTS

F. CARVALHO DA SILVA*, A. D'ANGELO,
A. GANDINI, V. RADO
Comitato Nazionale per l'Energia Nucleare,
Centro Studi Nucleari della Casaccia,
Rome,
Italy

ABSTRACT:

The second order sensitivity analysis relevant to neutron activations at the end of Fe and Na blocks shows that the discrepancy between the values obtained from the direct calculation and those which take into account the inaccuracy of the input data (average values) can be significant in cases of interest. It has been observed that, for a threshold detector response after a penetration larger than 50 cm in Fe blocks and 100 cm in Na blocks, the magnitude of this discrepancy (from 50% up to 100% of standard deviation) leads to the necessity of improving the existing accuracy of the inelastic cross-sections of Fe and Na. Moreover, the above discrepancy has been evaluated in terms of project parameters relevant to a power fast fission reactor, in particular, the Fe-displacement rate in the Fe/Na shield region and the Na-activation rate in the heat exchanger.

1. EXPECTED CORRECTIONS OF CALCULATIONAL VALUES

If a calculated quantity Q(p) is nonlinear with respect to parameters p_i, considering a second order Taylor expansion around the available values p_0, we can write, for the average value:

$$\overline{Q(p)-Q(p_0)} = \overline{Q(p)} - Q^{cal} = \sum_K \frac{\partial Q}{\partial p_K} \overline{(p_K - p_{0K})} + \frac{1}{2} \sum_{ij} \frac{\partial^2 Q}{\partial p_i \partial p_j} \overline{(p_i - p_{0i})(p_j - p_{0j})} \quad (1)$$

which represents the difference between the average value of Q and the result obtained from the calculation. Such quantity should then be considered as a correction to be introduced to obtain the best estimator (in the sense of the average value) of Q. Once the second order coefficients $\partial^2 Q / \partial p_i \partial p_j$ are available, together with the error variance-covariance data, this quantity can be easily calculated. In fact since, obviously, it is assumed that $\overline{p_K} = p_{0K}$,

---

(*) Permanent adress: Universidade Federal do Rio de Janeiro
COPPE/PEN - P.O. Box 68509, CEP 21910
RIO DE JANEIRO, RJ, BRASIL

if we define the quantity $\alpha_{ir} = \delta_{ir} + \delta_{jr}$, with δ_{ij} the Kronecker symbol, and the second order coefficient

$$s/_{ij} = \frac{2}{\alpha_i + \alpha_j} \frac{1}{Q^{cal}} \frac{\partial^2 Q}{\partial p_i \partial p_j} p_{oi} p_{oj} \quad , \qquad (2)$$

Eq. (1) can be re-written

$$\frac{\overline{Q(p)} - Q^{cal}}{Q^{cal}} = \sum_{j \geq i} s/_{ij} \varepsilon^2_{ij} \qquad (3)$$

where ε^2_{ij} represent the i,j-th element of fractional variance-covariance matrix associated with p_i. In relation to the evaluation of coefficient $s/_{ij}$, use of the higher order generalized perturbation theory /1,2,3/ should be made.

2. CONFIGURATIONS-CONSIDERED AND DETAILS OF ACTIVATION RATE CALCULATIONS

The significance of the discrepancy of the correction ($\overline{Q} - Q^{cal}$) due to nonlinear effects associated to the differential data uncertainties has been studied in relation to activation values in Na and Fe blocks with a fission spectrum distributed entering neutron source.

The significance of the above discrepancy in relation to the Fe displacement rate in the Fe/Na shield region and to the Na activation rate in the heat exchanger in a benchmark fast reactor shield /4,5/ has also been studied. The source spectrum considered of the neutrons entering into the radial shield is representative of a power fast reactor.

All the calculations in S_4, P_3 transport approximation have been made with the discrete ordinate code GIANT /6/.

The cross sections in a 45, shielding oriented, group structure, originated from ENDF/B-IV data, have been reduced to a 17 group for the Na and Fe block calculations. The structure of this latter library is very close to that pertinent to the variance-covariance matrix /7/ adopted in this work. The group collapsing has been performed by means of the ANISN Code.

3. RESULTS AND DISCUSSION

3.a) "Expected correction of activation rates in Fe and Na blocks."

In Table 1 through 4 the results obtained from the Fe and Na block are reported. They consist in the fractional values of the standard deviations and the expected corrections / Eq. (3)/.

From the results shown in these tables, indicating significant asymmetries of the probability distribution of threshold activations, and in view of a more reliable characterization of high energy spectra at deep penetration distances, the need follows for an improved accuracy of the Fe and Na inelastic cross-section.

3.b) "Expected correction of Fe displacement rate in the Fe/Na shield region and of activation rate of Na in the heat exchanger."

Once observed that the expected correction to the calculated values of a few response functions can be significant, this same correction has been considered in relation to two project parameters of interest for a fast power reactor.

In Table 5 the value relevant to the expected corrections are shown. It is noted that they do not exceed 20% of the standard deviation obtained by the usual linear procedure. This indicates that, for these two project parameters, this linear, i.e. first order, procedure can be considered satisfactory in a variety of practical cases. This, however, does not detract from the fact that the expected + 16% correction of the Na activation rate in the heat exchanger has some significance. In fact, even assuming that, as usual practice, correction factors are introduced to modify these calculated values, the starting ones should be in any case modified according to the expected corrections discussed above.

REFERENCES

/1/ A. GANDINI, Nucl. Sci. Eng., 67, 91 (1978); see also
Nucl. Sci. Eng., 70, 112 (1979)

/2/ A. GANDINI, Nucl. Sci. Eng., 73, 298 (1980)

/3/ A. GANDINI, Nucl. Sci. Eng., 77, 316 (1981)

/4/ J.Y. BARRE, "Fast Reactors: Definition of a Standard Configuration for the Comparison of Shielding Calculations", Proc. Specialist's Meeting on Sensitivity Studies and Shielding Benchmarks - OECD (Paris, October 1975)

/5/ S.D. LYMPANY, A.K. Mc CRAKEN, A. PACKWOOD, " Contribution to the Exercise on Sensitivity Studies for the NEA Theoretical Fast Reactor Benchmark", Proceedings of Specialist Meeting on Differential and Integral Nuclear Data Requirements for Shielding Calculations - Vienna 12-15 October 1976

/6/ G. PALMIOTTI, M. SALVATORES, "Transport Calculations of the Generalized Importance Functions for Sensitivity Analysis", Proc. Specialist's Meeting on Sensitivity Studies - OECD, Paris (1975)

/7/ J.D. DRISCHLER and C.R. WEISBIN, "Compilation of Multigroup Cross Section Covariance Matrices for Several Important Reactor Materials", ORNL-5318 (ENDF 235), 1977

TABLE 1

CALCULATED VALUE
EXPECTED CORRECTIONS

ACT. S(N,P)

DEPTH FE (CM)	STANDARD DEVIATIONS	EXPECTED CORRECTIONS
10	2.05E-01	2.64E-02
20	3.50E-01	7.21E-02
30	4.86E-01	1.37E-01
40	6.14E-01	2.17E-01
50	7.34E-01	3.08E-01
60	8.49E-01	4.07E-01
70	9.56E-01	5.15E-01
80	1.06E+00	6.21E-01
100	1.25E+00	8.67E-01
150	1.64E+00	1.49E+00

TABLE 2

CALCULATED VALUE
EXPECTED CORRECTIONS

ACT. RH(N,N')

DEPTH NA (CM)	STANDARD DEVIATIONS	EXPECTED CORRECTIONS
50	1.83E-01	3.47E-02
100	3.89E-01	1.31E-01
150	6.30E-01	3.04E-01
200	8.89E-01	5.73E-01
250	1.20E+00	9.68E-01

TABLE 3

CALCULATED VALUE
EXPECTED CORRECTIONS

ACT. IN(N,N')

DEPTH NA (CM)	STANDARD DEVIATIONS	EXPECTED CORRECTIONS
50	2.79E-01	5.61E-02
100	5.58E-01	2.05E-01
150	8.68E-01	4.69E-01
200	1.20E+00	8.64E-01
250	1.52E+00	1.48E+00

TABLE 4

CALCULATED VALUE
EXPECTED CORRECTIONS

ACT. S(N,P)

DEPTH NA (CM)	STANDARD DEVIATIONS	EXPECTED CORRECTIONS
10	1.18E-01	1.16E-02
20	2.03E-01	2.85E-02
30	2.81E-01	5.07E-02
40	3.58E-01	7.89E-02
50	4.35E-01	1.13E-01
60	5.12E-01	1.55E-01
100	8.29E-01	3.85E-01
150	1.23E+00	8.32E-01
200	1.65E+00	1.46E+00
250	2.04E+00	2.21E+00

TABLE 5

CALCULATED VALUE

EXPECTED CORRECTIONS IN FAST REACTOR BENCHMARK SHIELD

		STANDARD DEVIATION (%)	EXPECTED CORRECTION (%)
Fe D.P.A. at the end of SS/NA region	Fe	7	1
	Na	10	1
	TOTAL	13	+2
Na (n,γ) H.X.	Fe	8	—
	Na	75.5	16
	TOTAL	76	+16

NEUTRON FLUX AND SPECTRAL MEASUREMENTS FOR MATERIALS STUDIES*

L.R. GREENWOOD
Chemical Engineering Division,
Argonne National Laboratory,
Argonne, Illinois,
United States of America

Neutron characterization techniques are described at various fission reactors and particle accelerators used for materials studies. Nuclear data are required in several energy regions to improve spectral unfolding measurements. Realistic errors and covariances are also needed for all nuclear activation cross sections as well as for activity integrals and input flux spectra. Difficulties are often encountered in constructing the appropriate error matrices, especially for the input spectra, and more sensitivity studies are needed.

Characterization of Neutron Irradiation Facilities

Materials studies are conducted at a variety of neutron sources including fission reactors, 14 MeV T(d,n) sources, Be or Li(d,n) accelerators, and high-energy spallation devices. In order to understand fundamental materials behavior, it is necessary to characterize all facilities in terms of neutron flux and spectra as well as atomic displacements, gas production, and transmutation. These exposure parameters are vital to the correlation of property changes between facilities and for the extrapolation of materials behavior to new environments such as fusion reactors.

Neutron flux and spectral measurements are usually made with the multiple-foil activation technique. In the best cases, about 30 different reactions can be measured simultaneously and low-energy neutrons can be further defined using cadmium or other cover techniques and resonance self-cover or sandwich methods. Foils (or wires) are then either gamma- or beta-counted to determine activation integrals. Stable product monitors can also be used and helium measurements are now routine.(1) Corrections must then be applied for the irradiation history and decay time, gamma and neutron self-shielding, burnup of materials, burn-in of contaminants, flux and spectral gradients, and many other possible sources of error. The final saturated activity rates are then equal to a simple energy integral of the activation cross section times the flux spectrum.

The neutron flux spectrum is determined using a generalized least-squares procedure performed with the STAYSL computer code.(2) Errors and covariance matrices are defined for all input data, including the activities, cross

*Work performed under the auspices of the U.S. Department of Energy.

sections, and trial flux spectrum. All data is then simultaneously adjusted to minimize the chi-square parameter. Typical results for this procedure are shown in Figure 1. Such experiments have now been completed in a variety of fission reactors[3] including ORR, BSR, and HFIR at Oak Ridge National Laboratory, Omega West Reactor at Los Alamos National Laboratory (LANL), and LPTR at Lawrence Livermore Laboratory. The 14 MeV, T(d,n) accelerator RTNS II at Lawrence Livermore Laboratory has also been characterized as well as various Be(d,n) sources[4-6] and the IPNS spallation source[7] at Argonne National Laboratory.

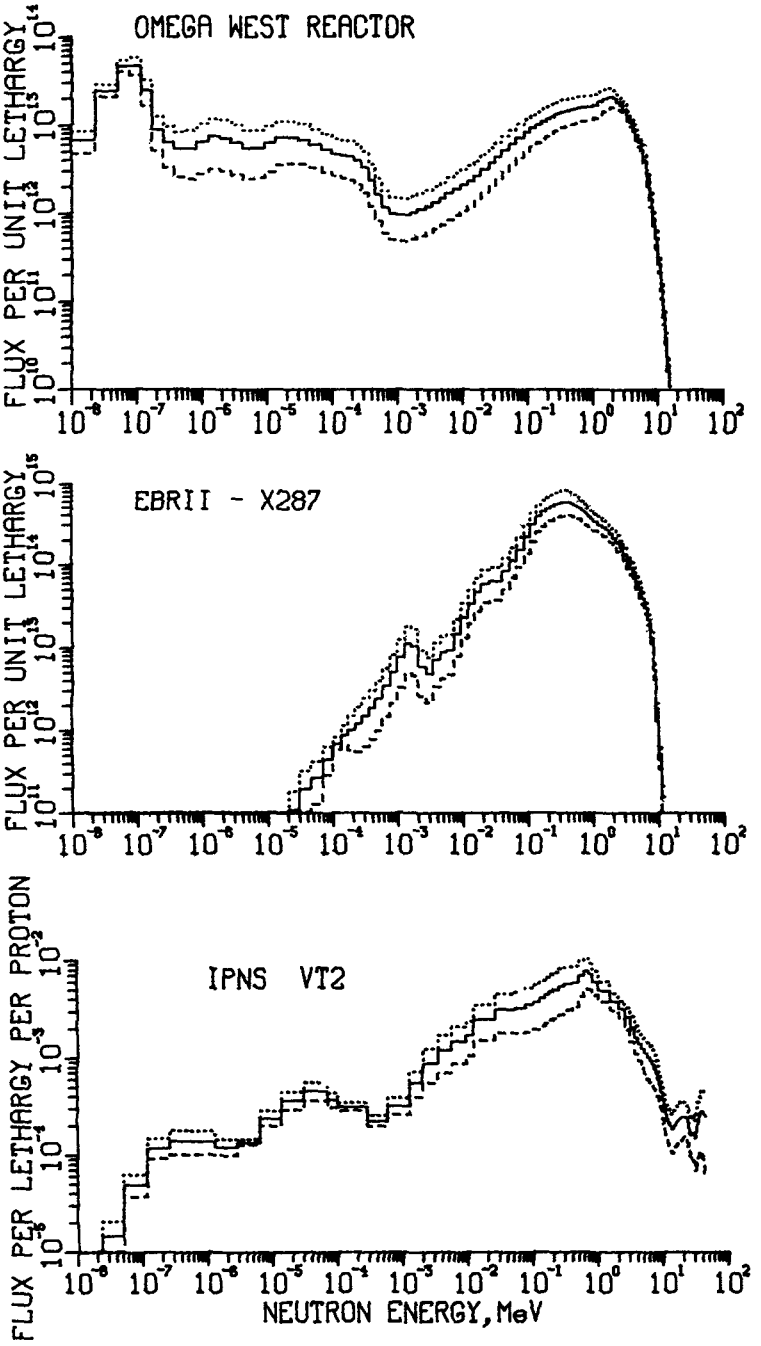

Figure 1. Neutron spectra unfolded at the Omega West Reactor (top), Experimental Breeder Reactor II (middle), and the newly-commissioned Intense Pulsed Neutron Source (bottom). The dotted and dashed lines represent one standard deviation. At least 28 activation reactions were measured in each case.

Status of Nuclear Data

Integral cross section experiments have been done for many years to assess the accuracy of differential nuclear data.[8] We have extended our cross section files to 44 MeV[9] for accelerator measurements mainly using differential data from LANL.[10] Integral cross section experiments have then been conducted in T(d,n) and Be(d,n) fields using time-of-flight spectrometry to determine the neutron spectra.[4,5] The results are listed in Table I using ENDF/B-V. As can be seen, the cross sections are sufficiently accurate that dosimetry can be performed reasonably well up to about 30 MeV thanks to

Table I. Results of Integral Cross Section Testing

Differential cross sections from ENDF/B-V, unless noted.
Estimated cross section errors are listed in percent.

	ORR[a]	RTNS II[b]	Be(d,n)[c]	
Reaction	Mixed-Spectrum	0°, 14.9 MeV	14-16 MeV	40 MeV
$^{27}Al(n,\alpha)^{24}Na$	-	+7	+6	-1
$^{45}Sc(n,2n)^{44m}Sc$[d]	-	-3	-15	+3
$Ti(n,x)^{46}Sc$	-1	+10	-1	+24
$Ti(n,x)^{47}Sc$	+25	-30	+6	-56
$^{48}Ti(n,p)^{48}Sc$	-2	-8	-1	+4
$Fe(n,x)^{54}Mn$	-3	-2	-3	+4
$^{54}Fe(n,\alpha)^{51}Cr$[d]	-17	+2	+1	-20
$^{56}Fe(n,p)^{56}Mn$	-	-	-2	-4
$^{55}Mn(n,2n)^{54}Mn$	-	-5	-	-
$^{59}Co(n,p)^{59}Fe$[d]	-	+26	-4	+5
$^{59}Co(n,2n)^{58}Co$	-	+4	+6	-3
$^{59}Co(n,\alpha)^{56}Mn$	-	-	-2	-5
$^{58}Ni(n,p)^{58}Co$	-3	+13	-3	+3
$^{58}Ni(n,2n)^{57}Ni$	-	-14	+1	+14
$^{60}Ni(n,p)^{60}Co$	+13	-21	-2	+3
$^{63}Cu(n,\alpha)^{60}Co$	-	-1	-	-
$Zr(n,xn)^{89}Zr$[d]	-	-4	+9	-1
$^{93}Nb(n,2n)^{92m}Nb$[d]	-	(+6)[b]	+6	+7
$^{107}Ag(n,2n)^{106m}Ag$[d]	-	+9	-	-
$^{169}Tm(n,2n)^{168}Tm$[d]	-	-	-	+10
$^{169}Tm(n,3n)^{167}Tm$[d]	-	-	-	-8
$^{197}Au(n,2n)^{196}Au$[d]	-1	0	-8	+1
$^{197}Au(n,3n)^{195}Au$[d]	-	-	-	+12
$^{197}Au(n,4n)^{194}Au$[d]	-	-	-	+1
$^{115}In(n,n')^{115m}In$	-	-	-2	-2
$^{235}U(n,f)$	-1	-	+8	+1
$^{238}U(n,f)$	-2	-	+4	-1
$^{238}U(n,2n)^{237}U$[d]	-	-	+1	-11

[a] Spectrum from neutronics calculation; values relative.

[b] T(d,n) source; values normalized to $^{93}Nb(n,2n)$, 463 mb ± 7%.

[c] See References 4 and 5.

[d] Cross section not in ENDF; see Reference 9.

the data of Reference 10 above 20 MeV. More cross sections are needed, especially above 28 MeV where there are no known measurements. At spallation sources, data are needed up to several hundred MeV and spallation cross sections themselves can be used for dosimetry as has been demonstrated with Cu.[11] Many of our cross section needs above 30 MeV can be met by a carefully planned mixture of calculations and measurements.

For fission reactors, there are a number of outstanding cross section discrepancies which should be resolved as shown in Table I. The agreement between integral and differential data is clearly much better now with ENDF/B-V; however, some reactions still appear to be in error, such as ^{47}Ti, ^{60}Ni(n,p), and ^{58}Ni(n,2n). At 14 MeV, cross section comparisons made at RTNS II also indicate some sizable errors in cross section ratios such as ^{58}Ni(n,p)/(n,2n).

In mixed-spectrum reactors, there continues to be a serious difficulty in finding reactions which are sensitive to the energy region between 1-500 keV, especially for longer irradiations. The ^{93}Nb(n,n') reaction appears to be the best candidate, but the data and measurement techniques still need development. More generally, there is an overall shortage of well-known cross sections leading to long-lived activation products for irradiations lasting several years or more. Table II lists the most important activation cross sections needed for fusion dosimetry.

Table II. Threshold Activation Reactions Desired for Fusion Dosimetry Listed by Material in Order of Priority.

Elements with multiple, long-lived products are favored. Many other reactions could also be used.

Reaction	Energy Range (MeV)	Reaction	Energy Range (MeV)
^{59}Co(n,p)^{59}Fe	4-28	^{90}Zr(n,p)^{90}Y	5-26
(n,2n)^{58}Co	10-30	Zr(n,x)^{89}Zr	12-36
(n,3n)^{57}Co	20-40	(n,x)^{88}Zr	18-45
(n,4n)^{56}Co	30-50	^{89}Y(n,p)^{89}Sr	4-25
^{197}Au(n,2n)^{196}Au	8-25	(n,2n)^{88}Y	12-34
(n,3n)^{195}Au	15-35	(n,3n)^{87}Y	22-50
(n,4n)^{194}Au	23-45	(n,α)^{86}Rb	8-28
Fe(n,x)^{54}Mn	1-40	^{169}Tm(n,2n)^{168}Tm	9-28
^{54}Fe(n,α)^{51}Cr	7-25	(n,3n)^{167}Tm	16-36
^{54}Fe(n,x)^{52}Mn	14-35	(n,5n)^{165}Tm	25-50
^{58}Ni(n,p)^{58}Co	2-25	^{23}Na(n,2n)^{22}Na	12-30
(n,2n)^{57}Ni	12-36	^{107}Ag(n,2n)^{106m}Ag	10-28
(n,3n)^{56}Ni	22-40	(n,3n)^{105}Ag	16-40
^{60}Ni(n,p)^{60}Co	3-30	^{238}U(n,2n)^{237}U	6-18
^{93}Nb(n,n')^{93m}Nb	0.1-10	(n,f)	1-50
(n,2n)^{92m}Nb	9-28	^{55}Mn(n,2n)^{54}Mn	11-28

Error Analysis

The reliability of spectral unfolding techniques has improved enormously with the advent of routine error analysis, including covariance effects. Such data are now being included in ENDF/B-V. However, there are still many cases where data are lacking or very poorly known. Cross-covariances between reactions are known in a few cases, but it is still a formidable task to assign appropriate values to unfolding problems involving 30 or more reactions. At present, self-covariances are assumed to be very small, possibly leading to systematic errors in unfolded spectra. Accurate error matrices can only be determined for the activation measurements. Yet, these errors are usually quite small (1-5%) compared to errors in cross sections (5-30%) and input spectra (30-100%).

There are also a variety of special problems in assigning errors which have not been solved. Neutron self-shielding errors, espeically at resonances, cannot yet be evaluated from the ENDF/B-V files, although computer codes are now being written. Similarly, errors are not properly assigned in cases using cadmium or other cover or sandwich techniques. Burnup or other spectral-dependent corrections also may be difficult to assess. For accelerators, one is always faced with steep flux and spectral gradients near the source, and corrections may be required to properly relate reaction rates in nearby foils. Finally, temporal variations in flux and spectra can introduce differences between short-lived and long-lived activity rates. At present, educated guesses are used to assign many of these errors. Sensitivity studies are needed to understand how such effects may influence spectral unfolding.

Of course, the worst problems encountered in assigning errors arise with the input spectrum. At accelerators, active spectrometry can be used far from the source; however, data are often inadequate to properly evaluate spectra near the source, and very-low and very-high energies often cannot be well-measured. In reactors, the situation is even worse since errors are not usually computed for neutronics calculations. It should also be pointed out that in many cases neutronics codes may have been adjusted to fit dosimetry data, especially fission rates. In any case, covariances exist between nuclear data used for neutronics and that used for dosimetry. Hence, systematic errors may be overlooked.

Gaussian self-covariances are usually assumed for the input spectrum. This certainly serves to smooth out sharp changes in the flux spectrum which are usually unphysical. However, this procedure does not take into account whatever knowledge of the spectrum which may be available. For example, we might want to insist that the thermal spectrum have a Maxwellian shape or that the fast spectrum resemble a pure fission shape. In a mixed-spectrum reactor, it is difficult to ensure that both conditions will be met simultaneously, and

it is often preferable to manually adjust the ratio of fast-to-thermal fluxes prior to unfolding. Covariance matrices might be constructed to solve this problem, although it is not clear what to do at intermediate neutron energies where the fast and thermal spectra must be joined. Sensitivity studies are needed to explore the whole problem of assigning error matrices to input spectra used in the unfolding technique.

References

1. See paper by H. Farrar, IV, in the proceedings of this conference.

2. F. G. Perey, "Least Squares Dosimetry Unfolding: The Program STAYSL," ORNL-TM-6062 (1977); modified by L. Greenwood (1979).

3. L. R. Greenwood, "Review of Source Characterization for Fusion Materials Irradiations," BNL-NCS-51245, p. 75 (1980).

4. L. R. Greenwood, R. R. Heinrich, R. J. Kennerley, and R. Medrzychowski, Nucl. Technol. 41, 109 (1978).

5. L. R. Greenwood, R. R. Heinrich, M. J. Saltmarsh, and C. B. Fulmer, Nucl. Sci. Eng. 72, 175 (1979).

6. D. W. Kneff, H. Farrar, L. R. Greenwood, and M. W. Guinan, "Characterization of the Be(d,n) Neutron Field by Passive Dosimetry Techniques," BNL-NCS-51245, p. 113 (1980).

7. M. A. Kirk, R. C. Birtcher, T. H. Blewitt, L. R. Greenwood, R. J. Popek, and R. R. Heinrich, J. Nucl. Mater. 96, 37 (1981).

8. M. F. Vlasov, A. Fabry, and W. N. McElroy, "Status of Neutron Cross Sections for Reactor Dosimetry," IAEA, INDC (NDS)-84-L+M (1977).

9. L. R. Greenwood, "Extrapolated Neutron Activation Cross Sections for Dosimetry to 44 MeV," ANL-FPP/TM-115 (1979).

10. B. P. Bayhurst, J. S. Gilmore, R. J. Prestwood, J. B. Wilhelmy, N. Jarmie, E. H. Erkkila, and R. A. Hardekopf, Phys. Rev. C12, 451 (1975).

11. J. T. Routti and J. V. Sandberg, Computer Physics Communications 21, 119 (1980).

NUCLEAR DATA NEEDS AND STANDARD SPECTRA FOR THE MEASUREMENTS AND ANALYSES OF D-Li NEUTRON SPECTRA

R. DIERCKX,
Joint Research Centre,
Ispra (Italy)

A. CESANA, M. TERRANI, V. SANGIUST,
Politecnico di Milano,
Milan,
Italy

SUMMARY

An experiment is in preparation to set up two standard spectra for D–Li neutron source dosimetry. These spectra are produced by 50 MeV D^+ failing on a thick Li target and the spectra emitted under 0° and 20° will be taken. These spectra will be measured by T.O.F. techniques and activation detectors will be irradiated at the same position of the T.O.F. detectors for calibration. With calibrated detectors, spectra in the vicinity of target will be measured.
A detector set is proposed and preliminary calculations are executed to find out which nuclear data are needed and in which energy region, to be able to analyze the measured reaction rates. The needed improvement of these data is discussed;after the execution of the measurements data needs and improvements will be revised.

INTRODUCTION.

The use of high energy neutron sources for damage studies connected with fusion reactors will be probably of great importance in the future. A programe in this direction has been planned at the JRC Ispra,and irradiations in Los Alamos have already been prepared and are now in execution. One of the point of importance when radiation damage experiments are performed is the knowledge of the neutron environment around the samples in study. Measurements with T.O.F. techniques are,if possible, of great utility,but in some cases the only convenient technique will be the M.F.A. (multiple foil activation).
In this context the preparation and validation of reference standard spectra is of importance together with the check of experimental techniques and data elaboration procedures. An irradiation experiment is in preparation (50 MeV D^+ on a thick Li target) and is here described and discussed.

THE EXPERIMENT.

50 MeV deuterons impinging on a thick Li target will generate a broad neutron spectrum peaking at 14 MeV but with a tail up to 40 MeV. The angular dipendence of the spectra will be considered, examining the energy distribution of neutrons emitted under 0° and 20°, The spectra will be measured by T.O.F. techniques with a counter 5 cm. in diameter at 6 m. from the target; a set of activation detectors will be irradiated at the same position of the T.O.F. detectors. The neutron spectra given by T.O.F. will so be used as reference spectra where the activations detectors will be calibrated for future use in other experiments. The calibrated detectors will also be used at the vicinity of the source (down to 40 cm) to search for a possible spectrum dipendence from the target distance. The source intensity will be of the order of $4 \cdot 10^{12}$ n/Sr s at 0°.

CHOICE OF DETECTOR SET AND RESPONSE EVALUATION.

When very high energy neutrons are involved the problem of interfering reactions has to be considered and imposes limitations on the choice of detectors and on their purity; reaction products of very short half-life will not be considered since the counting will be done with some delay after irradiations. The following materials were chosen: Co, Au, Fe, Ni, Ti, Al, Zr, In, Mn, Cu, ^{235}U, ^{238}U; the 25 reactions of possible use are listed.

$^{59}Co(n,\gamma)^{60}Co$	$^{197}Au(n,\gamma)^{198}Au$	$Fe(n,x)^{54}Mn$	$^{58}Ni(n,p)^{58}Co$
" $(n,p)^{59}Fe$	" $(n,2n)^{196}Au$	$^{56}Fe(n,p)^{56}Mn$	$^{60}Ni(n,p)^{60}Co$
" $(n,2n)^{58}Co$	" $(n,3n)^{195}Au$	$^{54}Fe(n,\alpha)^{51}Cr$	$^{58}Ni(n,2n)^{57}Ni$
" $(n,3n)^{57}Co$	" $(n,4n)^{194}Au$		
$Ti(n,x)^{46}Sc$	$^{27}Al(n,\alpha)^{24}Na$	$Zr(n,x)^{89}Zr$	$^{115}In(n,\gamma)^{116m}In$
$Ti(n,x)^{47}Sc$	$^{63}Cu(n,\gamma)^{64}Cu$		$^{115}In(n,n')^{115m}In$
$^{48}Ti(n,p)^{48}Sc$		$^{235}U(n,f)$	
$^{55}Mn(n,\gamma)^{56}Mn$		$^{238}U(n,f)$	

The energy response of these reactions was then evaluated using the 100 groups cross section library of Greenwood (1). In fig. 1 the energy interval of 90% response is reported together with the assumed flux shape. A reasonable energy coverage is reached up to 30 MeV, while at higher energies only $^{197}Au(n,3n)$ and $^{59}Co(n,3n)$ reactions are still of importance.

The full line counting rates with a Ge-Li of 40 cm^3, achievable with 1 hr irradiation, foils 1 mm thick and 0.8 cm in diameter, at 3 m from the Li target, were then evaluated. Unfortunately the counting rates from ^{60}Co, ^{195}Au and ^{51}Cr seem to low and the corresponding four reactions will probably not considered (2).

DATA UNCERTAINTIES AND IMPROVEMENTS

A preliminary evaluation of the uncertainties on reaction rates measured and cross sections, and on their propagation to the derived flux was made through STAY'SL (3).

If the flux adjustment as a result of absolute reaction rates measurement is here considered, the uncertainty evaluation shows a situation very far from satisfaction, the major errors coming from the cross sections. The cross section library, derived by Greenwood from the ENDF/B IV dosimetry file, is extrapolated up to 44 MeV through the TRESH code; errors up to 40% are foreseen for $E \geq 25$ MeV and will be propagated to the derived differential flux. However the integral flux, less affected by these errors for inter-correlation effects, will probably have uncertainties of the order of 15%.

An improvement in the cross sections of nearly all the reactions in the high energy region is highly desirable, particularly for $^{46}Ti(n,p)$, $^{197}Au(n,2n)$, $^{197}Au(n,4n)$ and $^{59}Co(n,3n)$.

As already observed (4), the situation is much improved if measurements in standard spectra are considered. Errors on decay data are by-passed, while errors on cross sections may be significantly reduced if unknown and reference spectra are similar in energy shape (5).

REFERENCES

1) L.R.Greenwood: ANL/FPP/TM - 115 (1978)

2) A.Cesana, V.Sangiust, M.Terrani: Internal Report

3) F.G.Perey: ORNL/TM - 6062, ENDF - 254 (1977)

4) A.Cesana, V.Sangiust, G.Sandrelli, M.Terrani: IAEA Advisory Group Meeting Vienna 12 - 16 October 1981

5) R.Dierckx: EUR - 2532e - (1965)

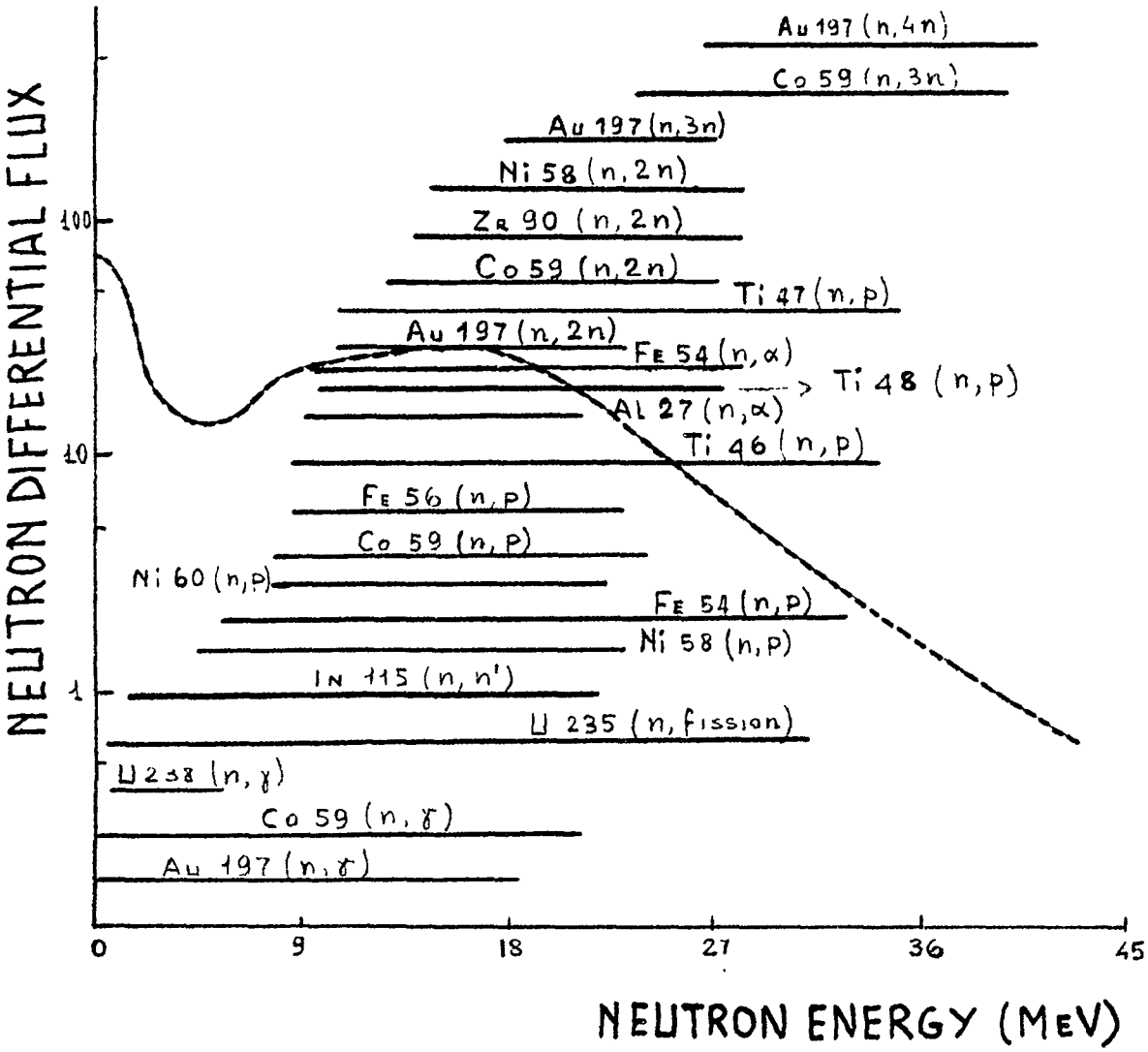
Au 197 (n,4n)
Co 59 (n,3n)
Au 197 (n,3n)
Ni 58 (n,2n)
Zr 90 (n,2n)
Co 59 (n,2n)
Ti 47 (n,p)
Au 197 (n,2n)
Fe 54 (n,α)
Ti 48 (n,p)
Al 27 (n,α)
Ti 46 (n,p)
Fe 56 (n,p)
Co 59 (n,p)
Ni 60 (n,p)
Fe 54 (n,p)
Ni 58 (n,p)
In 115 (n,n')
U 235 (n,fission)
U 238 (n,γ)
Co 59 (n,γ)
Au 197 (n,γ)
NEUTRON DIFFERENTIAL FLUX
100
10
1
0
9
18
27
36
45
NEUTRON ENERGY (MeV)

THE BASIC PRINCIPLES OF A COMPUTERIZED INFORMATION SYSTEM SAIPS

M.A. BERZONIS, H.Y. BONDARS
Latvijas Valsts Universitate,
Riga, Latvia,
Union of Soviet Socialist Republics

ABSTRACT

The information and computing system SAIPS used for planning neutron activation dosimetric experiments, unfolding of results of reaction rate measurements and analysis of final results is described. The system has unified input/output formats for different cross-section libraries and different unfolding codes.

At present a great number of various programs of neutron spectrum unfolding have been developed and used. The difference of these programs lies in the methods used to solve activation equations , in the program realization, the neutron cross- section and spectrum libraries , in the organization and formats of the data applied etc. The incorrect character of the problem to be solved and uncertainty of the data applied require additional exploration of the obtained solution. As a rule, intercomparison of the unfolding programs is done by different laboratories and only in some cases by separate laboratories (e.g. in [I]). Great care must be taken in generalizing the results as they can depend on the used detectors, errors in the reaction rates, the shape of the studied neutron spectrum, a priori information on the spectrum etc. On the other hand, a problem may be posed to determine requirements for a priori information, the detector set, the accuracy of the reaction rate measurements, errors in the cross-sections, applicability of the unfolding method etc. to obtain the required unfolding accuracy. Planning of the reaction rate measurements, spectra unfolding and studying of the obtained solution require time-consuming routine work. A computer-

ized information system SAIPS [2],[3],[4] performs automatization of this work and provides information and programs. At the present version of SAIPS this is achieved by unifying data output and input, cross-section and spectrum libraries for different unfolding programs.

Another essential feature of SAIPS is that its operation is divided into three levels providing the following possibilities:

1) to separate the use of the system from its desigh and development;

2) by means of the user language and cataloged procedures to obtain access to the system without need to go into programming problems;

3) to avoid information retrieval (unfolding programs, nuclear data, neutron spectra etc.) and its adaptation, aprobation and updating.

The centralized operation of the three-level system enables to avoid from the routine work duplicated in many laboratories and ensures higher reliability of information. On the other hand, the efficiency and development of the system depend on the feedback, i.e. users (physicists) and programmers.

SAIPS has been developed and tested on the ES 1022 computer controlled by the operational system OS ES . Because of the high degree of compatibility at both the software and hardware levels with computers IBM, SAIPS can also be employed.

In SAIPS unfolding programs are adapted without changes. But in the presented for calculation programs WINDOWS and RESP JUL criteria for the iterative process stops are calculated from the similar formula as in SANDII and in all programs the calculated neutron spectrum is presented in the same way. It is possible to refuse from these conditions. Because of necessity to expand the SAIPS possibilities and taking into consideration its deficiencies found during its operation the project has been reconstructed and a new modified version of SAIPS-2 system is being realized. In the new system a more simplified and expanded language of the user enables additional data processing , output data and auxiliary information.

This change is not felt by the user. The most essential changes come from the structure change of the neutron spectra and cross-section libraries and transformation of unfolding programs on PL/I: The existing structure taken from SAND II is not convenient for processing. The transfer to the PL/I unfolding programs will ease the work of the managing program, it will also enable the dynamic use of memory, as well as to unify separate parts of different programs. Thus, unfolding is adapted on the basis of the mathematical method without considering programmed realization.

REFERENCES

1. Kuijpers L.J.M. Experimental model studie for a fusion reactor blanket, 1976.

2. Бондарс Х.Я., Лапенас А.А. Методы расчета спектров нейтронов по измеренным скоростям реакций в SAIPS. Часть I. Обзор математических методов. Изв. АН Латв.ССР, Сер. физ.техн.наук, 1980, № 2.с.3-15. (Имеется перевод на английский язык изданный в Оакридже ORNL -tr-4669 и изданный в Вене МАГАТЕ L 80-23323).

3. Берзонис М.А., Бондарс Х.Я. Методы расчета спектров нейтронов по измеренным скоростям реакций в SAIPS. Часть 2. Программное и информационное обеспечение. Изв. А.Н. Латв.ССР. Сер. физ.техн.наук, 1981, № 1.с.9-13. (Имеется перевод на английский язык изданный в Вене МАГАТЕ L 80-23324).

4. Берзонис М.А., Бондарс Х.Я., Тайминя Д.Я. Методы расчета спектров нейтронов по измеренным скоростям реакций в SAIPS. Часть 3. Библиотеки сечений. Изв. АН Латв.ССР. Сер.физ.тех.наук (в печати).

NEUTRON DOSIMETRY FOR SURVEILLANCE TEST PURPOSES IN THE KFKI WWR-SM RESEARCH REACTOR*

J. VÉGH, I. VIDOVSZKY
Central Research Institute for Physics,
Hungarian Academy of Sciences,
Budapest,
Hungary

Abstracts

Irradiation experiments were performed on 15H2MFA steel /common RPV steel of a WWER-440 type PWR/ in the KFKI WWR-SM research reactor, to improve our fracture mechanics testing and neutron dosimetry methods. Here neutron dosimetry and damage calculations are discussed.

Neutron flux monitoring was carried out by the MFA technique, corresponding neutron spectra were unfolded. Neutron fluxes and spectra at the RPV wall and at the locations of surveillance specimens in an operating WWER-440 reactor were calculated for normalization purposes.

1. Experimental

1.1. Irradiation conditions

Irradiation of tension specimens, pre-cracked and V-notch Charpy impact specimens, cut from the 15H2MFA steel was performed in the KFKI WWR-SM research reactor. The WWR-SM is a swimming-pool type reactor, operated at max. 5MWth, the average thermal neutron flux is about $2 \cdot 10^{13}$ neutrons/cm^{2}sec. The irradiation rig was placed in the active core, at the location of a fuel assembly, it was heatable from 60°C up to 300°C electrically. The samples were given fast fluences /$E > 1.0$ MeV/ ranging from $1{,}0 \cdot 10^{19}$ to $4{,}2 \cdot 10^{19}$ neutrons/cm^2, which approximately correspond to a few years /3-5/ RPV exposure in a WWER-440 type nuclear power plant.

*This paper was not presented but sent by the authors for the meeting.

This material contains only the studies in the field of neutron physics, a similar publication on the mechanical aspects of the work is in preparation.

1.2. Neutron flux monitoring

Activation foils and wires were placed in a sealed aluminium capsule to avoid any damage from heat and moisture, or contamination.

The detector reactions were as follows: $^{54}Fe/n,p/^{54}Mn$, $^{58}Fe/n,\gamma/^{59}Fe$, $^{63}Cu/n,\alpha/^{60}Co$, $^{59}Co/n,\gamma/^{60}Co$, $^{46}Ti/n,p/^{46}Sc$, $^{93}Nb/n,n'/^{93}Nb^{m}$, $^{58}Ni/n,p/^{58}Co$, $^{60}Ni/n,p/^{60}Co$.

Activities of detector foils and wires were measured by a Ge/Li/ semiconductor detector coupled with a computerized data acquisition system based on a PDP11/10 computer and a CAMAC assembly. The analysis of gamma photopeaks was done by a fitting program: Gaussian peak-shape plus linear background were assumed.

The only exception was the $^{93}Nb/n,n'/^{93m}Nb$ reaction, where 16,6 KeV and 18,7 KeV X-ray peaks were measured with a Si/Li/ detector, although the evaluation was the same in this case as well.

2. Data evaluation and interpretation of results

2.1. Spectrum unfolding

Neutron spectrum evaluation was carried out by the unfolding code RFSP-JÜL [1], it calculates neutron flux density spectrum from measured saturated activities. The solution spectrum is tied to a trial spectrum: as a guess-spectrum we used a GRACE-result [2] plus a Maxwellian /T-380K/, the joining point between the Maxwellian and the intermediate neutron energy region was 0,17 eV. In our spectrum calculations SAND-II

and DOSCROS77 cross section libraries were used, with the exception of the $^{93}Nb/n,n'/^{93m}Nb$ reaction, where data were taken from the report EIR-195 [3].

On Fig.1. an unfolded solution spectrum and the guess spectrum can be seen in the 26 ABBN groups plus one thermal group representation.

2.2. Neutron flux at the RPV wall

For normalizing our experimental results to a real neutron environment in a WWER-440 type PWR, we had to carry out some calculations to give a reliable estimation for neutron flux values at the location of the RPV inner wall and the surveillance specimens.

With the aid of SABINE-3 [4], which is a one dimensional bulk shielding program, we calculated the neutron flux in 26 energy groups between 0.MeV and 15.MeV, results are shown in Fig.2. The fission source distribution in the active core was taken from a BIPR-5 result [5]: this program gives the radial flux distribution in the core of a WWER-440 reactor. The influence of inhomogenity in the core-flux distribution was investigated: a homogen flux /while the reactor is operated at the same power level/ gives cca.30 per cent higher flux values at the RPV location /see. Fig.3./.

On the base of SABINE-3 calculations, we could estimate the operating time, during which the above mentioned fluence values would be given to the RPV wall, in an operating WWER--440 reactor.

2.3. Irradiation damage calculations

Displacements per atom /dpa/ cross section curve for 15H2MFA steel was obtained with the aid of DAMSIG77 damage cross section library [6], using the formula:

$$\sigma_d(E_j) = \sum_{i=1}^{n} c_i \cdot \sigma_{di}(E_j) \qquad /1/$$

where

c_i : atomic per cent of the i-th element in the steel;

$\sigma_{di}(E_j)$: the corresponding displacement cross section value at the energy point E_j;

n : number of elements alloyed in the steel.

Alloying elements are: Fe, C, Mo, V, Cr, Mn. The last one has no damage cross section in the DAMSIG77, so the Mn was replaced by Cr in our calculations. Results of calculations are shown in Figs.4. and 5.: for comparison STEEL-L-DISPL from DAMSIG77 and ASTM E693-79 [7] recommendation are plotted together with 15H2MFA-STEEL respectively.

Spectrum averaged cross section data were calculated for Watt fission spectrum /E in MeV/:

$$\chi_w(E) = 0{,}484 \sinh(\sqrt{2E}) \cdot e^{-E} \qquad /2/$$

The average cross section values are presented in Table 1. for comparison.

Dpa values were calculated with the aid of formulas:

$$dpa/sec = \int_0^{+\infty} \sigma_d(E)\,\phi(E,t)\,dE \qquad /3/$$

$$dpa = \phi_{tot} \cdot t_{irr} \cdot \int_0^{+\infty} \sigma_d(E)\,\psi(E)\,dE \qquad /4/$$

$$dpa = F \cdot \langle \sigma_d \rangle_\psi \qquad /5/$$

where

$\phi(E,t)$: neutron flux density spectrum;

$\psi(E)$: normalized neutron flux density spectrum;

F : total fluence

$\langle \sigma_d \rangle_\psi$: the ψ-spectrum averaged dpa cross section value.

Final results of fluence measurements and damage calculations are shown in Table 2.

2.4. Conclusions

The described experimental technique and the evaluation of the neutron spectra /unfolding/ is suitable for the purpose of the RPV dosimetry program.

Other parts of the work should be improved as follows:

1/ the dpa prediction is not satisfactory yet;

2/ better dpa cross section data are needed for the 15H2MFA steel;

3/ the discussion of error propagation should be improved.

Our aim is to standarize the whole described procedure for making it suitable for the standard WWER-440 RPV surveillance program. Especially serious effort will be given to improve the error analysis.

References

1 Fischer,A., "RFSP-JÜL: A Program for Unfolding Neutron Spectra from Activation Data" Dec.-1977,Jül-1475

2 Szatmáry,Z., Valkó,J.: "GRACE - A Multigroup Fast Neutron Spectrum Code" KFKI-70-14 RPT

3 Hegedues,F., "Fast Neutron Fluence Detector Using the Reaction NB-93/N,N'/NB-93/Metastable/" R,EIR-195,7103

4 Ponti,C., Van Heusden,R., "SABINE-3, An Improved Version of the Shielding Code SABINE" EUR 5159 /1974/

5 Gadó,J., "Introduction to BIPR, a Program for Calculation the WWER-440 Reactors" KFKI-78-72 RPT

6 Zijp,W.L., et.al., "Damage Cross Section Library /DAMSIG77/" ECN-36 /1978/

7 "Standard Practice for Characterizing Neutron Exposures in Ferritic Steels in Terms of Displacement per Atom" ASTM E693-79

Table 1. Watt fission spectrum averaged dpa cross section values

Dpa cross section	$\langle\sigma_d\rangle_f$ [barns]
STEEL-L-DISPL /DAMSIG77/	840,5
ASTM E693-79	861,2
Draft ASTM standard*	863,6
15H2MFA-STEEL-DISPL	806,5
FE-L-DISPL /DAMSIG77/	822,9

*value from ECN-79-131 report, the other values were calculated with the aid of our program;

Table 2. Final results of fluence measurements and damage calculations

	WWR-SM irradiation location	WWER-440 RPV inner wall	WWER-440 surveillance probe's location
ϕ (E>0,1MeV)	0,43	$1,16 \cdot 10^{-3}$	$7,40 \cdot 10^{-3}$
ϕ (E>1,0MeV)	0,25	$5,72 \cdot 10^{-4}$	$3,27 \cdot 10^{-3}$
ϕ (total)*	1,0	$4,22 \cdot 10^{-3}$	$6,48 \cdot 10^{-2}$
$\langle\sigma_d\rangle$ [barns]	285,3	175,4	69,1
dpa/sec	1,0	$2,6 \cdot 10^{-3}$	$1,6 \cdot 10^{-2}$

* values are in arbitrary units, relative to the total value at the WWR-SM irradiation location;

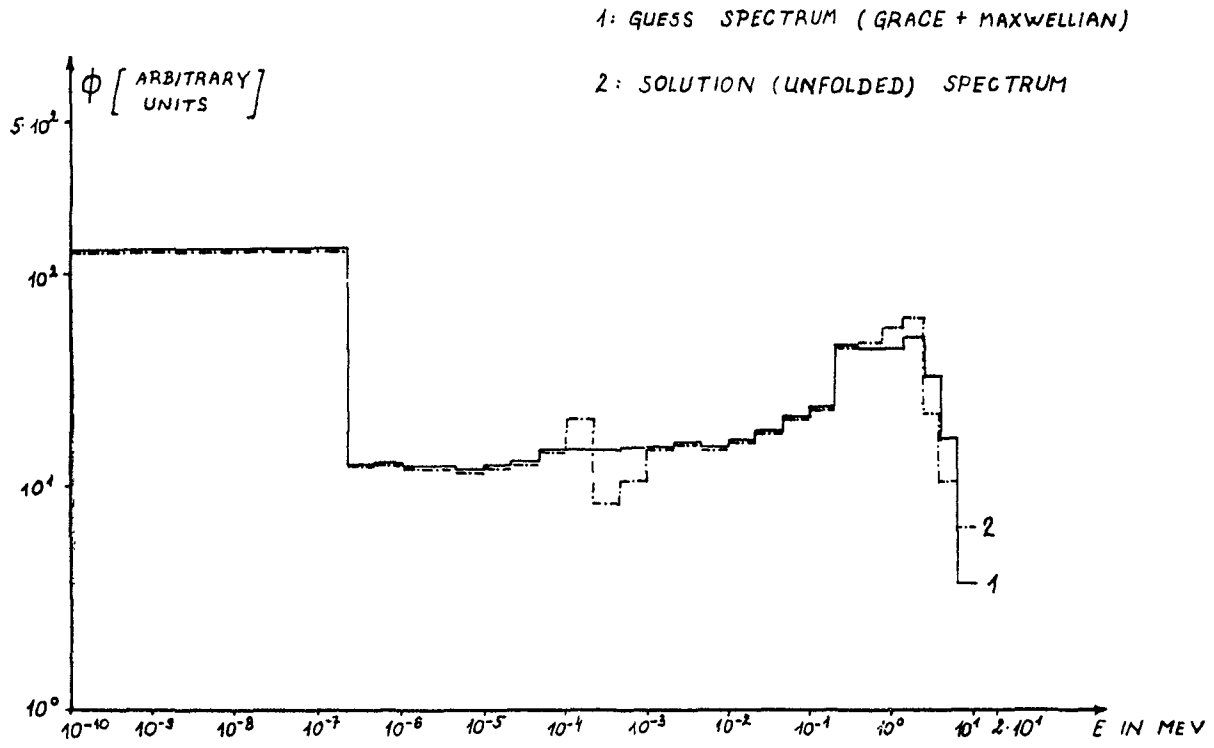

Figure 1.

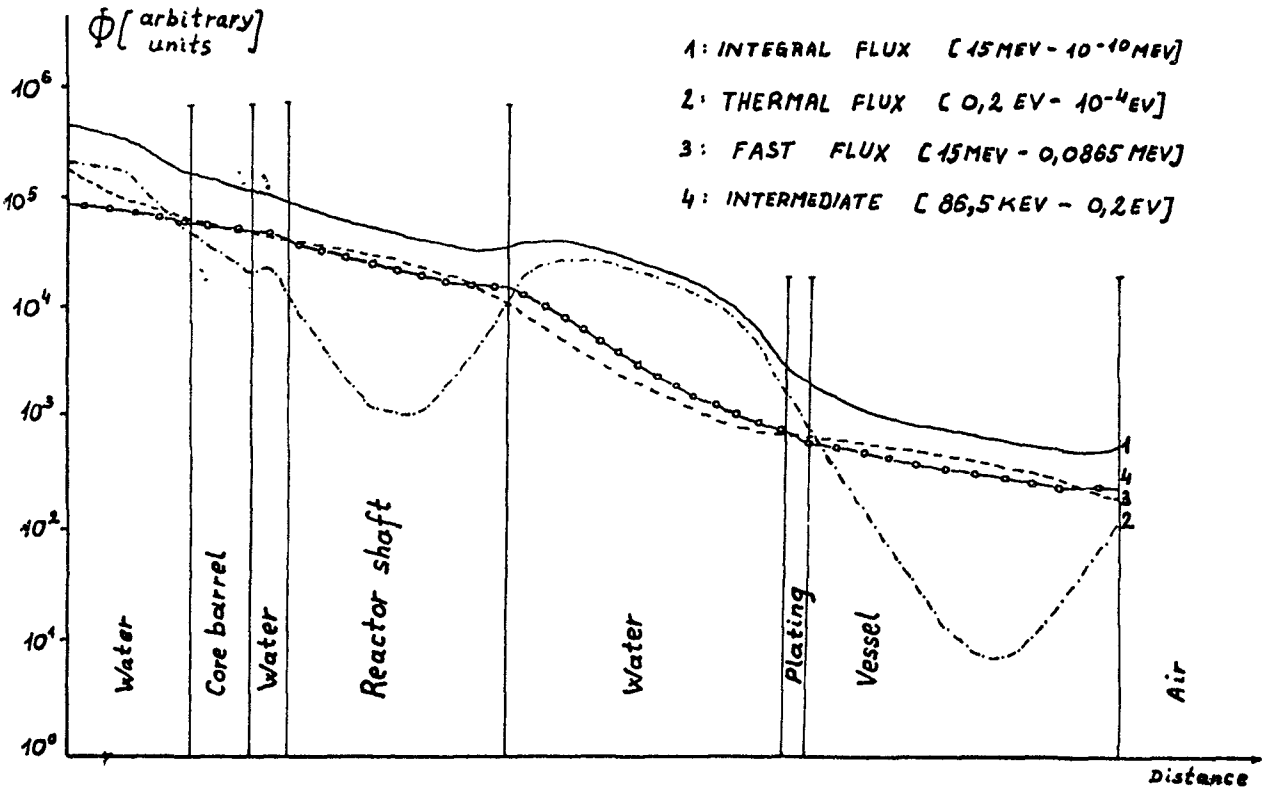

Figure 2. NEUTRON FLUX VS. DISTANCE FR. ZONE BOUNDARY

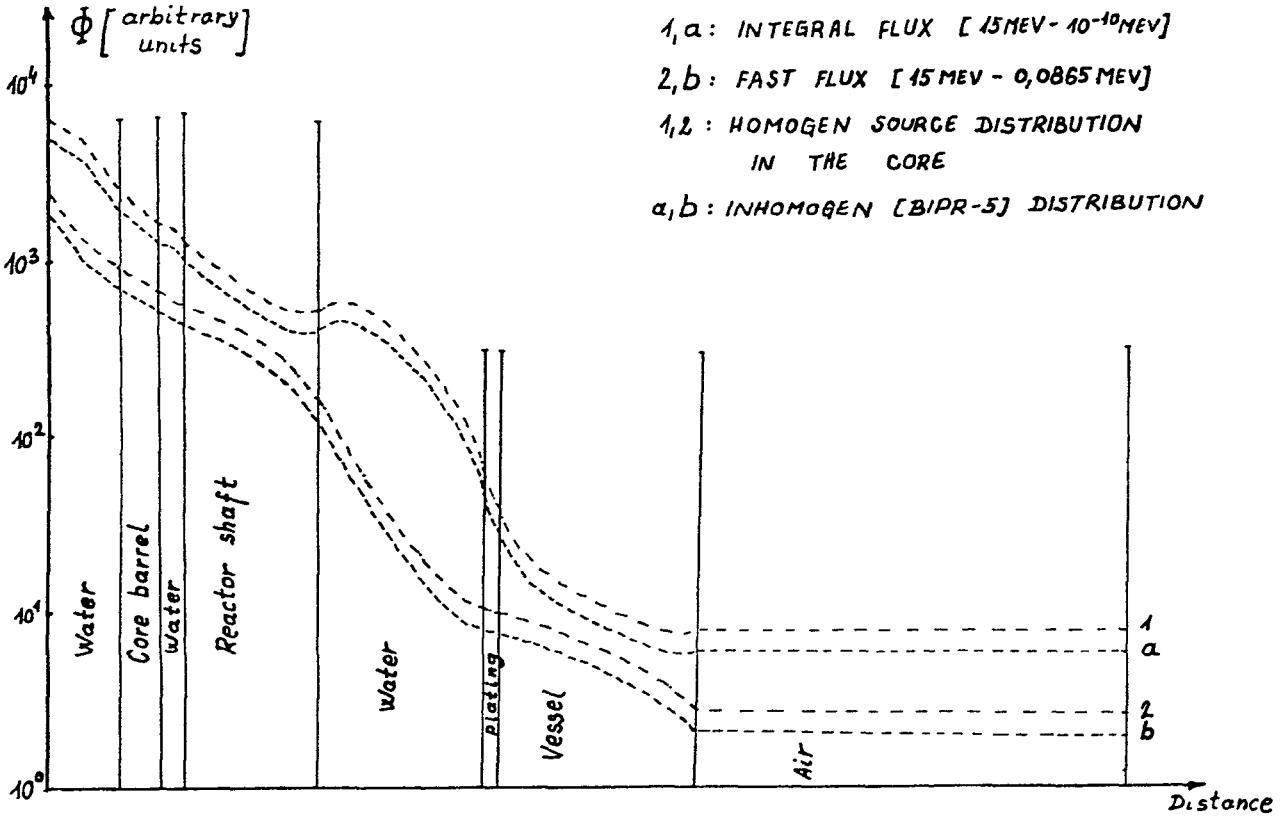

Figure 3. NEUTRON FLUX VS. DISTANCE FR. ZONE BOUNDARY

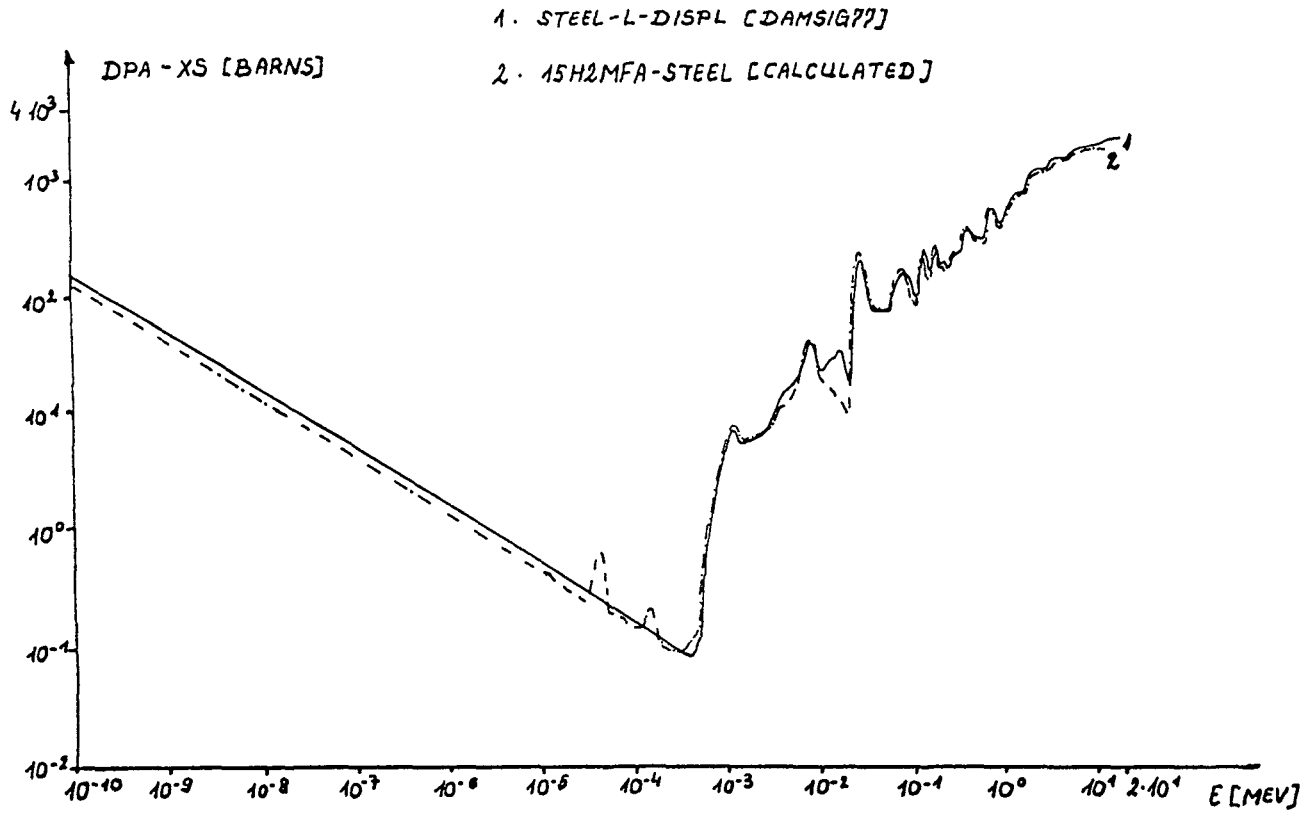

Figure 4.

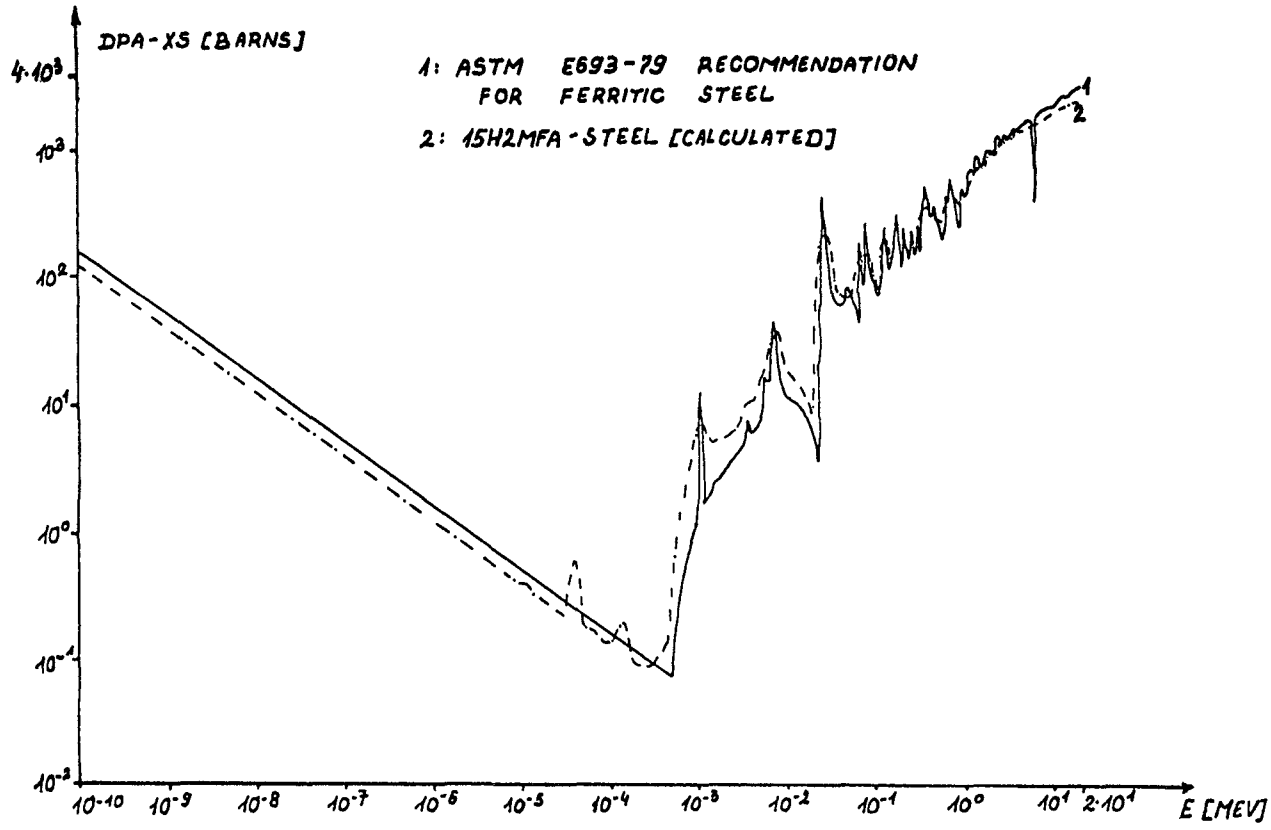
DPA-XS [BARNS]
1: ASTM E693-79 RECOMMENDATION FOR FERRITIC STEEL
2: 15H2MFA-STEEL [CALCULATED]
4·10³
10³
10²
10¹
10⁰
10⁻¹
10⁻²
10⁻¹⁰
10⁻⁹
10⁻⁸
10⁻⁷
10⁻⁶
10⁻⁵
10⁻⁴
10⁻³
10⁻²
10⁻¹
10⁰
10¹
2·10¹
E [MEV]

Figure 5.

RADIATION DAMAGE EXPERIMENT IN A SPALLATION NEUTRON SPECTRUM

R. DIERCKX
Joint Research Centre,
Ispra (Italy)

Short Communication

An irradiation is executed in a spallation neutron spectrum at the beam stop of LAMPF, LOS ALAMOS.
This neutron spectrum is harder than a fission spectrum, about 5-10% of the neutrons lie above 10 MeV and have energies up to 20-30 MeV. The irradiation has taken place in July 1981 for about one month, and reached a fluence of 10^{19} n/cm^2.
Temperature during irradiation is also measured.
The neutron spectrum is monitored by seven sets of monitor foils which are counted in different European laboratories.
The scope of this irradiation is to get some information on the radiation damage effect of high energy neutrons relative to fission neutrons.
As well as single crystals, TEM samples and tensile test samples are irradiated.
A mean feature will be the measurement of solid transmutation products in a number of selected materials interesting for fusion technology.

PRESSURE VESSEL SURVEILLANCE DOSIMETRY USING SOLID STATE TRACK RECORDERS

F.H. RUDDY, R. GOLD, J.H. ROBERTS
Westinghouse Hanford Company,
Hanford Engineering Development Laboratory,
Richland, Washington,
United States of America

Abstract

Solid state track recorders (SSTR) are among the methods being developed for light water reactor - pressure vessel surveillance (LWR-PVS). The research under way will result in the validation of a new ASTM method for application and analysis of SSTR monitors for reactor vessel and support structure surveillance. SSTR research and development has included physics-dosimetric measurements at the poolside facility (PSF), a high fluence metallurgical-dosimetry LWR-PVS mockup, and preparation of advanced SSTR dosimetry capsules for exposures at operating LWRs.

INTRODUCTION

In 1977 the United States Nuclear Regulatory Commission established the Light Water Reactor Pressure Vessel Surveillance (LWR-PVS) Dosimetry Improvement Program. The objective of this program is to improve, standardize, and maintain dosimetry, damage correlation, and the associated reactor analysis procedures used for predicting the integrated effects of neutron exposure to LWR Pressure Vessels and support structures.

Among the dosimetry methods being developed for LWR-PVS is the use of Solid State Track Recorders (SSTR). The research under way will result in the validation of a new American Society for Testing and Materials (ASTM) Method for application and analysis of SSTR monitors for reactor vessel and support structure surveillance.[1] Present SSTR research has concentrated on physics-dosimetric measurements at the Pool Critical Assembly (PCA) at ORNL, a low power mock-up of several thermal shield-pressure vessel surveillance configurations for LWRs; on measurements at the Poolside Facility (PSF), a high-fluence metallurgical-dosimetry LWR-PVS mock-up; and on preparation of advanced SSTR dosimetry capsules for exposures at operating LWRs.

The results of SSTR PCA measurements to date have been reported previously.[2,3] We summarize here the efforts which have provided SSTR dosimetry capsules for the higher fluence environments of the PSF and operating LWRs.

SSTR DOSIMETRY FOR THE PSF METALLURGICAL TESTS

The PSF at the Oak Ridge Reactor is being used to irradiate capsules filled with metallurgical test specimens of vessel and support structure steels as well as a variety of dosimetry sensors in a simulated thermal shield, pressure vessel wall, vessel cavity [void box (VB)] assembly. SSTR capsules have been included with the advanced dosimetry sensor capsules as shown in Figure 1. The SSTR subcapsules contain fissionable deposits of ^{237}Np, ^{238}U, and ^{235}U electroplated into nickel backing wafers placed in firm contact with natural quartz crystal SSTR as shown in Figure 2. The required fissionable deposits have mass densities in the picogram to nanogram per square centimeter range and active diameters of less than 3 mm. The fissionable deposit masses used in a typical PSF capsule are listed in Table I. The extremely low masses of these deposits result from the upper limit on scannable SSTR track density

and the anticipated high neutron fluences in the PSF irradiations. The production and quantification of these deposits required the development of special low mass electroplating and spiking techniques. Natural quartz crystal SSTR were used in the high temperature environs of the PSF because of the higher annealing temperature of this material relative to mica which is used in most SSTR dosimetry. SSTR capsules for a PSF perturbation experiment were irradiated for a much shorter length of time allowing mica SSTR to be used. In selected locations, Exploratory SSTR capsules were included. These capsules contained quartz SSTR with deposits of fissionable isotopes ^{234}U, ^{230}Th, and ^{226}Ra which are not conventionally used in SSTR dosimetry in addition to ^{235}U, ^{238}U, and ^{237}Np. The development of these isotopes for SSTR dosimetry will provide information on additional regions of the neutron spectrum. For instance, ^{226}Ra has a threshold of 3 MeV and may be useful for defining the extremely high energy region of the neutron spectrum. A typical Exploratory SSTR Dosimetry Capsule is shown in Figure 3. SSTR dosimetry packages of design similar to those shown in Figures 2 and 3 can now be made available for use for long term LWR pressure vessel and support structure surveillance at operating reactors.

LWR SSTR SURVEILLANCE DOSIMETRY

SSTR dosimetry capsules have been prepared for irradiation at several different operating LWRs. These irradiations are summarized in Table II. Analysis of the results from the completed irradiations is underway.

CONCLUSIONS

In addition to radiometric and SSTR dosimetry sets, helium accumulation fluence monitors, damage monitors, and temperature monitors are being studied. The ideal dosimetry set would monitor neutron fluence, damage, and temperature with as few materials as possible in order to reduce costs and required space. It is hoped that materials such as quartz SSTR and sapphire damage monitors can be developed as multipurpose materials. Sapphire for instance, might be used as a combined fluence and damage monitor (for example, analyzed for helium accumulation, Np^{237} fissions, and direct neutron damage).

Continuing research will result in the optimization of dosimetry packages for use in long term surveillance of LWR Pressure Vessels.

REFERENCES

1. "Application and Analysis of Solid State Track Recorder (SSTR) Monitors for Reactor Vessel Surveillance," American Society for Testing and Materials Standard Method E706 IIIB.

2. F. H. Ruddy, R. Gold, and J. H. Roberts, "Solid State Track Recorder Measurements in the Poolside Critical Assembly," Proceedings of the Third ASTM-EURATOM Symposium on Reactor Dosimetry, Ispra, Italy (1979).

3. F. H. Ruddy, R. Gold, and J. H. Roberts, "Solid State Track Recorder Measurements," in LWR Pressure Vessel Surveillance Dosimetry Improvement Program: PCA Experiments and Blind Test, W. N. McElroy (Ed.), NUREG/CR-1861, 1981, p 2.5-1.

TABLE I

CONTENTS OF SSTR DOSIMETRY CAPSULES EXPOSED IN THE PSF

Capsule Label	Location*	Isotopic and Mass Density (g/cm^2) ^{235}U	^{238}U	^{237}Np
S1	Surveillance Capsule	2.26×10^{-11}	2.76×10^{-9}	3.60×10^{-10}
S2	" "	2.37×10^{-11}	3.07×10^{-9}	3.83×10^{-10}
S3	" "	2.39×10^{-11}	3.15×10^{-9}	4.26×10^{-10}
S4	" "	2.43×10^{-11}	3.55×10^{-9}	4.57×10^{-10}
S5	Surface of Pressure Vessel	2.53×10^{-11}	3.66×10^{-9}	4.60×10^{-10}
S6	" " " "	2.72×10^{-11}	3.78×10^{-9}	4.94×10^{-10}
S7	T/4	2.75×10^{-11}	4.31×10^{-9}	5.15×10^{-10}
S8	T/2	5.32×10^{-11}	1.00×10^{-8}	7.93×10^{-10}
S9	Behind Void Box	1.83×10^{-10}	2.48×10^{-8}	2.20×10^{-9}
S10	" " "	1.98×10^{-10}	2.59×10^{-8}	6.00×10^{-9}

*T/4 and T/2 refer to locations 1/4 and 1/2 way through a simulated power vessel wall of thickness T.

TABLE II

SSTR DOSIMETRY CAPSULE EXPOSURES IN OPERATING LWRS

Location	Reactor Type	Isotopes Included	Time of Irradiation
Browns Ferry (3)	BWR	^{232}Th, ^{235}U, ^{238}U, ^{237}Np, ^{239}Pu	November, 1978 - August, 1979
McGuire (2)	PWR	^{232}Th, ^{235}U, ^{238}U, ^{237}Np	Februrary, 1981 - present
TIHANGE (1)	PWR	^{235}U, ^{238}U, ^{237}Np	May, 1980 - May, 1981

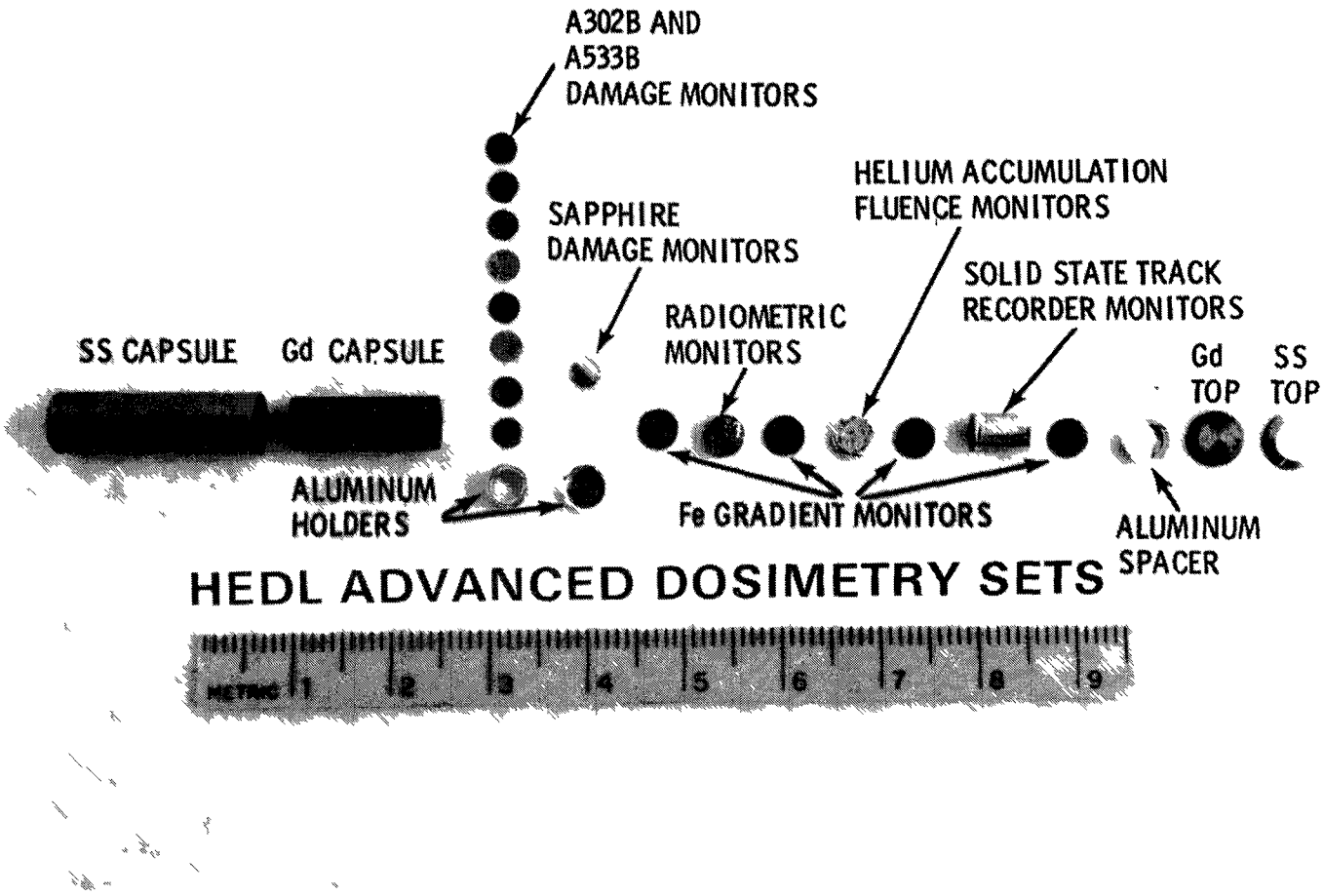

Figure 1. HEDL PSF Advanced Dosimetry Sets.

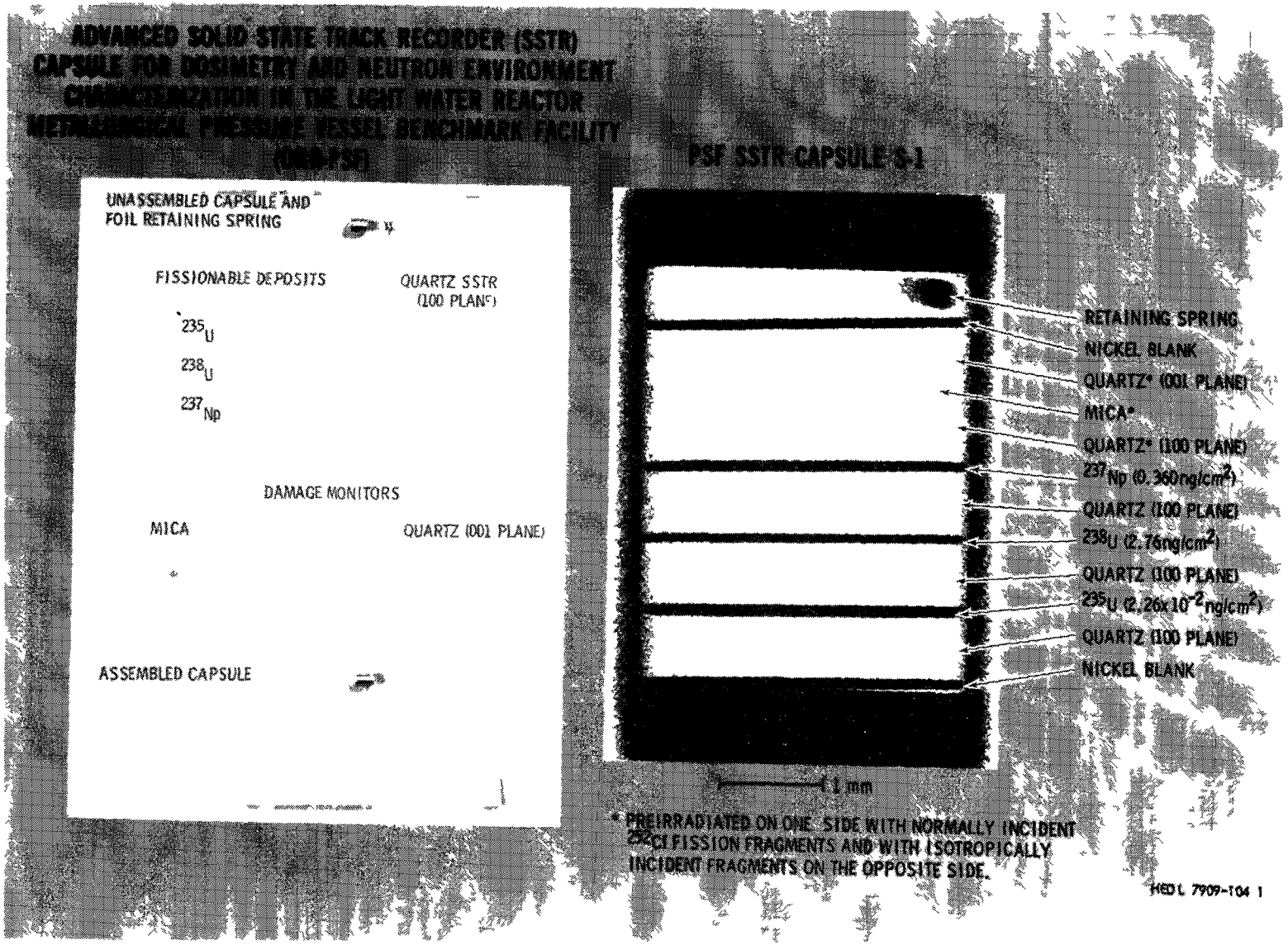

Figure 2. Advanced PSF Solid State Track Recorder Capsule.

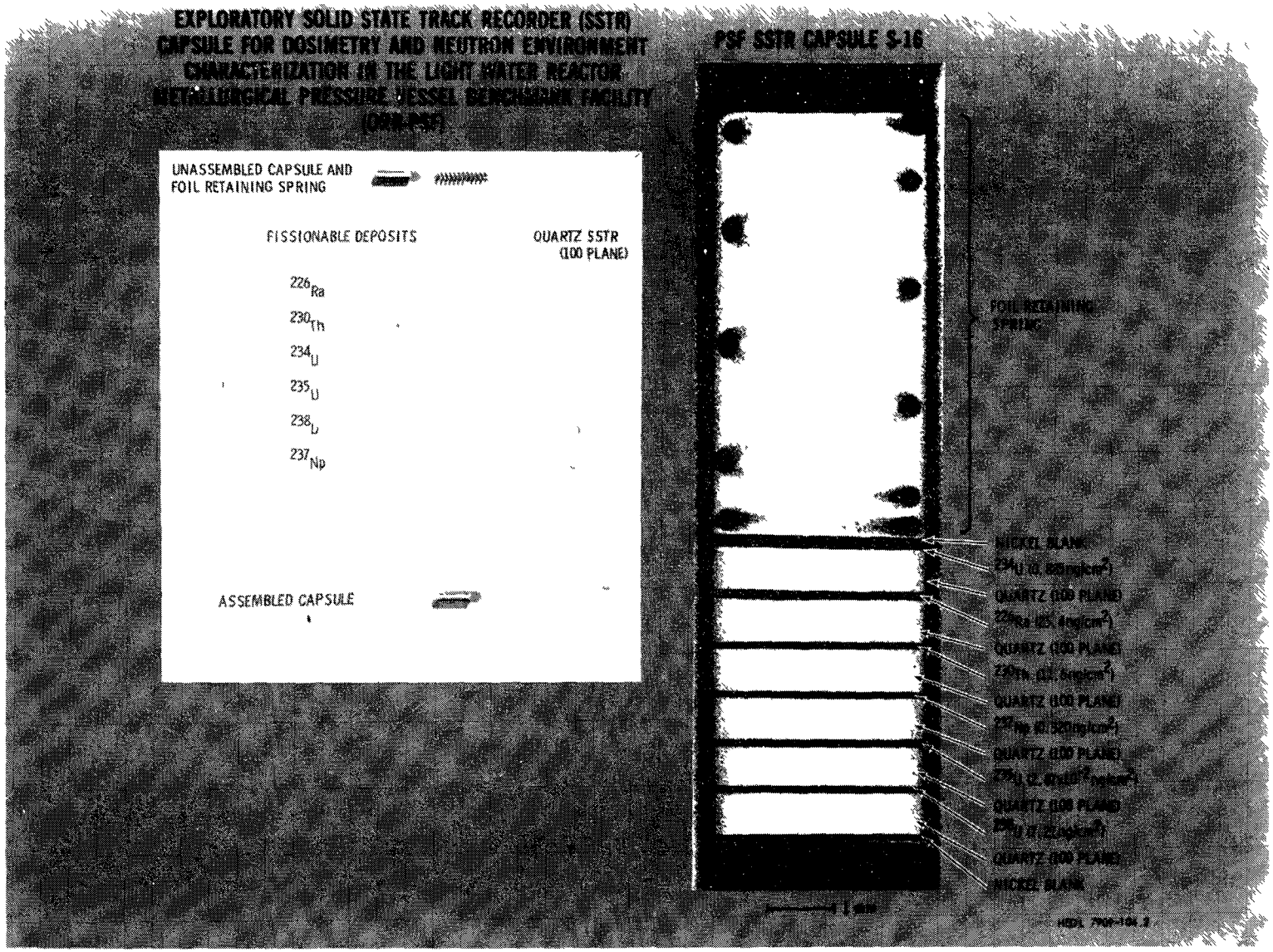

Figure 3. Exploratory PSF Solid State Track Recorder Capsule.

PROTON-RECOIL EMULSION OBSERVATIONS FOR INTEGRAL NEUTRON DOSIMETRY

R. GOLD, J.H. ROBERTS, F.H. RUDDY,
C.C. PRESTON, C.A. HENDRICKS
Westinghouse Hanford Company,
Hanford Engineering Development Laboratory,
Richland, Washington,
United States of America

Abstract

A new method of integral neutron dosimetry with nuclear research emulsions (NRE) is advanced. Two different integral relationships, based upon absolute proton-recoil reaction rates observed in NRE are derived. The method is illustrated with experimental data obtained from NRE which were irradiated in a light water reactor pressure vessel (LWR-PV) benchmark field. Experimental error is estimated for absolute proton-recoil reaction rates observed.

INTRODUCTION

Neutron dosimetry plays a crucial role in understanding the limitations of light water reactor pressure vessels (LWR-PV). The energy dependence of damage produced by neutrons in LWR-PV steel has been recognized for some time now. However, inherent limitations prevent differential measurement of neutron energy spectra in power reactor environments.[1] Integral measurements which can be conducted in power reactors, such as with radiometric, solid state track recorder (SSTR), or helium accumulation fluence monitor (HAFM) dosimeters, possess very limited energy resolution. Of even greater significance is that neutron induced radiation damage in iron is non-negligible in the 0.1-1.0 MeV energy region for these LWR-PV environments. Unfortunately, these passive high power techniques offer little coverage in this energy region. Hence, it is important to develop techniques which extend the applicability and accuracy of these integral methods.

It is possible to use nuclear research emulsions (NRE) to obtain both differential and integral spectral information. Emulsion work is customarily carried out in the differential mode.[2-4] In contrast, emulsion work in the integral mode is a new concept. In the integral mode, emulsions provide absolute integral reaction rates that can be used in spectral adjustment codes.[5] In the past, such adjustment codes have not utilized integral reaction rates based on emulsions. The beauty of emulsion integral reaction rates is their tie to the elastic scattering cross section of hydrogen. This $\sigma_{n,p}(E)$ cross section is universally accepted as a standard cross section and is known to an accuracy of roughly 1%. Hence, emulsion integral reaction rates will afford a significant new dimension for work with spectral adjustment codes.

INTEGRAL MEASUREMENTS WITH NRE

Two different integral relationships can be established using proton-recoil emulsion data. In contrast with NRE work in the differential mode in reactor environments, these integral reaction rates can be obtained with roughly an order of magnitude reduction in track scanning effort. Consequently, this integral mode is an important complementary alternative to the customary differential mode of NRE neutron spectrometry. The integral mode can be applied over extended regions, e.g., perhaps up to as many as 10 in-situ locations can be covered for the same scanning effort expended for a single differential measurement. Hence, the integral mode is especially advantageous for dosimetry applications that require extensive spatial mapping, such as exist in LWR-PV environments.

The first integral measurement follows directly the integral relation between the neutron spectrum and the observed proton spectrum. This relation can be written in the form

$$M(E_T) = n_p \cdot t \int_{E_T}^{\infty} \frac{\sigma_{np}(E)\phi(E)}{E}\, dE. \qquad (1)$$

where $\phi(E)$ is the neutron flux in neutrons/cm^2 per MeV per sec, t is the exposure time, E is the neutron or proton energy in MeV, n_p is the atomic hydrogen density in the emulsion in atoms/cm^3, and $M(E_T)$ is the proton spectrum in proton tracks per MeV per cm^3 observed in the emulsion at energy E_T. The integral in Eq. (2) can be defined as

$$I(E_T) = \int_{E_T}^{\infty} \frac{\sigma_{np}(E)}{E}\, \phi(E)\, dE. \qquad (2)$$

Here $I(E_T)$ possesses units of protons/(MeV-s) per hydrogen atom. Clearly $I(E_T)$ is a function of the lower proton energy cutoff E_T used for analyzing the emulsion data. Using Eq. (2) in Eq. (1), one finds the integral relation:

$$I(E_T) = \frac{M(E_T)}{n_p \cdot t} \qquad (3)$$

$I(E_T)$ is evaluated by using a least squares fit of the NRE scanning data in the neighborhood of $E = E_T$. Alternatively, since:

$$M(E_T) = M(R_T)\, \frac{dR}{dE}, \qquad (4)$$

where dR/dE is known from the proton range-energy relation in emulsions, one need only determine $M(R_T)$ in the neighborhood of $R=R_T$. Here M(R) is the proton-recoil range distribution in units of proton-recoil tracks per μ per cm^3 observed in the emulsion. Consequently, scanning efforts can be concentrated in the neighborhood of $R=R_T$ in order to determine $I(E_T)$. In this manner, the accuracy attained in $I(E_T)$ is comparable to the accuracy of the differential determination of $\phi(E)$, as derived from Eq. (1), but with a significantly reduced scanning effort.

The second integral relation can be obtained by integration of the observed proton spectrum $M(E_T)$. From Eq. (1), one has:

$$\int_{E_{min}}^{\infty} M(E_T)\, dE_T = (n_p \cdot t) \cdot \int_{E_{min}}^{\infty} dE_T \cdot \int_{E_T}^{\infty} \frac{\sigma_{np}(E)}{E}\, \phi(E)\, dE\ , \qquad (5)$$

where E_{min} is the lower proton energy cutoff used in analyzing the emulsion data. Introducing into Eq. (5) the definitions:

$$\mu(E_{min}) = \int_{E_{min}}^{\infty} M(E_T)\, dE_T \,, \tag{6}$$

and

$$J(E_{min}) = \int_{E_{min}}^{\infty} dE_T \int_{E_T}^{\infty} \frac{\sigma_{np}(E)}{E}\, \phi(E)\, dE \,, \tag{7}$$

one has

$$J(E_{min}) = \frac{\mu(E_{min})}{n_p \cdot t} \,. \tag{8}$$

Hence, the second integral relation, namely Eq. (8) can be expressed in a form analogous to the first integral relation, namely Eq. (3). Here $\mu(E_{min})$ is the integral number of proton-recoil tracks/cm^3 observed above an energy E_{min} in the emulsion. Consequently, the integral $J(E_{min})$ possesses units of tracks per second per hydrogen atom.

The integral $J(E_{min})$ can be reduced to the form

$$J(E_{min}) = \int_{E_{min}}^{\infty} \left(1 - \frac{E_{min}}{E}\right) \sigma_{np}(E)\, \phi(E)\, dE \,. \tag{9}$$

In addition, by using Eq. (4), the observable $\mu(E_{min})$ can be expressed in the form

$$\mu(E_{min}) = \int_{R_{min}}^{\infty} M(R)\, dR \,. \tag{10}$$

Hence, to determine the second integral relationship, one need only count proton-recoil tracks above $R=R_{min}$. Tracks considerably longer than R_{min} need not be measured, but simply counted. However, for tracks in the neighborhood of $R=R_{min}$, track length must be measured so that an accurate lower bound R_{min} can be effectively determined.

It is of interest to compare the differential energy responses available from these two integral relations. From Eqs. (2) and (9), one finds responses of the form $\sigma_{np}(E)/E$ and $(1-E_{min}/E)\sigma_{np}(E)$ for the first and second integral relations, respectively. (Note that the integrals $I(E_T)$ and $J(E_{min})$ possess different units, namely protons/MeV-s and protons/s, respectively.) These two responses are compared in Fig. 1, using a common cutoff of 0.5 MeV for both E_T and E_{min}. Since these two responses are substantially different, simultaneous application of these two integral relations is not only possible, but highly advantageous.

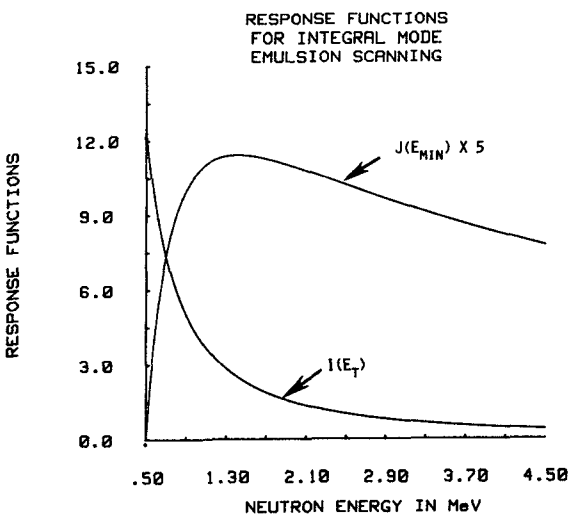

Figure 1. Response Factors for the Integral Reaction Rates $I(E_T)$ and $J(E_{min})$. $I(E_T)$ possesses units of barns/MeV and $J(E_{min})$ possesses units of barns.

ESTIMATION OF UNCERTAINTIES

Sources of systematic uncertainty for absolute neutron dosimetry with NRE are summarized in Table 1. Since these sources of uncertainty are essentially independent, the quadrature uncertainty for all systematic effects comes to roughly 5%. It should be stressed that Table 1 does not include uncertainties arising from the in-situ irradiation such as exist in exposure time t as well as in absolute power level.

TABLE 1
UNCERTAINTY ESTIMATES FOR ABSOLUTE NEUTRON SPECTROMETRY WITH NUCLEAR RESEARCH EMULSIONS

Source of Uncertainty	Approximate Relative Uncertainty (1σ)
1. Proton range straggling	2%
2. Proton energy based on range-energy relation	2%
3. Range measurements	2%
4. Volume of emulsion scanned	2%
5. Hydrogen density in the emulsion	3%
6. Hydrogen $\sigma_{np}(E)$ cross section	1%

Uncertainties in the absolute reaction rates $I(E_T)$ and $J(E_{min})$ follow from Eqs. (3) and (8), respectively. The relative variances for these absolute reaction rates are given by

$$\left(\frac{\delta I}{I}\right)^2 = \left(\frac{\delta M}{M}\right)^2 + \left(\frac{\delta n_p}{n_p}\right)^2 + \left(\frac{\delta t}{t}\right)^2 , \tag{11}$$

and

$$\left(\frac{\delta J}{J}\right)^2 = \left(\frac{\delta \mu}{\mu}\right)^2 + \left(\frac{\delta n_p}{n_p}\right)^2 + \left(\frac{\delta t}{t}\right)^2 . \tag{12}$$

PRELIMINARY RESULTS

Integral measurements have been obtained from emulsions irradiated at the 1/4 T location of the 8/7 and 4/12 SSC configurations of the LWR-PV mock-up at the Pool Critical Assembly (PCA) in Oak Ridge National Laboratory (ORNL).[6] Integral mode scanning of these two emulsions concentrated on the range between 4μ and 8μ, which corresponds to the energy region from 0.407 MeV to 0.682 MeV. Approximately 10^3 tracks were scanned in each emulsion. As can be seen in Figs. 2 and 3, a linear least squares fit of the observed proton-recoil range distribution is quite adequate for both emulsions. Consequently, a linear behavior was assumed in the 4μ to 8μ range, namely

$$m(R) = a + bR \tag{13}$$

where a and b are constants representing the intercept and slope, respectively. Here m(R) is the number of tracks per micron observed, so that

$$m(R) = V \cdot M(R) \tag{14}$$

where V is the volume of emulsion scanned in cm^3.

An attempt was made to optimize the linear least squares fit by changing the partitioning of the data in the 4μ to 8μ range. It was found that the linear least squares fit was quite insensitive to whether four points (tracks/micron) or 8 points (tracks/0.5 micron) were used in this range interval. The value of M(E), as obtained from the linear least squares fit, is given in Table 2 for both emulsions. Relative uncertainties at the 1σ level are also included in this table.

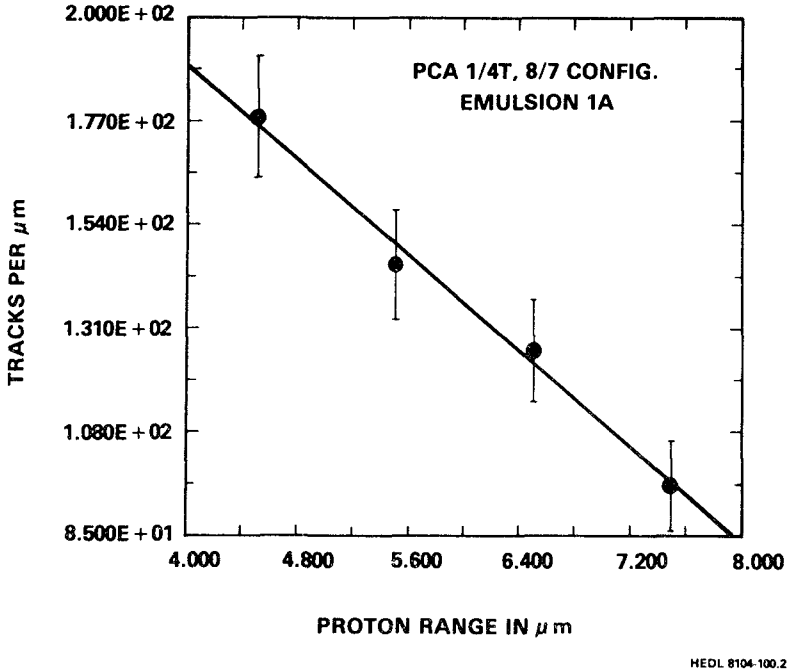

Figure 2. Linear Least Squares Fit of Range Data Observed in PCA Emulsion 1A Irradiated at the T/4 Location of the 8/7 Configuration.

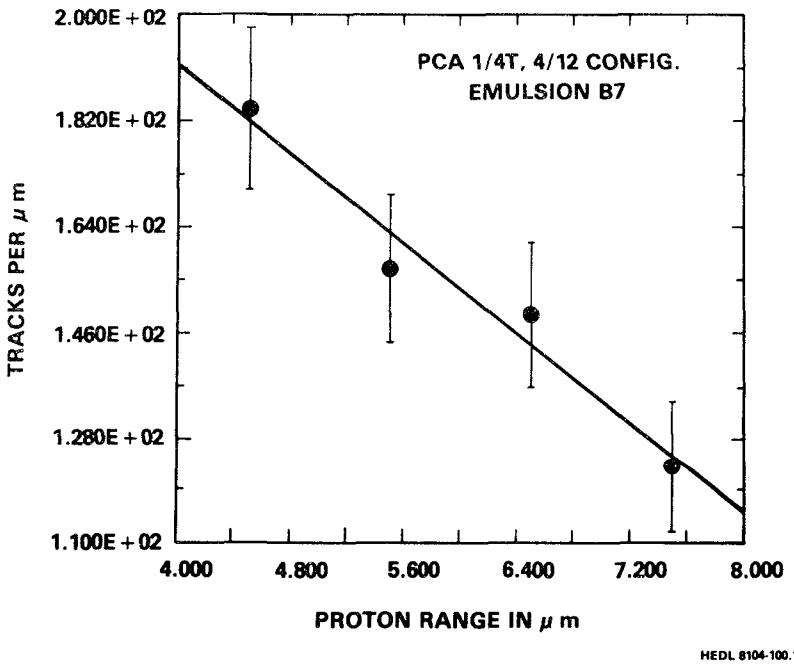

Figure 3. Linear Least Squares Fit of Range Data Observed in PCA Emulsion B7 Irradiated at the T/4 Location of the 4/12 SSC Configuration.

Results from the integral mode scanning for $\mu(E)$ are also presented in Table 2 for both emulsions. On this basis, the integral reaction rates I and J have been determined and can also be found in Table 2. It can be seen that I has been determined to better accuracy than J.

Reaction Rate	Units	Energy (MeV)	Emulsion 1A (1/4 T, 8/7 Configuration) Reaction Rate	Relative Uncertainties* (1σ) (%)	Emulsion B7 (1/4 T, 4/12 SSC Configuration) Reaction Rate	Relative Uncertainties* (1σ) (%)
M(E)	Protons/(MeV·cm^3)	0.519	2.63 x 10^7	5.4	2.76 x 10^7	5.2
μ(E)	Protons/cm^3	0.407	1.28 x 10^7	9.4	1.51 x 10^7	8.9
I(E)	Protons/(MeV·s)	0.519	6.87 x 10^{-19}	6.3	5.76 x 10^{-19}	6.1
J(E)	Protons/s	0.407	3.34 x 10^{-19}	9.9	3.16 x 10^{-19}	9.4
φ(E)**	Neutrons/(cm^2·s·MeV)	0.651	1.08 x 10^5	27.4	5.97 x 10^4	62.4

*Does not include an estimated 6% uncertainty from absolute power normalization.
**Differential neutron flux at energy E.

In addition to I and J, the absolute flux has been determined from these integral mode measurements. To this end, Figs. 4 and 5 present linear least squares fits of the log M(E) as a function of energy for the 8/7 and 4/12 SSC emulsions, respectively. Absolute flux is determined using the results of these least squares fit in Eq. (1). The resulting absolute flux, in units of neutrons/(cm^2 s MeV), is also included in Table 2 for both emulsions.

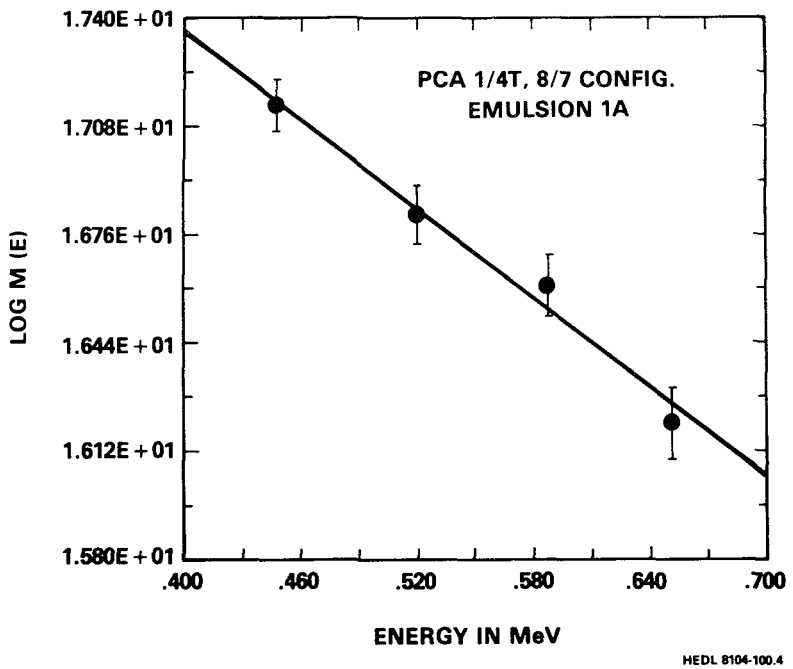

Figure 4. Linear Least Squares Fit of Log M(E) Data for PCA Emulsion 1A Irradiated at the T/4 Location of the 8/7 Configuration.

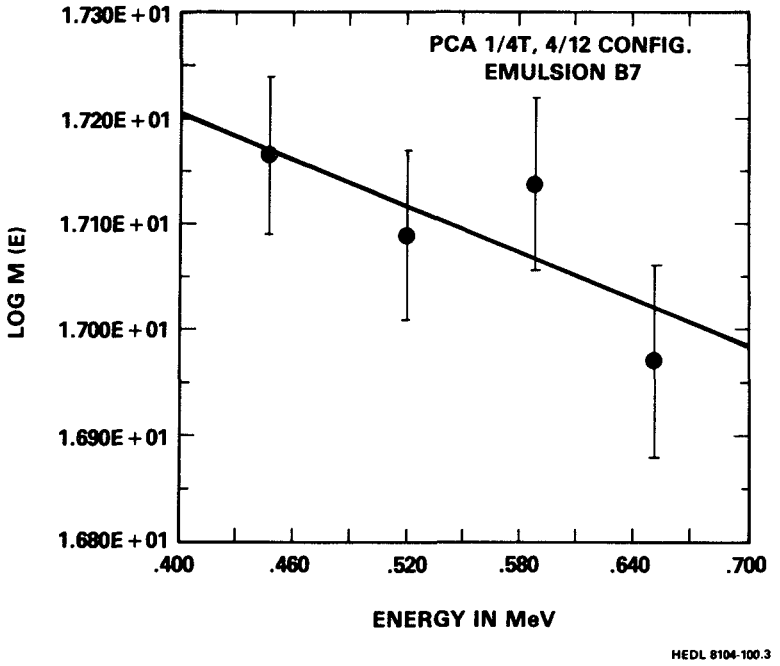

Figure 5. Linear Least Squares Fit of Log M(E) Data for PCA Emulsion B7 Irradiated at the T/4 Location of the 4/12 SSC Configuration.

Actually, the uncertainties in I, J and ϕ behave differently in the 4μ to 8μ interval, i.e., from 0.407 MeV to 0.682 MeV. The uncertainty in J is practically constant throughout this interval with the dominant contribution stemming from uncertainty in range observations. The uncertainty in ϕ decreases monotonically with increasing energy throughout this interval and is dominated by track collection statistics. The uncertainty in I attains a minimum in the interior of this interval, with approximately equal contributions from track statistics and systematic uncertainties (see Table 1). The results given in Table 2 correspond to the minimum uncertainty attained by each observable in this interval.

As one might have anticipated, the uncertainty attained in absolute flux is larger than uncertainties in I or J. Indeed, to expect an accurate absolute flux based on integral mode observation of approximately 10^3 tracks may be asking too much for every NRE measurement attempted. It may well be that the accuracy of the absolute flux determination will vary from case to case and, therefore, may not always be accurate enough for use in spectral adjustment codes. The validity of this conjecture will no doubt be tested as more experience is gained in the use of these integral mode NRE techniques.

REFERENCES

1. R. Gold, "Neutron Spectrometry for Reactor Applications: Status, Limitations, and Future Directions," First International ASTM-EURATOM Symposium on Reactor Dosimetry, Petten, 1975, Part I, 119, EUR-5667 (1977).

2. L. Rosen, "Nuclear Emulsion Techniques for the Measurement of Neutron Energy Spectra," Nucleonics 11, p. 32, 1953 and 12, p. 38, 1953.

3. J. H. Roberts, "Absolute Flux Measurements of Anisotropic Neutron Spectra with Proton Recoil Tracks in Nuclear Emulsions," Rev. Sci. Instr. 28, p. 667, 1957.

4. J. H. Roberts and A. N. Behkami, "Measurements of Anisotropic Neutron Spectra with Nuclear Emulsion Techniques," Nucl. Appl. 4, p. 182, 1968.

5. Current Status of Neutron Spectrum Unfolding, IAEA-TECDOC-221, International Atomic Energy Agency, Vienna, Austria, August 1979.

6. W. N. McElroy, Editor, "LWR Pressure Vessel Surveillance Dosimetry Improvement Program: PCA Experiments and Blind Test," NUREG/CR-1861, HEDL-TME 80-87 (1981).

A SIMPLE MODEL FOR CALCULATION OF FAST NEUTRON-INDUCED γ-RAY SPECTRA

B. BASARRAGTSCHA*, D. HERMSDORF, D. SEELIGER
Technical University Dresden,
Dresden,
German Democratic Republic

Abstract

A semiempirical model, the so-called R-parameter model, introduced by Howerton and Plechaty has been proved to be a simple but, nevertheless a very successful formalism for the description of γ-ray spectra emitted in the course of nuclear reactions induced by fast neutrons. By the single parameter R the γ-ray spectrum will be predicted with a satisfying reliability in a wide range of nuclear masses and neutron incidence energies. The formalism is limited by neutron incidence energies above the (n,2n)-threshold. Above this energy a modified ansatz proposed by the present work yields good results.

1. Introduction

With increasing application of neutron radiation in science, technology and medicine the transport of neutrons and induced by them secondary radiation (charged particles and γ-rays) a cross materials is of raising interest. Especially the γ-radiation field build up by fast neutron-induced nuclear reactions should be investigated to evaluate problems like energy deposition, induced radioactivity, radiation damage a.o. relevant for dosimetry, radiation protection and material testing. In all cases precise data for fast neutron-induced emission of γ, n, p, α, d ... radiation (angular distributions as well as energy spectra) are necessary. But, in many cases these data will be known very roughly or they are absent totally.

Considering neutron-induced γ-ray production cross sections the situation has been improved by carrying out systematical measurements of γ-ray spectra throughout the periodic system of nuclear masses /1/ and the simultaneous development of spectra unfolding methods /2/.

At present, experimentally obtained γ-ray spectra are known in a wide mass range for neutron incident energies from 1 to 20 MeV with a typical error of about 20 to 30 %. The spectra exhibits a more or less flat distribution arising from γ-transitions within

---

* Present address: State University of Ulan Bator, Mongolia.

the level continuum superimposed by peaks associated to transitions to low-lying states in the residual nuclei. Describing the gross behaviour responsible for the integral γ-ray production cross section the use of a probability distribution analogous to the Maxwellian type of neutron emission spectra is obvious also.

Basing on this idea, Howerton and Plechaty /3/ have introduced a semiempirical formula, the so-called R-parameter formalism, which has been applied very sucessful for explaining a great bulk of experimental data to a reasonable degree of confidence.

The present paper is reviewing the application of the model and will show possible further refinements.

2. Description of the R-parameter formalism

Analyzing experimental results of γ-ray spectra arising from $(n,x\gamma)$ reactions induced by neutrons of incident energies E_n higher than 4 MeV Howerton and Plechaty /3/ deduced a semiempirical formula proceeding from the well established fact that the spectrum of continuously emitted γ-radiation with energies $E_\gamma > 1$ MeV can be expressed in terms of a Maxwellian distribution

$$N(E_\gamma) = E_\gamma \exp(-R(E_n)\, E_\gamma) \tag{1}$$

In equation (1) a parameter R is introduced, which is assumed to depend on the neutron incidence energy E_n and the mass number A. The γ-ray spectrum is related to (1) using a normalization factor F given by

$$F(E_n) = \sigma_{n,x\gamma}(E_n) \int_0^{E_\gamma^{max}} N(E_\gamma)\, dE_\gamma \tag{2a}$$

and

$$\frac{d\sigma_{n,x\gamma}(E_n,E_\gamma)}{dE_\gamma} = F(E_n)\, N(E_\gamma)\,. \tag{2b}$$

An evaluation of equ. (2a) yields

$$F(E_n) = \frac{R^2(E_n)\,\sigma_{n,x\gamma}(E_n)}{1-(RE_\gamma^{max}+1)\exp(-RE_\gamma^{max})} \tag{3}$$

defining an averaged maximum of γ-ray energies by

$$E_\gamma^{max} = \frac{(E_n-\bar{E}_{n'})\,\sigma_{n,n'\gamma} + (E_n-Q_{n,n'}-2\bar{E}_{2n'})\,\sigma_{n,2n\gamma}}{\sigma_{n,n'\gamma} + \sigma_{n,2n\gamma}} \qquad (4)$$

Following symbols will be used in equ. (4):

$Q_{n,n'}$, $Q_{n,2n}$	- thresholds for (n,n') and (n,2n) reaction respectively;
$\bar{E}_{n'}$, $\bar{E}_{2n'}$	- mean energy of emitted neutrons from (n,n') and (n,2n) reaction respectively;
$\sigma_{n,n'\gamma}$, $\sigma_{n,2n\gamma}$	- cross section for (n,n') and (n,2n) reaction respectively.

Taking a Maxwellian typ for the neutron spectra the mean energies $\bar{E}_{n'}$ and $\bar{E}_{2n'}$ can be expressed by the well-known nuclear temperatures T and T'

$$\bar{E}_{n'} = 2T \approx 6\sqrt{\frac{E_n+8\ \mathrm{MeV}}{A}} \qquad (5a)$$

and

$$\bar{E}_{2n'} = 2T' \approx 6\sqrt{\frac{E_n-\bar{E}_{n'}}{A}} \qquad (5b)$$

Also the mean γ-ray energy is determined using equ. (1) to be

$$\bar{E}_\gamma = \frac{2\left[1-\left(\frac{R^2 E_\gamma^{max\,2}}{2} + RE_\gamma^{max} + 1\right)\exp\left(-R\,E_\gamma^{max}\right)\right]}{R\left[1-(R\,E_\gamma^{max} + 1)\exp\left(-R\,E_\gamma^{max}\right)\right]} \,. \qquad (6)$$

By this the γ multiplicity $\bar{M}_\gamma$ can be expressed

$$\bar{M}_\gamma = \frac{E_\gamma^{max}}{\bar{E}_\gamma} \qquad (7a)$$

applying equs. (4) and (6) or

$$\bar{M}_\gamma = \frac{\sigma_{n,x\gamma}}{\sigma_{n,n'\gamma} + \sigma_{n,2n\gamma}} \qquad (7b)$$

All equations are valid only for fast neutron induced reactions on non-fissile nuclei and neglect contributions from discrete γ-lines and neutron capture.

An extension to fissile nuclei will be done taking a multiplicity to be 7.4 /4/ resulting in

$$\sigma_{n,x\gamma} = \bar{M}_\gamma \left(\sigma_{n,n'\gamma} + \sigma_{n,2n\gamma} \right) + 7.4\, \sigma_{n,f\gamma} \qquad (8)$$

and adding a contribution $7.4\ \sigma_{n,f\gamma}\ N'(E_\gamma)$ to equ. (3). Here $N'(E_\gamma)$ means the spectrum of γ-quanta from the fast neutron-induced fission which may be different from $N(E_\gamma)$.

3. Application of the model

3.1. Determination of the functional dependences of R

The formalism discussed above is determined totally by only one parameter depending on neutron incidence energy and mass number $R(E_n,A)$.

These dependencies have been studied systematically by Howerton and Plechaty /3/ also. At neutron incident energies of 4.1 and 14.8 MeV they had deduced values of R in a wide range of atomic masses. This is carried out by a least-squares-method to fit equ. (1) to the experimental γ-ray spectra, or easily by a eye-guided definition of the shope of a straight line resulting from a plot $N(E_\gamma)/E_\gamma$ against E_γ.

Clearly a linear dependence on A could be justified. Keeping E_n fixed

$$R\ (4.1\ \text{MeV}) = 0.00395\ A + 0.940 \qquad (9)$$

and

$$R\ (14.8\ \text{MeV}) = 0.00585\ A + 0.335 \qquad (10)$$

have been obtained. This is summarized in fig. 1.

From this a parametrization was proposed:

$$R\ (E_n,A) = 0.00395\ A + 0.940 + \frac{E_n - 4.1\ \text{MeV}}{14.8\ \text{MeV} - E_n}\ (0.0019\ A - 0.605) \qquad (11)$$

(E_n in units MeV, R in MeV^{-1}).

Recently the energy dependence has been investigated in more detail by Hino et al. /5/ for Sn and Ba and by the authors for ^{93}Nb. The obtained results are also included in fig. 1.

As most striking feature of the results extracted from ^{93}Nb an energy dependence of R appears, which is clearly different from that predicted from eq.(11) (fig. 2a).

So, an ansatz of the type

$$R\ (E_n,A) = a\ (E_n)\ A + b\ (E_n)$$

has been followed. Using all available informations known for R such a relation can be approximated by

$$R\ (E_n,A) \approx 0.6\ (1-e^{-0.274\ E_n})\ A + e^{-0.15\ E_n} + 0.2 \qquad (12)$$

(E_n in MeV, R in MeV^{-1}). This is shown in fig. 2b.

Equ. (12) may be proposed for an more consistent with experimental interpolation formula for R.

3.2. Description of experimental γ-ray spectra and γ-ray production cross sections

To demonstrate the very satisfying application of the R-parameter formalism three examples obtained from ^{93}Nb+n will be choosen. In figs. 3, 4 and 5 measured γ-ray spectra at 4, 6 and 14 MeV neutron incident energies taken from refs /6/ and /7/ are shown together with their interpretation in the simple R-parameter model as well as in terms of the most refined model available at present for description of γ-ray emission from highly excited nuclei basing on the Hauser-Feshbach formalism (H-F model) for nuclear reactions /8,9/.

Such a comparison leads to the following conclusions on the limitations and the reliability of the semiempirical R-parameter model:
At neutron incident energies above 4 MeV and quite below the (n,2n)-threshold the spectra can be well described in terms of the simple model defined by equs. (1) and (2). The results using a constant parameter R are nearly equivalent to that obtained with high complex and time-consuming calculations.

Above this threshold the situation is worse because of a strong component resulting from low-energetic γ-ray emission from (n,2nγ) reaction, which disturbes the simple spectral shape. From fig. 5 clearly can be seen that the spectrum is composed of two different distribution functions which may accounted for by two different values of Ralso.

Less sensitive against such differential effects the integrated over γ-ray energies cross section $\sigma_{n,x\gamma}$ appear. As shown in fig. 6 the γ-ray production cross section for ^{93}Nb+n can be well predicted by the simple R-parameter model in reasonable agreement with experimental results taken from refs. /6,7,10/.

4. Improvements of the R-parameter model

Starting from our investigations of γ-ray spectra produced by neutrons with energies above the (n,2n)-threshold an improvement of the simple Howerton's ansatz (1) seems reasonable. Therefore, equation (1) has been modified to read

$$N(E_\gamma) = E_\gamma \exp(-R(E_n, E_\gamma) E_\gamma) \qquad (13)$$

assuming the parameter R to be dependent on the γ-ray energy E_γ also.

For an investigation of this dependency, a differential fit has been carried out dividing the experimental γ-ray spectra into small energy bins. After smoothing the experimental data this procedure results in really γ-ray dependent values of R shown in fig. 7 for ^{93}Nb+n.

In deed, for neutron energies below the (n,2n)-threshold R may be considered constant approximately for $E_\gamma > 1.5$ ...2MeV.

On the other hand, above this threshold (in fig. 7 at 14 MeV) the function $R(E_\gamma)$ shows clearly two ranges. In each range the values of R are nearly constant also but they are changing rapidly in a small intervall of E_γ. The functional dependence on E_γ may be expressed as a simple jump. Inserting such a jump in R into the formalism a much better agreement between experiments and the model predictions is obviously seen in fig. 5.

It may be reserved for the next future to analyze all experimental spectra obtained at neutron energies above the (n,2n)-threshold in terms of the ansatz (13).

5. Conclusions

The R-parameter model introduced by Howerton and Plechaty is a very simple but efficient and succesful approach to describe γ-ray spectra produced in the course of inelastic scattering of fast neutrons in the energy range from about 4 MeV up to the (n,2n)-threshold. It provides for a quick estimation of unmeasured γ-ray spectra using R-parameters evaluated from an interpolation in mass and neutron energy dependences.

The simple model holds true only as long as the (n,2n)-reaction is still closed. If the neutron incidence energy exceeds this threshold a modified version including γ-ray energy dependent R is favoured yielding better results. In this case no simple interpolation shema is known up to now.

References

/1/ J.K. Dickens et al., Nucl. Sci. Eng. 62 (1977) 515

/2/ Y. Hino et al., Nucl. Sci. Techn. 15 (1978) 85

/3/ R.J. Howerton, E.F. Plechaty, Nucl. Sci. Eng. 32 (1968) 178

/4/ H. Goldstein, in Reactor Handbook, Vol. III, part B, p. 16, New York, 1962

/5/ Y. Hino et al., private communication, 1981

/6/ D.M. Drake, J.C. Hopkins, C.S. Young, H. Condé, Nucl. Sci. Eng. 40 (1970) 294

/7/ C.S. Young et al., in Proc. Int. Conf. on Neutron Cross Section Technology, Washington, 1975

/8/ M. Uhl, B. Strohmaier, Report IRK-76/01, 1976

/9/ B. Basarragtscha, D. Hermsdorf, D. Seeliger, in Proc. 2nd Int. Symp. on Neutron Induced Reactions, Smolenice, 1979, Physics and Applications Vol. 6, p. 381, Bratislava, 1980;
B. Basarragtscha, D. Hermsdorf, E. Paffrath, submitted to J. of Physics G: Nucl. Phys.

/10/ D.L. Broder et al., Atomn. Ehnerg. 16 (1964) 103

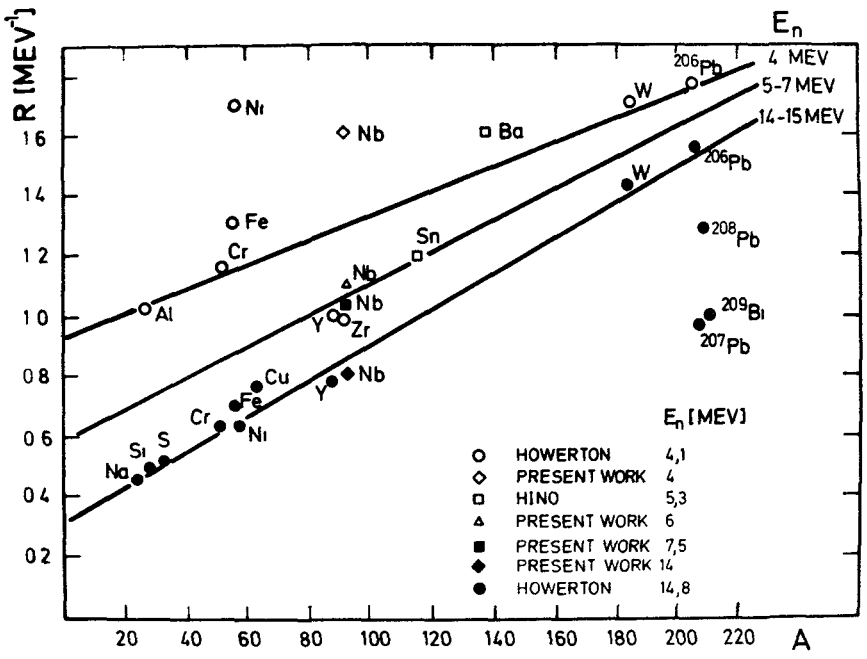

Fig. 1 Systematics of mass dependence of R at constant neutron incidence energies E_n.
Values of R extracted at different neutron energies may be fitted by straight lines.

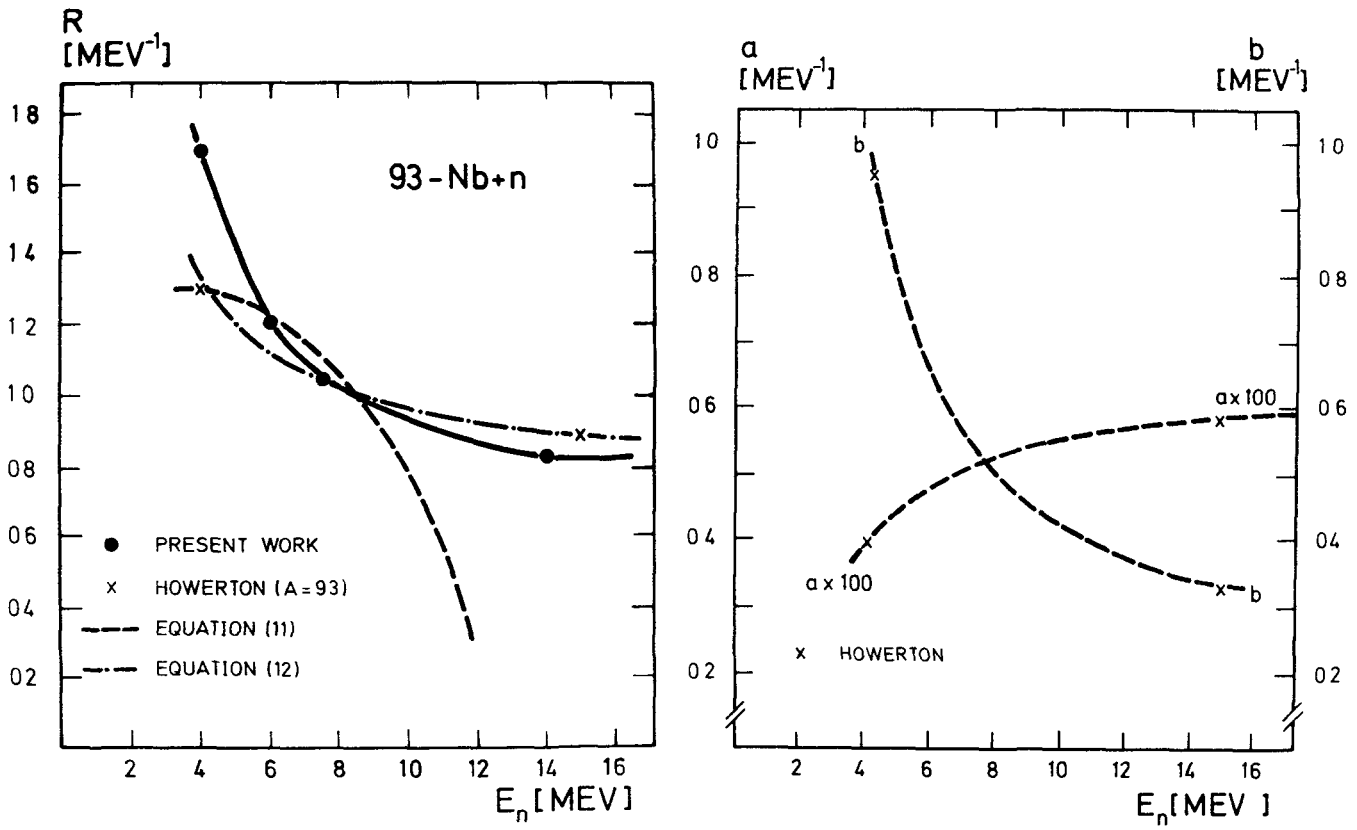

Fig. 2 Dependence of R on the neutron incidence energy E_n.
a) Experimental and predicted by the R-parameter model energy dependencies for A = 93,
b) expected energy dependence of R in terms of the ansatz R = a (E) A + b (E).

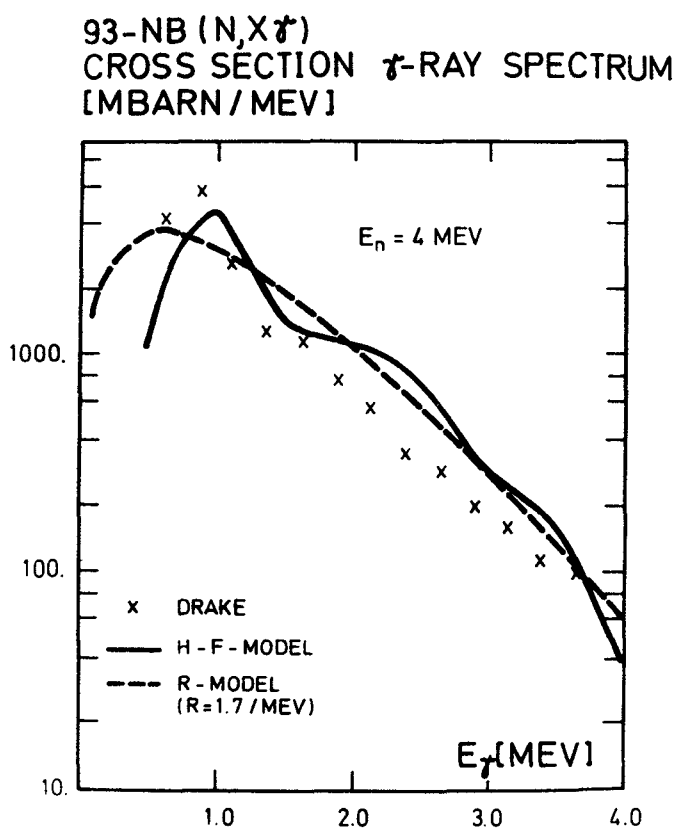

Fig. 3 γ-ray spectra produced by ^{93}Nb bombarded with neutrons of 4 MeV.
Experimental data taken from Drake et al. /6/ are compared the theoretical predictions in the frame of the statistical model (H-F) and the R-parameter model.

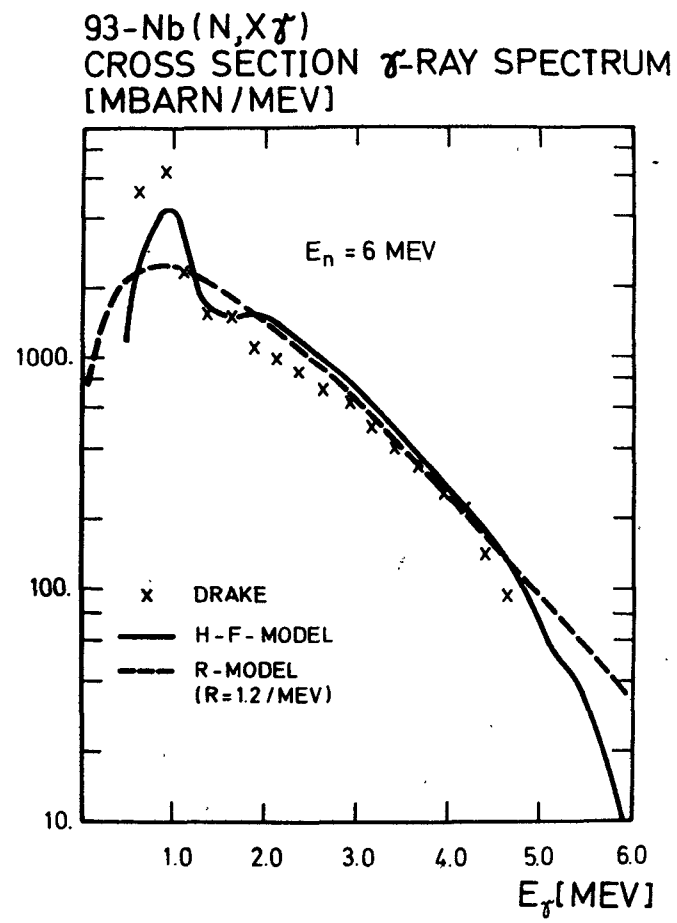

Fig. 4 Same as in fig. 3 for 6 MeV neutrons.

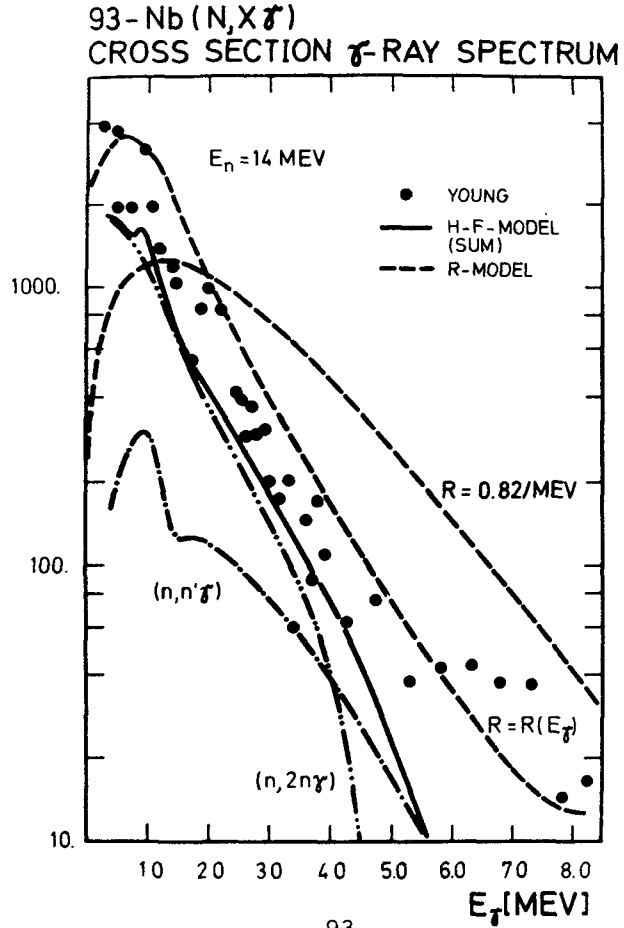

Fig. 5 γ-ray spectra produced by ^{93}Nb bombarded with neutrons of 14 MeV.
Experimental data taken from Young et al. /7/ are compared with theoretical predictions in the frame of the statistical model (H-F) and the R-parameter model in simple version of equ. (1) and the modified one (equ. (13)).

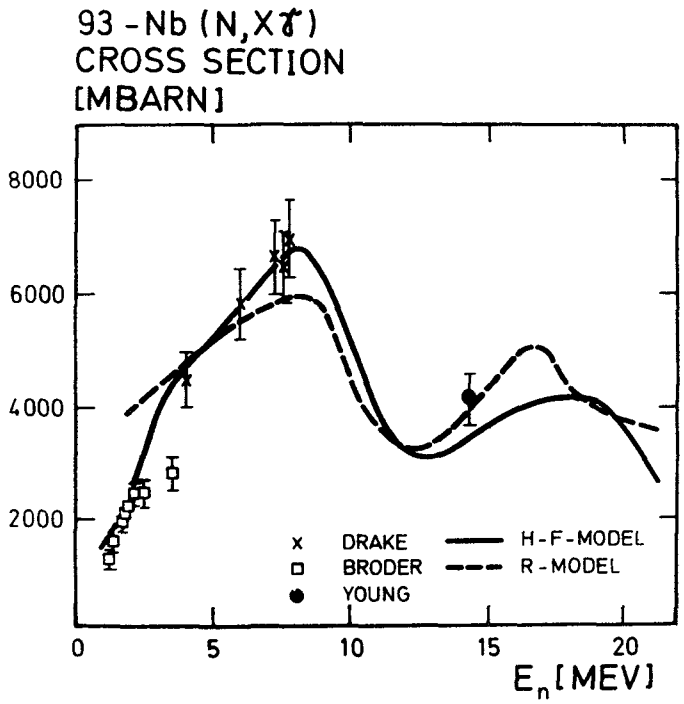

Fig. 6 γ-ray production cross section for ^{93}Nn+n.
Experimental data from refs. /6,7 and 10/ are compared with statistical model (H-F) and the simple R-parameter model.

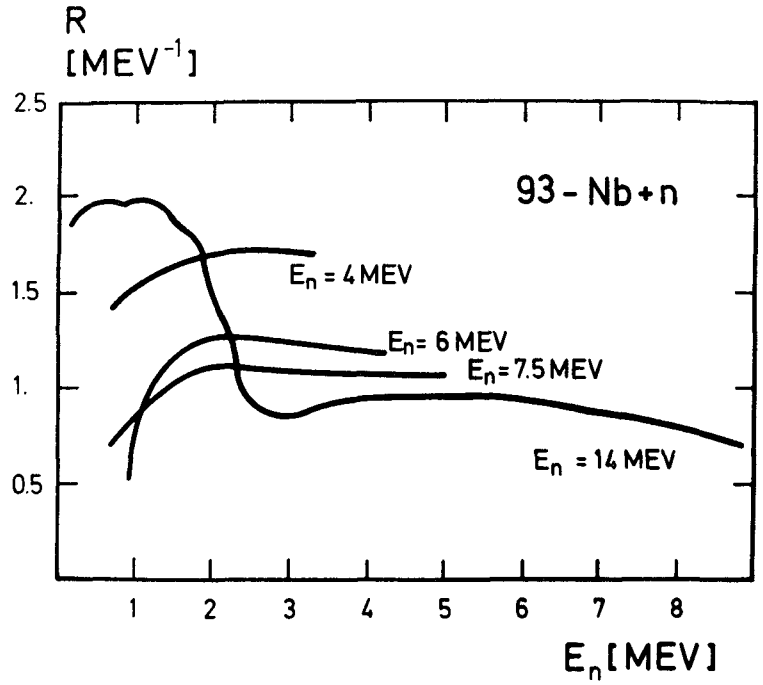

Fig. 7 Dependence of R on the γ-ray energy E_γ at constant mass A = 93 and different neutron incidence energies E_n. At neutron energies below the (n,2n)-threshold R is approximately constant for $E_\gamma > 2$ MeV, whereas above this threshold R is really divided into two ranges according to γ-quanta from (n,n'γ) and (n,2nγ) reactions respectively.

NEUTRON CROSS SECTION CALCULATIONS FOR ^{52}Cr, ^{55}Mn, ^{56}Fe AND $^{58,60}Ni$ FOR INCIDENT ENERGIES UP TO 30 MeV*

B. STROHMAIER, M. UHL, W. REITER
Institut für Radiumforschung und Kernphysik der
Universität Wien,
Vienna,
Austria

Abstract

Neutron induced cross sections for the most abundant isotopes of Cr, Mn, Fe and Ni were calculated up to an incident energy of 30 MeV. The emission of neutrons, protons, alpha particles and photons was considered. The choice of a consistent set of model parameters is described and a comparison of calculated cross sections with experimental data is presented.

1. Introduction

For the most abundant isotopes of Cr, Mn, Fe and Ni we calculated the following neutron induced reaction cross sections to 30 MeV incident neutron energy:
. total
. differential elastic
. activation cross sections for particular reaction paths, e.g. (n,pn) and (n,np)
. production spectra of emitted particles and photons integrated over the full solid angle
. production cross sections of all residual nuclei summed over all considered reaction paths
. H and He production cross sections

The large amount of experimental data which exists for several of the above cross sections, though mostly below 20 MeV, was exploited for the adjustment and verification of model parameters.

2. Procedure

For an incident neutron energy of 30 MeV, reactions with up to 3 or 4 emitted particles are allowed by energy conservation. As different types of emitted particles we considered neutrons, protons and alpha-particles. This means that for a given target nucleus 27 to 81 reaction paths have to be considered.
The following nuclear reaction models were applied for the cross section calculations:
- compound nucleus evaporation model for the treatment of multiple emission of particles and gamma-rays
- exciton model for first chance precompound emission
- optical model for the total and the elastic cross sections and for the creation of the transmission coefficients required for the above named models.

For the computations, we used the code STAPRE /1/ which incorporates the former two models, and and the optical model code ABACUS II /2/. In a later stage, we plan to include direct reaction contributions to inelastic neutron scattering populating low excited collective levels.
The results of the calculations critically depend on a set of model parameters. We attempted to find a consistent set of model parameters which in the mass region of interest reproduces simultaneously :
. total and differential elastic neutron cross sections
. average resonance data as spacings and strength functions
. cross sections for competing reactions of the type (n,nx), (n,px) and (n,αx)
. cross sections for (p,nx) and (α,nx) reactions.

---

*Work partly supported by EURATOM, CCR Ispra (Italy)

3. Determination of the model parameters

On the basis of the above explained general principles the particular choice of the model parameters and their adjustment by comparison to experimental data was performed as follows:

3.1. Transmission coefficients

i. Neutrons
We utilized the optical potential by Arthur and Young /3/, who made very extensive calculations of neutron induced reaction cross sections for $^{54,\ 56}Fe$.

The energy dependence of the volume absorptive potential between 0 and 10 MeV was slightly changed.
This potential reproduces the total and the differential elastic cross section of iron very well. As it gives also acceptable fits to the total and differential elastic cross sections and the strength functions of the other considered isotopes, we used it for all nuclei.

ii. Protons
For protons we chose the optical potential by Mani et al. /4/. Its applicability was additionally made sure of by reproducing experimental (p,n) cross section data; the calculated cross sections were corrected for isospin effects employing the model of Grimes et al. /5/ with a mixing parameter $\mu = 0.4$.

iii. Alpha-particles
For alpha-particles we used a potential derived from that of McFadden et al./6/. The potential could be verified by reproduction of experimental (α,n) cross sections. In contrast to the potential by Huizenga et al. /7/, the modified McFadden potential reproduces experimental (n,α) cross sections with level density parameters which are consistent with resonance data.

iv. Photons
For E1 radiation we used the Brink-Axel model /8/ which relates the strength function to the photo-absorption cross section. In spite of the severe fragmentation of the giant dipole resonance for $A<60$ we approximated it by a single Lorentz curve with resonance energy $75/A^{1/3}$ MeV and width 5.5 MeV. These values are reasonably consistent with the compilation by Berman et al. /9/. For improving the reproduction of the experimental 14 MeV photon production spectra, the E1 strength function was reduced by a factor of 0.55 below 6 MeV. For the strength functions of the other multipole types, the Weisskopf model /10/ was used. They were normalized relative to the E1 strength function at the neutron binding energy according to the systematics of McCullagh et al./11/ in the case of M1 radiation and according to Weisskopf's estimate for E2, M2 and E3. An overall normalization factor was determined so as to reproduce experimental capture cross sections for some nuclei, however, without consideration of valence capture. A weighted average over the thus obtained normalization factors was taken for those nuclei for which no experimental capture cross sections are available.

3.2. Exciton model parameters

The particle-hole state densities were calculated with the Pauli principle corrected formula of Williams /12/ with a global expression for the single particle state density $g = 6/\pi^2 * A/8$ and with a simple pairing correction. The emission rates for nucleons account for the type of the projectile as proposed by Gadioli et al. /13/, those for α-particles are based on the model of preformed α-clusters /14/ with a global preformation factor $\varphi = 0.2$. For the internal transition rates we used Williams' /15/ expressions. The quantity FM which via the relation $|M|^2 = FM\ A^{-3}\ U^{-1}$/16/ defines the squared transition matrix elemnet for given excitation energy U, was adjusted so as to reproduce the high energy portion of (n,pγ) excitation functions and the high energy tail of proton production spectra at 15 MeV incident neutron energy. The parameters were further verified by comparing neutron production spectra with measurements. In order to check the applicability of this parametrization of preequilibrium decay also at higher incident energies, we calculated some (p,xnγ) excitation functions for incident energies to 40 MeV.

3.3. Levels and level density parameters

The level density is calculated in the frame of the back-shifted Fermi gas model /17/. We redetermined the parameters a and Δ for those nuclei for

which more recent data on levels /18/ and resonance spacings (mostly refs. 19,20) were available; the rigid body value with r_o = 1.25 fm was assumed for the effective moment of inertia. If required for the reproduction of experimental cross sections we varied the level density parameters within their uncertainties. If no resonance information was available we used systematics and whenever possible we chose the level density parameters so as to fit experimental cross sections simultaneously.
Also for the explicit consideration of levels, the information was taken from ref 18.

4. Results and discussion

We found that for incident energies to 30 MeV only reaction paths with three emission steps at most have to be considered. Among these, paths with three charged particles can be neglected. For most of the paths with two charged particles, a Weisskopf-Ewing version of the STAPRE code was used.
The calculations reproduce the available experimental data in general within 20 %, in many cases much better. Therefore, we estimate errors of 20 - 30 % for extrapolated cross sections which at some energy are confirmed by experimental data. Only slightly diminished accuracy applies to the prediction of unknown cross sections which involve nuclei whose level dnesity is confirmed by other data. For reactions which populate nuclei far from the line of beta stability, the errors may be much larger. As in general these reactions contribute only little to the gas production cross sections, we estimate an accuracy of 20 - 20 % for these quantities as well as for the particle production spectra with exception of the highest energy contributions which are dominated by direct reactions.

References

/1/ B. Strohmaier and M. Uhl, Proc. Winter Course Nucl. Theory for Applications, Trieste, 1978, IAEA-SMR-43 (1980), p. 318
/2/ E. H. Auerbach, Rept. BNL-6562 (1962)
/3/ E. D. Arthur and P. G. Young, Rept. LA-8626-MS (ENDF-304) and Proc. Int. Symp. Neutron Cross Sections from 10 to 50 MeV, Brookhaven 1980, p. 731
/4/ G. S. Mani, M. A. Melkanoff and I. Iori, Rept. C.E.A.-2379 (1963)
/5/ S. M. Grimes, J. O. Anderson, A. K. Kerman and C. Wong, Phys. Rev. C5 (1972) 85
/6/ L. McFadden and G. R. Satchler, Nucl. Phys. 84 (1966) 177
/7/ J. R. Huizenga and G. J. Igo, Rept. ANL-6373 (1961)
/8/ D. M. Brink, Thesis, Oxford University (1955) and P. Axel, Phys. Rev. 126 (1962) 671
/9/ B. L. Berman and S. C. Fultz, Rev. Mod. Phys. 47 (1975) 713
/10/ J. M. Blatt and V. F. Weisskopf, "Theoretical Nuclear Physics", John Wiley and Sons Inc., (1952)
/11/ C. M. McCullagh, M. L. Stelts and R. E. Chrien, Phys. Rev. C23 (1981) 1394
/12/ F. C. Williams, jr., Nucl. Phys. A166 (1971) 231
/13/ E. Gadioli, E. Gadioli-Erba and P. G. Sona, Nucl Phys. A217 (1973) 589
/14/ L. Millazzo-Colli, G. M. Braga-Marcazzan, Nucl. Phys. A210 (1973) 297
/15/ F. C. Williams, jr., Phys. Lett. 31B (1970) 184
/16/ C. Kalbach-Cline, Nucl. Phys. A210 (1973) 590
/17/ W. Dilg, W. Schantl, H. Vonach and M. Uhl, Nucl. Phys. A217 (1973) 269
/18/ C. M. Lederer and V. S. Shirley (eds.), "Table of Isotopes", Seventh edition, John Wiley and Sons Inc., N. Y. (1978)
/19/ G. Rohr, Proc. Specialists' Meeting Neutron Data of Structural Materials for Fast Reactors, Geel, 5-8 Dec. 1977, Pergamon Press (1979), p. 614
/20/ F. H. Froehner, Proc. Int. Conf. Neutron Physics and Nucl Data for Reactors and other Applied Purposes, Harwell, 25-29 Sept. 1978, p. 268
/21/ A. Pavlik and G. Winkler, priv. comm.

SPECTRAL INDICES OF SOME THRESHOLD REACTIONS MEASURED IN URANIUM 235 FISSION SPECTRUM

I.N. ACQUAH*, B. GLUMAC, I. REMEC, M. NAJŽER
University E. Kardelj,
Jožeph Štefan Institute,
Ljubljana,
Yugoslavia

ABSTRACT

Spectral indices of nine treshold reactions $^{24}Mg(n,p)$, $^{27}Al(n,alpha)$, $^{56}Fe(n,p)$, $^{64}Zn(n,p)$, $^{19}F(n,2n)$, $^{115}In(n,n')$, $^{47}Ti(n,p)$, $^{58}Ni(n,p)$ and $^{127}I(n,2n)$ were measured in the uranium 235 fission spectrum of a fission plate driven by thermal neutrons from the thermalizing column of the 250 kW TRIGA reactor. The reaction rates were calculated from the activities of irradiated foils determined by a calibrated Ge-Li spectrometer. Results were corrected for the fission spectrum distortions calculated by the ANISN transport code. Measured values are compared with the data from the Fabry's evaluation.

1. INTRODUCTION

Fission spectrum averaged cross sections are among most important nuclear data for reactor neutron dosimetry. Several measurements in U 235 fission spectrum have been performed in various neutron fields such as core of thermal and fast reactors (1,2), spherical fission cavities (6,7) and uranium fission plates (1,2,3,4,5). The latter method was used in our work described in this paper.

Cross section measurement requires the absolute determination of neutron fluence during irradiation. This difficult task was avoided by measuring only spectral indices relatively to the monitoring reactions. The following indices were experimentally determined: $^{24}Mg(n,p)$, $^{27}Al(n,alpha)$, $^{56}Fe(n,p)$, $^{64}Zn(n,p)$ and $^{19}F(n,2n)$ relatively to $^{115}In(n,n')$, $^{47}Ti(n,p)$and $^{58}Ni(n,p)$ relatively to $^{27}Al(n,alpha)$ and $^{127}I(n,2n)$ relatively to $^{58}Ni(n,p)$.

Only a very short description of the work is given here. More details regarding the experimental arrangement can be found in papers describing our older measurements (3,4). All details of this work are available in a PhD thesis (8).

2. EXPERIMENTAL ARRANGEMENT

Activation foils were irradiated in the fast neutron field of a 260 mm dia 1,5 mm thick fission plate made of 20% enriched uranium cladded by 0,8 mm of aluminium. It was located in a large (2,4x2,4x3,6 m) exposure room). The plate was driven by thermal neutrons from the thermalizing column of our 250 KW TRIGA reactor. The irradiation position was 40 mm behind the fission plate.

*Present address, Ghana Atomic Energy Commission, Legon, Accra, Ghana.

The actual fast neutron spectrum was slightly different from the fision spectrum due to:

i) fast neutron background of core fast neutrons leaking through the thermalizing column. The resulting background activity of irradiated foils was experimentally determined and subtracted from the measured activity,

ii) fast neutrons scattered in the walls of the exposure room and returned to the irradiation position. Their contribution to the measured activities was found to be negligible (8),

iii) scattering and absorption of fast neutrons in the fission plate itself. In our older work (4) we estimated that this distortion can not effect the Al(n,alpha) - In(n,n') spectral index for more than 2 to 3%. Later these effects were also calculated by the ANISN (9) transport code in a 100 energy group approximation. Group cross-sections were taken from DLC library. Results are listed in Table I. In the last column is given the ratio of spectral index in pure fission spectrum to spectral index in our fission plate spectrum. This ratio represents the correction factor by which the measured values should be multiplied. It can be seen that corrections are quite small and much less than the estimated experimental error.

Detector foils of Mg, Al, Fe, Zn, In, Ti and Ni were cut from high purity grade 1 metals, fluorine foil was cut from gaflon (C_2F_4) while iodine detector was made in form of pellets containing pressed C_6I_6 power with small addition of organic bonding material. Iodine detector was 30 mm while all others were 50 mm in diameter.

Detectors were irradiated sandwiched between the monitoring foils. Indium was used as monitoring foil for Mg, Al, Fe, Zn and F, aluminium for Ti and Ni and nickel for I detectors.

Reaction rates were calculated from the absolute activities. They were measured by a closed end Ge-Li detector 49,5 mm dia in close geometry. The energy resolution of ^{60}Co, 1,33 MeV gamma line was 2,1 KeV. Efficiency of the spectrometer was determined by 50 mm dia calibrated point gamma sources ^{57}Co, ^{139}Ce, ^{203}Hg, ^{113}Su, ^{85}Sr, ^{137}Co, ^{54}Mn, ^{65}Zn and ^{60}Co and ^{144}Ce, ^{141}Ce, ^{203}Hg, ^{103}Ru, ^{85}Sr, ^{137}Cs, ^{95}Nb, ^{54}Mn, ^{60}Co and ^{88}Y. The 1 σ standard error of efficiency calibration was between 1,5 and 3% depending on gamma ray energy. Correction factors for coincidence summing, selfabsorption in detector foils and finite foil thickness were experimentally determined.

3. RESULTS AND DISCUSSION

Results are given in Table II. Measured values of spectral indices, these values multiplied by correction factors from the last column in Table I, data from Fabry evaluation (10) and ratio of corrected measured to Fabry values are given in columns 3,4,5,6 respectively. Errors quoted in column 3 are 1 σ standard deviation. They include the error of the specified reaction rate and the error of the reference reaction rate.

Agreement between measures values and Fabry's evaluation is within the range of 4% for all but one reaction as can be seen from the ratios given in the last column. Only the ^{58}Ni(n,p) Al(n,alpha) spectral index is 7,5% higher than Fabry evaluation.

References

1. Kimura I., et al., Neutron Cross Sections for Reactor Dosimetry, Vol.2, 265 Vienna (1978), IAEA-208.
2. Kobayashi K. and Kimura I., Proc.Third ASTM-EURATOM Symposium on Reactor Dosimetry, EUR 6813 EN-FR, Vol. II,1004 (1980).
3. Najžer M., Rant J., Šolinc H., Proc.IAEA Conf. on Nuclear Data for Reactors Vol.2, 571, Helsinki (1970).
4. Najžer M. and Rant J., Neutron Cross-Sections for Reactor Dosimetry, Vol. 2, 247, Vienna (1978), IAEA-208.
5. Bresesti A.M. et al., Nucl.Sci. Enging. 40,331 (1970).
6. Fabry A. et al., Proc.IAEA Conf. on Nuclear Data for Reactors, Vol. 2.535, Helsinki (1970).
7. Fabry A., BLG-465 (1972).
8. Acquah I.N. PhD thesis, University of Maribor, Maribor, Yugoslavia (1980).
9. Seltsez R.G., WANL-TMI-1967.
10. Fabry A. et al., Neutron Cross Sections for Reactor Dosimetry, Vol.1,233 Vienna (1978), IAEA-208.

TABLE I

Effects of scattering in fission plate on the reaction rates

Reaction	Reaction rate				Spectral index		
	Fission plate /rel.unit/	True fission /rel.unit/	Fission/ f.plate	Ref. react.	Fission plate	True fission	Fission/ f.plate
$^{24}Mg(n,p)$	1,401E-3	1,434E-3	1,0236		7,997E-3	8,025E-3	1,0035
$^{27}Al(n,\alpha)$	6,271E-4	6,414E-4	1,0228	$^{115}In(n,n')$	3,579E-3	3,589E-3	1,0028
$^{56}Fe(n,p)$	9,225E-4	9,444E-4	1,0237		5,265E-3	5,285E-3	1,0038
$^{64}Zn(n,p)$	3,829E-2	3,930E-2	1,0264		2,186E-1	2,199E-1	1,0059
$^{115}In(n,n')$	1,752E-1	1,787E-1	1,0200		1	1	
$^{47}Ti(n,p)$	2,132E-2	2,186E-2	1,0253	$^{27}Al(n,\alpha)$	34,00	34,08	1,0024
$^{58}Ni(n,p)$	1,004E-1	1,030E-1	1,0259		160,1	160,6	1,0031
$^{127}I(n,2n)$	6,129E-4	6,255E-4	1,0206	$^{58}Ni(n,p)$	6,105E-3	6,073E-3	0,9948

TABLE II

Measured spectral indices

Reference reaction	Reaction	Spectral index: This work measured	This work corrected	Evaluation by Fabry	Ratio Measured Evaluated
$^{115}In(n,n')$	$^{24}Mg(n,p)$	$7,795 \pm 0,39 \times 10^{-3}$	7,822	$7,831 \times 10^{-3}$	0,999
	$^{27}Al(n,\alpha)$	$3,575 \pm 0,17 \times 10^{-3}$	3,585	$3,730 \times 10^{-3}$	0,961
	$^{56}Fe(n,p)$	$5,655 \pm 0,23 \times 10^{-3}$	5,677	$5,476 \times 10^{-3}$	1,037
	$^{64}Zn(n,p)$	$0,163 \pm 0,0065$	0,164	0,158	1,038
	$^{19}F(n,2n)$	$3,556 \pm 0,20 \times 10^{-5}$	-	-	-
$^{27}Al(n,\alpha)$	$^{47}Ti(n,p)$	$26.68 \pm 1,2$	26,74	26,70	1,002
	$^{58}Ni(n,p)$	$165,0 \pm 6,8$	165,5	153,9	1,075
$^{58}Ni(n,p)$	$^{127}I(n,2n)$	$9,82 \pm 0,32 \times 10^{-3}$	9,77	$9,677 \times 10^{-3}$	1,010

NEUTRON MEASUREMENT WITH THE $^{93}Nb(n,n')^{93m}Nb$ REACTION

K. SAKURAI
Division of Japan Materials Testing Reactor,
Japan Atomic Energy Research Institute,
Ibaraki-ken,
Japan

Abstract

This note describes the measurement of neutron fluence above 0.1 MeV with the $^{93}Nb(n,n')^{93m}Nb$ reaction in the JMTR and the unfolding of YAYOI neutron spectrum with 13 foils including the $^{93}Nb(n,n')^{93m}Nb$ reaction.

(1) Neutron fluence measurement

The $^{93}Nb(n,n')^{93m}Nb$ has some advantages to monitor neutron fluence above 0.1 MeV. These advantages are as follows; (1) the threshold energy is as low as about 30 keV; (2) the isomer life is as long as 13.6 years; (3) the shape of the neutron cross section is similar to that of damage function. Therefore, the $^{93}Nb(n,n')^{93m}Nb$ reaction has been tried to monitor neutron fluence above 0.1 MeV of the LWR pressure vessel.

Neutron fluence above 0.1 MeV was measured with the $^{93}Nb(n,n')^{93m}Nb$ reaction at the second beryllium reflector region in the Japan Materials Testing Reactor (JMTR). The used niobium dosimeters were wires 0.020 inches in diameter, 99.833% in purity and supplied by Reactor Experiments Inc.. The irradiation hole in which niobium wires were irradiated is at J-12 of the second beryllium reflector region. The niobium wires of about 1.6 mg were set in the material capsule which was scheduled to be irradiated at J-12. The iron wires about 1 mg were also set at the same position as niobium wires in the capsule in order to monitor neutron fluence. The material capsule was irradiated at the 45th cycle (Jan. 13 ∿ Feb. 16, 1979), the 46th cycle (Mar. 29 ∿ Arp. 24, 1979) and the 47th cycle (Jan. 17 ∿ Jul. 13, 1979).

The transition from ^{93m}Nb is M4 which means about 100% internal conversion. The neutron fluence above 0.1 MeV is calculated from the data of the absolute activity determined by KX-ray measurement, the neutron spectrum and the $^{93}Nb(n,n')^{93m}Nb$ cross section. KX-ray emitted from ^{93m}Nb after 415 days cooling time were measured with a high purity 200 $mm^2 \times 7$ mm Ge detector. The effective cross section above 0.1 MeV of the $^{93}Nb(n,n')^{93m}Nb$ reaction is defined by the following equation,

$$\sigma_{0.1} \equiv \frac{\int_0^\infty \phi(E)\sigma(E)dE}{\int_{0.1}^\infty \phi(E)dE}$$

where $\phi(E)$ is the neutron spectrum and $\sigma(E)$ is the $^{93}Nb(n,n')^{93m}Nb$ cross section. The used data are the falf life of 13.6 ± 0.3 years[1] and branching ratio of 0.116 ± 0.0035[2]. The neutron spectra were calculated by using ANISN code[3] with the slab model for JMTR core[4].

The $^{93}Nb(n,n')^{93m}Nb$ cross section determined by Hegedüs[5] was used to calculate the effective cross section above 0.1 MeV. Hegedüs used the half-life of 11.4 years and the branching ratio of 0.122[5]. The relation of the present nuclear data (the cross section $\sigma(E)$, the half-life $T^1/2$ and the branching ratio I_{KX}) and the nuclear data used by Hegedüs (the cross section $\sigma'(E)$, the half-life $T'^1/2$ and the branching ratio I'_{KX}) is expressed by the following equation[6].

$$\sigma(E) = \frac{T^1/2}{I_{KX}} \frac{I'_{KX}}{T'^1/2} \sigma(E) = \frac{13.6}{0.116} \frac{0.122}{11.4} \sigma'(E) = 1.25\ \sigma'(E)$$

The effective cross section above 0.1 MeV of the $^{93}Nb(n,n')^{93m}Nb$ reaction is 75.2 mb. The effective cross section above 0.183 MeV was also calculated in order to compare the neutron fluence above 0.183 MeV monitored

with the $^{93}Nb(n,n')^{93m}Nb$ reaction with the neutron fluence above 0.183 MeV calculated for the JMTR core[4], and the value is 84.7 mb.

The accuracy of the neutron fluence above 0.183 MeV monitored with the $^{93}Nb(n,n')^{93m}Nb$ reaction can be evaluated by comparison with the neutron fluence above 0.183 MeV monitored with the reaction and the neutron fluence above 0.183 MeV calculated for JMTR core. The effective cross section of the $^{54}Fe(n,p)^{54}Mn$ reaction was calculated by using the ANISN spectrum and the $^{54}Fe(n,p)^{54}Mn$ cross section in the ENDF/B-IV. The value above 0.1 MeV is 25.8 mb and the value above 0.183 MeV is 29.9 mb.

The neutron fluence above 0.1 and 0.183 MeV monitored with the reactions and the neutron fluence above 0.183 MeV calculated for JMTR core are given in Table.

Method	>0.183 MeV (n/cm^2)	>0.1 MeV (n/cm^2)
JMTR calculation	2.21×10^{20}	——
$^{54}Fe(n,p)^{54}Mn$.	2.12×10^{20}	2.46×10^{20}
$^{93}Nb(n,n')^{93m}Nb$	2.61×10^{20}	3.03×10^{20}

The uncertainty of the neutron fluence above 0.1 MeV measured with the $^{93}Nb(n,n')^{93m}Nb$ is small than 30% including the uncertainties of the half-life, the branching ratio, the $^{93}Nb(n,n')^{93m}Nb$ cross section and the ANISN spectrum.

(2) Neutron spectrum measurement

Neutron spectrum of YAYOI glory-hole was measured by using resonance detectors such as $^{197}Au(n,\gamma)^{198}Au$ and $^{55}Mn(n,\gamma)^{56}Mn$, and threshold detectors such as $^{93}Nb(n,n')^{93m}Nb$, $^{115}In(n,n')^{115m}In$, $^{58}Ni(n,p)^{58}Co$, $^{24}Mg(n,p)^{24}Na$ and $^{27}Al(n,\alpha)^{24}Na$[7]. Irradiation condition at YAYOI glory-hole was the reactor power of 500 W and the irradiation time of 30 minutes. The niobium foil was 0.5 inches in diameter and 0.005 inches in thickness. The KX-ray spectrum was measured with the high purity Ge detector for the counting time of 26 hours and the cooling time of 137 days after the irradiation.

International intercomparison study of unfolding code had projected by IAEA. For the neutron spectrum unfolding, the reaction rates at YAYOI glory-hole, the guess spectrum and the neutron cross sections were offered to each participator by IAEA[8]. These data were also used for the neutron spectrum unfolding in addition to the reaction rate of the $^{93}Nb(n,n')^{93m}Nb$ reaction and the neutron cross section. The data for the neutron spectrum unfolding are shown in Table.

The neutron spectrum unfolding was performed with following two cases; one was analysis with reaction rates measured by author, the other was analysis with reaction rates and the neutron cross sections offered from IAEA. For the latter case, the neutron spectrum unfolded with 12 reaction rates and the reaction rate of the $^{93}Nb(n,n')^{93m}Nb$ reaction is shown in Figure. The guess spectrum and the neutron spectra unfolded with 12 and 13 reaction rates were shown in this figure. Ratio of the measured reaction rate (M) to the calculated reaction rate (C) is given in Table. The neutron spectrum unfolding was performed with SAND II [9].

Reaction	YAYOI glory-hole reaction rate (dps/atom)		Neutron cross section for unfolding
	(7)(8) REAL-80 data set	(7) Sakurai's data set	
$^{93}Nb(n,n')^{93m}Nb$	——	1.98 - 14 (±4%)	Hegedüs[5]
$^{59}Co(n,\alpha)^{56}Mn$	1.47 - 17+(±2.4%)	——	ENDF[8]
$^{55}Mn(n,\gamma)^{56}Mn$	8.48 - 16 (±2.8%)	8.24 - 16 (±3%)	"
$^{56}Fe(n,p)^{56}Mn$	1.00 - 16 (±2.8%)	——	"
$^{27}Al(n,p)^{27}Mg$	3.87 - 16 (±8.4%)	——	"
$^{27}Al(n,\alpha)^{24}Na$	6.74 - 17 (±2.9%)	6.91 - 17 (±3%)	"
$^{24}Mg(n,p)^{24}Na$	1.47 - 16 (±3.1%)	1.40 - 16 (±3%)	"
$^{23}Na(n,\gamma)^{24}Na$	7.85 - 17 (±4.1%)	——	"
$^{47}Ti(n,p)^{47}Sc$	1.68 - 15 (±11.5%)	——	"
$^{48}Ti(n,p)^{48}Sc$	2.57 - 17 (±3.8%)	——	"
$^{58}Ni(n,p)^{58}Co$	1.07 - 14 (±2.4%)	1.01 - 14 (±3%)	"
$^{115}In(n,n')^{115m}In$	2.12 - 14 (±3.9%)	2.14 - 14 (±3%)	"
$^{186}W(n,\gamma)^{187}W$	1.16 - 14 (±4.9%)	——	"
$^{197}Au(n,\gamma)^{198}Au$	2.82 - 14 (±3.8%)	3.14 - 14 (±4%)	"

+ 1.47 - 17 means 1.47×10^{-17}

Reaction	12 foils M/C		12 foils + Nb M/C	
	Zeroth	Final	Zeroth	Final
$^{93}Nb(n,n')^{93m}Nb$	—	—	1.3490	1.1305
$^{59}Co(n,\alpha)^{56}Mn$	0.8582	1.0261	0.8333	1.0253
$^{55}Mn(n,\gamma)^{56}Mn$	1.1910	0.9312	0.8821	0.9309
$^{56}Fe(n,p)^{56}Mn$	0.9086	1.0465	0.8821	1.0493
$^{27}Al(n,p)^{27}Mg$	0.9402	1.0774	0.9128	1.0857
$^{27}Al(n,\alpha)^{24}Na$	0.7968	0.9699	0.7736	0.9679
$^{24}Mg(n,p)^{24}Na$	0.8186	0.9855	0.7948	0.9839
$^{23}Na(n,\gamma)^{24}Na$	1.0811	0.9353	1.0497	0.9319
$^{47}Ti(n,p)^{47}Sc$	0.7596	0.8798	0.7375	0.8587
$^{48}Ti(n,p)^{48}Sc$	0.7899	0.9459	0.7669	0.9454
$^{115}In(n,n')^{115m}In$	1.0936	1.0824	1.0618	0.9305
$^{186}W(n,\gamma)^{187}W$	1.3886	1.0619	1.3483	1.0314
$^{197}Au(n,\gamma)^{198}Au$	1.3737	1.0581	1.3336	1.0535
Standard deviation (%)	22.38	6.76	23.29	7.36

References

(1) C. Michael Lederer and Virginia S. Shirley, "Table of Isotopes (Seventh Edition)", John Wiley and Son, Inc. (1978).

(2) W.L. Zijp and J.H. Board, "Nuclear Data Guide for Reactor Neutron Metrology", Part I, ECN-70 (1979).

(3) W.W. Engle Jr., "A User's Manual for ANISN", K-1693 (1967).

(4) H. Iida, et al., "Effect of the Neutron Spectrum in Evaluation of the Fast Neutron Fluxes", JAERI-M 6205 (1975).

(5) F. Hegedüs, "Détecteur de Fluence de Neutrons rapides base la Réaction $^{93}Nb(n,n')^{93m}Nb$", EIR-BERICHT NR-195 (1971).

(6) F. Hegedüs, "Comments on Summary of the Technical Discussion on Niobium as Fluence Detector Published in Reactor Radiation Metrology-Newsletter (Aug. 1979)", Reactor Radiation Metrology-Newsletter, No.13 (1980).

(7) M. Nakazawa, et al., "The YAYOI Intercomparison on Multiple-Foil Reaction Rate Measurements", UTNL-R-0099 (1981).

(8) D.E. Gullen, "Summary of ORR and YAYOI data for the REAL-80 Project Distributed 6 Feb. 1981", IAEA-NDS-33 (1981).

(9) W.N. McElroy, et al., "A Computer - Automated Iterative Method for Neutron Flux Spectra Determination by Foil Activation", I and II, AFWL-TR-67-41 (1967).

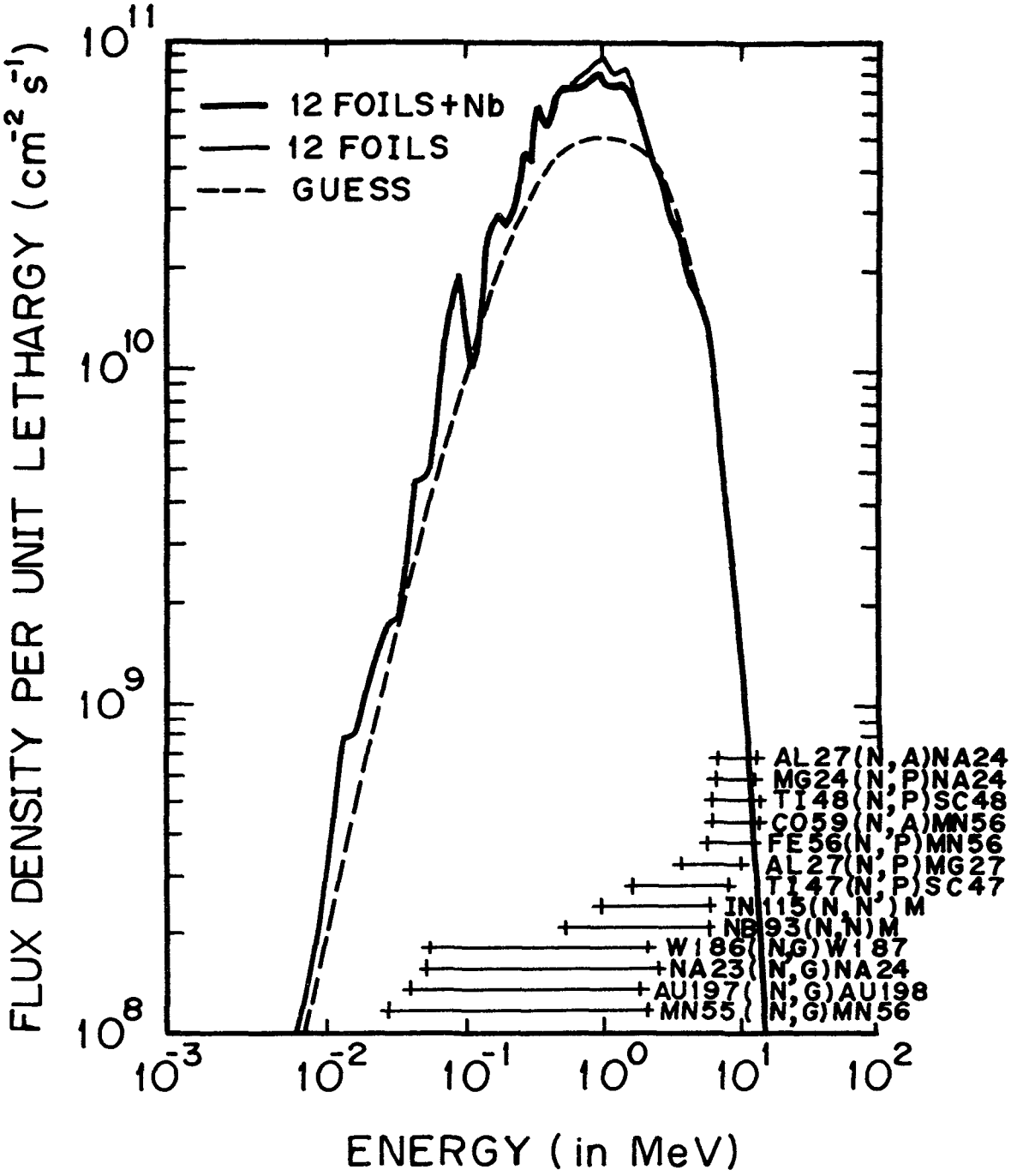
12 FOILS+Nb
12 FOILS
GUESS
FLUX DENSITY PER UNIT LETHARGY (cm⁻² s⁻¹)
ENERGY (in MeV)
AL27(N,A)NA24
MG24(N,P)NA24
TI48(N,P)SC48
CO59(N,A)MN56
FE56(N,P)MN56
AL27(N,P)MG27
TI47(N,P)SC47
IN115(N,N')M
NB93(N,N)M
W186(N,G)W187
NA23(N,G)NA24
AU197(N,G)AU198
MN55(N,G)MN56

NEUTRON SPECTRA CALCULATION IN MATERIAL IN ORDER TO COMPUTE IRRADIATION DAMAGE

C. DUPONT, J. GONNORD, A. LE DIEU DE VILLE,
J.C. NIMAL, B. TOTTH
CEA, Centre d'études nucléaires de Saclay,
Service d'études des réacteurs et de mathématiques appliquées,
Gif-sur-Yvette,
France

SUMMARY :

This short presentation will be on neutron spectra calculation methods in order to compute the damage rate formation in irradiated structure. Three computation scheme are used in the French C.E.A. :

- 3 dimensional calculations using the line of sight attenuation method (MERCURE IV code), the removal cross section being obtained from an adjustment on a 1 dimensional transport calculation with the discrete ordinate code ANISN
- 2 dimensional calculation using the discrete ordinates method (DOT 3.5 code), 20 to 30 group library obtained by collapsing the 100 group a library on fluxes computed by ANISN
- 3 dimensional calculations using the Monte Carlo method (TRIPOLI system). The cross sections which originally came from UKNDL 73 and ENDF/B3 are now processed from ENDF B IV.

1 - INTRODUCTION -

The damage formation rate (d.p.a) from neutron irradiation suppose the knowledge of the energy repartition of neutron flux in different points $\vec{r}$ of the irradiated structure. From this spectrum $\varphi(\vec{r}, E)$ the number of d.p.a or the zone formation rate, is evaluated as a reaction rate :

$$(1) \qquad \tau(\vec{r}) = \int_0^\infty \varphi(\vec{r}, E) * R(E)\, dE$$

in the French C.E.A. three methods are commonly used :

a) line of sight attenuation method using removal cross section adjusted on a 1 D transport calculation

(codes ANISN and MERCURE IV)

b) 2 dimensional calculation by the discrete ordinates method using a 20 to 30 groups library obtained by collapsing the 100 groups standard library on fluxes computed by 1 or several 1 dimensional transport calculation.

(codes ANISN and DOT 3.5)

c) 3 dimensional calculation by the Monte Carlo method which solves exactly the transport equation.

(TRIPOLI system)

Finally we shall review the different cross sections library which have been used and are now in use in our laboratory.

2 - LINE OF SIGHT ATTENUATION METHOD USING REMOVAL CROSS SECTION -

We use in that case the codes ANISN and MERCURE IV. This computation scheme allows the representation of three dimensional geometries and source distribution.

2.1. MERCURE IV code [1] [2]

This code integrate the line of sight attenuation kernel for gamma ray (biologic dose, heating) and for fast neutron (biologic dose, damage formation rate). The code uses a simple formula given by relation (2) where the kernel $G(\vec{r}, \vec{r_o}, g)$ caracterises the attenuation of particles in group g, born at $\vec{ro}$ and arriving at $\vec{r}$.

$$(2) \qquad \tau = \iiint_{Vs} d\vec{r_o} \sum_{g=1}^{N} S(\vec{r_o}, g)\, G(\vec{r}, \vec{r_o}, g)$$

V_s is the volume containing the sources and τ the reaction rate.
In MERCURE IV, the kernel G is computed using the line of sight attenuation formalism, only the distances along the straight line joining $\vec{r_o}$ to $\vec{r}$, through the different material have to be taken into account.

The kernel $G(\vec{r_o}, \vec{r}, g)$ takes thus the following expression :

$$(3) \qquad G(\vec{r_o}, \vec{r}, g) = A_R \left(\sum_i \mu_i t_i, g\right) \frac{e^{-\sum_i \mu_i t_{i,g}}}{4\pi (\vec{r} - \vec{r_o})^2}$$

where ti is the straight line distance a cross the i^{th} material
μg is the linear attenuation coefficient in the i^{th} material for particles belonging to group g (removal neutron section).

A_R is a coefficient taking into account the diffusion of particles and the particule flux conversion in reaction rate, dose, damage according to the response R (E) we consider before (1).

For gamma ray A_R is a product of the accumulation factor and the mean value Rg of the response in group g.

For fast neutron A_R is a factor computed from a transport calculation as we shall see later on ; this factor depends on the response R (E) required.
In MERCURE IV the calculation of integral (2) is carried on by the Monte Carlo method. The source space is divided in meshes ΔVk in three dimensions. ΔVk is a discretisation in cartesian, cylindrical or spherical coordinates.

The source intensity S ($\vec{r_o}$, g) can be :

- either a constant in the ΔVk mesh
- or obtained from a bilinear interpolation of S values at the nodes of the mesh.

An importance function Ikg is then computed for each mesh k in each group g. A sampling of particles is then generated according to the Ikg assumed to be uniform inside each ΔVk. The integral (2) is then evaluated by scoring the contribution of each particle. It has been demonstrated that such a game gives the optimum variance on final integral τ . Further more, generating the particles inside ΔVk suppresses the systematic bias of the analytic codes which focus the source at the center of each ΔVk and thus neglect the self absorbtion.

Let us examine now the geometrical capability of MERCURE IV which uses the TRIPOLI geometry package. The space is divided in finite homogeneous volumes. Each volume can be limited by any portion of planes or quadratic surfaces and support all types of boundary conditions.

Cross section library :

- for gamma rays the code uses a library allowing to process gamma from 8.5 MeV to 105 keV
- for fast neutron a library is generated for each case using the following method.

2.2. ANISN [3] [4]

ANISN is a well known U.S. code solving the integro differential form of the transport equation by the discrete ordinates method (discretisation of angular flux on a spatial and angular mesh). The cross sections have a multigroup structure and are represented by an expansion on Legendre polynomial at order N (P_N) ; generally N equals 3 for neutrons and 5 for gamma rays. The geometry is one dimensional in cartesian, cylindrical or spherical coordinates.

The code computes scalar fluxes and higher moments and the angular repartition of fluxes. It allows to collapse the original cross section library in a large group library using the computed flux as weighting function :

$$\sigma_G = \frac{\sum_g \sigma_g \phi_g}{\sum_g \phi_G}$$

2.3. Computation scheme

The computation scheme is divided in 3 parts :

2.3.1. one or several 1 D transport calculation with ANISN in a simplified geometry preserving the thickness of the material along the direction joining the source to the calculation point. ANISN gives reaction rates

(d.p.a): τ^*_{jR} at each interface j between two different material for the response R.

2.3.2. For each response R a MERCURE IV calculation on the same 1 dimensional geometry in order to adjust a coefficient A_R and removal cross section µig on the τ^*_{jR} computed by ANISN.

2.3.3. Finally a 3 dimensional MERCURE IV using the adjusted A_R and removal cross section gives the result for the 3 dimensionnal source.

This scheme is use for pressure vessel irradiation survey when the configurations are not too far from 1 dimensional (PWR for example).

3 - CALCULATIONS USING THE DISCRETE ORDINATES METHOD

The computation scheme is simpler but applies only to 2 dimensional configurations, X-Y or R-Z. The scheme begins by one or several 1 dimensional transport calculations with 100 groups in energy using the ANISN code which collapse the original 100 groups library in 20 to 30 larger groups (2.2.). The cross sections are computed for each homogeneous space zone, these zones being some times divided to take into account the variation of neutron spectrum.

The same ANISN calculations are then redone with the new collapsed library for validation. Then the larger group library is used in a two dimensional transport calculation using the discrete ordinates S_N code DOT. [5].

In SACLAY the DOT-4 version is now used instead of DOT 3.5 .

The next table gives an example of large groupe structure used for damage rate calculation.

4 - CALCULATIONS USING THE MONTE CARLO METHOD

4.1. Method

The Monte Carlo method has two advantages :

- the exact 3 dimensional geometry can be represented
- a fine representation of the interaction process can be handled (anisotropy - cross section).

The TRIPOLI system [6] [7] solves the transport of neutron or gamma-rays - time depending or not - for source or critical problems. In the case of damage formation studies we are essentially interest by the fast neutrons which reduce considerably the computing time compare to those of a complete calculation from 15 MeV to thermal energy (there is no thermal neutron diffusion).

E limit (MeV)	Group DOT
14.918	
	1
10.	
	2
9.048	
	3
8.187	
	4
7.408	
	5
6.703	
	6
6.065	
	7
4.966	
	8
4.066	
	9
3.329	
	10
2.725	
	11
2.231	
	12
1.827	
	13
1.496	
	14
1.225	
	15
1.003	
	16
0.821	
	17
0.498	
	18
0.302	
	19
0.183	
	20
0.0866	
	21
0.0318	
	22
0.0248	
	23
0.0193	
	24
0.0055	
	25
$4.1\ 10^{-7}$	
	26
0.	

The 3 dimensional geometry is a collection of homogeneous volumes limited by parts of first or second order surfaces. These surfaces are defined by there equations :

$$f(x, y, z) = 0$$

The boundary conditions can be :

- void
- albedo
- reflexions
- translations
- rotations

the last three conditions allows to process repetitive geometries.

The distribution of sources in space angle and energy is quite general and given by the relation (5) :

$$(5)\quad S(\vec{r}, \vec{\Omega}, E) = \sum_J C_{m,j}\, S_{1j}(\vec{r}) * \frac{S_{2j}(E)}{\int S_{2j}(E)\, dE} * \frac{S_{3j}(\vec{\Omega})}{\int S_{3j}(\vec{r})\, d\vec{\Omega}}$$

Each function S_{1j} can be defined in a cartesian, cylindrical or spherical system. $C_{m,j}$ is a modulation coefficient for each volume.

Concerning the interaction handling by the TRIPOLI system we shall limit to the fast neutron interaction as we interest here to the damage rate. The interactions handled in the fast range are the following :

- elastic scattering with any type of anisotropy
- n n' - n 2 n - n 3 n reaction isotropic in the center of mass system
- absorption ($n\gamma$ np $n\alpha$).

In TRIPOLI application for damage problems a fine multigroup mesh is used for the representation of cross section. The number of fine group is not limited, only a few of them being simultaneously in the computer memory. TRIPOLI use generaly 200 groups from 15 MeV to 1 keV and around 300 for all energy range.

4.2. Some applications

We chose two examples of application that could be compared to experimental results.

The first one is about an irradiation of an HTR block in the PEGGY loop of PEGASE reactor. The geometry is shown on figure 1. It is exactly the geometry input in the TRIPOLI system. A borated water screen placed on the hot face of the loop in order to flat the power distribution is missing on the figure. The figure 2 shows the equivalent indium fission flux computed by TRIPOLI in the UO2 pins. The figure 3 shows the ratio of the computed values to the experimental measures.

The second example is about a dosimetry in a loop simulating a PWR vessel irradiation ; it is the DOMPAC experiment realise by the S.P.S in Saclay [8]. The figure 4 shows the computed responses of detectors on the iron block axis compared to experiment.

5 - CROSS SECTIONS LIBRARY

Two types of libraries are used in the three schemes that we presented :

- 100 groups library developped on Legendre Polynomials :
  P3 for neutron P5 for gamma-rays
  used by the S_N codes
- ponctual library used by the TRIPOLI system.

During a long time these two libraries had different origin and different processing :

- the neutron multigroup library was DLC 2 [9] from RSIC and has been replaced by VITAMIN/C [10] collapsed on the 100 groups of DLC 2.
- the gamma P5 multigroup library came from LASL
- the punctual TRIPOLI library called LINDA was processed from UKNDL 73

Two complete new coherent library are now processed and tested in the laboratory from ENDF/ B IV and B V.

The punctual processing is done using the NJOY system[11]. From this punctual data two libraries are derived :

- a MICROS library used by the TRIPOLI 2 system
- an AMPX master which can be used after collapsing and format conversion by the S_N codes.

The cross section has been reconstruct from resonance parameters with a tolerance of 1 % at 6 temperatures (0°K, 20°K, 300°K, 573°K, 1000°K, 1700°K).

From the punctual data a 315 group P3 neutron library has been generated. The mesh includes VITAMIN/E, BABEL and APOLLO mesh plus a fine description of iron and sodium resonance. The table shows the diagram of the cross section processing from ENDF/B to the TRIPOLI and S_N libraries.

CROSS SECTION PROCESSING FROM ENDF/B

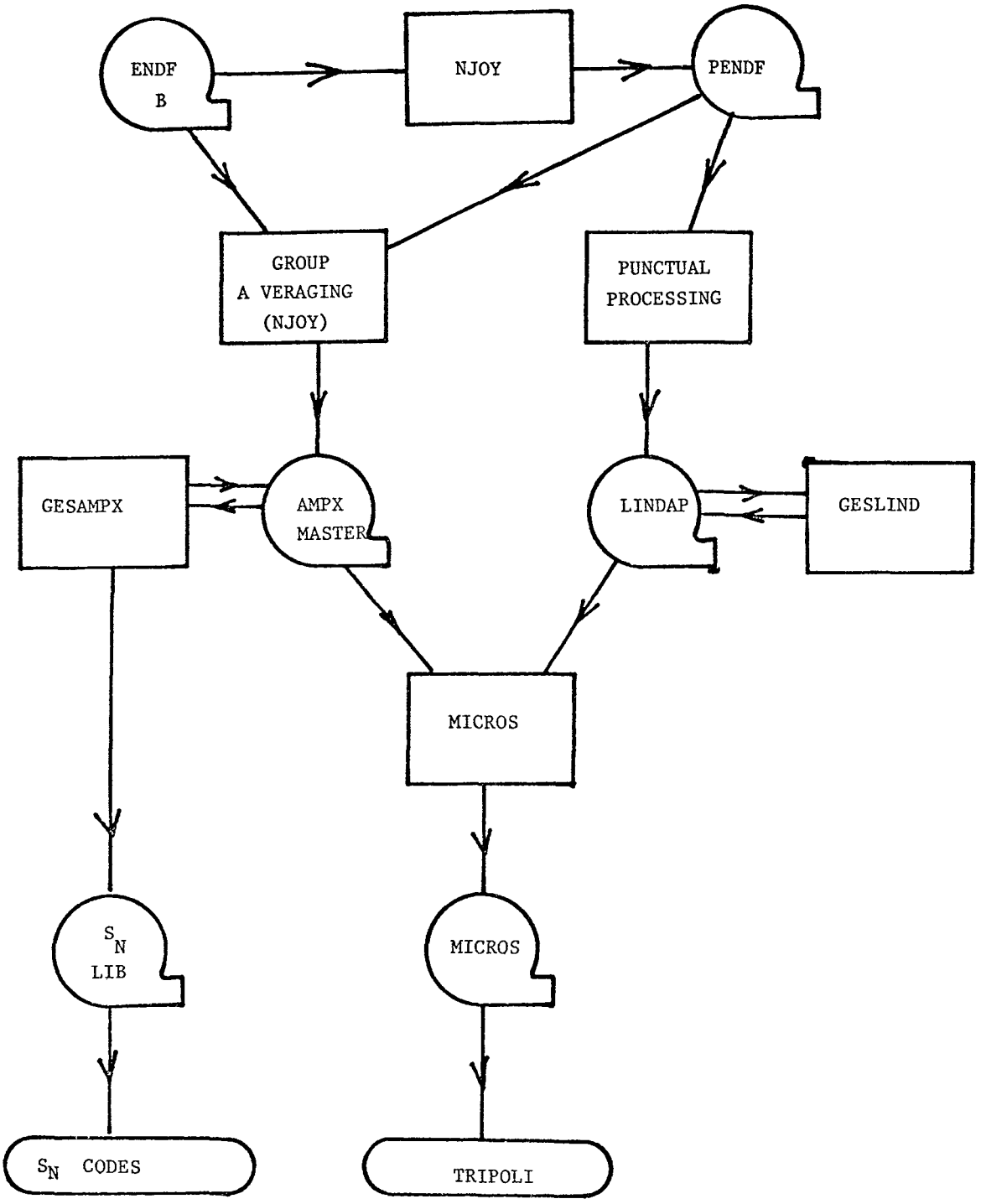

BIBLIOGRAPHIE

[1] C. DEVILLERS - C. DUPONT
MERCURE IV : Un programme de Monte Carlo à trois dimensions pour l'intégration de noyaux ponctuels d'atténuation en ligne droite
NOTE C.E.A. - N. 1726 (juillet 1974)

[2] C. DUPONT - J.C. NIMAL
MERCURE IV : Un programme de Monte Carlo à trois dimensions pour l'intégration de noyaux ponctuels d'atténuation en ligne droite
RAPPORT interne (juillet 1980)

[3] C. DEVILLERS
Système ANISN : Description et mode d'utilisation du programme aux ordonnées discrètes ANISN et des programmes auxiliaires
NOTE C.E.A. - N. 1358 (octobre 1970)

[4] W.W. ENGLE
A users Manual for ANISN - A one Dimensional Discrete Ordinates Transport code with Anisotropic Scattering
AEC Research and Developpement Report K 1693

[5] G. BRANDICOURT
Mode d'utilisation du programme de transport aux ordonnées discrètes à deux dimensions DOT 3
RAPPORT interne (janvier 1976)

[6] J.C. NIMAL et collaborateurs
Programme de Monte Carlo polycinétique à trois dimensions
TRIPOLI 01 (tomes 1 à 7)
NOTE C.E.A. - N. 1919 (septembre 1976)

[7] A. BAUR - L. BOURDET - G. DEJONGHE - J. GONNORD - A. MONNIER - J.C. NIMAL - T. VERGNAUD -
Programme de Monte Carlo polycinétique à trois dimensions TRIPOLI 02 (tomes 1 à 4)
NOTE C.E.A. à paraître

A. BAUR - L. BOURDET - G. DEJONGHE - J. GONNORD - A. MONNIER - J.C. NIMAL - T. VERGNAUD
TRIPOLI II : Prepared for Monte Carlo Seminar-Workshop- Three dimensional polyenergetic Monte Carlo radiation transport program (Vol. 1 and 2)
OLS 80 110

[8] A. ALBERMAN - M. FAURE - M. THIERRY - O. HOCLET - A. LE DIEU DE VILLE - J.C. NIMAL - P. SOULAT
Communication au 3ème *symposium* ASTM/EURATOM (ISPRA *Italie Octobre* 1979) sur la dosimétrie des rayonnements de Réacteurs
Expérience de dosimétrie "DOMPAC" simulation neutronique de l'épaisseur de la cuve d'un réacteur PWR - Caractérisation des dommages d'irradiation

[9] DLC 2 R.S.I.C.

[10] VITAMIN/C DLC 41 R.S.I.C.

[11] NJOY Nuclear Data Processing System
R.E. Mac FARLANE L.A.S.L.

1

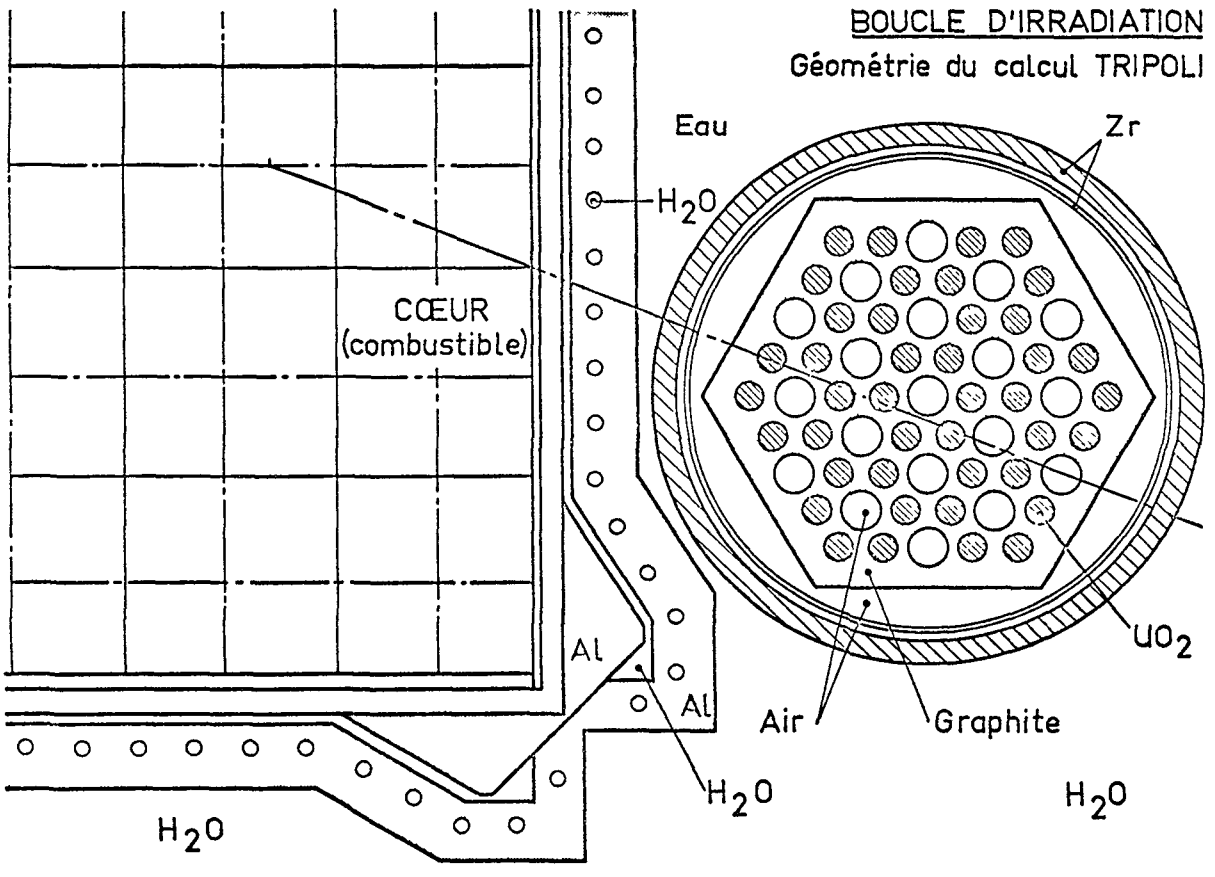

FIG. 1

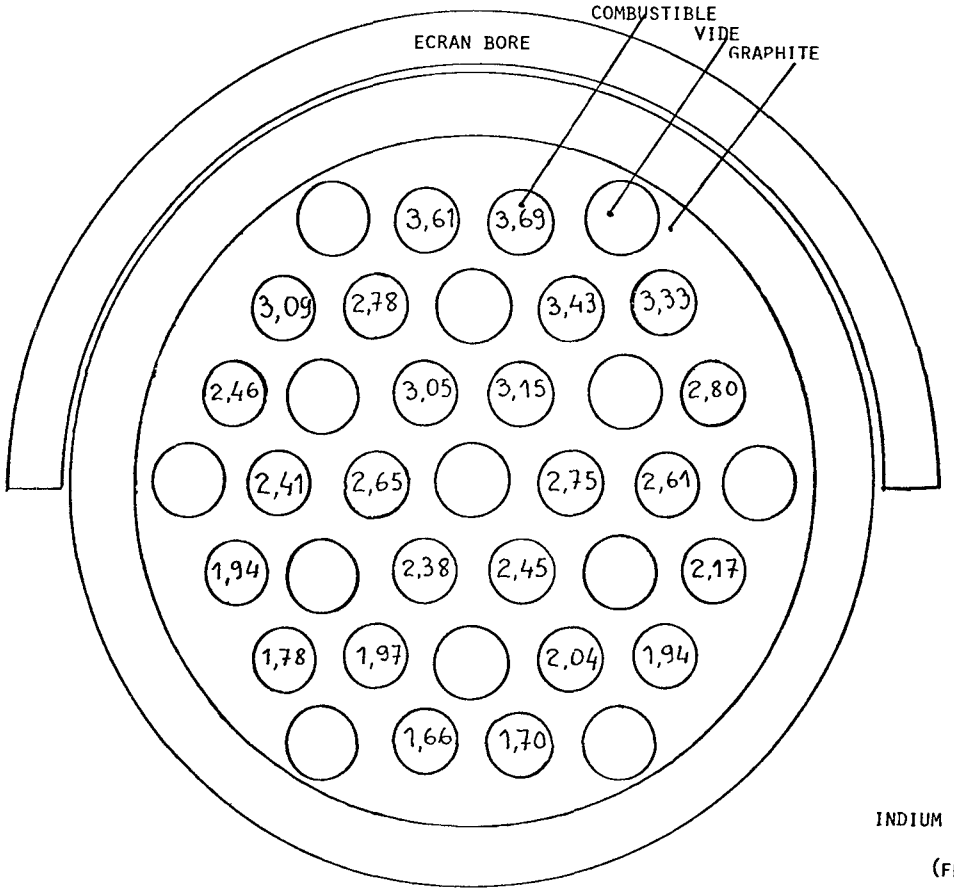

FIG. 2.

BIP-01

INDIUM EQUIVALENT, SUPERIEUR A 1 MEV

(FLUX EN 10^{13} N/CM^2/S)

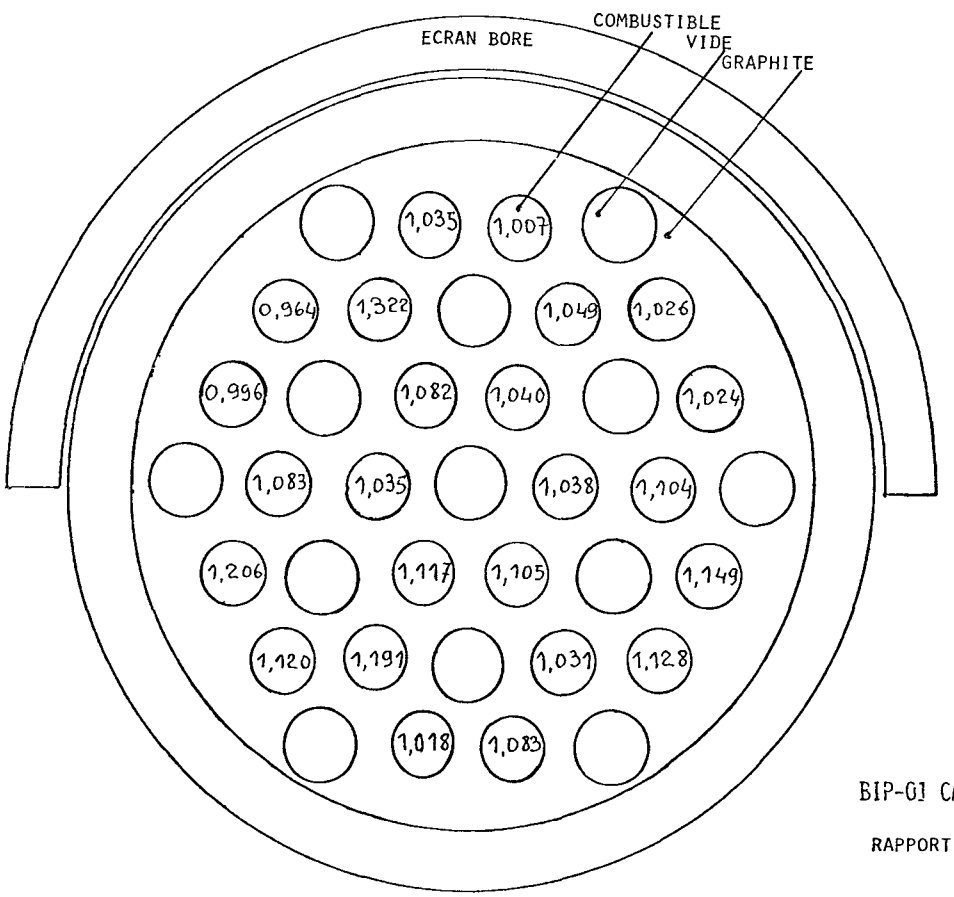

FIG. 3.

BIP-01 CALCUL TRIPOLI ET EXPERIENCE

RAPPORT CALCUL / EXPERIENCE POUR L'INDIUM

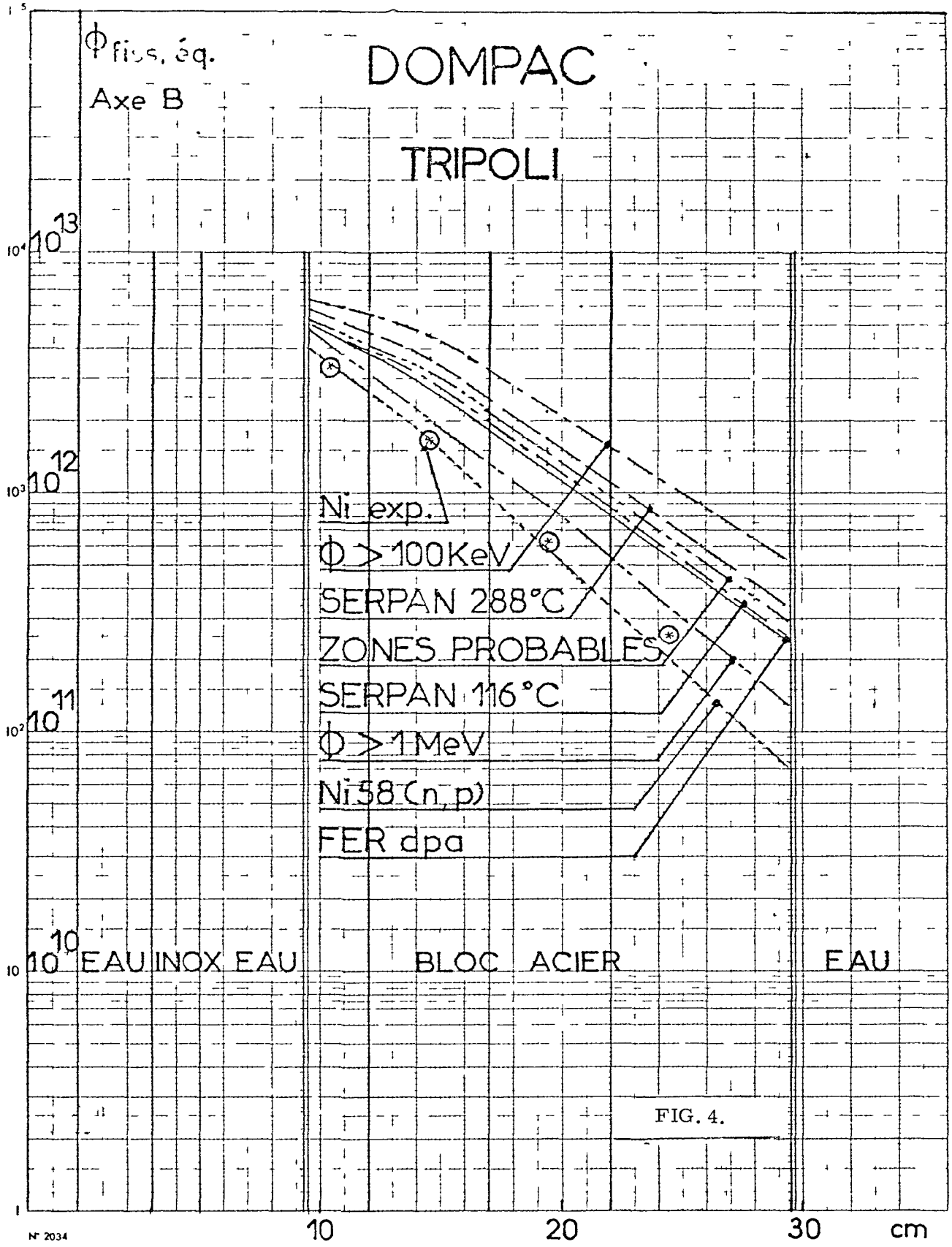
DOMPAC
TRIPOLI
Φ fiss. éq.
Axe B
10^13
10^12
10^11
10^10
Ni exp.
Φ > 100 KeV
SERPAN 288°C
ZONES PROBABLES
SERPAN 116°C
Φ > 1 MeV
Ni 58 (n, p)
FER dpa
EAU INOX EAU
BLOC ACIER
EAU
10
20
30
cm
N° 2034

FIG. 4.

STATUS OF DISPLACEMENT CROSS SECTIONS

P. STILLER
Swiss Federal Institute for Reactor Research,
Würenlingen,
Switzerland

Abstract

In this paper the status of displacement cross sections is described which are available for common use from the data centers in form of multigroup cross section data sets. In addition some of the further developments in view of an improvement of the components needed in calculating displacement cross sections are reported.

Introduction

Today under the aspects of reactor safety the property changes and the resulting behaviour of irradiated reactor structure materials are of special interest in view of radiation damage effects. Examples are the pressure vessel of a thermal fission reactor, the LMFBR materials development or the first wall region of a fusion reactor. For relating the radiation induced changes in a material to the condition of this material the irradiation exposures have to be expressed in an unit which is physically correlated to the damage mechanism.

The damage mechanism common to all neutron and charged particle irradiations of solids and the primary source of radiation damage is the displacement of atoms from their normal lattice sites. Thus an appropriate damage exposure index is the number of times on the average that an atom has been displaced in particle collisions during the irradiation of the material. Hence, the standard procedure for characterizing neutron or charged particle irradiations is to give the average number of displacements per atom (dpa) in the irradiated materials. In radiation damage and especially reactor materials research it is of major interest and of fundamental importance to have such a basic quantity for comparing the effectiveness of different kinds of irradiations or the effects of different neutron spectra on the mechanical properties of materials. That is why it has been recommended that irradiation test data on reactor structural materials should include in addition to fluence the displacing dose expressed as the average number of displacements per atom.

The number of dpa associated with a particular irradiation depends on the amount of energy deposited in the material and therefore on the energy spectrum of the radiation causing radiation damage. Hence, if the particle flux spectrum and the total fluence are available this practice can be applied to any material for which displacement cross sections are known. Based on these informations the calculated spectrum sensitive parameter dpa serves as an appropriate starting point for relative correlations of

material property changes and associated environments as well as an exposure unit that is common to both neutron and charged particle irradiations.

Not only the use of a spectrum-dependent exposure unit but also the development of semiempirical effective damage functions to describe the energy dependence of a particular damage state have been supported by the need to account for the neutron energy dependence of radiation damage. Both developments have converged on the need for displacement cross sections and their application to define displacement rates in existing and proposed irradiation facilities. If the displacement process is considered to be the dominant damage mechanism and not the helium production or the formation of foreign atoms via nuclear transmutations the assumed shape of the effective damage function is generally the displacement cross section.

After the definition of the displacement cross section the status of four different displacement cross section sets for neutrons is described.

Displacement Cross Section

The general expression for the displacement cross section $\sigma_d(E)$ at neutron energy E due to a reaction of type i is, according to Doran (1), given by equation (1):

$$\sigma_d^i(E) = \sigma^i(E) \int_{-1}^{\mu_{max}} p[T(E,\mu)]\,\nu[T(E,\mu)]\,d\mu \qquad (1),$$

where $\sigma^i(E)$ is the reaction cross section at energy E. T is the kinetic energy of the primary knock-on atom (PKA) in the laboratory system, μ is the cosine of the scattering angle ϕ of the PKA in the center-of-mass system (CMS). The probability for the production of a primary recoil atom of energy T by a neutron of energy E is given by $p[T(E,\mu)]$. A secondary displacement model, the displacement function $\nu(T)$, describes the average number of secondary displaced atoms produced in a cascade initiated by a PKA of energy T. By using an energy partition model the fraction $\beta(T)$ of the primary recoil energy T is defined which is not dissipated to electrons during the slowing down process. Hence, the damage energy $T_{DAM} = \beta(T)T$ is available to cause displacements. Based on Lindhard's theoretical treatment for the stopping cross sections (2,3,4) Robinson has shown that the damage energy fraction $\beta(T)$ for Lindhard's energy partition model is well represented by a numerical approximation (5,6,7).

The conversion from the damage energy T_{DAM} to the average number of displacements $\nu(T)$ is done by a proportionality factor (8,9) $f = \kappa/2T_d$ according to equation (2):

$$\nu(T) = \frac{\kappa}{2T_d} \cdot T_{DAM} \qquad (2)$$

where $\nu(T)$ is generally expressed in a modified Kinchin-Pease form.
κ is a potential form factor introduced to account for anisotropic scattering and for the softness of real potentials. Thus the deviation from hard sphere collisions is described if physically real potentials for the collision process are present. This is a modification of the old Kinchin-Pease model (10) in which hard sphere (isotropic) scattering was assumed.

T_d is the effective anisotropic displacement threshold energy averaged over crystallographic directions and is required to displace a lattice atom.

At the IAEA Specialists Meeting on Radiation Damage Units held in Harwell on 2nd-3rd November 1976 the following *interim procedure for calculating secondary displacements* was recommended: $\nu(T)=bT_{DAM}$ where $b=10keV^{-1}$ for iron, steels and nickel based alloys, and T_{DAM} is estimated on the base of the Lindhard model. The justification for these recommendations are given in the report by Norgett, Robinson and Torrens (reports CEA No. 4389, AERE No. TP/494).
Thus in comparison to the damage function which is an experimentally derived quantity to relate neutron fluence to a property change after irradiation the atomic displacement cross section is theoretically derived to relate neutron fluence to the number of atoms initially displaced from lattice positions.

The calculation of a displacement cross section requires the following information be included: reaction cross sections dependent on energy and angular distributions to calculate the primary recoil atom energy distribution, a model describing the partition of deposited energy between electronic excitation and kinetic energy of the atoms to calculate the damage energy, and a secondary displacement model.

Displacement Cross Section Sets

There are several data sets of displacement cross sections for neutrons published between 1972 and 1979. In common use for calculating dpa are multigroup displacement cross section libraries based on different point cross section sets, collision models or displacement criteria and different procedures in generating multigroup data. The status and content of these libraries known to the autor and generally available are described in the section that follows.

Displacement Cross Section Library DAMSIG77

This displacement cross section library in the 620 neutron group SAND-II/CCC-112 format was contributed by the Netherlands Energy Research Foundation, Petten, in 1978 (11). DAMSIG77 is now included in the data library collection DLC-81/DOSDAM77-81. Displacement cross sections for the following materials are available: C, Al, Si, Cr, Fe, Ni, Cu, Zr, Mo, W, V, Nb, stainless steel. A number of these materials have more than one displacement cross section set originating from different evaluations.

The 620 groups structure of the displacement cross section values, which is used in SAND-II (12), was obtained by converting the original group structure applying extrapolation and interpolation procedures. This group structure is as fine or finer than the group structure in which the neutron flux is generally available. The procedure how to collapse this group structure to match the flux group structure is given in ref. (13).

The two carbon displacement cross section sets included were based on data presented by Reed (14) in 1967, respectively by Morgan (15) in 1974.

The source for Reed's total neutron scattering cross sections for carbon was the Winfrith and Aldermaston Nuclear Data Library of 1963 (16). Reed published these point cross sec-

tions for 95 energies from 1 keV to 14 MeV together with the Thompson-Wright displacement function $\nu(T)$ for graphite (17, 18) for 21 neutron energies. A displacement threshold T_d=60 eV as reported by Lucas and Mitchell (19) has been used. This atomic displacement model of Thompson and Wright which is the most universally acceptable model for graphite has been recommended by IAEA (20) in 1972 and by ASTM (21) in 1974 to be used for carbon. Calculating the product of both data sets after interpolation or extrapolation point values for the displacement cross sections were obtained at ECN which were then converted to group data.

The displacement cross section for graphite as presented by Morgan is based on cross section data from the ENDF/B-III file, the Lindhard damage model and the modified Kinchin-Pease model. The used displacement efficiency κ is equal to 1. A value of 31 eV for T_d has been chosen on the basis of measurements, (22, 23, 24, 25). The displacement cross sections have been calculated for 78 groups from 79 eV up to 14.92 MeV in the standard General Atomic Multigroup (GAM-II) neutron energy group structure (26) using the 1/E plus Watt fission spectrum weighting function. By extrapolation the data were extended to 17.9 MeV. Anisotropic elastic scattering and isotropic inelastic scattering of neutrons have been included in the displacement cross section calculation but assuming that all energy lost by a neutron in an inelastic scattering event appears as kinetic energy of a primary displaced atom. Hence, ignoring the excitation of the residual nucleus a shift of the PKA spectrum to higher energies is the result and thus an overestimation of the total number of atoms displaced by inelastic scattering. The contributions of the (n,γ) reaction and of high energy reactions such as (n,p), (n,α) and (n,2n) have been also omitted. The average value for the displacement cross section set based on the data of Morgan and averaged over a Watt spectrum is about 40 % higher and using an 1/E spectrum 50 % higher in comparison to the average value obtained with the cross section set based on Reed's values.

The sources of the two displacement cross section sets for Al, Cr, Fe, Ni, Zr and Mo are the paper of Lott et al. (27) in 1973 and the report of Genthon et al. (28) in 1975. Lott et al. provided also displacement cross sections for Si, Cu and W. In addition a displacement cross section set for V and Nb is included in DAMSIG77, calculated with the ENDF/B-III cross section data and supplied by A. Albermann (CEN, Saclay, France) in 1975/76.
In Lott's work neutron cross sections of the UKNDF library were applied. The displacements were calculated by using the Lindhard universal model and the modified Kinchin-Pease model corresponding to the IAEA recommendation (20) of 1972. The displacement efficiency κ had a value of 0.8. A displacement threshold T_d of 40 eV has been used.
The group data were generated for the GAM-II energy group structure with an 1/E- and a fission spectrum. Neutron reactions taken into account were the elastic scattering with anisotropic angular distribution, the inelastic scattering, (n,γ) and (n,2n). The contribution of the (n,γ) reaction was calculated without considering the kinetic energy of the neutron and with the simplification that no angular correlation exists between emitted gammas. The treatment of the (n,2n) reactions assumed isotropic neutron emission in the center-of-mass system and no correlation in view of the directions of the emitted neutrons. The values presented by Lott are given from an epithermal neutron energy of

0.414 eV up to 14.92 MeV and have been extended by ECN to 10^{-4} eV, respectively to 17.9 MeV with the exception of the data for iron which stop at 10.6 MeV.

The displacement cross section for steel is the summation of the values for Fe (74 %), Cr (18 %) and Ni (8 %) weighted by the element composition.

In the displacement cross section tables of the EWGRD recommendation based on the UKNDF library and published by Genthon et al. (28) the (n,γ) contribution is absent. Thus, the displacement cross sections are given for neutron energies from 720 eV up to 14.1 MeV.

The spectrum averaged displacement cross section values for the same material differ about 2 % for the 1/E and Watt fission neutron spectrum with the exception of the data for Zr which differ about 5 % for the Watt spectrum.

The displacement cross sections for V and Nb listed by Alberman also do not contain the contribution of the (n,γ) reaction and hence start at 450 eV respectively 720 eV and stop at 14.1 MeV.

DLC-55 / RECOIL

For correlating radiation damage effects in different neutron environments, fission reactors or future fusion devices the data collection DLC-55/RECOIL (29), published in 1976 is a useful basic data library. The recoil energy being a fundamental quantity in descriptions of radiation effects primary recoil energy distributions in 104 energy groups have been prepared at ORNL.

The data of this multigroup library are provided for 105 neutron energy groups from 10^{-4} eV up to 14.918 MeV in the 100 GAM group structure (30,31) and for five additional groups up to 20 MeV. An analysis code RECOIL (29) is included to derive all the radiation effects parameters as primary recoil atom spectra, damage energy and displacement cross sections from these primary recoil energy distributions.

Primary recoil energy distributions are given for 27 elements, respectively isotopes: ^{6}Li, ^{7}Li, Be, ^{10}B, ^{11}B, C, N, O, Mg, Al, Si, Ti, N, Cr, Mn, Fe, Co, Ni, Cu, Zr, Nb, Mo, Ta, ^{181}W, ^{182}W, Au and Pb.

In order to evaluate displacement cross sections in the analysis code RECOIL the Lindhard theory as used by Robinson (32) is employed to determine that fraction of the kinetic energy of the PKA which will produce further nuclear displacements. The number of displaced atoms per primary knock-on atom is calculated by using again the modified Kinchin-Pease model. The displacement threshold T_d is a free input parameter of the analysis code RECOIL. The displacement efficiency κ has a value of 0.8.

Calculating the primary recoil energy distributions all neutron reactions significant for the materials have been processed from ENDF/B-IV: (n,n), (n,n'),(n,2n), (n,n'α), (n,n'3α), (n,2nα), (n,3nα), (n,n'p), (n,γ), (n,p), (n,d), (n,t), (n,^{3}He), (n,α), (n,2α) and (n,3α). For the elastic scattering and if available also for inelastic resolved scattering reactions the angular distributions were included calculating the energy distributions.

The effect of gamma rays emitted after inelastic and non-elastic reactions on the heavy ion recoil energy distribution is small and was not included in the calculations.

For (n,γ) reactions the secondary gamma-ray energies, along with their emission probabilities, were obtained from the nuclear data sheets. The incident neutron energy has been taken into account to conserve total energy and momentum, and isotropic emission of gamma rays in the rest system has been assumed. In view of capture-level probabilities valid for thermal neutron energies it was assumed that they apply for all neutron energies. Also fast emission of the gamma rays was assumed so that no interaction with other nuclei takes place until the full deexcitation of the residual nucleus.

For the reactions (n,2n), (n,3n), (n,n'α), (n,n'p) etc. the recoil spectra were obtained by using a one-neutron emission model (33) corresponding to the inelastic scattering with a level energy equal to the reaction threshold. The secondary neutron spectra given in ENDF/B-IV were assumed to be applicable at all angles in the center-of-mass system. The effect of the emission of the second particle on the recoil spectra was not thought to be large.

In case of neutron absorption reactions, such as (n,p), (n,d), (n,t), (n,^{3}He), (n,α) etc., the neutron evaporation model with the inclusion of the emitted particle mass was assumed to apply to all these reactions (34). In addition an effective Coulomb barrier was used as the lower energy at which a charged particle can be emitted.

MACKLIB-IV

MACKLIB-IV (35) is a library of nuclear response functions for all materials presently of interest in fusion and fission applications for neutronics analysis of nuclear systems. The atomic displacement cross sections listed in 1978 in this multigroup data library were taken from the work of Doran (36) in 1976.

The displacement cross sections are based on ENDF/B-IV and are given in the CTR energy group structure of 171 neutron groups (37) with an upper energy limit of 17.333 MeV. Displacement cross sections are available for Al, V, Cr, Fe, Ni, Cu, Nb, Mo, Ta, W, Pb. The effective displacement threshold T_d assumed in generating the displacement cross sections for the various materials are the following: Al 25 eV, V40 eV, Cr 40 eV, Fe 40 eV, Ni 40 eV, Cu 30 eV, Nb 60 eV, Mo 60 eV, Ta 90 eV, W 90 eV, Pb 25 eV. The Lindhard energy partition model was used to define the damage energy T_{DAM}. The conversion to the number of displacements per PKA was done by the proportionality factor $\kappa/2T_d$ (9) with the displacement efficiency κ=0.8. Using T_d=0.04 keV for Cr, Fe and Ni the IAEA recommendation that this factor should be equal to 10 keV^{-1} for iron, steels and nickel-based alloys (8) has been fulfilled.

In the treatment of elastic and inelastic scattering the anisotropy was included when appropriate data were given. For elastic scattering the corrected maximum scattering angle ϕ_{max} of the PKA of the mass A in the center-of-mass system $\mu_{max} = \cos\phi_{max} = 1-(2T_d/T_{max})$ was used instead of $\mu_{max} = +1$ (head-on collision), $T_{max} = 4AE/(A+1)^2$ being the maximum knock-on energy in an elastic collision of a neutron with an atom of atomic weight A. This results in a lower maximum recoil energy T at a neutron energy E and is important for low energy elastic scattering in connection with heavier recoils.

Calculating the displacement cross sections Doran omitted the (n,γ) contribution estimating this neutron reaction to be negligible in various fast and thermal neutron spectra.

The (n,2n) and (n,3n) reactions were taken into account using the sequential emission formulation (38) and its modification (39) for these (n,xn) processes (1)and the secondary neutron emission spectra of the ENDF/B file which do not distinguish between the emitted neutrons. The (n,2n) contribution was calculated applying the 2-n model: the emission of the first neutron with energy E_m in the center-of-mass system (CMS) will result in a recoil energy which was taken to be the same average recoil energy as after the scattering of an incident neutron of energy E having the energy E_m (CMS) after the scattering. In dependence of this average recoil energy and the permissible emission energy of the second neutron which depends on the binding energy of this neutron and on the emission energy of the first neutron the recoil energy for the (n,2n) process was determined. An analogous treatment was used for (n,3n) reactions.

The contributions to the displacement cross section due to the heavy recoils of the charged-particle-out reactions (n,c) were included because displacements are primarily caused by the recoil energy of the residual nucleus. The excitation energy of the residual nucleus and the Coulomb barrier has been taken into account for the calculation of the effective neutron energy threshold. The recoil energy distribution has been based on the evaporation model.

The (n,n'p) and (n,n'α) reactions with two particles being emitted were included by simple adding the neutron cross sections to the (n,p) and (n,α) cross sections, respectively.

No spectrum weighting was used in collapsing the pointwise calculated data to the 171 neutron group structure.

ASTM Standard E693-79 for Iron

In connection with "The Recommended Standard Practice for Characterizing Neutron Exposure in Ferritic Steels in Terms of Displacements per Atom (dpa)" (13) in 1979, the American Society for Testing and Materials issued a data set of displacement cross sections for iron with the fixed designation E693-79. This practice is under the jurisdiction of ASTM Committee E-10 on Nuclear Technology and Application. It is assumed that this displacement cross section for iron is an adequate approximation for any ferritic steel.

The recommended displacement cross section for iron is available for 640 neutron energy groups from 10^{-4} eV up to 20 MeV. 620 groups are given in the SAND-II group structure (12) up to 18 MeV. 20 groups equally spaced in energy are added up to 20 MeV. Thus, the data cover the energy range of primary interest for both fission and fusion reactor applications. The displacement cross sections for iron listed in this data set for 640 neutron energy groups are based on data calculated by Doran from ENDF/B-IV neutron cross sections for iron (MAT=1192) for the 171 CTR neutron energy groups structure and published (36) in 1976. Whereas the (n,γ) contribution to the displacement cross section has been omitted by Doran the neutron reactions included are the elastic and inelastic scattering, (n,2n), charged-particle-out reactions (n,c) as (n,α), (n,p), (n,d), (n,t), (n,^{3}He) and (n,n'α), (n,n'p). The missing (n,γ) contribution was added by ASTM.

The treatment of the elastic scattering as reported in a previous work (33) is the same as in the description given for the displacement cross sections of MACKLIB-IV. Anisotropy has been considered for elastic and inelastic scattering.

For neutron spectra having a significant soft component it may be important for the displacement cross section to include the effect of recoil atoms produced by the emission of energetic gammas in (n,γ) reactions. Thus, an estimate to the displacement cross section of the (n,γ) process was added by ASTM easily obtained by multiplying the energydependent (n,γ) cross section by the damage energy $T_{DAM} = \beta(T_\gamma)T_\gamma$. The recoil energy T_γ due to gamma ray emission was given in terms of the gamma-ray energy E_γ and the mass M of the recoiling atom by $T_\gamma = \overline{E_\gamma^2}/2Mc^2$. The mean square gamma energy $\overline{E_\gamma^2}$ was determined from the gamma-ray energies and tabulated abundances (40). The recoil energy was taken to be independent of the neutron energy because for higher neutron energies the (n,γ) cross section can be neglected relative to other neutron cross sections.

The (n,2n) reaction was approximately treated using the 2-n model.

The contributions of the charged-particle-out reactions (n,c) in which only one particle is emitted were calculated considering the Coulomb barrier and using an evaporation model similar to that used for inelastic scattering. A compound nucleus formation was assumed with isotropic particle emission.

The (n,n'p) and (n,n'α) reactions were included by adding the cross sections to the (n,p) and (n,α) cross sections, respectively.

Comparison of Iron Data

Fig. 1 shows the displacement cross section set for iron recommended by ASTM. In the Fig. 2-5 the displacement cross sections for iron of the group data libraries DAMSIG77 (including Lott's data and the EWGRD set), RECOIL and MACKLIB-IV are compared with the ASTM recommended data set.

Comparing Lott's data with the ASTM data set it is obvious that in Lott's work the contributions of the charged-particle-out reactions to the displacement cross section are missing. The great deviations in the energy region from 1 to 10 keV, for example 400 % at a neutron energy of 1 keV, where elastic scattering is the dominant reaction may result from a different procedure in interpolating point cross sections and from the different maximum cosine of the scattering angle allowed in the CMS. For neutron energies less than 450 eV the displacement cross sections are determined only by the (n,γ) reaction in case of commonly used T_d values. In this region Lott's data are constantly 24 % lower than the ASTM recommended values. This may result from different basic nuclear data. The applied simplified model to calculate the recoil energies after gamma emission is the same in both calculations.

The displacement cross sections published by Genthon et al. (EWGRD) (Fig.3) differ by a broader group structure. In this data set also the high energy charged-particle-out reactions were not taken into account. In the neutron energy region where elastic scattering dominates also an overestimation of the displacement cross sections in comparison to the ASTM values can be observed with the same tendency of an increasing deviation if the neutron energy decreases as in Lott's data. The (n,γ) contribution has been omitted.

The displacement cross sections of iron calculated for a broader group structure on the base of the primary recoil energy distribution library RECOIL show good agreement with the ASTM data also again with the exception of the energy region of dominant

elastic scattering (Fig.4). The point cross sections being the same the procedure used to calculate the recoil energy distribution after elastic neutron scattering may be responsible for the deviations.

In Fig.5 two displacement cross section sets are compared which differ only by the neutron energy group structure and by the fact that in the data set included in the MACKLIB-IV library the (n,γ) contribution has been omitted. The procedure for the data generation as well as the point data base (ENDF/B-IV) are the same. The resonance at about 1 keV only present in the ASTM displacement cross section set results from the (n,γ) reaction.

Developments

Some efforts were made both to improve the displacement cross sections of neutrons for a more accurate estimation of the produced defects in metals and to calculate displacement cross sections for nonmetals:

Revised Nuclear data

Based on ENDF/B-V the displacement cross sections have been reviewed (41) for possible significant changes due to revised nuclear data. The displacement cross sections have been revised for 26 elements also of interest to the fusion materials program. First indications are that most changes are relatively small. Spectral-averaged cross sections generally agree within 10 % of those computed using ENDF/B-IV. The damage parameter file will be extended for Cr, Fe, Ni, Cu, Nb and Au to 44 MeV for applications at Be or Li (d,n) accelerators or spallation neutron sources using calculated and measured neutron cross sections. Further details have been reported by Greenwood and Smither at this meeting in the paper "Displacement Damage Calculations with ENDF/B-V".

Primary Recoil Energy Distribution

a) (n,γ)

The average number of Frenkel pairs $\bar{\nu}$ is a function of the primary recoil energy distribution as result of different neutron reactions. Thus, in the case of emission processes after neutron capture the goal of recent calculations has been to obtain improved recoil energy distributions. Considering neutron flux spectra and the energy dependence of the (n,γ) cross section it is obvious that low energy neutrons may be just as efficient or even more than high energy neutrons in producing damage if a large fraction of the neutrons will be slow enough that (n,γ) reactions become important. That is why an accurate knowledge of the (n,γ) recoil may be of importance.

A new model for (n,γ) capture has been developed and beta-decay effects are also included to calculate (n,γ) displacements (42).

In the past a number of simplifying approximations were generally made to include the (n,γ) reaction in the calculation of atomic displacements: all gammas following capture have been usually considered independently, the effect of the neutron energy, gamma cascades, gamma-gamma angular correlations, angular correlation between the reaction momentum and the γ-ray recoil momentum, life times of intermediate states just as the effect of the momentum of the captured neutron and beta decay effects were ignored.

Now the treatment of the generation of primary recoil atom energy distributions includes all these circumstances accompanied with the (n,γ) process.

Gammas emitted successively in a cascade can be highly correlated in direction. This effects greatly the recoil energy which resulting from (n,γ) reactions is near the displacement threshold energy T_d. Therefore, the assumption of isotropic gamma emission can have major consequences on theoretical predictions. Hence, gamma-gamma correlations and decay schemes for the activated nucleus are needed to determine correctly the recoil energy distribution.

Thus, in case of a s-wave capture the isotropic emission of the first gamma is included whereas in case of a p-wave capture the existing angular distribution of the emitted gamma relative to the neutron momentum is considered.

If the half life of the intermediate state is short compared to the time between collisions the recoil energy distribution produced by two gamma rays in a cascade is a broad distribution whereas the recoil energy spectrum for the long-lived intermediate state cascade is just two sharp lines.

Kinney (43) performed exact calculations of nuclear recoil energies from prompt gamma decays resulting from neutron capture for the sake of an accurate determination of the primary recoil energy distribution from (n,γ) reactions. The calculated recoil energy distribution has been based on detailed nuclear level structures and measured branching ratios taking into account the angular correlations between successive gammas. The results have been compared with previous values of the recoil energy obtained by using simplifications and approximations. The significance of the results discussed in terms of current displacement models is not yet known to the author. Further particulars can be taken from the previously mentioned paper of Greenwood and Smither presented at this meeting.

b) Beta decay

There are many (n,γ) reactions producing short-lived product nuclei which decay by beta and possible further gamma emission. This provides a contribution to the primary recoil energy distribution. In case of a high end-point beta energy of a few MeV there may be enough recoil momentum from the beta decay to displace the product atom. Hence, a significant increase of the number of displacements is possible. The recoil energy is a function of the beta and the neutrino energy depending on the beta-neutrino angular correlation which has been considered as well as the beta-gamma angular correlation in calculating recoil energies (42).

Displacement Efficiency

The secondary displacement model used assumes proportionality between displacements and damage energy. This assumption is physically questionable. For energies well above the displacement threshold T_d an efficiency factor $\kappa = 0.8$ is predicted by analytic theories and binary collision calculations. The significant dependence of κ on the damage energy of the primary recoils as result of radiation damage experiments has been investigated by molecular dynamic calculations of energetic displacement cascades (44) modelling the experimental result of an initial rise of κ in the vicinity of the displacement threshold and of a subsequent drop of κ to 0.3 for damage energies greater than 30 keV for W and Mo. However, it is concluded from

the calculations and the experiments that the reduced damage rates for these damage energies are primarily caused both by recombination of normally stable Frenkel pairs and by high defect mobility induced by lattice agitation during cooling of the cascade.

Displacement Cross Sections for Nonmetals

Displacement cross sections for nonmetals have been calculated by Goland and Dell (45) for evaluating the effects of neutrons on their properties. In view of an application as electrical insulators in fusion reactors ceramics are of current interest. Calculational methods for evaluating displacement cross sections analogous to those in metals have been adapted to these multicomponent solids as Al_2O_3, Si_3N_4 or $MgAl_2O_4$. The damage analysis program DON (46) has been used in conjunction with the damage energy of Coulter and Parkin (47) for multicomponent systems.

Damage cross section library DAMSIG81

In a private communication given by W. L. Zijp from the Netherlands Energy Research Foundation (ECN), Petten, an updated version of the damage cross section library DAMSIG77 has been announced. This new library named DAMSIG81 will be based mainly on ENDF/B-IV neutron cross sections and will be available in 1982.

Conclusion

The displacement cross section data sets described in this paper and available for the calculation of dpa values have been published until 1979. However, these data represent at best the state of the art of 1976 when ENDF/B-IV neutron cross sections have been used together with nuclear models employed at that time for the calculation of displacement cross sections. Therefore if necessary and if available the application of ENDF/B-V neutron cross sections for structural materials and of improved nuclear models for the calculation of the displacement cross sections is recommended.

References

(1) D. G. Doran, N. J. Graves, "Neutron Displacement Damage Cross Sections for Structural Metals", in Irradiation Effects on the Microstructure and Properties of Metals, ASTM STP 611. (1976) 463.

(2) J. Lindhard, V. Nielsen, M. Scharff, P. V. Thomsen, Mat. Fys. Medd. Dan. Vid. Selsk. 33, No 10, (1963)

(3) J. Lindhard, M. Scharff, H. E. Schrott, Mat. Fys. Medd. Dan. Vid. Selsk. 33, No 14, (1963).

(4) J. Lindhard, V. Nielsen, M. Scharff, Mat. Fys. Medd. Dan. Vid. Selsk. 36, No 10 (1968).

(5) M. T. Robinson, Phil. Mag. 17 (1968) 639.

(6) M. T. Robinson, "Nuclear Fusion Reactors", Culham, (1969) 364.

(7) M. T. Robinson, Proceedings of Conference on Radiation-Induced Voids in Metals, Conf-71-61, (1972) 397.

(8) "Recommendations for Displacement Calculations for Reactor/Accelerator Studies in Austenitic Steel", IAEA Specialist Meeting on Radiation Damage Units, Seattle 1972, Nucl. Eng. Design, 33 (1975) 91.

(9) D. G. Doran, J. R. Beeler, N. D. Dudey, M. J. Fluss, "Report on the Working Group on Displacement Models and Procedures for Damage Calculations", HEDL-TME-73-76, (1973).

(10) G. H. Kinchin, R. S. Pease, "The Displacement of Atoms in Solids by Radiation", Rep. Progr. Phys. 18 (1955) 1.

(11) W. L. Zijp, K. H. Appelman, H. J. Nolthenius, H. C. Rieffe, "Damage Cross Section Library (DAMSIG77)", ECN-36, (1978).

(12) W. N. McElroy et al., "SAND-II Neutron Flux Spectra Determinations by Multiple Activation Iterative Method", RSIC-CCC-112 (1969).

(13) ASTM recommended practice E 693-79, Annual Book of ASTM Standards, Part 45 (1980).

(14) D. L. Reed, "The comparison of carbon atom displacement rate in graphite in the Dragon reactor, the Petten HFR and low enrichment HTR", Dragon project report DP-559, 1967.

(15) W. C. Morgan, "Atomic displacement cross section for carbon from ENDF/B-III data", Journal of Nuclear Materials, 51 (1974) 209.

(16) E. P. Barrington, A. L. Pope, J. S. Story, "The data in the Winfrith Nuclear Data Library", AEEW-R-553, 1963.

(17) M. W. Thompson, S. B. Wright, "A new damage function for predicting the effect of reactor irradiation of graphite in different neutron spectra", AERE-R-4701, 1964.

(18) M. W. Thompson, S. B. Wright, Journal of Nuclear Materials 16 (1965) 146.

(19) M. W. Lucas, E. M. J. Mitchell, Carbon 1 (1964) 345.

(20) Specialists Meeting on Radiation Damge on Graphite and on Ferritic and Austenitic Stell, Battelle Seattle Research Center, (1972).

(21) ASTM "Standard Recommended Practice for Reporting Dosimetry Results on Nuclear Graphite", ANSI/ASTM E525-74, Annual Book of ASTM Standards, Part 45, (1980).

(22) T. Iwata, T. Nihira, Phys. Letters 23 (1966) 631.

(23) G. L. Montet, G. E. Myers, Carbon 9 (1971) 179.

(24) T. Iwata, T. Nihira, J. Phys. Soc. Japan, 31 (1971) 1761.

(25) G. L. Montet, Carbon 11 (1973) 89.

(26) G. D. Joanou, J. S. Dudek, General Atomic Report, GA-4265, (1963).

(27) M. Lott, J. P. Genthon, F. Gervaise, P. Mas, J. C. Mougniot, Nguyen van Doan, Proceedings of the IAEA Conference on Nuclear Data in Science and Technology, Vol. 1. p. 89, Paris, March 1973.

(28) J. P. Genthon et al., "Recommendations on the measurement of irradiation received by the structural materials of reactors", EUR 5274 d, e, f, n, 1975.

(29) T.A. Gabriel, J.D. Amburgey, N.M. Greene "Radiation-Damage Calculations: Primary Recoil Spectra, Displacement Rates and Gas-Production Rates", ORNL-TM-5160, (1976).

(30) R.W. Roussin, "Abstracts of the Data Library Packages Assembled by the Radiation Shielding Information Center", ORNL-RSIC-30, Vol.I (1972).

(31) D.M. Plaster, R.T. Santoro, W.E. Ford III, "Coupled 100-Group Neutron and 21-Group Gamma-Ray Cross Sections for EPR Calculations", ORNL-TM-4872, (1975).

(32) M.T. Robinson, "Nuclear Fusion Reactors", Proc. British Nuclear Energy Society Conference, Culham Lab., (1969) 364.

(33) D.G. Doran, Nucl. Sci. Eng. 49 (1972) 130

(34) D.M. Parkin, A.N. Goland, "A Computational Method for the evaluation of Radiation Effects Produced by CTR-Related Neutron Spectra", BNL 50434 (1974).

(35) Y. Gohar, M.A. Abdou, "MACKLIB-IV, A Library of Nuclear Response Functions Generated with the MACK-IV Computer Program from ENDF/B-IV", ANL/FPP/TM-106, (1978).

(36) D.G. Doran, N.J. Graves, "Displacement Cross Sections and PKA Spectra: Tables and Applications", HEDL-TME-76-70, (1976).

(37) R.W. Roussin et al., "The CTR Processed Multigroup Cross Section Library for Neutronics Studies", ORNL/RSIC-37, (1977).

(38) M. Segev, "Inelastic Matrices in Multigroup Calculations", ANL-7710, (1971) 374

(39) G.R. Odette, Trans. Am. Nucl. Soc. 15 (1972) 464

(40) V.J. Orphan, N.C. Rasmussen, T.L. Harper, "Line and Continuum Gamma Ray Yields from Thermal Neutron Capture in 74 Elements", Technical Report GA-10248, DASA-2500, (1970).

(41) L.R. Greenwood, "Revision of Displacement Cross Sections with ENDF/B-V", DOE/ER-0046/5, May 1981, p. 35.

(42) R.K. Smither, L.R. Greenwood, "Description of Neutron Capture and Beta-Decay Process Leading to Displacement Production", DOE/ER-0046/5, May 1981, p. 29.

(43) J.H. Kinney, "Exact Calculations of Nuclear Recoil Energies from Prompt γ Decays Resulting from Neutron Capture", Second Topical Meeting on Fusion Reactor Materials, Aug. 9-12, 1981, Session 3F-2, to be published in J. of Nuclear Materials.

(44) M.W. Guinan, L.R. Greenwood, "Molecular Dynamic Calculations of Energetic Displacement Cascades", Second Topical Meeting on Fusion Reactor Materials, Aug. 9-12, 1981, Session 3F-1, to be published in J. of Nuclear Materials.

(45) A.N. Goland, D.F. Dell, DOE/ER-0046/3 (1980) p. 34

(46) D.M. Parkin, A.N. Goland, Radiation Effects 28 (1976) 31

(47) C.A. Coulter, D.M. Parkin, J. Nuclear Mater. 88 (1980) 249

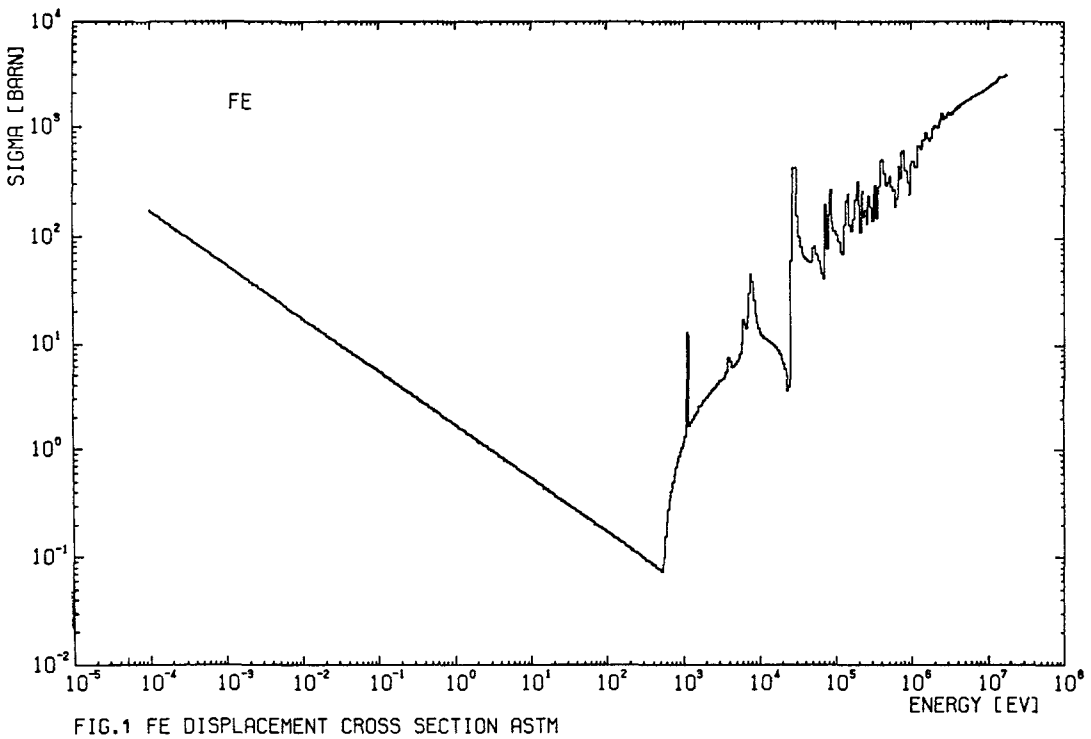

FIG.1 FE DISPLACEMENT CROSS SECTION ASTM

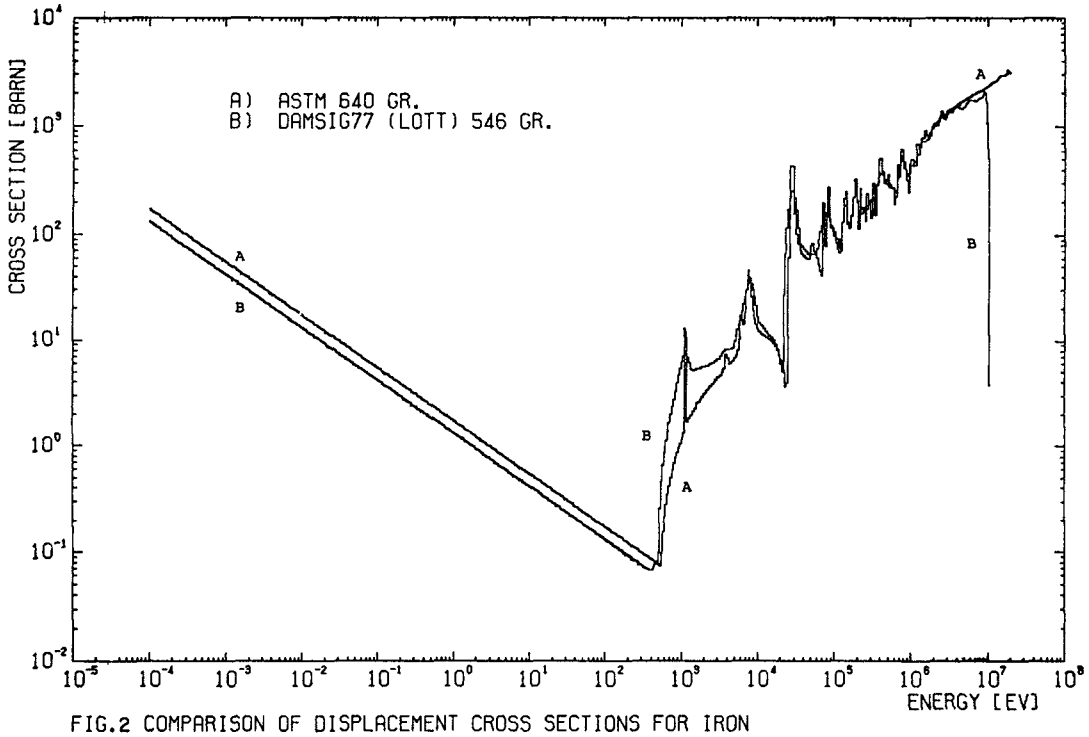

FIG.2 COMPARISON OF DISPLACEMENT CROSS SECTIONS FOR IRON

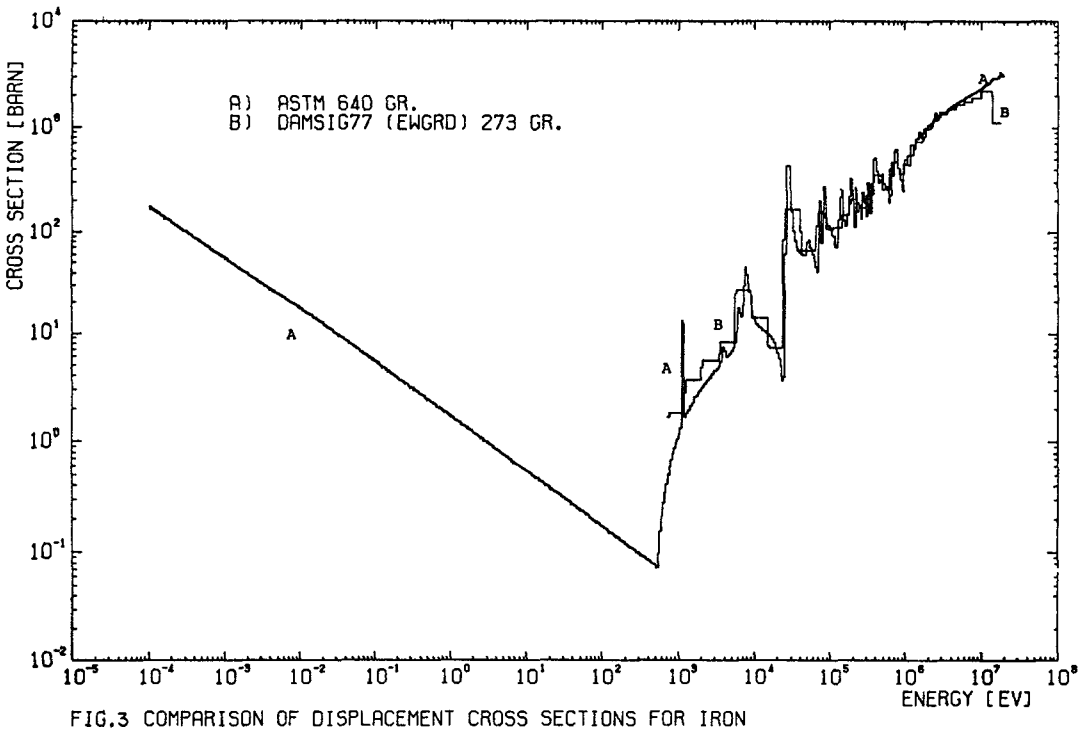

FIG.3 COMPARISON OF DISPLACEMENT CROSS SECTIONS FOR IRON

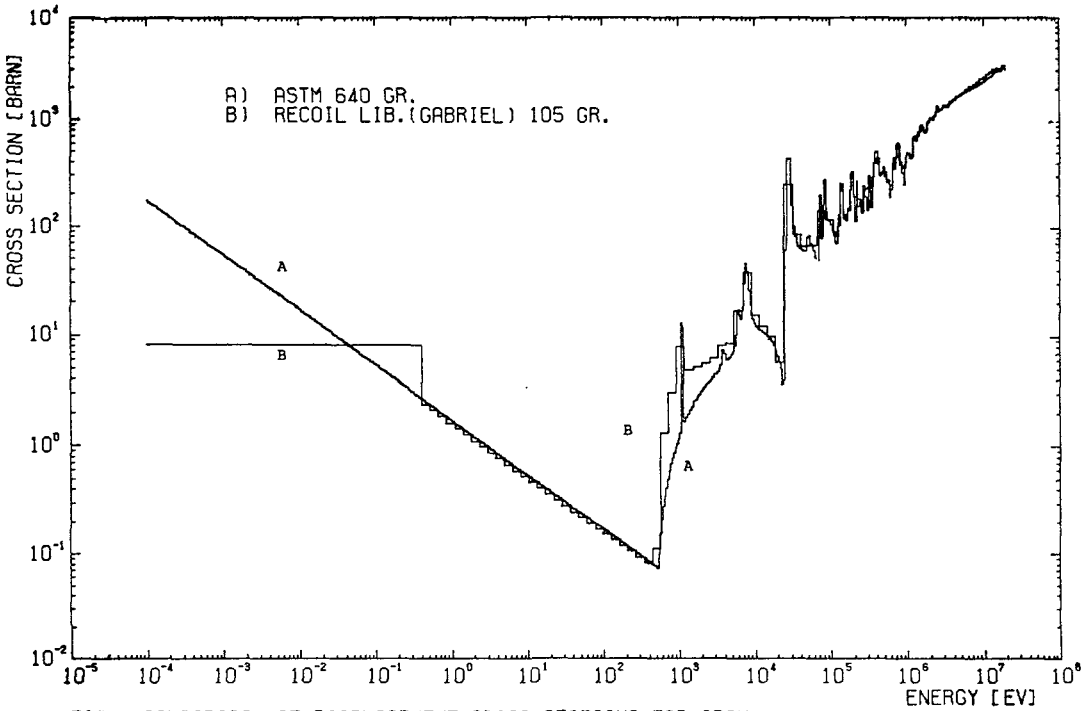

FIG.4 COMPARISON OF DISPLACEMENT CROSS SECTIONS FOR IRON

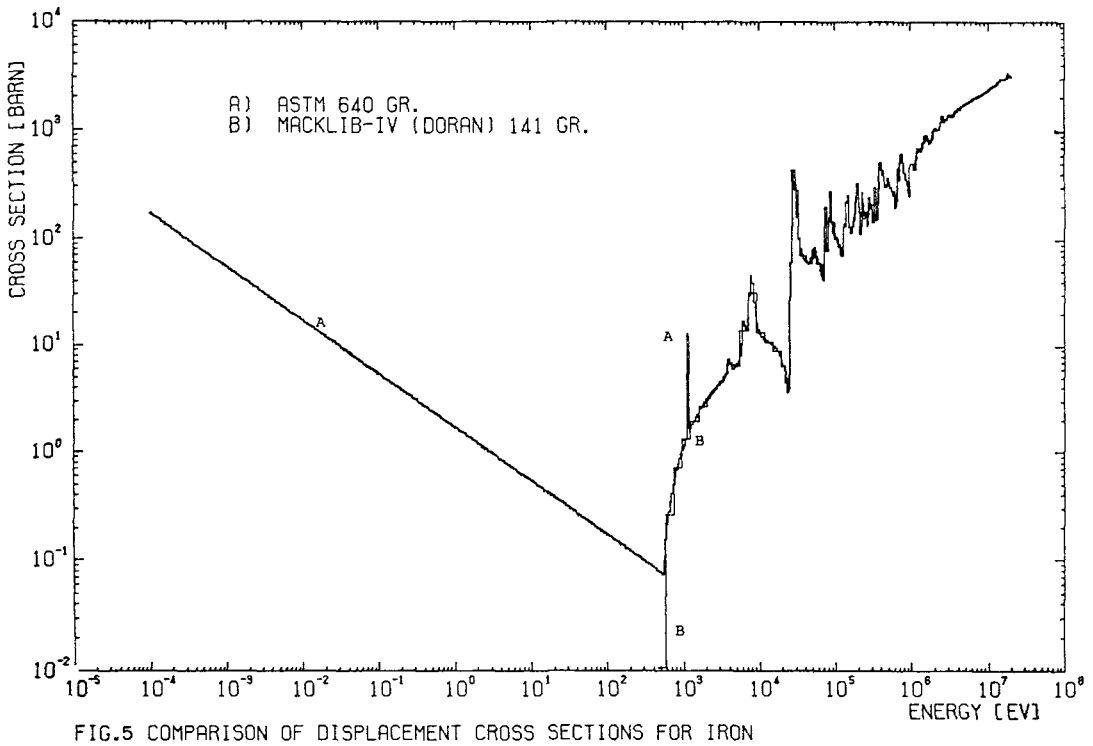

FIG.5 COMPARISON OF DISPLACEMENT CROSS SECTIONS FOR IRON

DISPLACEMENT CROSS SECTIONS IN NEUTRON-IRRADIATED METALS

T. IWATA, S. TAKAMURA, H. MAETA, T. ARUGA
Tokai Research Establishment,
Japan Atomic Energy Research Institute,
Tokai-mura, Ibaraki-ken,
Japan

A b s t r a c t

Resistivity damage rate data for various metals (21 elements) neutron-irradiated at liquid helium temperatures have been compiled. Experimental displacement cross sections have been derived from these data and compared with theoretical ones to clarify the present status of displacement cross sections.

1. Introduction

Experimental and theoretical data on the displacement cross sections in neutron-irradiated metals are compiled and they are compared to make clear the need for nuclear data and the need for experiments and theories on damage production.

The displacement cross sections for neutron irradiations have been studied through the measurement of resistivity damage rates in Argonne National Laboratory[3-5] and Oak Ridge National Laboratory.[1,6-10] Some other laboratories also have obtained experimental data on damage production rates, although their primary concern was in the study of fundamental properties of lattice defects.[21-35]

The displacement cross section σ_d is defined as

$$n_F = \sigma_d \Phi ,$$

where n_F is the concentration of Frenkel defects produced by irradiation and it is equivalent to the displacements per atom (dpa) if dpa < 1. Φ is the total neutron fluence.

2. Experimental determination of σ_d

Neutron irradiation is usually performed at liquid helium temperatures to prevent defects from annealing thermally. The resistivity increase, $\Delta\rho$, by irradiation is measured at such low temperatures as a function of Φ, and

$d(\Delta\rho)/d\Phi$ is plotted against $\Delta\rho$. Then, σ_d is obtained from

$$\left.\frac{d(\Delta\rho)}{d\Phi}\right|_{\Delta\rho=0} = \rho_F \sigma_d ,$$

where ρ_F is the characteristic resistivity of a Frenkel defect.

3. Theoretical calculation of σ_d

The defect concentration n_F is calculated by the following formula;

$$n_F = \Phi \iint \phi(E)\, \sigma(E,T)\, \nu(T)\, dE\, dT,$$

where $\phi(E)$ is the fraction of neutrons with energy between E and E+dE, $\sigma(E,T)$ is the differential cross section for a neutron with energy E to produce a primary knock-on atom (PKA) with energy between T and T+dT, and $\nu(T)$ is the total number of atoms displaced in the subsequent series of atom-atom collisions initiated by a PKA with energy T. Therefore,

$$\sigma_d = \iint \phi(E)\, \sigma(E,T)\, \nu(T)\, dE\, dT.$$

In the NRT model of atomic displacement cascades,[2] $\nu(T)$ is given by the modified Kinchin-Pease formula;

$$\nu(T) = \kappa \frac{f(T)\, T}{2E_d} ,$$

where κ is the displacement efficiency and is assumed to be 0.8 and E_d is the directional average of the threshold energy for displacing an atom from a lattice point. f(T) is the fraction of energy available for elastic collisions during the cascade and it is given by the LSS theory.[11,12] The LSS theory does not consider the so-called atomic number dependence of stopping powers (i. e. Z-oscillation), which has been observed experimentally.[13]

σ_d is often expressed as

$$\sigma_d = 0.8 \frac{\langle \sigma T \rangle}{2E_d} ,$$

and $\langle \sigma T \rangle$ is called the damage-energy cross section.

4. Comparison of experiments and calculations on σ_d

Table I shows the experimental results of initial damage rates obtained in several fission reactors. The results of ANL, München and ORNL were obtained from the extrapolation of the $d(\Delta\rho)/d\Phi$ vs $\Delta\rho$ plot. The others show the averaged data of $\Delta(\Delta\rho)/\Delta\Phi$ on a few specimens in the region of small $\Delta\rho$. The low-temperature irradiation facilities and neutron fields

are described in references cited.[14-20] In the LHTL of JAERI, a cylindrical fuel element made of 90 % enriched uranium-zircalloy alloy surrounds the end of an irradiation tube to convert thermal neutrons into fission ones. Between the fuel element and the irradiation tube, there is inserted a cylindrical shield of B_4C to cut thermal neutrons.[16] The neutron flux and energy spectrum for the VT53 position in ANL CP-5 were recently remeasured and analyzed based on recent advances in theoretical and computer treatments.[5]

Table II shows theoretical data of the damage-energy cross sections calculated by various researchers.

The values of ρ_F and E_d for use in reducing the displacement cross sections are shown in Table III.

Table IV compares the experimental and calculated displacement cross sections for the VT53 position in ANL CP-5.

In Table V are shown the results of experiments performed in the other fission reactors, which are compared with the calculated displacement cross sections for the fission neutron spectrum. The LHTL of JAERI and the LTIF of ORNL are considered to have virtually unmoderated fission neutron spectrum.

Table VI shows the results for Be(d,n) neutron irradiations, where the initial damage rates were obtained from the slope of the $\Delta\rho$ vs Φ plot.

Table VII is the results for T(d,n) neutron irradiations.

5. Conclusion

Tables I-VII show the present status of experiments and calculations on the displacement cross sections. Here we will neither discuss nor evaluate the respective results in various metals. We can draw, however, some requirements for the future studies.

(a) The neutron flux and energy spectrum should be remeasured in the low-temperature neutron irradiation facilities as was done in the VT53 of ANL CP-5.

(b) Displacement cascade models should be developed.

(c) The atomic number dependent energy loss of knock-on atoms should be studied to be used in the displacement calculations.

(d) Damage rate measurement should be extended to various metals and alloys in various neutron energy spectra.

(e) Experimental determination of ρ_F and E_d should be made more accurately and they should be measured also in alloys.

References

1) M. T. Robinson: Fundamental Aspects of Radiation Damage in Metals, ed. M. T. Robinson and F. W. Young, Jr., U. S. ERDA CONF-751006-P1 (1976) p. 1.

2) M. J. Norgett, M. T. Robinson and I. M. Torrens: Nucl. Eng. Des. 33 (1974) 50.

3) J. A. Horak and T. H. Blewitt: Phys. Stat. Sol. (a) 9 (1972) 721.

4) B. S. Brown, T. H. Blewitt, T. L. Scott and A. C. Klank: J. Nucl. Mat. 52 (1974) 215.

5) M. A. Kirk and L. R. Greenwood: J. Nucl. Mat. 80 (1979) 159.

6) J. B. Roberto, C. E. Klabunde, J. M. Williams, R. R. Coltman, Jr., M. J. Saltmarsh and C. B. Fulmer: Appl. Phys. Lett. 30 (1977) 509.

7) J. B. Roberto and M. T. Robinson: J. Nucl. Mat. 61 (1976) 149.

8) J. B. Roberto, M. T. Robinson and C. Y. Fu: J. Nucl. Mat. 63 (1976) 460.

9) R. R. Coltman, Jr., C. E. Klabunde and J. M. Williams: Oak Ridge National Laboratory Report ORNL-5640 (1980) p. 125.

10) T. A. Gabriel, J. D. Amburgey and N. M. Greene: Oak Ridge National Laboratory Report ORNL/TM-5160 (1976).

11) J. Lindhard, M. Scharff and H. E. Schiøtt: Mat. Fys. Medd. Dan. Vid. Selsk. 33 (1963) No. 14.

12) J. Lindhard, V. Nielsen, M. Scharff and P. V. Thomsen: Mat. Fys. Medd. Dan. Vid. Selsk. 33 (1963) No. 11.

13) C. Lehmann: Interaction of Radiation with Solids and Elementary Defect Production (North-Holland, Amsterdam, 1977).

14) A. C. Klank, T. H. Blewitt, J. J. Minarik and T. L. Scott: Bull. Inst. Int. Froid Suppl. 5 (1966) 373.

15) D. J. Mackinnon and G. R. Piercy: Chalk River National Laboratory Report CRRM-1057 (1961).

16) H. Suzuki, S. Okuda, H. Kumamoto, K. Daimon and K. Akasi: Proc. 1st Int. Cryogenic Eng. Conf. (Heywood-Temple Industrial Publications, London, 1968) p. 251.

17) H. Kayano, M. Narui, M. Watanabe and S. Ohuchi: Japan Atomic Energy Research Institute JAERI-memo 3478 (1969).

18) H. Meissner, W. Schilling and H. Wenzl: Euronuclear 2 (1965) 277.

19) R. R. Coltman, Jr., C. E. Klabunde and J. M. Williams: Oak Ridge National Laboratory Report ORNL-5486 (1979) p. 105.

20) J. M. Williams, J. K. Redman, C. E. Klabunde and R. R. Coltman, Jr.: Oak Ridge National Laboratory Report ORNL-5135 (1976) p. 80.

21) M. L. Swanson and G. R. Piercy: Can. J. Phys. 42 (1964) 1605.

22) S. Takamura, H. Maeta and S. Okuda: J. Phys. Soc. Jpn. 25 (1968) 418.

23) S. Takamura, H. Maeta and S. Okuda: J. Phys. Soc. Jpn. 26 (1969) 1120.

24) S. Takamura, H. Maeta and S. Okuda: J. Phys. Soc. Jpn. 26 (1969) 1125.

25) S. Okuda, S. Takamura and H. Maeta: Phys. Stat. Sol. 36 (1969) 531.

26) R. Hanada, S. Takamura, S. Okuda and H. Kimura: Trans. JIM 11 (1970) 434.

27) S. Takamura, R. Hanada, S. Okuda and H. Kimura: J. Phys. Soc. Jpn. 30 (1971) 1091.

28) S. Takamura, R. Hanada and S. Okuda: J. Phys. Soc. Jpn. 30 (1971) 1360.

29) S. Takamura and S. Okuda: J. Phys. Soc. Jpn. 35 (1973) 750.

30) S. Takamura and M. Kobiyama: Radiat. Eff. 49 (1980) 247.

31) H. Maeta, S. Takamura and S. Okuda: Phys. Lett. 75A (1979) 131.

32) S. Ono, S. Takamura, T. Iwata and F. E. Fujita: to be published.

33) M. Nakagawa, K. Böning, P. Rosner and G. Vogl: Phys. Rev. B 16 (1977) 5285.

34) M. Nakagawa, W. Mansel, K. Böning, P. Rosner and G. Vogl: Phys. Rev. B 19 (1979) 742.

35) U. Theis and H. Wollenberger: J. Nucl. Mat. 88 (1980) 121.

36) D. M. Parkin and A. N. Goland: Radiat. Eff. 28 (1976) 31.

37) T. Aruga and K. Shiraishi: to be published.

38) P. Lucasson: Fundamental Aspects of Radiation Damage in Metals, ed. M. T. Robinson and F. W. Young, Jr., U. S. ERDA CONF-751006-P1 (1976) p. 42.

39) P. Vajda: Rev. Mod. Phys. 49 (1977) 481.

40) M. W. Guinan and C. E. Violet: cited in refs. 5 and 9.

41) M. G. Miller and R. L. Chaplin: Radiat. Eff. 22 (1974) 107.

42) T. Iwata and T. Nihira: J. Phys. Soc. Jpn. 31 (1971) 1761.

43) T. Iwata, T. Nihira and H. Matsuo: J. Phys. Soc. Jpn. 33 (1972) 1060.

44) W. C. Morgan: J. Nucl. Mat. 51 (1974) 209.

45) J. McIlwain, R. Gardiner, A. Sosin and S. Myhra: Radiat. Eff. 24 (1975) 19.

Table I. Resistivity damage rates for metals neutron-irradiated in fission reactors, $\left.\frac{d(\Delta\rho)}{d\Phi}\right|_{\Delta\rho=0}$ ($\times 10^{-25}$ Ω cm^3).

	ANL CP-5,VT53 (14,5)	CRNL NRU,D-3 (15)	JAERI JRR-3,LHTL (16,17)	München, FRM CC (18)	München, FRM OC	ORNL BSR,LTIF (19,20)
(1) FCC metals						
Al	1.49(3,5)	2.6 (21)	2.2 (28)	2.94(33)	1.50(35)	2.19(9)
Ni	1.14(3,5)			2.27(33)		1.71(9)
Cu	0.424(3,5)	1.00(21)	0.7(23,24, 25,28)	0.88(33) 1.33(35)	0.945(35)	0.723(9)
Pd				2.16(33)		
Ag	0.295(3,5)			0.85(33)		
Pt	0.818(3,5)			1.88(33)		1.76(6)
Au	0.328(3,5)	0.75(21)	0.6(23,28)	0.73(33)		
(2) BCC metals						
V	4.8 (4,5)					7.17(9)
Fe	3.33(3,5)		6.5 (24)	7.5 (34)		
Nb	2.19(4,5)		6.5 (29)			3.43(9)
Mo	1.86(3,5)		3.4(22,24, 26)	10 (34)		3.38(9)
Ta	1.30(4,5)			3.3 (34)		
W			3.9 (27)	4.7 (34)		
(3) HCP metals and graphite						
C(graphite)			5.5×10^4(32)			
Mg			9 (30)			
Ti			35 (30)			
Co	2.42(3,5)					
Zn		6.50(21)	8 (31)			
Zr			27 (30)	23 (34)		
Cd	3.0 (4,5)	7.10(21)				
Sn				1.33(34)		

Table II. Damage-energy cross sections calculated for fission neutron spectrum. $<\sigma T>$ ($\times 10^{-20}$ eV cm^2)

	Robinson (1) [ENDF/ B-I]	Parkin & Goland (36,1) [ENDF/ B-III]	Gabriel et al (10,1) [ENDF/ B-IV]	Kirk & Greenwood (5) [ENDF/ B-IV]	Aruga & Shiraishi (37) [ENDF/ B-IV]	Aruga & Shiraishi (37) [JENDL-I]
(1) FCC metals						
Al	9.48		10.2	9.44	8.10	10.55
Ni			9.17	7.78	8.32	
Cu	8.02	8.32	9.07	7.73	8.16	8.25
Pd						
Ag		7.2			7.17	
Pt		8.14				
Au	4.89	5.09	5.88		5.02	
(2) BCC metals						
V			10.7		9.85	
Fe					8.46	8.43
Nb	8.00	7.47		7.49	8.02	
Mo		8.22	10.0	8.00	5.17	8.75
Ta					5.57	
W					5.13	
(3) HCP metals and graphite						
C					5.17	5.21
Mg					7.52	
Ti					9.49	
Co			9.33		8.50	
Zn						
Zr						
Cd					6.71	
Sn						

Nuclear data files used in the calculations are shown in parentheses.

Table III. Frenkel defect resistivity (ρ_F) and average threshold energy for defect production (E_d) for various metals.

	ρ_F (10^{-4} Ω cm)	E_d (eV)
(1) FCC metals		
Al	3.9 (38)	27 (38)
Ni	6 (38)	33 (38)
Cu	2.0 (38)	29 (38)
Pd	9 (38)	41 (38)
Ag	2.1 (38)	39 (38)
Pt	9.5 (39)	44 (38)
Au	2.2 (38)	43 (38)
(2) BCC metals		
V	18 (9)	57(41,38)
Fe	30 (39)	44 (38)
Nb	16 (38)	78 (38)
Mo	13 (38)	60-70 (38)
Ta	17 (38)	80-90 (38)
W	14 (38)	100 (38)
(3) HCP metals and graphite		
C (graphite)	4.9×10^4 (43)	28 (42)
Mg	4 (38)	20 (38)
Ti	10 (38)	30 (38)
Co	15 (39)	36 (38)
Zn	15 (39)	29 (38)
Zr	40 (38)	40 (38)
Cd	5 (39)	30 (38)
Sn	1.1 (45)	33(45,38)

Table IV. Displacement cross sections for metals irradiated in the VT53 of CP-5, ANL.[3-5]

	σ_d (Experiment) ($\times 10^{-22}$ cm^2)	$\langle \sigma T \rangle$ (5) ($\times 10^{-21}$ eV cm^2)	σ_d (Theory) ($\times 10^{-22}$ cm^2)
(1) FCC metals			
Al	3.8	76.2	11.3
Ni	1.9	59.0	7.2
Cu	2.1	56.3	7.8
Ag	1.40	47.3	4.9
Pt	0.86	(32.4)*	(2.9)*
Au	1.49	32.4	3.0
(2) BCC metals			
V	2.7		
Fe	1.1	50.7	4.6
Nb	1.4	55.7	2.9
Mo	1.3	61.2	3.8
Ta	0.8		
(3) HCP metals			
Co	1.6	56.0	6.2
Cd	6		

*) $\langle \sigma T \rangle$ for Au was substituted for Pt.

Table V. Comparison of experimental and calculated displacement cross sections. $\sigma_d(10^{-22}cm^2)$.

	Experiment in fission reactors				Calculation for unmoderated fission neutrons					
	CRNL NRU,D-3	JAERI JRR-3,LHTL	München FRM,CC	ORNL BSR,LTIF	Robinson ENDF/B-I	Parkin & Goland ENDF/B-III	Gabriel et al ENDF/B-IV	Kirk & Greenwood ENDF/B-IV	Aruga & Shiraishi ENDF/B-IV	Aruga & Shiraishi JENDL-I
(1) FCC metals										
Al	6.7	5.6	7.5	5.62	14.0		15.1	14.0	12.0	15.6
Ni			3.8	2.9			11.1	9.4	10.1	
Cu	5.0	3.5	4.4, 6.7	3.62	11.1	11.5	12.5	10.7	11.3	11.4
Pd			2.4							
Ag			4.0			7.4			7.4	
Pt			2.0	1.85		7.4				
Au	3.4	2.7	3.3		4.5	4.7	5.5		4.7	
(2) BCC metals										
V				4.0			7.5		6.9	
Fe		2.2	2.5						7.7	7.7
Nb		4.1		2.14	4.1	3.8		3.8	4.1	
Mo		2.4	7.7	2.41		5.1	6.2	4.9	3.2	5.4
Ta			1.9						2.6	
W		2.8	3.4						2.1	
(3) HCP metals and graphite						Morgan(44) ENDF/B-III				
C		11.5				11.2			7.4	7.4
Mg		22							15.0	
Ti		35							12.7	
Zn	4.3	5.3								
Zr		6.8	5.8							
Cd	14.2								8.9	
Sn			12.1							

Table VI. Be(d,n), ORNL[6-8]

	$\frac{d(\Delta\rho)}{d\Phi}\Big\|_{\Delta\rho=0}$ (10^{-25} Ω cm^3)	σ_d (exp) (10^{-22} cm^2)	$<\sigma T>$ (10^{-21} eV cm^2)	σ_d (cal) (10^{-22} cm^2)
Cu	2.11 (6)	10.6	276 (8)	38.1
Pt	4.72 (6)	5.0	(198)*) (8)	(18.0)
Nb	10.1 (6)	6.3	252 (8)	12.9

*) $<\sigma T>$ for Au was substituted.
Deuteron energy, 40 MeV.

Table VII. T(d,n), LLL[40,5,9]

	$\frac{d(\Delta\rho)}{d\Phi}\Big\|_{\Delta\rho=0}$ (10^{-25} Ω cm^3)	σ_d (exp) (10^{-22} cm^2)	$<\sigma T>$ (10^{-21} eV cm^2)	σ_d (cal) (10^{-22} cm^2)
Nb	11.26 (40)	7.0	247 (1)	12.7
			273 (36,1)	14.0
			281 (10,1)	14.4
			263 (5)	13.5
Mo	10.11 (40)	7.2	277 (10,1)	17.0
			259 (5)	15.9

DISPLACEMENT DAMAGE CALCULATIONS WITH ENDF/B-V*

L.R. GREENWOOD, R.K. SMITHER
Chemical Engineering Division,
Argonne National Laboratory,
Argonne, Illinois,
United States of America

DISPLACEMENT DAMAGE CALCULATIONS WITH ENDF/B-V

Neutron displacement damage cross sections have been calculated for 30 elements using nuclear cross sections from ENDF/B-V. Six elements have been extended to 44 MeV for accelerator-based neutron sources. Spectral-averaged damage cross sections are found to agree within 10% of those calculated previously using ENDF/B-IV. Nuclear data is needed to improve the quality of the files and to provide for error assignments. The treatment of some reactions also needs improvement, especially (n,γ), β-decay, and secondary-particle emission above 14 MeV.

Displacement Damage Calculations

Neutron cross sections for the displacement of atoms have been calculated for 30 elements using the DISCS[1] computer code. Nuclear kinematics are used for each reaction to calculate primary knock-on-atoms (PKA) at each neutron energy as a function of recoil atom energy. Exact calculations are performed for elastic scattering using angular distributions directly from ENDF/B-V.[2] For inelastic scattering and nonelastic events we assume a compound nuclear reaction mechanism. An evaporation model is used to describe the energy distribution of emitted particles, and angular distributions are assumed to be isotropic in the center-of-mass coordinate system. Although these assumptions are not entirely correct, deviations from this model are not very significant below 14 MeV, since most of the damage is due solely to elastic and inelastic scattering. Multiple-particle emission is treated using a Monte Carlo procedure to determine the recoil atom energy; however, only the (n,2n) reaction is treated exactly.

Capture gamma events are also included; however, such events are relatively unimportant except in a purely thermal spectrum. At present, all gamma rays are assumed to be emitted independently. The capture gamma spectra of Orphan[3] are thus summed to give an average recoil energy. The effective recoil energy also includes the number of gammas per capture and cut-off energy required to remove an atom from its lattice site. Table I lists cut-off energies and average and effective gamma recoil energies which are used in our calculations. Calculations are now in progress to treat (n,γ) and β-decay events more exactly, as will be discussed later.

*Work performed under the auspices of the U.S. Department of Energy.

Table I. Displacement Energies and (n,γ) Recoil Energies

The effective recoil energy is the true average PKA energy above E_d times the gamma multiplicity per neutron capture.

	Displacement Energy	(n,γ) Recoil Energy, eV	
Element	E_d, eV	True	Effective
Be	31	1188	1912
C	31	683	891
Na	25	297	566
Mg	25	279	745
Al	27	506	640*
Si	25	334	730
K	40	209	413
Ca	40	206	468
Ti	40	367	481
V	40	360	380*
Cr	40	515	590*
Mn	40	281	385
Fe	40	404	420*
Co	40	264	362
Ni	40	530	530*
Cu	40	383	380*
Zr	40	112	140*
Nb	40	102	97*
Mo	60	132	100*
Ag	60	117	136
Ta	90	102	3*
W	90	115	13*
Au	30	71	68
Pb	25	140	140*

*Efficiency factor between 0.8 and 1.0 included from Reference 7.

Once PKA spectra have been calculated, we must assess the probability that an atom of given recoil energy will knock secondary atoms out of their lattice sites. This can be done very simply using the Lindhard model to partition the available particle energy between nuclear events and electronic energy losses (which are ignored). The available nuclear energy is then divided by twice the energy required to remove an atom from its lattice site (typically 40 eV) and multiplied by an efficiency factor of 0.8 to obtain secondary displacements as a function of recoil energy.[4] The total displacement cross section is then obtained by integrating the PKA distributions times the secondary displacement function over the recoil energy spectrum. Displacement cross sections for several elements are shown in Figure 1. Partial cross sections are shown for Fe in Figure 2.

In order to compute displacements at Be or Li(d,n) (FMIT) or spallation (IPNS) neutron sources, it is necessary to have cross sections extending up to 50 and 500 MeV neutron energies, respectively. However, in each case there

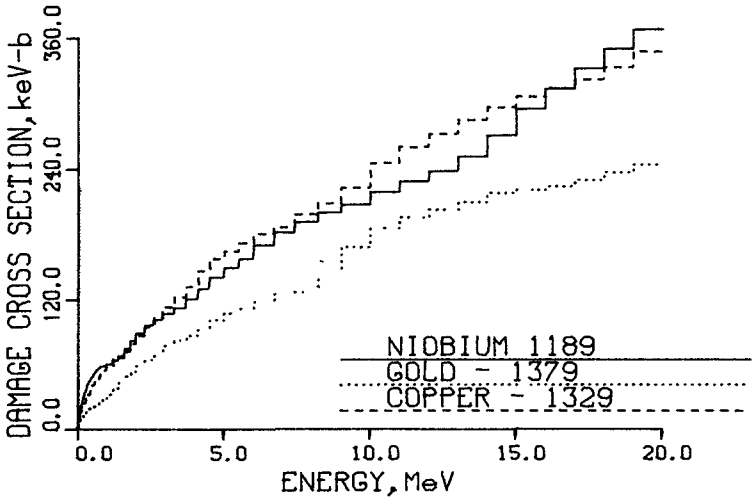

Figure 1. Damage energy cross sections are compared for Cu, Nb, and Au.

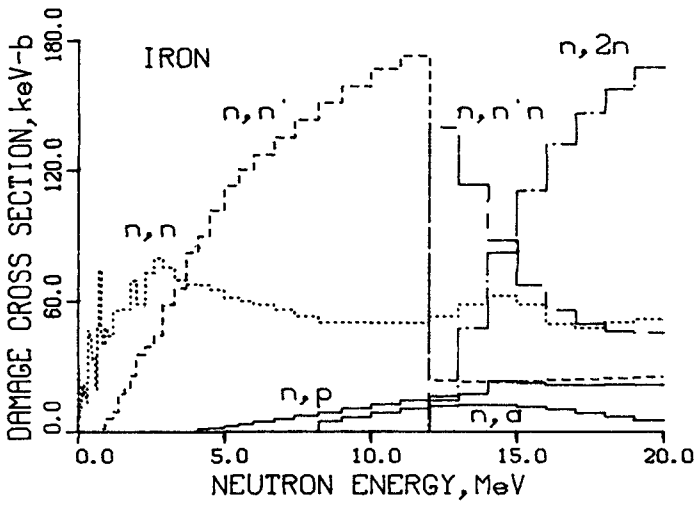

Figure 2. Partial damage energy cross sections are shown for various reactions for iron. Note that the elastic, inelastic, and (n,xn) reactions dominate at all energies.

are very few neutrons above about 30 MeV. We have been able to calculate cross sections to 44 MeV for six elements including Cr, Fe, Ni, Cu, Nb, and Au using a mixture of calculated and measured cross sections. This has proven adequate for existing accelerator neutron sources; however, more calculations are needed for other elements, and some reactions should be treated more exactly at higher neutron energies.

Spectral-Averaged Cross Sections

Spectral-averaged cross sections are listed for a variety of spectra in Table II. The fission-spectrum values are also listed for ENDF/B-IV. As can be seen, all values agree within 10% (this is also true at 14 MeV). In order to assess the importance of various energy regions, the damage rates in Ni are listed in Table III for several broad-energy groups for a mixed-fission reactor

Table II. Spectral-Averaged Damage Energy Cross Sections

To obtain displacement cross sections, multiply by $400/E_d$ (eV, Table I).

Element	$\langle\sigma_D\rangle$, keV - barn			
			^{235}U Fission	
	Thermal (n,γ)[a] (2200 m/s)	14.5 MeV	V[b]	IV[b]
Be	0.018	23.1	35.3	35.9
C	0.0030	39.0	52.0	51.3
Na	0.300	139.9	97.1	-
Mg	0.047	159.8	92.8	91.1
Al	0.147	176.9	96.3	98.3
Si	0.117	191.4	96.0	94.1
K	0.867	256.7	89.3	-
Ca	0.201	273.1	95.4	-
Ti	2.93	243.7	92.8	95.7
V	1.92	269.9	100.9	97.1
Cr	1.83	278.4	94.8	91.6
Mn	5.12	259.6	94.6	98.2
Fe	1.07	290.1	84.4	80.3
Co	13.47	294.1	81.7	85.7
Ni	2.35	300.1	85.0	82.2
Cu	1.44	296.0	79.2	81.3
Zr	0.026	258.9	86.0	73.1
Nb	0.112	270.9	79.5	79.5
Mo	0.265	259.2	83.5	83.4
Ag	8.65	229.6	71.1	71.2
Ta	0.094	215.5	53.5	-
W	0.241	197.2	50.8	-
Au	6.72	217.7	50.2	50.5
Pb	0.024	203.4	59.6	59.1

[a] Thermal cross sections from Reference 8; neutron self-shielding must be included in most applications.

[b] Values are compared for ENDF/B-V and -IV.

Table III. Spectral Dependence of Displacement Damage in Ni

Percent of displacements are shown in each energy range.

Fission Reactors			Accelerator Source[c]	
Energy, MeV	ORR[a]	EBRII[b]	Energy, MeV	Be(d,n), 40 MeV
<0.1	3.7	4.3	<1	2
0.1-0.4	9.2	25.8	1-5	4
0.4-1	13.8	27.3	5-10	11
1-2	24.8	20.0	10-15	23
2-4	32.2	15.9	15-20	28
4-6	11.2	4.8	20-25	19
>6	5.2	2.0	25-30	8
			>30	5

[a]Oak Ridge Research Reactor; mixed-spectrum, flux half-thermal and half-fast at core center.

[b]Experimental Breeder Reactor II at Argonne National Laboratory; fast spectrum in blanket region (row 7).

[c]Zero degree spectrum measured at Oak Ridge Isochronous Cyclotron.

(ORR), a fast reactor (EBR-II), and a Be(d,n) neutron source. In the fission case, the most important thing to note is that significant damage (20-30%) is generated by neutrons below 1 MeV. Hence, more work is often needed to define neutron spectra in the 0.1-1 MeV region. For Be(d,n) sources, the neutrons below 1 MeV and above 30 MeV are relatively unimportant.

Nuclear Data Needs

In principle, the nuclear data needs for displacement damage calculations are nearly overwhelming since all nuclear reaction cross sections, angular distributions, and secondary particle distributions must be known for most elements from 0-50 MeV. Fortunately, many reactions do not have to be treated exactly since they contribute very little to the total damage. A mixture of nuclear model calculations and measurements should thus prove adequate for most materials studies. Of course, above 14 MeV nuclear data is often very poorly known and measurements are needed for damage assessments at Be or Li(d,n) and spallation neutron sources. In all cases, elastic and inelastic scattering and multiple neutron emission reactions dominate the damage. Hence, most of the effort should go into improving our knowledge of these reactions. For fusion materials studies, data is needed mainly for Fe, Ni, Cr, Al, Cu, W, Sn, Ti, and V, roughly in order of priority, up to 35 MeV.

Improvements in Nuclear Models

As detailed in the first section, some assumptions have been made in our treatment of the nonelastic reactions. Of course, many of these assumptions are required since nuclear data is simply not available. Nevertheless, work is needed to assess inaccuracies which arise because of these nuclear models.

In particular, we need a model of secondary particle emission, especially for charged particle reactions. Multiple-particle reactions such as (n,3n) or (n,np) should also be treated more exactly. Of course, neither of these two problems are very important below 14 MeV and generally contribute less than 10% of the total displacements.

Improvements are also needed in our treatment of the (n,γ) reactions. Nuclear lifetimes are typically less than recoil stopping times. Hence, gamma cascades and angular correlations should be taken into account. At the very least, PKA spectra should be calculated since we now only have a spike at the average recoil energy (see Table I). We are now working on this problem, and preliminary results are shown in Figure 3.(5)

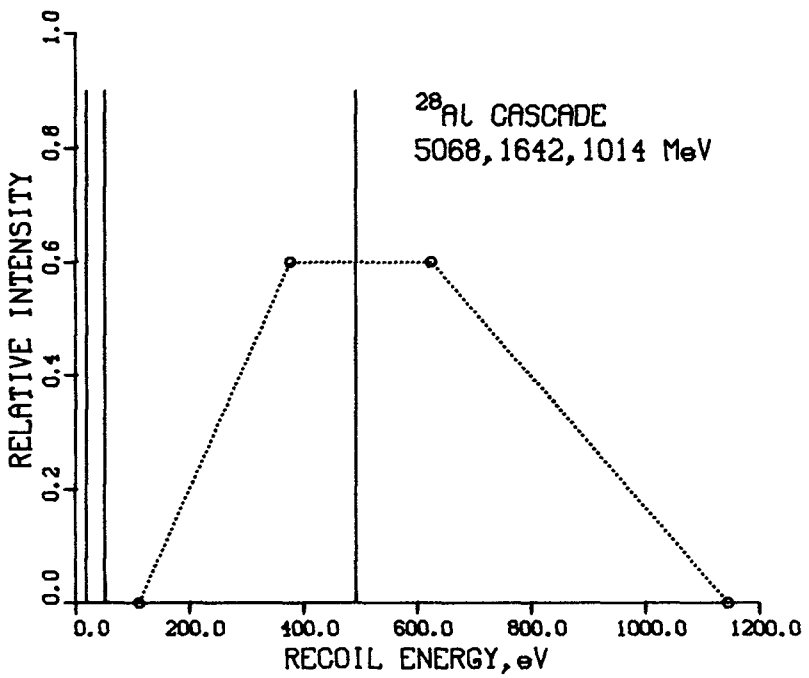

Figure 3. Recoil spectra are shown for the $^{27}Al(n,\gamma)^{28}Al$ reaction leading to a three-gamma cascade. The three solid lines represent the case where lifetimes are much longer than stopping times, and each gamma is treated separately. The dotted line assumes prompt gamma emission with isotropic angular correlations. The average energy is the same for both cases.

In the case of (n,γ) reactions, it should also be pointed out that neutron self-shielding effects may very strongly suppress displacements in a finite sample and will also tend to produce more displacements on the surface of a sample than inside. For example, in ORR a 25 micron Au foil actually sees only half the displacements predicted for an infinitely dilute foil. Hence, some care is needed to apply (n,γ) displacements calculated for typical metallurgical specimens.

Beta-decay is also very important for some nuclei, and although usually neglected it can often add significantly to the damage. For example, capture in ^{27}Al leads to a prompt decay from ^{28}Al. The end point energy is 2.8 MeV resulting in recoils up to 210 eV. The PKA spectrum has been calculated and is shown in Figure 4.(5) Of course, β-decay may often be followed by subsequent gamma emission (e.g., a 1.8 MeV gamma in ^{28}Si). The net effect of beta-decay in aluminum will be about half that of neutron capture and will thus significantly increase the total damage. All prompt β-decay should thus be included in our displacement damage calculations. However, long-lived products will have to be treated separately, since displacements will continue to occur slowly long after an irradiation has been completed.

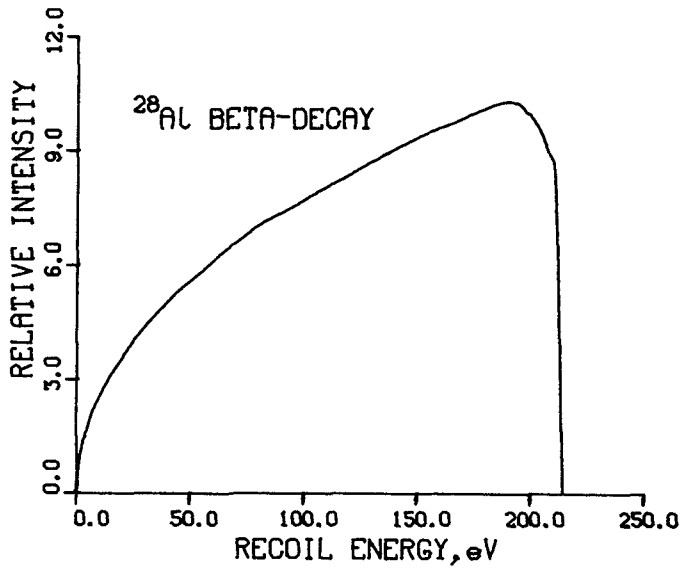

Figure 4. Recoil spectra for ^{28}Al (2.2 m) beta decay following neutron capture in ^{27}Al.

There is also some question about the validity of the Lindhard model used in our secondary displacement calculations. Recent studies indicate significant differences at low recoil energies and alternate models have been proposed.(6) Of course, energies required to produce a displacement must also be reviewed, especially since no experimental data exists for many elements.

Error Analysis

One of the most important deficiencies in our calculation of displacement damage is the lack of a rigorous error analysis. The best guess at present is that displacement cross sections are generally accurate to 10-20%; however, errors increase rapidly with energy and are probably 30-50% above 14 MeV. In principle, error files in ENDF/B-V (although not complete) could be processed for some reactions. However, errors in nuclear models (as discussed above)

might be as large as those given for a specific cross section. This problem requires either more rigorous calculations to test the models or sensitivity studies to determine how important various assumptions really are. Finally, one must consider that displacement cross sections are generally combined with activation measurements to determine the DPA rate for a given experiment. Hence, covariances should also be considered including self-covariances for each reaction, correlations between reaction cross sections, and correlations between displacement cross sections and activation cross sections. Such covariance effects are now routinely considered for spectral unfolding. Covariance matrices for an adjusted flux spectrum should then be combined with that for a displacement cross section to obtain exposure parameters for each irradiation. At present, only the flux-spectral errors are treated properly. Assuming adequate spectral response with activation reactions, it is now generally possible to determine DPA rates to 10-15% accuracy, assuming zero error for the displacement cross sections. Depending on the energy range, an additional 10-20% error is usually added for the unknown error in the displacement calculations.

References

1. G. R. Odette and D. R. Doiron, Nucl. Tech. 29, 346 (1976).

2. Evaluated Nuclear Data File - Version V, National Neutron Cross Section Center, Brookhaven National Laboratory (1979).

3. V. J. Orphan, "Line and Continuum Gamma-Ray Yields from Thermal-Neutron Captures in 75 Elements," GA-10248 (1970).

4. "Recommendations for Displacement Calculations for Reactor/Accelerator Studies in Austenitic Steels," IAEA Specialists Meeting, Nucl. Eng. Des. 33, 91 (1975).

5. R. K. Smither and L. R. Greenwood, "Description of Neutron Capture and Beta-Decay Processes Leading to Displacement Production," DOE-ER-0046-5, p. 29 (May 1981).

6. R. L. Simons, "The Correlation of Irradiation Effects Using Primary Recoil Spectra," DOE-ER-0046-3, p. 41 (November 1980).

7. D. G. Doran and N. J. Graves, "Displacement Cross Sections and PKA Spectra," HEDL-TME-76-70 (1976).

8. Neutron Cross Sections, BNL-325, Third Edition (1976).

EFFECT OF UNCERTAINTIES IN NEUTRON SPECTRA AND FLUENCES DETERMINATION ON THE WWER PRESSURE VESSEL LIFETIME PREDICTION

M. BRUMOVSKÝ *, B. OŠMERA†, V. VALENTA*
*Škoda Concern,
Plzeň

†Nuclear Research Institute,
Řež,
Czechoslovakia

Neutron spectra and dpa calculations in the positions of surveillance specimens and pressure vessel inner surface; the neutron spectra and fluence determination in test reactor. Influence of the uncertainties in neutron spectra and fluences on dpa prediction, estimation of resulting errors and pressure vessel lifetime uncertainty.

The pressure vessel (PV) lifetime prediction of WWER in principle is being performed on the basis of both calculated and experimental data.

The material property changes are determined by irradiation experiments in experimental reactors /1/. The real changes of PV material are continuously monitored by means of the surveillance specimens and thus the PV lifetime prediction could be improved.

The change in transition temperature depending on the neutron fluence according to the relation (1)

$$\Delta T_k = A_\phi \, (\phi t \times 10^{-22})^{1/3} \qquad (1)$$

ϕt = neutron fluence

is used as the main parameter for the PV lifetime study.

The uncertainties of the PV lifetime could be studied from several points of view:

- computation of the neutron spectrum and flux falling on the inner surface of the PV
- neutron spectrum and flux determination in experimental test reactors
- Changes in the mechanical properties (ΔT_k)

- influence of the different spectra on the ΔT_k
- neutron fluence determination for the surveillance specimens
- determination of the property changes of surveillance specimens.

The influence of the neutron spectrum and flux uncertainties on the PV lifetime determination are discussed further.

I. WWER Computations

For the WWER reactor the neutron fluxes falling on the PV inner surface and surveillance specimens placed on the basket of active zone have been computed using JEXD code (a MAC-RAD diffusion - removal code version with 15 groups Greenborg library). The ratio of neutron fluxes for $E \geqslant 0.4$ MeV has been found to be equal about 11 for the surveillance specimens and inner surface fluxes.

The effects of various spectra and fluxes has been compared using dpa.

II. The spectrum of experimental reactor VVR-S, which is being used for irradiation experiments, has been determined experimentally by activation method with SAND-II unfolding technique.

The null approximation of the neutron spectrum for activation measurements in the irradiation channel was taken from the differential measurements carried out in the ŠR-0 reactor loaded with the same type of fuel elements. To obtain better irradiation conditions for the specimens, the ŠR-0 reactor core was rearranged in such a way to imitate precisely the environment of irradiation rig in the VVR-S reactor. All necessary spectrometric and subsidiary measurements were performed in this reactor assembly /2/.

III. The neutron spectrum influence on ΔT_k

The change in the mechanical properties represented by ΔT_k and caused by different neutron spectra could be expressed by means of dpa using relation

$$\Delta T_k^{PV} = \left(\frac{dpa^{PV}}{dpa^{exp}}\right)^{1/3} \Delta T_k^{exp} \qquad (2)$$

The dpa above energy E = 0.4 MeV computed for VVR-S, PV - WWER, surveillance specimens and fission spectra differ in the range of 7 % which corresponds to ~ 2 % change in ΔT_k according to (2). The fraction of dpa above E = 0.4 MeV is equal or greater then 70 % of dpa in the whole energy range; 30 % of dpa, i.e. dpa below E = 0.4 MeV can cause 12 % change of ΔT_k, see fig. 1.

In order to compare computing methods and group libraries a set of computations in plane geometry (isotropic plane U^{235} fission spectrum source, neutron penetration through Fe and Fe + H_2O layers) was performed /3/. Several diffusion - removal codes and group libraries and ANISN (DCL-2 , EURLIB libraries)were used.

The greatest differences were found for ABB and MAC-RAD libraris in diffusion - removal codes (spectrum at x = 10 cm in 30 cm Fe layer). The fluxes above E = 0.4 MeV differ 25 times, i.e. $\phi_{ABBN}\ (E \geq 0.4) \simeq 25\ \phi_{MAC-RAD}\ (E \geq 0.4)$ then $\langle dpa_{ABBN} \rangle \simeq 11 \langle dpa_{MAC-RAD} \rangle$ which coresponds to 220 % change in ΔT_k. For normalized spectra, dpa above 0.4 MeV differ 2.3 times (~ 30 % of ΔT_k).

IV. Neutron Fluence

Uncertainty of dpa depends linearly on the fluence, $(\Delta T_k) \propto (dpa)^{1/3}$, (1), (2), dominant error in test reactor is caused by the error in monitor integral cross section (spectral effect).

Property changes of PV material could be estimated relatively accurately on the basis of surveillance specimen results using relative changes of fluxes and spectra.

V. PV lifetime prediction

The PV lifetime estimation is being performed in two steps (design, exploatation). During the design stage the results of flux computations and material investigations in experimental reactors are taken into account predominantly. The main uncertainties are caused by computed fluxes and measured fluences in experimental reactors.

Real error in determined fluences in test reactors is about 30 % (9 % in ΔT_k) and about 300 % in computing estimation of neutron fluxes which could result in 40 % error in ΔT_k. Further improvement in the PV lifetime prediction could be achieved after 1, 3, 5 and 10 years from the beginning of exploatation, including surveillance specimens results; with respect to the flux ratio it is done with sufficient time reserve.

To decrease the uncertainties in energy space dependent neutron flux calculation and to improve neutron monitoring for surveillance purposes, further computational and experimental studies (benchmarks on physical assemblies) will be performed.

References:

/1/ M. Brumovský, S. Havel, Radiation Damage and annealing in Cr-Mo-Vsteel , Škoda report ZJE 239(1979)

/2/ B. Ošmera et al., Neutron Spectra Measurements and Neutron Flux Monitoring for Radiation Damage Purposes, ÚJV 5081-R

/3/ Hep J., Valenta V., Rataj J., Some Remarks to neutron spectra calculations, Physical problems of WWER, conference Karlovy Vary, 1980 (in czech)

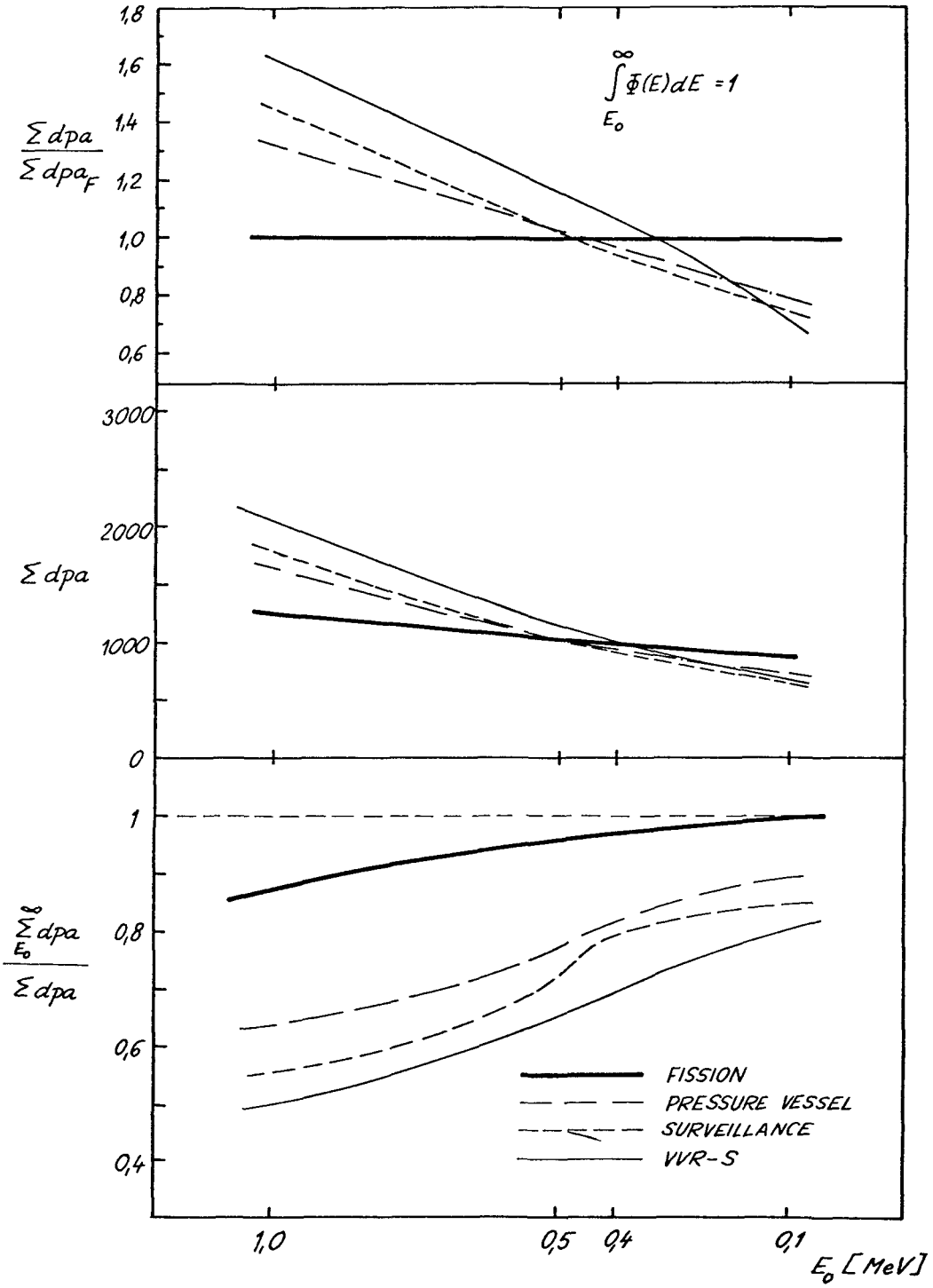

Fig.1 – dpa values for different neutron spectra:
- fission spectrum U^{235}
- pressure vessel inner surface } WWER-440
- surveillance specimens
- VVR-S experimental test reactor

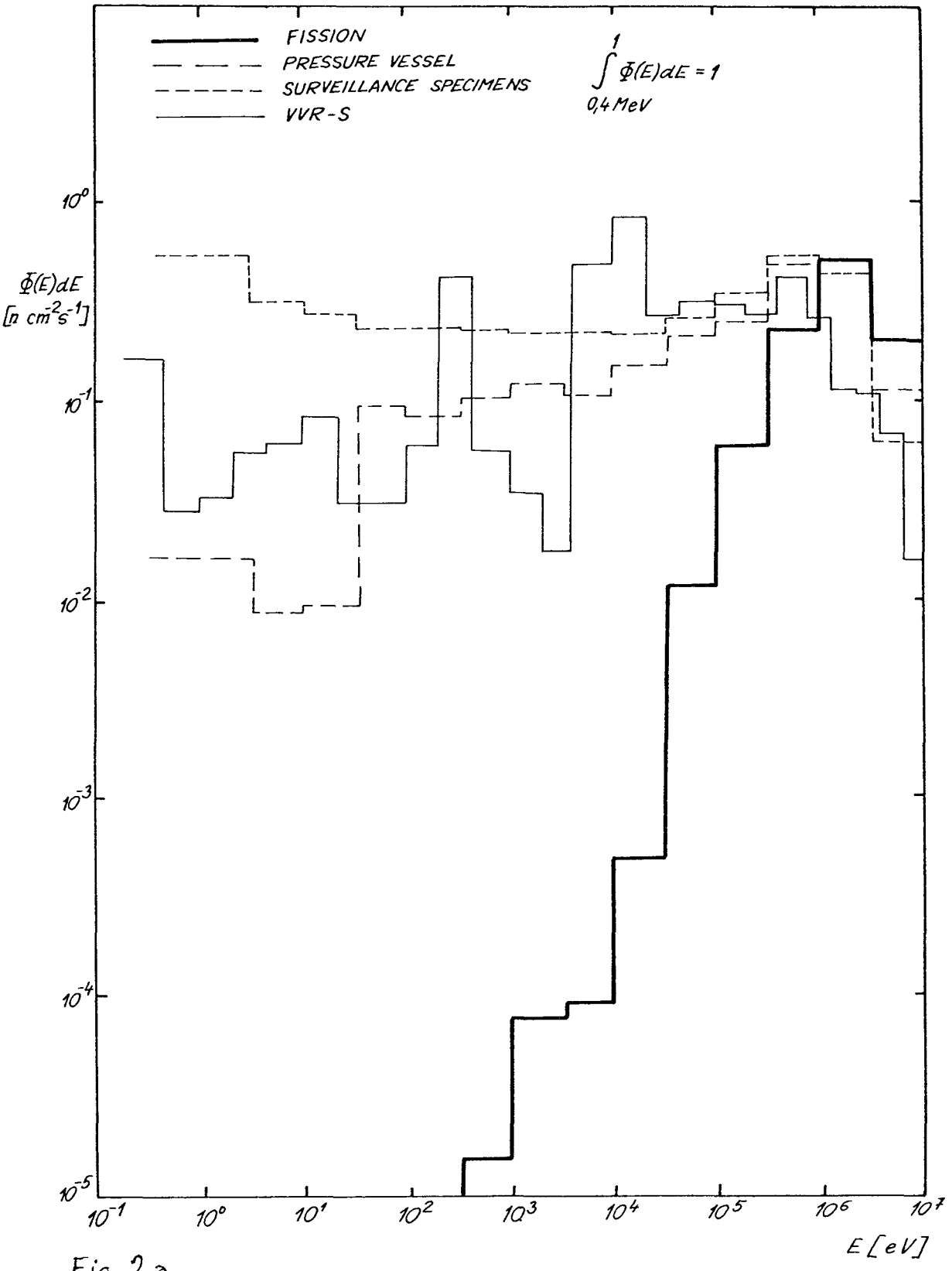

Fig. 2a

Fig. 2 – Group fluxes, normalized to 0,4 MeV (a) and 1.0 MeV (b)
- fission spectrum U^{235}
- pressure vessel inner surface } WWER-440 (calculated)
- surveillance specimens
- VVR-S experimental test reactor (measured)

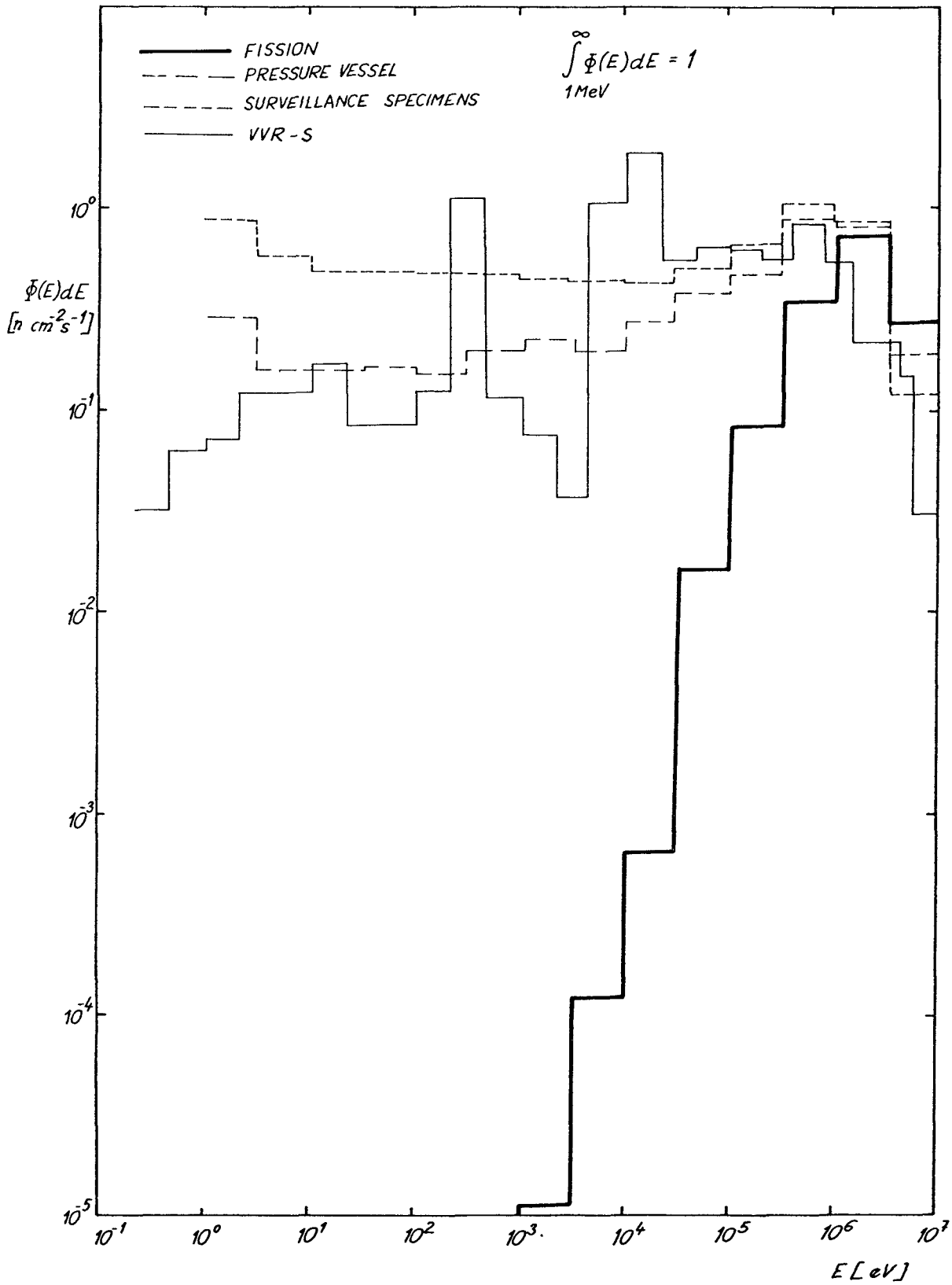
FISSION
PRESSURE VESSEL
SURVEILLANCE SPECIMENS
VVR-S
$\int_{1MeV}^{\infty} \Phi(E)dE = 1$
$\Phi(E)dE$
[n cm^{-2}s^{-1}]
10^{0}
10^{-1}
10^{-2}
10^{-3}
10^{-4}
10^{-5}
10^{-1}
10^{0}
10^{1}
10^{2}
10^{3}
10^{4}
10^{5}
10^{6}
10^{7}
E [eV]

Fig. 2 b

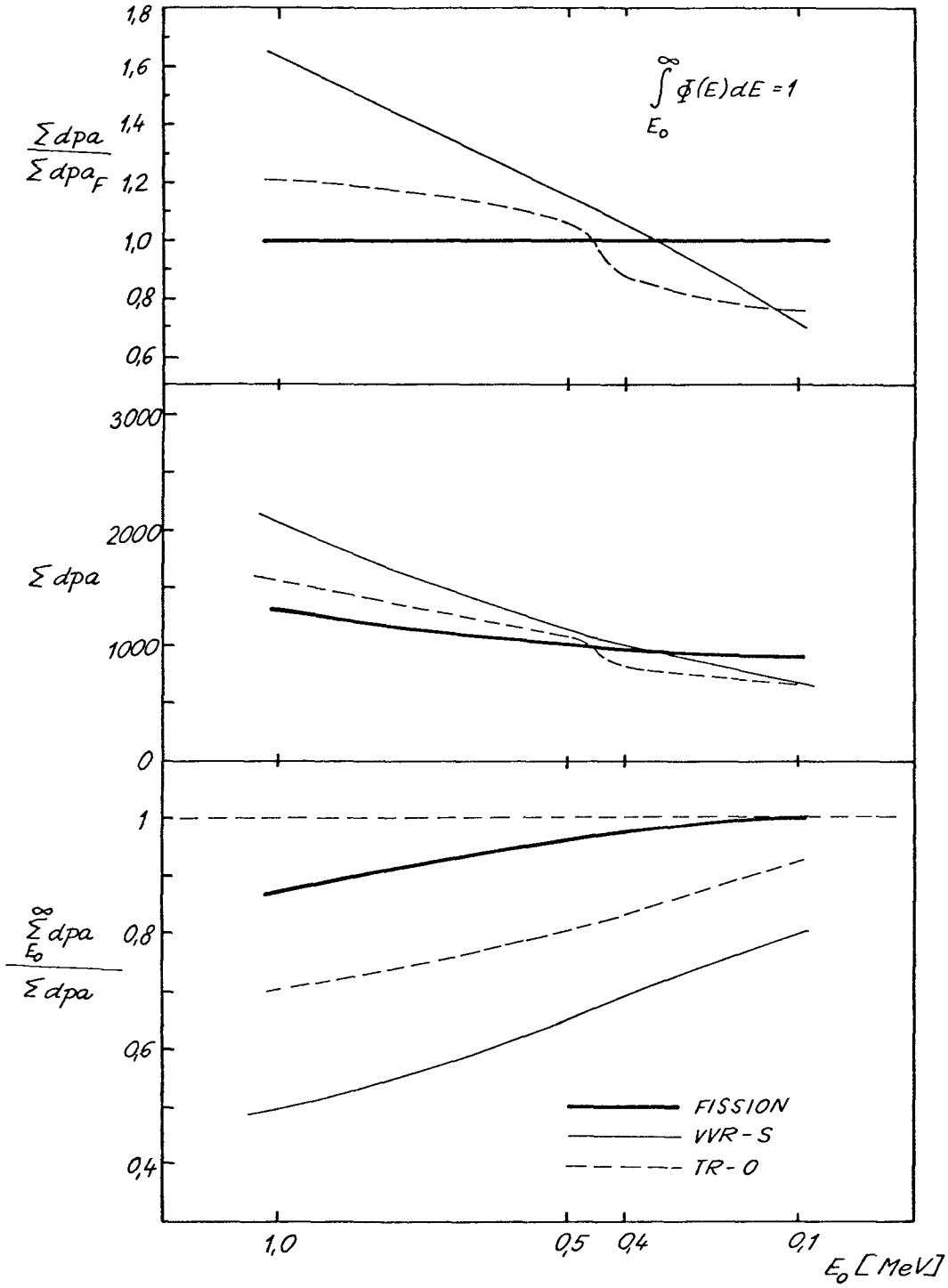

Fig.3 — dpa values for irradiation in light-water (VVR-S) and heavy-water (TR-O) reactors

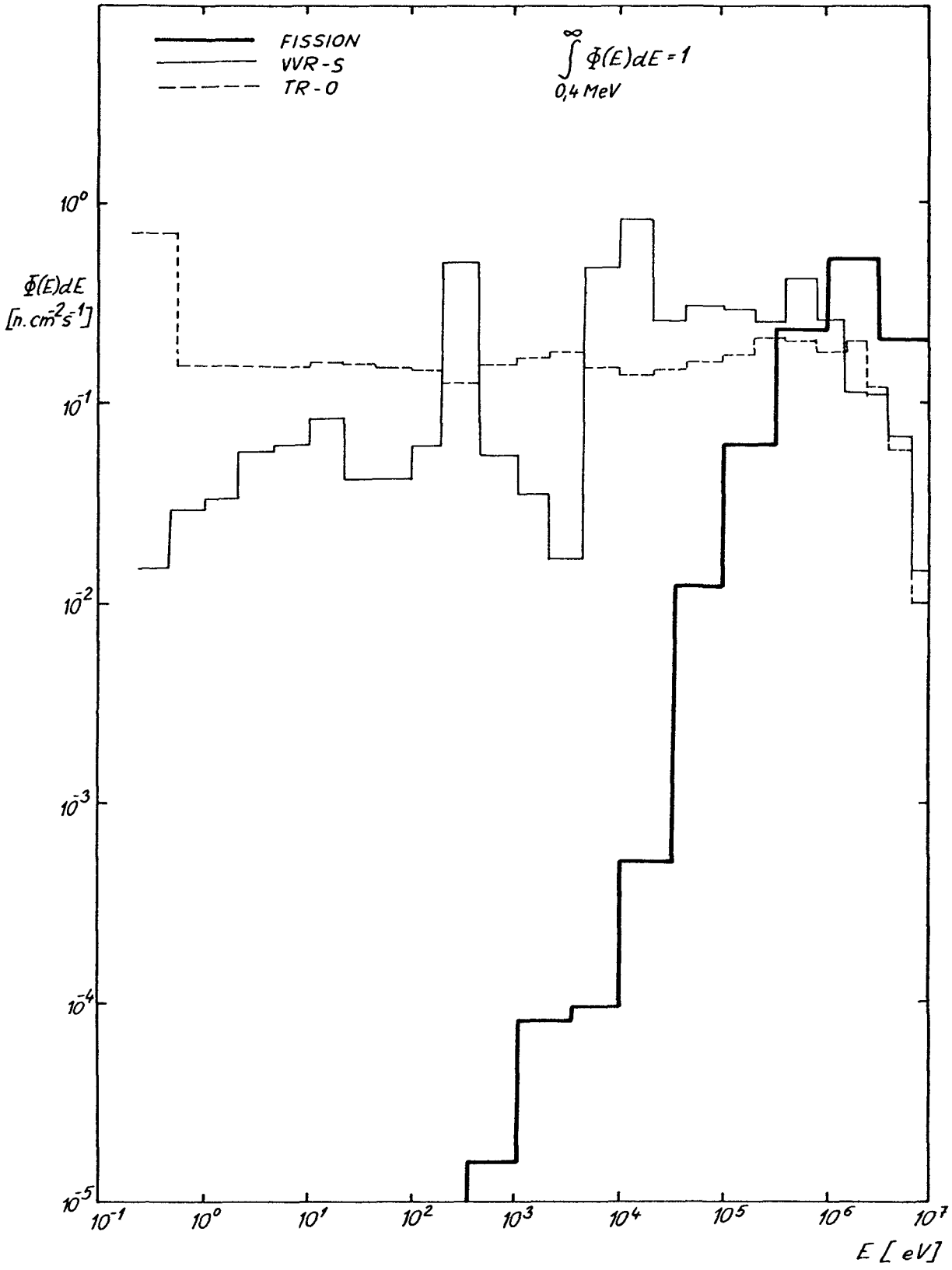

Fig.4 – Group fluxes, normalized to 0.4 MeV for irradiation in light-water (VVR-S) and heavy-water (TR-O) reactors

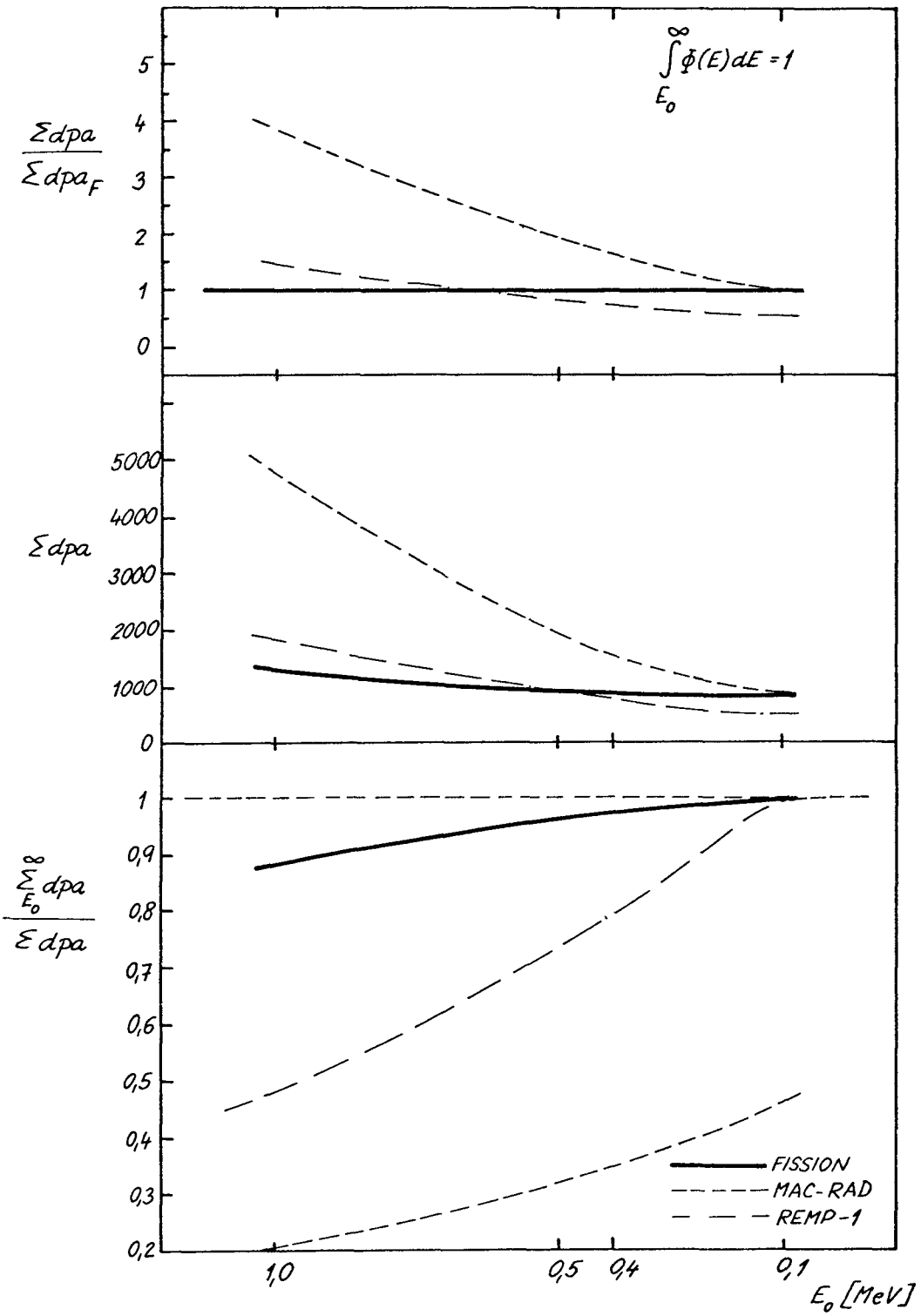

Fig.5 - dpa values for 2 most different spectra (maximum difference from intercomparison of group libraries and computation codes)
spectrum at x = 100 mm in 300 mm Fe layer, isotropic plane U^{235}, fission spectrum source,

USE OF 14 MeV GENERATORS FOR RADIATION DAMAGE STUDIES

J. CSIKAI
Institute of Experimental Physics,
Kossuth University,
Debrecen,
Hungary

Abstract. The paper outlines the present status of radiation damage studies based on the 14 MeV neutron generators. Results for sputtering yields, particle release, range of recoil atoms, chunk emission are discussed. Some new results for the average range of recoils in metals are given.

INTRODUCTION

Recent studies on the Controlled Thermonuclear Reactor (CTR) show that the energy will probably be released in the D-T-Li fuel cycle. During the operation of a D-T reactor its first wall is expected to reach 600-1000 ^{o}C and simultaneously will be bombarded by a 14 MeV neutron flux density of about 10^{14} n/cm^{2}s.

Investigations on the interaction of fast neutrons with structural materials are of primary importance for the design of the thermonuclear reactors. It should be noted, however, that the neutron source facilities are presently not available for the engineering testing of the working conditions of fusion reactors. Recently a number of measurements were carried out on sputtering yields, i.e. the mean number of target atoms ejected per neutron, blistering, particle release, desorption of gases and range of recoil atoms using 14 MeV neutron generators [1-12].

The minimum fluence needed to study the surface effects is about $\sim 10^{17}$ to 10^{18} n/cm^2, while to observe any bulk effects a value of $>10^{20}$ n/cm^2 should be assured [13]. The surface radiation effects involves the study of blistering, sputtering, and particle emission lead to wall erosion and plasma contamination. The bulk neutron fluence can change the physical and mechanical properties of structural materials, including the creep strength, ductility and swelling.

The experimental information available on these processes are very scarce and contradictory.

Measurements on the radioactive recoil emission yields give a possibility to calculate the mean range of energetic atoms in the sample. The mean projected range $\langle R \rangle$ of recoil atoms is equal to the first momentum of the range distribution.

$$\langle R \rangle = \frac{N_f - N_b}{N_t} d,$$

where N_f and N_b are the number of recoil atoms emitted from a target foil of thickness d, in the forward and backward directions, respectively, while N_t is the total number of radioactive recoils [3].
The method of producing radioactive recoil atoms by nuclear reactions in a target and collecting the emitted atoms on catcher foils was proposed by Fluegge and Zimen [20], and refined for nonmonoenergetic recoils by Biersack and Zimen [21]. The energies of fission fragments and recoils from (n,α), (n,p) and (n,2n) reactions produced by 14 MeV neutrons are in the MeV and a few 100 keV ranges, respectively.

EXPERIMENTS

Typical experimental set-ups used for neutron sputtering and recoil experiments are shown in Fig. 1 [3]. The apparatus used in Debrecen for the measurements of the forward and backward emission yields is shown schematically in Fig. 2. Neutrons were produced generally by intense D-T sources [22, 23]. The total neutron dose in sputtering experiments was about 2×10^{13} to 2×10^{16} n/cm^2 using an average flux density of 10^{10} to 10^{12} n/cm^{2}s.

For the determination of the range of radioactive recoil atoms the small neutron generators of about 10^{11}n/s yield can be applied. The number of atoms collected on the catcher foils and through it the activity to be measured depend on the type of reaction. In our experiment [26] thick target foils of Fe, Zn, Cu, and Au were irradiated with 14 MeV neutrons. In this case the values of N_f and N_b can be neglected to N_t and so the mean range of recoils is determined by comparing the activity on the catcher with the activity of the target. The ratio of released atoms (N_f+N_b) to the total number of produced radioactive nuclei (N_t) as a function of target thickness are indicated in Fig. 3 for ^{24}Na and ^{27}Mg [24].

As can be seen in Fig. 3 the ratio depends strongly on the thickness of the target foil at 14 MeV neutron energy. The activities of the targets and catcher foils were measured by a GM counter and a NaI detector. For Zn the 670 keV, while for Cu and Au the 511 keV gamma lines were used.

RESULTS AND DISCUSSION

Results for sputtering yields (S) and the emission of chunks obtained in the 14 MeV neutron experiments are summarized in Table I.

A round-robin experiment [4] shows that the sputtering ratio of Nb has no larger value than 10^{-4} and the results do not allow a definite conclusion to be drawn for the chunk emission.

Spherically and cylindrically shaped chunks containing up to 5×10^{12} atoms per piece were found on the catcher foils. Beckscattered sputtering yield is lower by one order of magnitude than the forward one. The sputtering yields for amorphous materials were calculated by Sigmund [25] using the linear Boltzmann transport theory.

These calculations need accurate cross section data. It should be noted, however, that the experimental results for sputtering are also not reliable enough for comparision with theory. He has shown that for fast neutrons the yield is proportional to the specific damage energy, which is given by:

$$\langle \sigma E_D \rangle = \int_0^\infty E_D \, d\sigma$$

where $d\sigma$ is the differential cross section for transferring an energy T to a target atom by a collision with a fast neutron, E_D is the energy available for the displacement cascade.
As it can be seen in Fig. 4 the $\langle \sigma E_D \rangle$ values for different materials as a function of neutron energy are uncertain [3].

Data obtained for the mean ranges of recoil atoms in solids are summarized in Table II. The errors are due to uncertainties in determining N_t, N_f and N_b and to the geometrical uncertainties.

Biersack has applied the biatomic repulsive potential of Firsov [27] for calculation of stopping power, range straggling of recoil atoms of energies between 100 and 1500 keV. Good agreement was found between the experimental data for the mean ranges in polycrystalline metals or amorphous oxide layers except at the highest energies (see Table II.). Results of Gähler et al. [6] show that the measured range depends strongly on the condition of the surface.

REFERENCES

[1] BEHRISCH, R., GAHLER, R., KALUS, J., J. Nucl. Materials 53 (1974) 183.

[2] KAMINSKY, M., IEEE Transactions Nucl. Sci. 18 (1971) 208.

[3] BEHRISCH, R., Nucl. Instr. and Meth. 132 (1976) 293.

[4] BEHRISCH, R., HARLING, O.K., THOMAS, M.T., BRODZINSKI, R.L., JENKINS, L.H., SMITH, G.J., WENDELKEN, J.F., SALTMARSH, M.J., KAMINSKI, M., DAS, S.K., LOGAN, C.M., MEISENHEIMER, R., ROBINSON, J.E., SHIMOTOMAI, M., THOMPSON, D.A., J. Appl. Phys. 48 (1977) 3914.

[5] BIERSACK, J.P., Z.f. Phys. 211 (1968) 495

[6] GÄHLER, R., KALUS, J., BEHRISCH, R., Nucl. Instr. and Meth. 130 (1975) 203.

[7] KAMINSKY, M., PEAVEY, J.H., DAS, S.K., Phys. Rev. Letters 32 (1974) 599.

[8] OBERHAUSER, R., WIECHMANN, W., Nukleonik 8 (1966) 59.

[9] ERTEL, D., ZIMEN, K.E., Nukleonik 5 (1963) 256.

[10] ZIMEN, K.E., ERTEL, D., Nukleonik 4 (1962) 231.

[11] KELLER, K., Plasma Physics 10 (1968) 195.

[12] BEHRISCH, R., Nuclear Fusion 12 (1972) 695.

[13] PERSIANI, P.J., ANL/CTR-75-1 (1975)

[14] GARBER, R.I., DOLJA, G.P., KALYADA, V.M., MADLIN, A.A., FEDORENKO, A.I., Zh. Eksperim. Teor. Fiz. Pisma 7 (1968) 375.

[15] KAMINSKY, M., DAS, S.,K., IEEE Trans. Nucl. Sci. NS-21 (1974) 37.

[16] KAMINSKY, M., DAS, S.K., Proc. 1st. Topical Meeting on the technique of controlled nuclear fusion, San Diego, USA (April 1974).

[17] KAMINSKY, M., DAS, S.K., J. Nucl. Materials 53 (1974) 162.

[18] KAMINSKY, M., DAS, S.K., Proc. Int. Summer Inst. Univ. of Wisconsin, Milwaukee (August 1975).

[19] HARLING, O.K., THOMAS, M.T., BRODZINSKI, R.L., RANCITELLI, L.A., Phys. Rev. Lett. 34 (1975) 1340.

[20] FLUEGGE, S., ZIMEN, K.E., Z.physik Chemie B42 (1939) 179.

[21] BIERSACK, J.P., ZIMEN, K.E., Z. Naturforsch. 16a (1961) 849.

[22] BARSCHALL, H.H., UWFDM-331 Univ. of Wisconsin (1979).

[23] CSIKAI,J., INDC/NDS/-114/GT, IAEA (1980).

[24] CSIKAI J., BORNEMISZA, P., HUNYADI, I., Nucl. Instr. and Meth. 24 (1963) 227.

[25] SIGMUND, P., Phys. Rev. 184 (1969) 398, 399, 403 and 408.

[26] CSIKAI, J., PETŐ, G., to be published

[27] FIRSOV, O.B., Soviet Phys. JETP 5 (1957) 1192: 6 (1958) 534, 7 (1958) 308.

Table I.

Summary of the neutron sputtering yields

Target material	S atoms/neutron	Chunks size and density	Ref.
Au	$< 6 \times 10^{-4}$		[11]
	3×10^{-3}		[14]
Nb cold rolled 5 /um microfinish	5×10^{-5} to 3.7×10^{-2}	0.3-5 /um 5-30, max. 1000 cm^{-2}	[7]
Nb annealed 0.5 to 2 /um microfinish	1×10^{-4} to 6×10^{-4}	0.3-1 /um 0-20, max.100 cm^{-2}	[15-18]
Nb single crystal	5×10^{-5} to 2×10^{-4}	no	
Au	2×10^{-4} to 2×10^{-5}		[3]
Nb cold rolled as annealed as well	1.1×10^{-5} to 5.9×10^{-4}	→	[19]
Au	2.5×10^{-5}		
Nb	$< 1.3 \times 10^{-3}$ to 1.3×10^{-5}	0.2-2 /um 0-39	[4]

Table II.

Mean ranges of recoil atoms

Recoil atom	$\langle R_f \rangle$	$\langle R_b \rangle$	$\langle R \rangle_{th}$	Reaction	Recoil energy (keV)	Ref.
$^{196}Au^+$	107 Å ± 25 %	7-14 Å	87 Å	(n,2n)	71	[6]
	28.6 Å	-	-	(n,2n)	71	[1]
	188 Å	20±10 Å	-	(n,2n)	71	[26]
$^{92}Nb^+$	296 Å ± 16 %	-	275 Å	(n,2n)	143	[6]
	193 Å	-	-	(n,2n)	143	[1]
^{92}Nb (annealed)	569 Å ± 16 %	26-65 Å	275 Å	(n,2n)	143	[6]
$^{27}Mg^+$	29 x 10^3 Å	-	-	(n,p)	max. 1950	[24]
$^{24}Na^+$	55 x 10^3 Å	-	-	(n,α)	max. 3810	[24]
$^{56}Mn^+$	2060 Å	-	-	(n,p)	260	[26]
$^{62}Cu^+$	1180 Å	-	-	(n,2n)	230	[26]
$^{64}Cu^+$	1170 Å	195 Å	-	(n,2n)	223	[26]
$^{63}Zn^+$	1275 Å	83 Å	-	(n,2n)	226	[26]

+ polycrystal

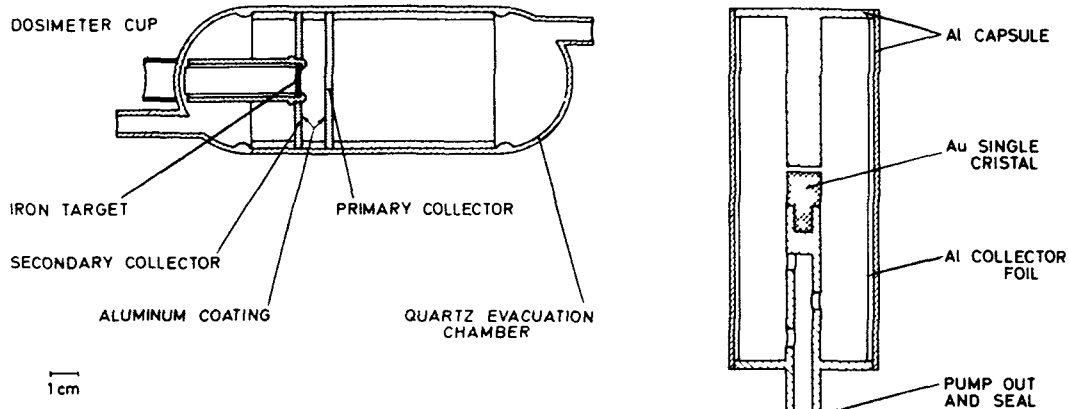

UNIVERSITY OF CINCINNATI
(BATELLE NORTH WEST)

ARGONNE

SCHEMATIC OF THE APPARATUS USED FOR SPUTTERING MEASUREMENTS WITH REACTOR NEUTRONS

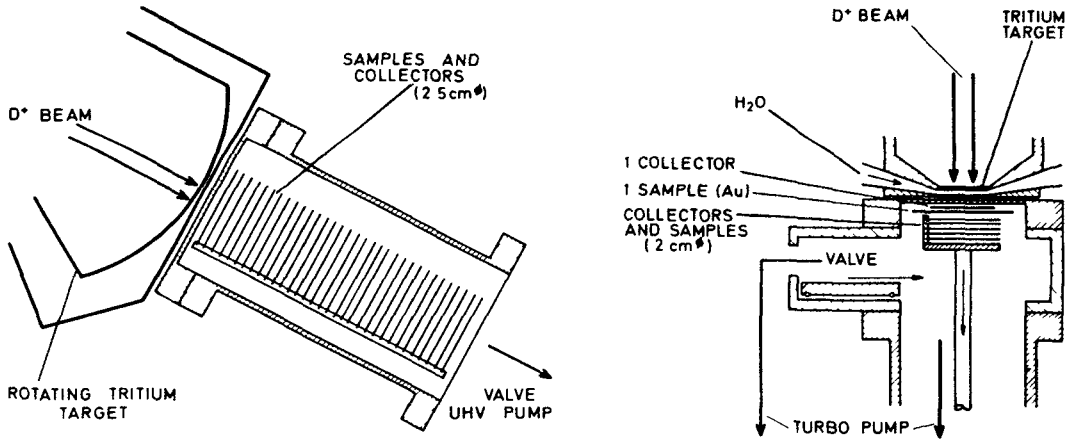

LIVERMORE

GARCHING
(UNIVERSITY OF MAINZ)

SCHEMATIC OF THE APPARATUS USED FOR SPUTTERING MEASUREMENTS WITH 14 MeV NEUTRONS

Fig. 1. Experimental arrangements used in sputtering and recoil experiments.

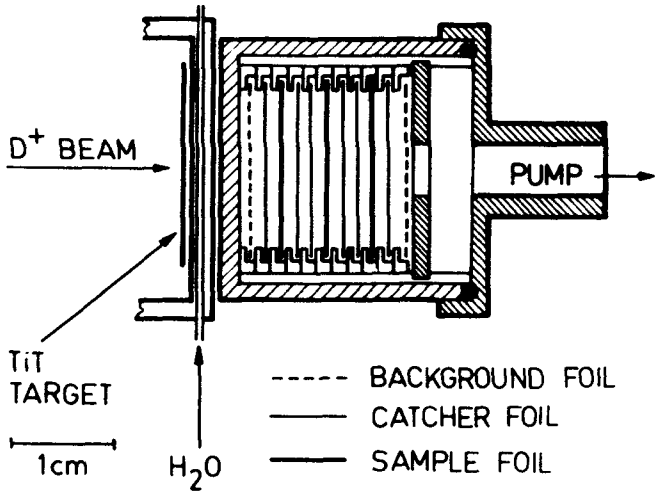

Fig. 2. Apparatus used for neutron recoil experiments in Debrecen.

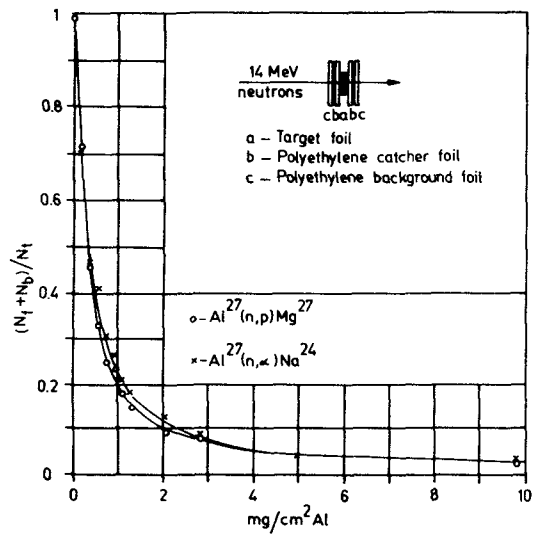

Fig. 3. Ratios of (N_f+N_b) to N_t as a function of sample thickness.

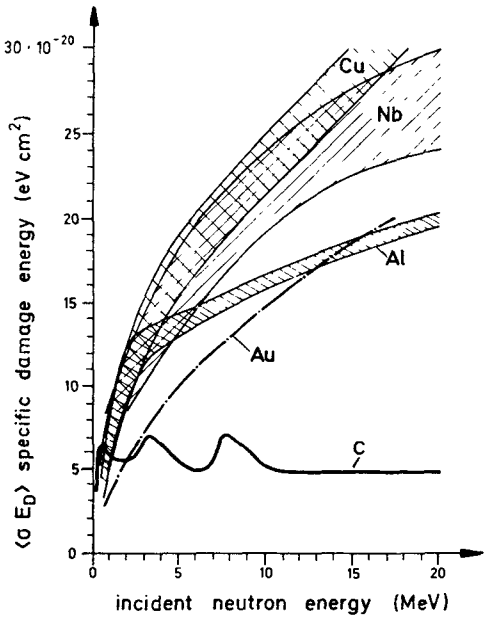

Fig. 4. Specific damage energy for various elements.

STATUS OF NEUTRON DATA REQUIRED FOR CALCULATIONS OF GAS PRODUCTION AND TRANSMUTATION

J. CSIKAI
Institute of Experimental Physics,
Kossuth University,
Debrecen,
Hungary

ABSTRACT. The review outlines the present status of nuclear data needed for calculations of gas production and transmutation for reactor structural materials. The sources of experimental and evaluated data, the systematics and the theoretical models available are discussed.

INTRODUCTION

The nuclear technology related to the design, construction and operation of fission and fusion reactors needs a number of accurate data on nuclear structure, decay and reaction. Study of the properties of structural components of reactors subjected to intense neutron field has social and economic importance. The main sources of radiation damage are as follows: a/ displacement of atoms from the lattice sites b/ formation of foreign atoms by nuclear transmutations. The presence of foreign atoms may strongly influence the development of the damage microstructure, especially the gases like hydrogen and helium produced in /n,xp/ and /n,xα/ reactions are able to stabilize a void in metal against surface tension forces. At working temperature of a fusion reactor the hydrogen diffuse rapidly out of structural material, therefore, especially the helium has a great influence on the void formation and hence swelling. In fast breeder and fusion reactors the release of radioactive foreign atoms by diffusion or nuclear recoil as well as the gas produced embrittlement are also important.

In a thermal reactor the gas production and transmutation are not serious for the low neutron energies involved. The two stage reactions like ^{58}Ni/n,γ/^{59}Ni/n,α/ can be a significant source of He in some spectra. It is evident that the radiation damage depends strongly on the fluence and spectral shape of neutrons. The numbers of primary knock-on atoms /PKA/ and transmutations per neutron show maxima as a function of bombarding energy because the relevant reaction cross sections achieve also peak values between 10 and 20 MeV. This is the reason while the data at around 14 MeV are very important. Starting

from the fact that about one third of the elements are used or considered as reactor structural materials [1,3,4], therefore, a survey on the present status of neutron data is indispensable.

Fig. 1 shows the neutron spectra for thermal and fast reactors compared with that expected at the first wall of a fusion reactor [1]. Accurate excitation functions and double differential cross sections for secondary particles would be necessary in the bombarding neutron energy range given in Fig.1 for the calculation of gas production and transmutation. There is no existing neutron generating facility that can produce transmutation in potential structural materials at the rates calculated by Dudziak [2] e.g. for Al_2O_3 as the first-wall insulator in a fusion reactor.

In this respect the data for /n,charged particle/ reactions should be studied. Among these, however, the /n,t/, /n,^{3}He/ and /n,2p/ processes are unimportant because of low cross sections. The major reactions are as follows: /n,p/, /n,n'p/, /n,d/, /n,α/ and /n,n'α/.

Gas production can be estimated directly from a nuclear data library prepared for activation calculations. Using the library /RECOIL/ [10] Gabriel et al. [11] has calculated the gas production for several alloys and pure elements for a first wall neutron spectrum. Results obtained by Jarvis [7] show that good agreement is rarely found between the two sets of calculations. The discrepancies were attributed to the nuclear cross sections. The expected gas production rates for several materials for fast breeder and fusion reactors are given in Table I.

Table I.

Gas production in structural materials

Parameter	Fast breeder core	Fusion reactor first wall	Ref.
Neutron flux or loading	8.5×10^{15} n/cm^{2}s	3.5 MW/m^2	[1]
Hydrogen gas production (at.ppm/yr)*	700	2000 /SS 316/ 400 /Nb/ 970 /Al_2O_3/	[1] [1] [2]
Helium gas production (at.ppm/yr)	30	660 /SS 316/ 110 /Nb/ 1680 /Al_2O_3/	[1] [2]

*Atomic parts per million per year.

Jarvis [7] has calculated the transmutation rates for five alloys /Nb-1Zr, TZM,V-20Ti, Al2024 and SS316/ considered as CTR first wall materials and compared with the results of Vogelsang et al. [8]. The agreement between the two sets of calculations was rather poor. The largest transmutation rate was observed for Nb-1Zr, where, the Zr content increased to 5.3 % after 37.5 MW-yr/m^2, reducing the ductility of the metal.

In simulation experiments high energy charged particle bombardment is used to simulate the effects of neutrons. Such experiments, however, do not give the same information on the damage as the neutrons [69].

NUCLEAR DATA REQUIREMENTS

According to the latest list issued by the IAEA [5] there is a large number of /n,p/, and /n,α/ cross sections requested for the determination of radiation damage including the hydrogen and helium accumulation as well as the transmutation of elements. As indicated in Table II. most of the data are needed for /n,tot H/ and /n,tot He/ between 9 and 14 MeV with an accuracy of about 10 %. Double differential neutron emission and /n,2n/ cross sections are also requested.

In the case of /n,p/ and /n,α/ reactions the energy-angle differential cross sections (DDCS) are requested only at 14 MeV.

In addition to the /n,p/ and /n,α/ reactions the transmutation products result from neutron capture are also important in the interior of the reactors where the flux density of thermal neutrons is high. The /n,γ/ cross sections at thermal energy and the resonance integrals for epi-thermal neutrons leading to radioactive isotopes are well known [34-38]. The contribution of /n,γ/ reaction to the transmutation products in MeV region can be neglected.

The transmutation caused by the /n,2n/ reaction is more serious for monoisotopic elements than for elements having several stable isotopes since the /n,2n/ reaction can produce an other stable isotope and through it the physical and chemical properties of the material remain the same. For the calculation of transmutation rates the excitation functions of /n,2n/ reactions leading to radioactive isotopes are needed in the energy range given in Fig. 1.

Table II.

Requisted data for radiation damage

Element	Reaction	Energy	Accuracy (%)
^{6}Li	n,α	1 keV - 18 MeV	10
^{7}Li	n,p	14 MeV	DDCS
	n,α	14 MeV	DDCS
	n,tot H	9 - 14 MeV	10
	n,tot He	9 - 14 MeV	10
^{9}Be	n,p	14 MeV	DDCS
	n,α	14 MeV	DDCS
	n,α	8 - 15 MeV	10
	n,tot H	9 - 14 MeV	10
	n,tot He	9 - 14 MeV	10
	(n,2n)	up to 15 MeV	20
^{10}B	n,p	14 MeV	DDCS
	n,α	14 MeV	DDCS
	n,tot H	9 - 14 MeV	10
	n,tot He	9 - 14 MeV	10
	n,tot	1 keV - 18 MeV	10
^{11}B	n,p	14 MeV	DDCS
	n,α	14 MeV	
	n,tot H	9 - 14 MeV	10
	n,tot He	9 - 14 MeV	10
C	n,p	14 MeV	DDCS
	n,α	14 MeV	DDCS
	n,tot H	9 - 14 MeV	10
	n,tot He	9 - 14 MeV	10
^{14}N	n,p	14 MeV	DDCS
	n,α	14 MeV	DDCS
	n,tot H	9 - 14 MeV	10
	n,tot He	9 - 14 MeV	10
O	n,p	14 MeV	DDCS
	n,α	14 MeV	DDCS
	n,tot H	9 - 14 MeV	10
	n,tot He	9 - 14 MeV	10
^{16}O	n,α	up to 15 MeV	15

Element	Reaction	Energy	Accuracy (%)
^{19}F	n,p	14 MeV	DDCS
	n,α	14 MeV	DDCS
	n,tot H	9 - 14 MeV	10
	n,tot He	9 - 14 MeV	10
^{27}Al	n,p	14 MeV	DDCS
	n,α	14 MeV	DDCS
	n,p	up to 15 MeV	15
	n,d	up to 15 MeV	15
	n,t	up to 15 MeV	15
	n,tot H	9 - 14 MeV	10
	n,tot He	9 - 14 MeV	10
Si	n,p	14 MeV	DDCS
	n,α	14 MeV	DDCS
	n,tot H	9 - 14 MeV	10
	n,tot He	9 - 14 MeV	10
Ti	n,p	14 MeV	DDCS
	n,α	14 MeV	DDCS
	n,p	up to 15 MeV	15
	n,α	up to 15 MeV	15
	n,tot H	9 - 35 MeV	10
	n,tot He	9 - 35 MeV	10
V	n,p	14 MeV	DDCS
	n,α	14 MeV	DDCS
	n,p	up to 15 MeV	10
	n,α	up to 15 MeV	10
	n,tot H	9 - 35 MeV	10
	n,tot He	9 - 35 MeV	10
^{50}V	(n,2n)	up to 15 MeV	20
^{51}V	n,α	up to 15 MeV	10
Cr	n,p	14 MeV	DDCS
	n,α	14 MeV	DDCS
	n,p	up to 15 MeV	20
	n,α	up to 15 MeV	20
	n,tot H	9 - 35 MeV	10
	n,tot He	9 - 35 MeV	10
^{52}Cr	(n,2n)	up to 15 MeV	15
Fe	n,p	14 MeV	DDCS
	n,α	14 MeV	DDCS
	n,p	up to 15 MeV	10
	n,α	up to 15 MeV	10
	n,tot H	9 - 35 MeV	10
	n,tot He	9 - 35 MeV	10

Element	Reaction	Energy	Accuracy (%)
Ni	n,p	14 MeV	DDCS
	n,α	14 MeV	DDCS
	n,p	up to 15 MeV	20
	n,α	up to 15 MeV	10
	n,t	up to 15 MeV	15
	n,tot H	9 - 35 MeV	10
	n,tot He	9 - 35 MeV	10
Cu	n,p	14 MeV	DDCS
	n,α	14 MeV	DDCS
	n,p	up to 15 MeV	15
	n,α	up to 15 MeV	15
	n,tot H	9 - 35 MeV	10
	n,tot He	9 - 35 MeV	10
Zr	n,p	up to 15 MeV	15
	n,α	up to 15 MeV	15
^{92}Nb	n,α	up to 15 MeV	30
^{93}Nb	n,p	14 MeV	DDCS
	n,α	14 MeV	DDCS
	n,p	up to 15 MeV	15
	n,α	up to 15 MeV	15
	n,tot H	9 - 35 MeV	10
	n,tot He	up to 35 MeV	10
	n,tot	up to 15 MeV	15
	(n,2n)	up to 15 MeV	10
Mo	n,p	14 MeV	DDCS
	n,α	14 MeV	DDCS
	n,p	up to 15 MeV	15
	n,α	up to 15 MeV	15
	n,tot H	9 - 14 MeV	10
	n,tot He	9 - 14 MeV	10
	(n,2n)	up to 15 MeV	10
Sn	n,p	14 MeV	DDCS
	n,α	14 MeV	DDCS
	n,tot H	9 - 35 MeV	10
	n,tot He	9 - 35 MeV	10
W	n,p	14 MeV	DDCS
	n,α	14 MeV	DDCS
	n,tot H	9 - 14 MeV	10
	n,tot He	9 - 14 MeV	10

Element	Reaction	Energy	Accuracy /%/
Pb	n,p	14 MeV	DDCS
	n,α	14 MeV	DDCS
	n,tot H	9 - 14 MeV	10
	n,tot He	9 - 14 MeV	10
Energy-angle differential neutron emission cross section /DDNE/			
C	DDNE	9 - 15 MeV	10
N	DDNE	9 - 15 MeV	10
O	DDNE	9 - 15 MeV	10
F	DDNE	9 - 15 MeV	10
Al	DDNE	15 - 35 MeV	10
Ti	DDNE	15 - 35 MeV	10-40
V	DDNE	up to 15 MeV	10
Cr	DDNE	15 - 35 MeV	10
Fe	DDNE	15 - 35 MeV	10
Ni	DDNE	15 - 35 MeV	10
Cu	DDNE	15 - 35 MeV	10
^{93}Nb	DDNE	20 - 35 MeV	10-50
Sn	DDNE	15 - 35 MeV	10
Na	n,γ	100 eV -100 keV	10 up to 10 keV 20 above 10 keV
^{40}Ar	n,γ	up to 10 MeV	20
^{45}Sc	n,γ	100 keV- 18 MeV	10
^{50}Cr	n,γ	100 eV - 15 MeV	25
^{62}Ni	n,γ	100 eV - 1 MeV	25
^{64}Zn	n,γ	25 MV - 15 MeV	20
^{107}Pd	n,γ	1 keV- 1 MeV	10

The structural materials are concentrated in the mass number ranges $45 < A < 65$ /Ti, V, Cr, Mn, Fe, Co, Ni/ and $90 < A < 100$ /Zr, Nb, Mo/. Among these the data for Cr, Fe, Ni are the most important. The resonance cross sections for radiative capture σ_γ up to 0.5 MeV are requested with accuracies indicated in brackets for each elements: Fe/$\pm$5 %/, Ni/$\pm$ 8%/, Cr/$\pm$12 %/, Mn/$\pm$10 %/, Mo/$\pm$ 10 %/ [15].

The radioactive decay data is well established and can be taken from the literature [6, 70].

STATUS OF NUCLEAR DATA

Bychkov et al. [9] has given an exhaustive review of the experimental information on the /n,2n/, /n,p/ and /n,α/ threshold reactions and discussed the theoretical models as well as the empirical and semi-empirical systematics used to evaluate the cross-sections. In /n,p/ and /n,α/ reactions effective thresholds are present because the Coulomb barrier of the nucleus prevents the emission of charged particles.

The authors summarized in tables and figures all the available experimental information on the cross sections form the reaction threshold to 20 MeV and in the range of nuclei with $Z > 20$. Recommended excitation functions obtained by theoretical models for various isotopes as well as evaluated cross sections at 14.5 MeV were given. Experimental data published up to 1977 were taken into account.

The recommended cross sections were obtained form the experimental data taking into account the N-Z systematics. In selecting the recommended cross sections they have given preference to measurements based on the activation method, radiochemical separation, enriched isotopes and semiconductor detector. Cross section was not recommended for contradictory data.

Excitation functions calculated for /n,p/, /n,α/ and /n,2n/ reactions were extended for isotopes given in Table III.

It should be noted, however, that the data are very scarce and contradictory in the given energy range. The recommended values /large full points/ together with all the available data for /n,p/, /n,α/ and /n,2n/ cross sections at 14.5 MeV [12] are summarized in Figs. 2, 3 and 4. The deadline date for the literature survey

for small points was 1969, while the crosses represent the modern data.

The numbers shown above the question marks denote the target mass numbers of those nuclides for which data are not available. Data for /n,2n/ cross sections are summarized only for structural materials.

Table III.

Excitation functions given in Ref. [9].

Reaction	Isotope
/n,p/	^{45}Sc, ^{46}Ti, ^{51}V, ^{52}Cr, ^{54}Fe, ^{56}Fe, ^{59}Co, ^{58}Ni, ^{60}Ni, ^{64}Zn, ^{66}Zn, ^{75}As, ^{74}Se, ^{68}Sr, ^{89}Y, ^{90}Zr
/n,α/	^{45}Sc, ^{51}V, ^{54}Fe, ^{59}Co, ^{63}Cu, ^{75}As, ^{79}Br, ^{58}Rb, ^{93}Nb, ^{112}Cd, ^{118}Sn, ^{127}I, ^{133}Cs, ^{140}Ce, ^{197}Au
/n,2n/	^{45}Sc, ^{46}Ti, ^{50}Cr, ^{52}Cr, ^{55}Mn, ^{54}Fe, ^{56}Fe, ^{59}Co, ^{52}Ni, ^{63}Cu, ^{65}Cu, ^{64}Zn, ^{66}Zn, ^{69}Ga, ^{75}As, ^{74}Se, ^{84}Sr, ^{89}Y, ^{90}Zr, ^{93}Nb, ^{103}Rh, ^{127}I, ^{142}Nd, ^{146}Nd, ^{148}Nd, ^{150}Nd, ^{148}Sm, ^{150}Sm, ^{152}Sm, ^{154}Sm, ^{169}Tm, ^{175}Lu, ^{181}Ta, ^{197}Au, ^{203}Tl, ^{209}Bi.

In the case of /n,2n/ reaction mass numbers leading to radioactive isotopes are only indicated. As it can be seen in Figs. 2, 3 and 4 the spread is significant both in old and modern data.

The majority of the recent fast neutron cross sections for /n,p/, /n,α/ and /n,2n/ reactions has been determined for D-T neutrons in the interval of 13.5-15 MeV and similarly to the earlier measurements, in most cases the activation method was used. The possible sources of errors are discussed elsewhere [12].

The techniques used for the determination of reaction cross sections can be divided into three groups, namely activation, accumulation and spectrum methods. The latter is rather difficult because it needs the measurements of the double differential

cross section for the emitted particles in a high background. Recently a charged-particle magnetic quadrupole spectrometer /MQS/ has been constructed [16] for H and He. The improvement in the spectrum methods for the emitted charged particles and neutrons has been surveyed by Qaim [13,14] and Vonach [39]. The accumulation method is simple because only the emitted particles should be collected.

Using a MQS Haight and Grimes [17] have measured the charged particle production cross sections for structural materials at 14-15 MeV. Spectra of protons for ^{46}Ti and ^{48}Ti show the importance of /n,n'p/ reaction /see Fig. 5./. By integrating such spectra over energy and angle the p, d and α emission cross sections were determined. As can be seen in Fig. 6 the total hydrogen and helium production cross sections show large variations from element to element. Both the spectral shapes and angular distributions of /n,p/, /n,n'p/, /n,pn/, /n,d/, /n,α/ and /n,n'α/ processes can be well described in first approximation by the equilibrium mechanism. The hybrid model of Blann [18] reasonable agreements with the angle-integrated data for proton and alpha emission. It was concluded that within an element the pre-equilibrium component is usually more significant for the heavier isotopes. Results obtained by MQS method are also indicated in Fig. 2 and 3. In the case of Cr, Fe and Ni the $\sigma_{n,d}$ is about 10 mb and so its contribution to the total hydrogen content is not higher than 15 %.

Total helium production cross sections for several elements and separated isotopes were measured by Kneff et al. [19] using high-sensitivity gas mass spectrometry /GMS/ [20]. Data obtained by the GMS and MQS methods are summarized in Table IV.

Cross section measured by different methods agree within the quoted uncertainties. The sums of the isotopic cross sections for Ni and Cu weighted by the isotopic abundances, are 102 ± 7 mb and 52 ± 4 mb. These values are in good agreement with the 100 ± 7 mb and 51 ± 3 mb pure element cross sections, respectively. The measured stainless steel Type 316 cross section is 57 ± 4 mb, while the weighted sum of the components Fe, Cr, Ni, Mo and C is 52 ± 3 mb. Preliminary cross section results have also been obtained for C, V, Zr, Nb, Mo, ^{92}Mo, ^{94}Mo, ^{95}Mo, ^{96}Mo, ^{97}Mo, ^{98}Mo, ^{100}Mo, and Pt [22, 23].

Table IV.
Total helium generation cross sections in mb
for 14.8 MeV neutrons

Material	GMS [19]	MQS [17]
Al	145 ± 10	121 ± 25
Ti	37 ± 3	34 ± 7
Cr	34 ± 4	38 ± 6
Fe	48 ± 3	43 ± 7
Ni	100 ± 7	97 ± 16
^{58}Ni	116 ± 8	106 ± 17
^{60}Ni	79 ± 6	76 ± 12
^{61}Ni	53 ± 4	-
^{62}Ni	18 ± 6	-
^{64}Ni	61 ± 4	-
Cu	51 ± 3	42 ± 7
^{63}Cu	67 ± 5	56 ± 10
^{65}Cu	17 ± 2	-
Au	0.72 ± 0.09	-

The energy and angular distributions of alpha particles for 14 MeV neutron induced reactions show the following features; for very light nuclei the /n,α/ reaction seems to proceed mainly as a direct process; there is an intermediate region in which no mechanism dominates; for medium weight nuclei the compound and pre-equilibrium processes seem to dominate; for heavy nuclei the pre-equilibrium and direct processes become dominant [48,49,50].

The /n,n'α/ and /n,n'p/ reactions were studied systematically at 14 MeV by Qaim and Stöcklin [21] and it was shown that their values are high enough to take into account in radiation damage calculations.

In spite of the extensive investigations in recent years the data for /n, charged particle/ reactions are very scarce and contradictory, therefore, the theoretical models and systematics are indispensable to estimate the unknown cross sections. It was shown by Qaim [13] that the /n,np/ and /n,nα/ cross sections depend on the (N-Z)/A asymmetry parameter similarly to the /n,p/ and /n,α/ processes.

Most recently Frehaut et al. [42] determined the excitation functions for /n,2n/ reactions between threshold and 15 MeV for about 50 elements and separated isotopes using a large gadolinium-loaded liquid scintillator tank and pulsed

Table V.

Average cross sections for ^{252}Cf neutrons

Reaction	$\sigma_{n,p}$ [mb]		Reaction	$\sigma_{n,p}$ [mb]	
$^{19}F(n,p)^{19}O$	1.07 ±0.08	[32]	$^{54}Fe(n,p)^{54}Mn$	92.5 ±5.0	[32]
				84.6 ±2.0	[24]
$^{27}Al(n,p)^{27}Mg$	5.11 ±0.43	[32]		87.0 ±5.4	[25]
	4.90 ±0.32	[25]		90.0 ±5.1	[26]
	4.67 ±0.37	[30]		87 ±3	[28]
	3.8 ±0.2	[31]			
$^{28}Si(n,p)^{28}Al$	9.66 ±0.55	[32]	$^{56}Fe(n,p)^{56}Mn$	1.45±0.06	[32]
$^{29}Si(n,p)^{29}Al$	1.79 ±0.79	[32]		1.45±0.035	[24]
$^{32}S(n,p)^{32}P$	72.4 ±4.8	[25]		1.43±0.08	[25]
$^{24}Mg(n,p)^{24}Na$	1.95 ±0.12	[25]		1.18±0.08	[28]
				1.084±0.068	[30]
$^{46}Ti(n,p)^{46}Sc$	13.4 ±1.1	[32]	$^{59}Co(n,p)^{59}Fe$	1.96±0.01	[32]
	13.8 ±0.3	[24]			
	15.0 ±1.0	[26]	$^{58}Ni(n,p)^{58}Co$	113.4 ±4.8	[32]
	12.4 ±1.2	[28]		118 ±3	[24]
				119 ±6	[25]
$^{47}Ti(n,p)^{47}Sc$	22.0 ±0.9	[32]		118.8 ±5.4	[26]
	18.9 ±0.4	[24]		105 ±5	[28]
	20.2 ±1.9	[26]		94.6 ±4.5	[30]
	20.3 ±1.1	[28]			
	19.0 ±1.5	[31]	$^{64}Zn(n,p)^{64}Cu$	46.4 ±2.3	[32]
				39.4 ±1.0	[24]
$^{48}Ti(n,p)^{48}Sc$	0.38 ±0.02	[32]		41.7 ±2.7	[25]
	0.42 ±0.01	[24]		36.6 ±1.5	[30]
	0.434±0.036	[26]			
	0.41 ±0.023	[31]	$^{90}Zr(n,p)^{90m}Y$	0.045±0.006	[32]
			$^{92}Mo(n,p)^{92m}Nb$	16.8 ±0.7	[32]
$^{51}V(n,p)^{51}Ti$	0.93 ±0.10	[32]		10.2 ±1.1	[31]
	0.71 ±0.11	[25]	$^{95}Mo(n,p)^{95m}Nb$	0.144±0.013	[32]
			$^{95}Mo(n,p)^{95}Nb$	21.99±2.00	[32]

Reaction	$\sigma_{n,\gamma}$ [mb]		Reaction	$\sigma_{n,\gamma}$ [mb]	
$^{23}Na(n,\gamma)^{24m+g}Na$	0.335± 0.015	[33]	$^{110}Cd(n,\gamma)^{111m}Cd$ + $^{111}Cd(n,n')$	110 ± 4	[30]
$^{51}V(n,\gamma)^{52}V$	2.8 ± 0.3	[33]		204 ± 7	[31]
$^{55}Mn(n,\gamma)^{56}Mn$	2.96 ± 0.21	[33]	$^{116}Cd(n,\gamma)^{117}Cd$	38 ±14	[31]
$^{59}Co(n,\gamma)^{60m+g}Co$	6.97 ± 0.34	[33]	$^{134}Ba(n,\gamma)^{135m}Ba$ + $^{135}Ba(n,n')$	180 ±11	[30]
$^{63}Cu(n,\gamma)^{64}Cu$ + $^{65}Cu(n,2n)$	10.95 ± 0.51	[27]		255 ±28	[31]
	17.6 ± 1.4	[31]	$^{136}Ba(n,\gamma)^{137m}Ba$ + $^{137}Ba(n,n')$	293 ±29	[31]
$^{65}Cu(n,\gamma)^{66}Cu$	8.0 ± 1.2	[33]			
$^{68}Zn(n,\gamma)^{69m}Zn$	1.84 ± 0.12	[30]	$^{138}Ba(n,\gamma)^{139}Ba$	1.29± 0.26	[30]
$^{75}As(n,\gamma)^{76}As$	26.0 ± 1.6	[31]		3.8 ± 0.4	[31]
$^{84}Sr(n,\gamma)^{85}Sr$	242 ±27	[31]	$^{181}Ta(n,\gamma)^{182m+g}Ta$	119.9 ± 6.5	[33]
$^{86}Sr(n,\gamma)^{87m}Sr$ + $^{87}Sr(n,n')$	129 ± 6	[30]		105.5 ± 6.1	[27]
	182 ±22	[31]		119.1 ± 5.2	[33]
$^{94}Zr(n,\gamma)^{95}Zr$	8.75 ± 0.65	[33]	$^{197}Au(n,\gamma)^{198}Au$	76.2 ± 1.8	[24]
$^{96}Zr(n,\gamma)^{97}Zr$	4.17 ± 0.21	[33]		79.9 ± 2.9	[27]
				95.5 ± 2.3	[29]
$^{98}Mo(n,\gamma)^{98}Mo$ + $^{100}Mo(n,2n)$	26.3 ± 1.3	[33]		77.6 ± 3.1	[30]
	24.8 ± 1.2	[27]		90.6 ± 5.5	[31]
	23.2 ± 1.4	[31]			
			$^{198}Hg(n,\gamma)^{199m}Hg$ + $^{119}Hg(n,n')$	168 ± 6	[31]
$^{100}Mo(n,\gamma)^{101}Mo$	14.85 ± 1.11	[33]	$^{232}Th(n,\gamma)^{233}Th$	87.8 ± 4.0	[27]

Table V. (cont.)

Reaction	$\sigma_{n,\alpha}$ [mb]	
$^{27}Al(n,\alpha)^{24}Na$	1.08 ±0.05	[33]
	1.006±0.022	[24]
	1.060±0.075	[26]
	0.86 ±0.05	[28]
$^{51}V(n,\alpha)^{48}Sc$	0.043±0.002	[33]
$^{59}Co(n,\alpha)^{50}Mn$	0.20 ±0.01	[33]
	0.217±0.015	[25]
	0.20 ±0.01	[28]
$^{93}Nb(n,\alpha)^{90m}Y$	18.3 ±1.5	[33]
$^{92}Mo(n,\alpha)^{89m+g}Zr$	0.42 ±0.02	[33]

neutron source. Data normalized to the $\sigma_{n,f}$ of ^{238}U were obtained with a relative accuracy of 4-10 % for several natural elements /Ti, V, Cr, Fe, Cu, Ga, Zr, Mo, W, Pt, Pb/ and isotopes which are considered as structural materials. It was concluded that the /n,2n/ cross sections appear to be very sensitive to the local behaviour of the level density distributions. Shell effects were also observed in the cross sections.

Ratios of experimental $\sigma_{n,2n}$ to compound nucleus calculations [43] as a function of target mass number for $U_R=E_n+Q/n,2n/=$ 6 MeV are shown in Fig. 7. The calculated cross sections generally overestimate the measured values by about 10 % [44]. According to our investigations [45] the excitation functions of /n,2n/, /n,t/, /n,α/ and /n,p/ reactions can be well described by the Hauser-Feshbach model [46,47] if the level density parameter in the neutron channel is determined from the fit of the calculated /n,α/ excitation function to the experimental data. Further data with higher accuracy are needed to determine the exact contribution of pre-equilibrium emission to the differential and integral cross sections. Both the measured and calculated excitation functions can be checked by the determination of spectrum averaged cross sections. The ^{252}Cf has a good standard Maxwellian spectrum with T_M= 1.42 MeV to control the microscopic data.

As it can be seen in Table V the agreement between data obtained in different laboratories for /n,p/, /n,α/ and /n,γ/ reactions are satisfactory. Average /n,2n/ cross

Table VI.

Average (n,2n) cross-sections for ^{252}Cf and ^{235}U neutrons

Target nuclide	T for (n,2n) (MeV)	$\langle\sigma_{n,2n}\rangle$ for T_M=1.42 MeV (mb)	$\langle\sigma_{n,2n}\rangle$ (mb) Cranberg	Target nuclide	T for (n,2n) (MeV)	$\langle\sigma_{n,2n}\rangle$ for T_M=1.42 MeV (mb)	$\langle\sigma_{n,2n}\rangle$ (mb) Cranberg
N-14	1.46	0.0033	0.0008	Br-81	1.30	0.847	0.2512
F-19	2.50	0.025	0.0063	Rb-85	1.17	0.944	0.2685
Na-23	1.75	0.014	0.0025	Rb-87	1.08	1.81	0.5710
P-31	1.64	0.0033	0.0006	Se-84	1.20	0.0744	0.0164
K-39	1.00	0.0012	0.0002	Y-98	0.93	0.453	0.1119
Sc-45	0.090	0.14	0.0348	Zr-90	1.06	0.264	0.0593
Ti-46	1.42	0.017	0.0030	Mo-92	0.70	0.0526	0.0110
Cr-50	1.59	0.0093	0.0017	Rh-103	0.90	1.50	0.5339
Cr-52	1.11	0.112	0.0246	Ag-107	1.72	1.23	0.4752
Mn-55	1.20	0.632	0.1858	Cd-106	0.94	0.530	0.1446
Fe-54	1.10	0.0047	0.0008	Cd-116	0.97	3.45	1.3555
Co-59	1.05	0.569	0.1624	In-113	1.12	2.33	0.8007
Ni-58	1.31	0.010	0.0022	In-115	1.22	2.45	1.0106
Cu-63	1.64	0.265	0.0678	Sn-112	0.91	0.954	0.2674
Cu-65	1.30	0.840	0.2598	Sb-121	1.32	2.24	0.7855
Zn-64	1.92	0.0640	0.0136	Sb-123	1.17	2.65	0.9719
Zn-66	1.27	0.343	0.0874	I-127	1.26	2.46	0.8811
Ga-69	1.31	0.702	0.2033	Oe-140	1.19	2.54	0.8979
Ge-70	1.24	0.252	0.0602	Pr-141	1.18	2.29	0.7828
Ge-76	2.36	0.963	0.3130	Sm-144	1.30	0.967	0.2708
As-75	1.30	0.825	0.2440	Tm-169	1.14	6.20	2.6156
Se-74	1.09	0.140	0.0306	Au-197	0.87	7.85	3.3985
Se-76	0.91	0.463	0.1206	Tl-203	2.83	3.50	1.4580
Br-79	1.14	0.641	0.1771	Pb-204	1.02	5.15	2.1007

sections for the ^{252}Cf and ^{235}U fission spectra were calculated using the following relations [40,41]

$$\langle\sigma\rangle = \int_{E_{th,2n}}^{E_{th,3n}} \sigma(E)\, N(E)\, dE, \quad \text{where}$$

$\sigma(E) = \sigma_0 \left[1 - (1 + \frac{E}{T}) e^{-\frac{E}{T}}\right]$. The T and σ_0 parameters in Weisskopf formula were fitted to the experimental points.

The calculated values given in Table VI show that the $\sigma_{n,2n}$ data depend strongly on the spectral shape accepted for ^{252}Cf. A change of 10 % in T_M results in a factor of two in $\sigma_{n,2n}$, which means that the neutron spectra in a reactor should be determined with high accuracy to obtain reliable data for the calculation of gas production and transmutation.

THE DATA BASE FOR CALCULATIONS

The status of computer codes and the major requirements of their use for gas production and transmutation calculations were discussed by Jarvis [7]. There are two codes written for fission reactor applications, namely the FISPIN [51] and the ORIGEN [52]. Data libraries for fission reactor applications are available with both codes, it is necessary, however, to provide a group-averaged reaction cross section data library for fusion calculations. The available nuclear cross section library for activation and transmutation for (n,γ), (n,2n), (n,α), (n,p), (n,d), (n,t), (n,nα) and (n,n') reactions is listed in Ref. [7]. The constraction of a multigroup nuclear cross section library from the original literature would require a great effort. Neutron data for fission reactor design and an index to the literature can be found in the CINDA [53]. List of data collections for gas production and transmutation calculations prepared by Jarvis [7] is summarized in Table VII. The following well-documented evaluated data libraries are available at NDS [55]: ENDF/B-IV [56], ENDL [57], KEDAK [58] and ENDF/B-V [59]. The use of nuclear models in the evaluation of nuclear data has been reviewed by Prince [60]. Among the computer codes for gas production and transmutation calculations the THRESH [61], FISPRO [62] and GNASH [63] are recommended to use. Some computer codes and their possible applications are listed in table VIII.

Table VII.

List of data collections for gas production and transmutation calculations

1.	The Evaluated Data Files; /See IAEA tech.report 146/	UKNDL /U.K./ ENDF /U.S./ LLL /U.S./ KEDAK /Germany/ "Benzi" - Italian fission product library "Cook" - Australian fission product library
2.	ENDF/B-IV Dosimetry File. ed. by B.A. Magurno.	BNL-NCS-50446 /1975/
3.	UCRL-50400 Vol 18 /1977/	"ACTL-Evaluated Neutron Activation Cross-section library"
4.	BNL-325, supplement 2 /1966/	
5.	W.E. Alley and R.M. Lessler, "Neutron Activation Cross-Sections",	Nuclear Data Tables 11 /1973/ No's 8 and 9.
6.	"Handbook on nuclear activation cross-sections",	IAEA technical report 156 /1974/
7.	"Compilation of Threshold Reaction Neutron Cross-Sections", A. Schett, K. Okamoto, L. Lesca, F.H. Frohner, H. Liskien and A. Paulsen, EANDC 95 U, Centre de Compilation de Donnees Neutroniques, Saclay /1974/	
8.	"Evaluated reference cross-section library", R.L. Simons and W.N. McElroy, BNWL-1312 /1970/	
9.	"Multigroup reaction cross-sections for FTR application", R.B. Kidman, HEDL-TME-72-135 /1972/.	
10.	"Table of Nuclear reactions and subsequent radioactive decays induced by 14 MeV neutrons" K. Tsukada JAERI 1252 /1977/.	
11.	DLC-33/Montage 400. "100 Group neutron activation cross-section data for fusion reactor structure and coolant materials" R.S.I.C. Oak Ridge /1976/.	
12.	Compilation of Actinide Neutron Nuclear Data KDK-35 NEANDC /OR/ 153L, Stockholm /1979/	

Table VIII.
List of computer codes

1.	THRESH /A statistical model code which computes the particle emission cross section induced by neutrons in the energy range 0-20 MeV./
2.	FISPRO-II. /Can be used to compute radiative capture cross sections over the energy range 1 keV to 10 MeV/.
3.	GNASH /A modern code incorporating pre-equilibrium emission followed by a multi-step Hauser-Feshbach calculation/
4.	STAPRE /A statistical model code for calculating particle induced cross sections using discrete /Hauser-Feshbach/ evaporation and pre-equilibrium /exciton model/ formalisms. Gamma decay is described by means of a cascade model./
5.	OVERLAID ALICE /Evaporation cascade including fission plus pre-equilibrium emission based on Hybrid Model using neutrons, protons and deuterons as projectiles./
6.	ING. /A two-step Hauser-Feshbach code with precompound decays and gamma-ray cascades designed for calculating nuclear reaction cross sections below 20 MeV. Binary-reaction, tertiary-reaction and gamma-ray-production cross sections such as /n,gamma/, /n,p/, /n,2n/, /n,n'gamma/ may be calculated. Energy distributions of secondary particles and gamma rays may be output in ENDF/B formats./
7.	MODESTY /Calculates all energetically possible reaction cross sections and particle spectra within a nuclear decay chain following the method of Uhl [67]./
8.	MSPQ /The code calculates the cross sections of /i,xn/, /i,xnp/, /i,xnalpha/, /i,p/ and /i,alpha/ reactions using the /evaporation/ statistical model with inclusion of preequilibrium emission. The incident particle /i/ can be a neutron, a proton, a deuteron, a triton or an alpha-particle. The number of emitted neutrons /x/ can vary from 1 to 3. The code gives also the neutron spectra of /i,n'/ and /i,2n/ reactions. No angular momentum and parity conservations are taken into account./
9.	AMALTHEE /The code is described for calculations of the energy spectra of particles emitted in /i,x/ and /i,xy/ reactions within the master equation approach of the Griffin model. The incoming /i/ and outgoing /x,y/ particles can be neutrons, protons, deuterons, tritons, helium 3 or alpha particles. The set of master equations describing the equilibration of the composite nucleus is solved exactly by a matrix method./

Gas production extimates can be made directly from a nuclear data library prepared for activation calculations. The RECOIL [10] data base has advantage because it contains the total hydrogen and helium production cross sections for elements. There are a number of investigations at present to study the applicability of the different evaluations. Among the most recent studies the following are mentioned.

In Fig. 8 a comparision of experimental cross sections for the $^{52}Cr/n,p/^{52}V$ reaction with three evaluations is shown. As it can be seen the KEDAK-2 and the ENDF/B-V evaluations do not agree well with the experimental data [64]. The solid line was calculated using the code GNASH.

The $^{63}Cu/n,\alpha/^{60}Co$ reaction cross sections curve was compared with the ENDF/B-IV and ENDF/B-V evaluations. Results show that the agreement with the ENDF/B-V is satisfactory [65].

The spectra derived by means of data on the reaction $^{58}Ni/n,p/$ from the BOSPOR-78 [66] and ENDF/B-IV. libraries gave minimum deviations from the experimentally obtained spectra. The cross section data from the UKNDL library showed considerably greater deviations for $^{58}Ni/n,p/$ and $^{56}Fe/n,p/$ reactions.

Further data are needed in a wide range of neutron energy with about 10 % accuracy for the calculation of gas production and transmutation.

Status of fission product nuclear data is summarized in Ref. [68]. The role of fission products in gas production and transmutation has not been included in this review.

REFERENCES

[1] Jarvis, O.N., Proc. Int. Conf. on Neutron Physics and Nuclear Data, Harwell /Sept. 1978/, p. 1073

[2] Dudziak, D.J., Proc. 1st Topl. Mtg. Technology of Controlled Nuclear Fusion, San Diego, DONF-740402, Vol. II.p. 114. /1974/

[3] Steiner, D., Nucl. Sci. Eng. 58 /1975/ 107

[4] Vook, F.L., Physics Today 28 No 9/1975/ 34

[5] Muir, D.W., WRENDA 79/80, INDC SEC -73/URSF IAEA, Vienna /1979/; DayDay, N., WRENDA 81/82, INDC(SEC)-78/URSF IAEA, Vienna /1981/

[6] Lederer, C.M., Shirley, V.S. Table of Isotopes, John Wiley and Sons, Inc., New York /1978/

[7] Jarvis, O.N., IAEA-TECDOC-223, Vienna /1979/ p.47

[8] Vogelsang, W.F., Kulcinski, G.L., Lott, R.G., Sung, T.Y., Nucl. Technology 22 /1974/ 329

[9] Bychkov, V.M., Manokhin, V.N., Pashchenko, A.B., Plyaskin, V.I., INDC/CCP/-146/LJ, IAEA, Vienna, /1980/

[10] Gabriel, T.A., Amburgey, J.D., Greene, N.M., Nucl. Sci. Eng. 61 /1976/ 21

[11] Gabriel, T.A., Bishop, B.L., Wiffen, F.W., Nucl. Technology 38 /1978/ 427

[12] Csikai, J., in Course on Nuclear Theory for Applications, /Trieste, 1980/, SMR/68/I-17.

[13] Qaim, S.M., Proc. Int. Conf. on Neutron Physics and Nuclear Data, Harwell /Sept. 1978/ p.1088

[14] Qaim, S.M., Nucl. Cross Section and Technology, Vol. II. NBS-SP 425 /1975/ p.664

[15] Frõhner, F.P., Proc. Int. Conf. on Neutron Physics and Nuclear Data, Harwell, /Sept. 1978/ p.268

[16] Alvar, K.R., Barschall, H.H., Borchers, R.R., Grimes, S.M., Haight, R.C., Nucl. Instr. and Meth. 148 /1978/ 303

[17] Haight, R.C., Grimes, S.M., Symp. on Neutron Cross Sections from 10 to 50 MeV, Brookhaven /May 1980/, BNL-NCS-51245, p.245

[18] Blann, M., Phys. Rev. Lett. 27 /1971/ 337; Nucl. Phys. A213 /1973/ 570

[19] Kneff, D.W., Oliver, B.M., Nakata, M.M., Farrar IV.,H., Symp. on Neutron Cross sections from 10 to 50 MeV, Brookhaven /May 1980/, BNL-NCS-51245,p. 289

[20] Farrar, IV. H., McElroy, W.N., Lippincott, E.P., Nucl. Technol., 25/1975/ 305

[21] Qaim, S.M., Stõcklin, G., Proc. 8th Symp. Fusion Technology, EUR 518e /1974/ 939

[22] Farrar IV. H., Kneff, D.W., Trans. Am. Nucl. Soc. 28 /1978/ 197

[23] Kneff, D.W., Farrar IV.H., Mann, F.M., Schenter, R.E., Nucl. Technology 49 /1980/ 498

[24] Alberts, W.G., Günther, E., Matzke, M., Rassl, G., EVR 5667 ef, Part II /1977/ 131

[25] Kobayashi, K., Kimura, I., Proc. 3rd ASTM-EURATOM Symp. Reactor Dosimetry, Ispra, Italy, /Oct., 1979/

[26] Spiegel, V., Eisenhower, C.M., Grundl, I.A., Martin, G.C., Proc. 2nd ASTM-EURATOM Symp. Reactor Dosimetry, Palo Alto, Calif. /Oct. 1977/, NUREG/CP-0004, Vol.2., /1978/ p.959

[27] Green, L., Nucl. Sci. Eng. 58 /1975/ 361

[28] Kironac, G.J., Eiland, H.M., Slavic, C.J., Proc. Topl. Mtg. Irradiation Experimentation in Fast Reactors, Jackson Lake, Wyoming /Sept. 1973/ CONF.730910, V.S. AEC /1973/ p.412

[29] Pauw, H., Aten, A.H.W., J. Nucl. Energy, 25 /1971/ 457

[30] Ben Abdallah, H., PhD. Thesis, Univ. Mohammed V., Rabat /1981/

[31] Józsa, I., Pető, G., Csikai, J., Vinh Long, K.D., ATOMKI Közl. 16/4/1974/ p.339

[32] Dezső, Z., Csikai, J., Proc. VII. Int. Symp. Interactions of Fast Neutrons with Nuclei,/Nov. 1977/, Gaussig, ZfK 376, p.44

[33] Dezső, Z., Csikai, J. Proc. IV. All. Union Conf. on Neutron Physics, Kiew, /April, 1977/

[34] Garber, D.I., Kinsey, R.R., BNL 325, INDC /USA/-58 /1976/

[35] Gruppelaar, H., Tables of RCN fission product cross section evaluation, Vol. 1. ECN-13 /1977/; Vol. 2. ECN-33 /1977/

[36] Technical Report No. 107, IAEA, Vienna /1970/

[37] Van der Linden, R., De Corte, F., Hoste, J., J. Radioanal. Chem. 20 /1974/ 695

[38] Mughabghab, S.F., Garber, D.I., Neutron Cross Sections, BNL 325 /1973/

[39] Vonach, H., Proc. 2nd Int. Symp. on Neutron Induced Reactions, /Smolenice, 1979./ p.59

[40] Bődy, Z.T., ATOMKI Közl. 16 /1974/ 351

[41] Csikai, J., Some physical, dosimetry and biomedical aspects of ^{252}Cf, IAEA-SR-3/23 /1976/ p.28

[42] Frehaut, J., Bertin, A., Bois, R., Jary, J., Symp. on Neutron Cross Sections from 10 to 50 MeV Brookhaven /May 1980/ BNL-NCS-51245,p.399

[43] Holub, E., Cindro, N., Bersillon, O., Jary, J., Z.f. Physik. A289 /1979/ 421

[44] Holub, E., Cindro, N., Proc. 2nd. Int. Symp. on Neutron Induced Reactions, /Smolenice 1979/ p. 133

[45] Sudár, S., Csikai, J., Nucl. Phys. A319 /1979/ 157

[46] Hauser, W., Feshbach, M., Phys. Rev. 87 /1952/ 366

[47] Fu, C.Y., Atomic Data and Nuclear Data Tables 17 /1976/ 128

[48] Staudt, G., Mőrike, M., Rohwer, T., Schilling, B., Schiessle, E., Proc. 2nd. Int. Symp. /Smolenice 1979/ p. 35

[49] Turkiewicz, J., Proc. 2nd. Int. Symp. /Smolenice 1979/ p. 13

[50] Augustiniak, W., Glowacka, L., Jaskola, M., Turkiewicz, J., Zemlo, L., Le Van Khoi, Kozlowsky, M., Proc. 2nd. Int. Symp. /Smolenice 1979/ p. 43

[51] Richardson, B.L., "FISPIN-4", UKAEA Reactor Group, TRG Memorandum 6907 /1976/

[52] Bell, M.J., "ORIGEN", ORNL-4628 /1973/

[53] CINDA-An Index to the Literature on Microscopic Neutron Data, IAEA, Vienna

[54] Tsukada, K., JAERI 1252 /1977/

[55] Pronyaev, V., Schmidt, J.J., INDC/P /81/-26

[56] Garber, D.I., Brewster, C., BNL-17100 /1975/

[57] UCRL-50400 /1976/

[58] Goel, B., KfK-2233 /1975/

[59] DayDay, N., Lemmel, H.D., IAEA-NDS-15 /1980/

[60] Prince, A., IAEA-190, Vol 1. /1976/; IAEA-SMR-43/1980/

[61] Pearlstein, S., J. Nucl. Energy 27 /1973/ 81

[62] Benzi, V., Reffo, G., E.N.E.A. CCDN NW/10 /1969/

[63] Young, P.G., Arthur, E.D. "GNASH" LA-6947 /1977/

[64] Smith, D.L., Meadows, J.W., Nucl. Sci. Eng. 76 /1980/ 43

[65] Winkler, G., Smith, D.L., Meadows, J.W., Nucl. Sci. Eng. 76 /1980/ 30

[66] Zolotarev, K.I., Bychkov, V.M., Pashchenko, A.B., Plyaskin, V.I., Manokhin, V.N., Chernov, L.A., INDC /CCP/ -147/LJV /1980/

[67] Uhl, M., Acta Phys. Austr. 31 /1970/ 245

[68] Proc. 2nd Advisory Group Meeting on Fission Product Nuclear Data, Petten /Sept. 1977/, IAEA-213 /1978/

[69] Qaim, S.M., IAEA-TECDOC-223, AG-150/A4 Vienna /1979/, p.75

[70] Lorenz, A., INDC /NDS/ - 83/LN, IAEA, Vienna, /1977/, INDC/P(81)-25, Vienna, /1981/

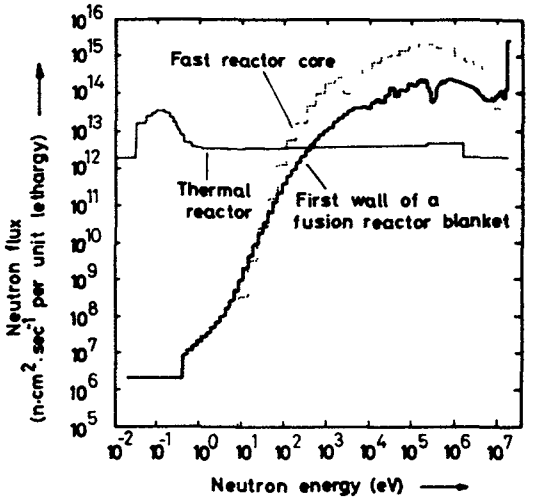

Fig. 1 Neutron spectra for fusion and fission reactors [1]

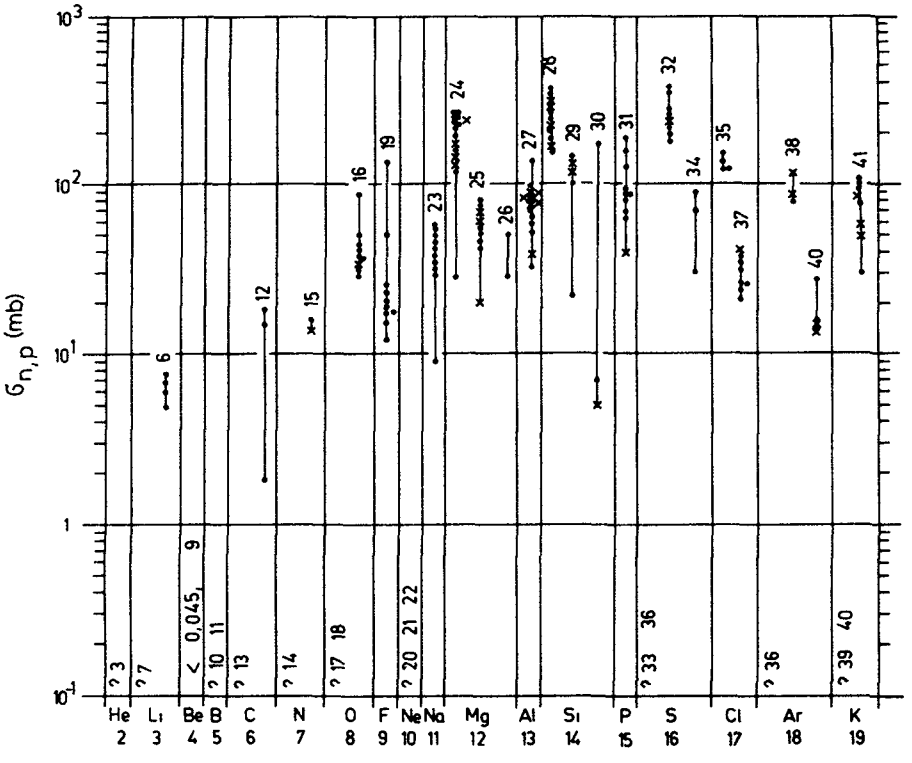

Fig. 2 a-e. Activation and hydrogen production cross sections for (n,p) reactions at 14.5 MeV

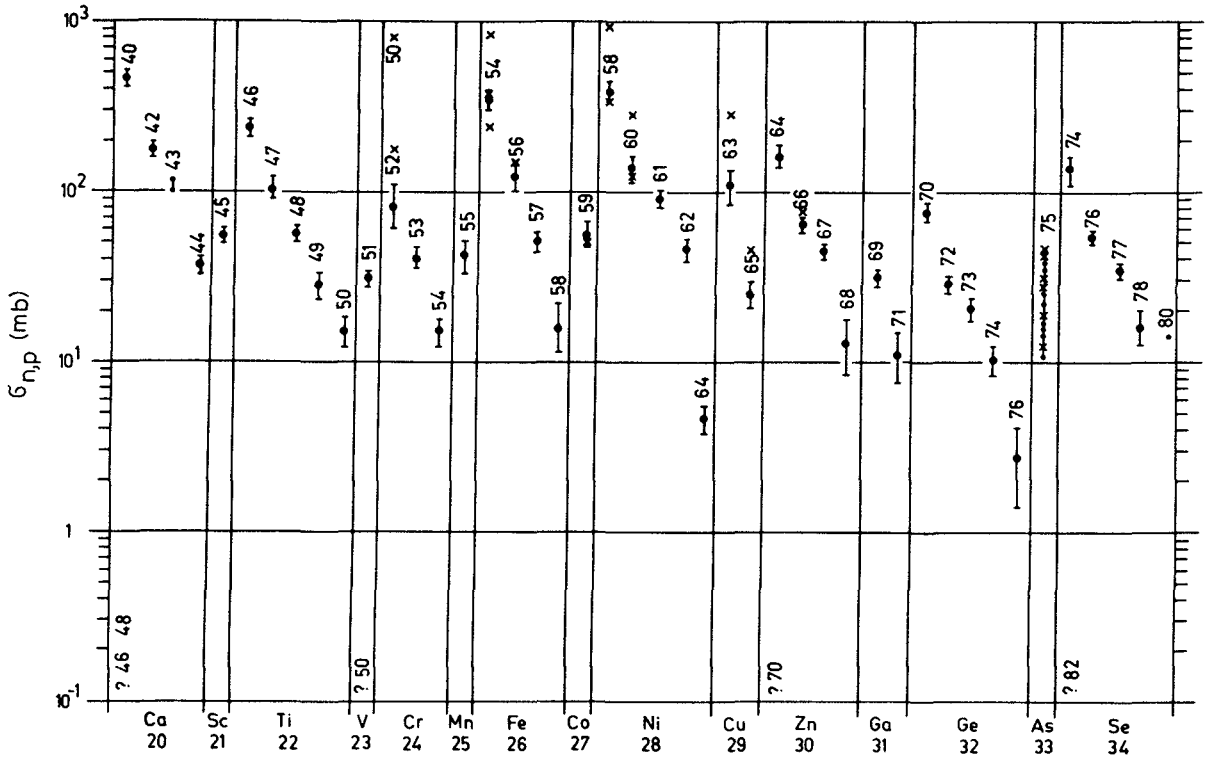
$\sigma_{n,p}$ (mb)
Ca 20
Sc 21
Ti 22
V 23
Cr 24
Mn 25
Fe 26
Co 27
Ni 28
Cu 29
Zn 30
Ga 31
Ge 32
As 33
Se 34

Fig. 2 b.

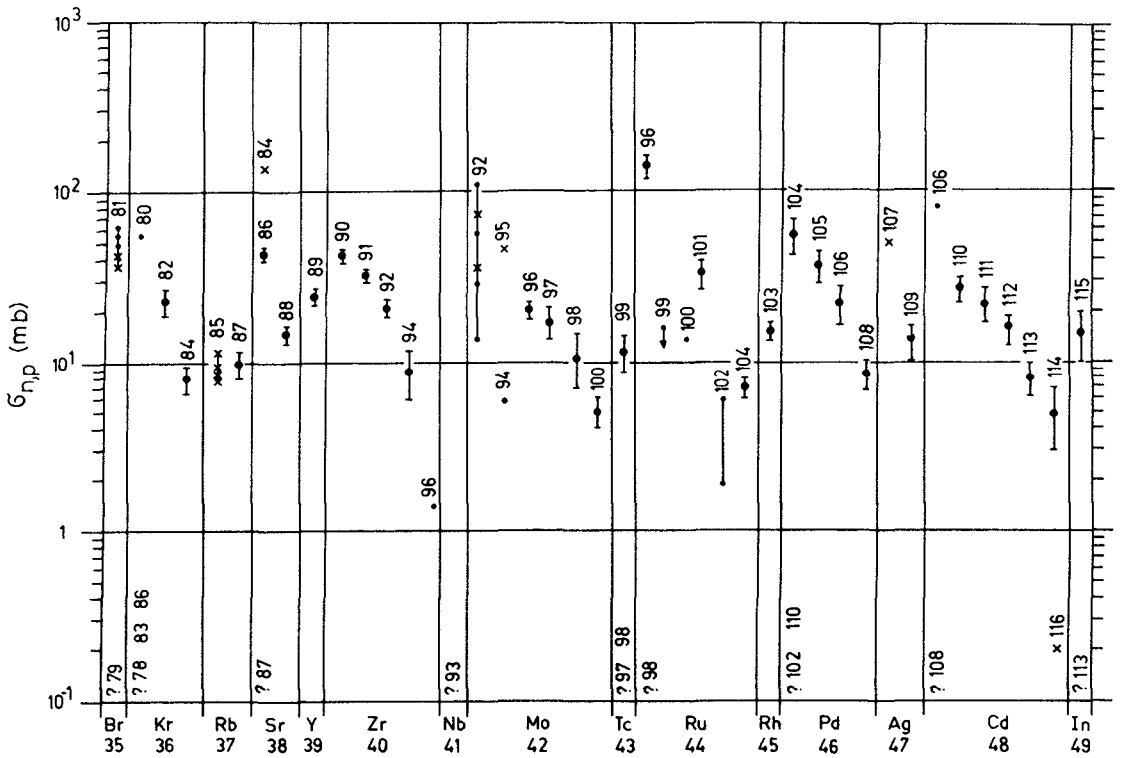
$\sigma_{n,p}$ (mb)
Br 35
Kr 36
Rb 37
Sr 38
Y 39
Zr 40
Nb 41
Mo 42
Tc 43
Ru 44
Rh 45
Pd 46
Ag 47
Cd 48
In 49

Fig. 2 c.

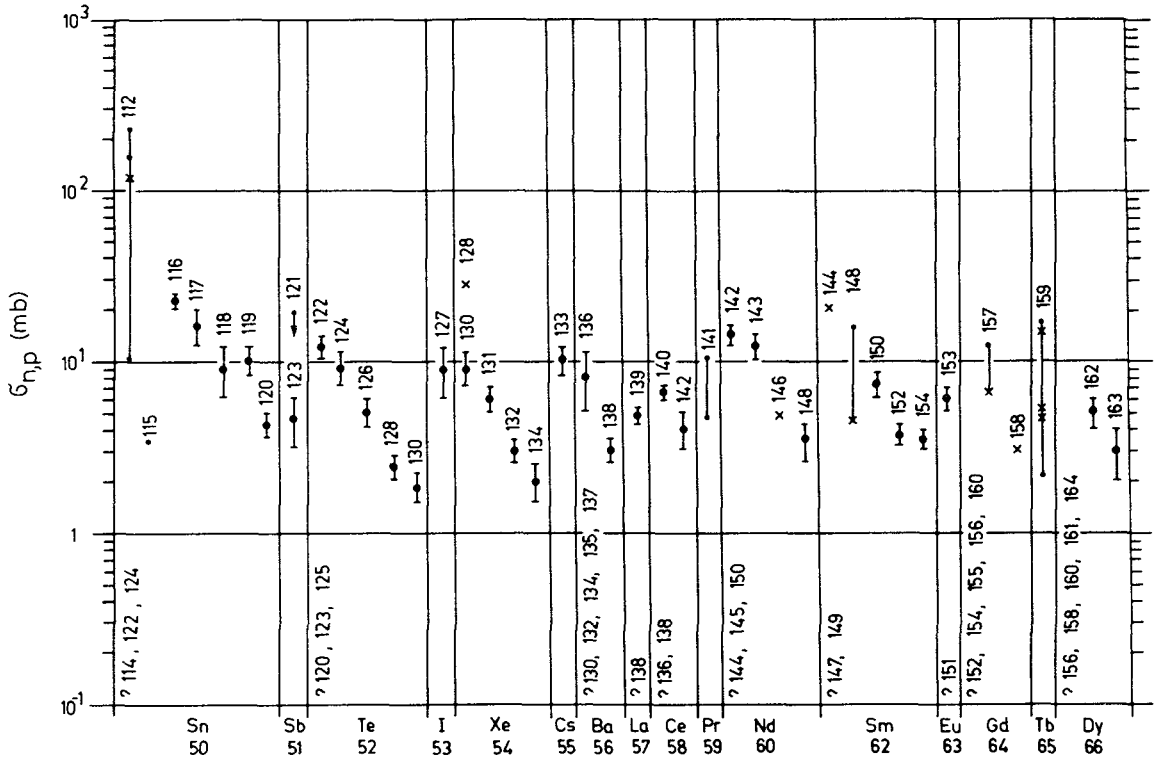
σn,p (mb)
Sn 50
Sb 51
Te 52
I 53
Xe 54
Cs 55
Ba 56
La 57
Ce 58
Pr 59
Nd 60
Sm 62
Eu 63
Gd 64
Tb 65
Dy 66

Fig. 2 d.

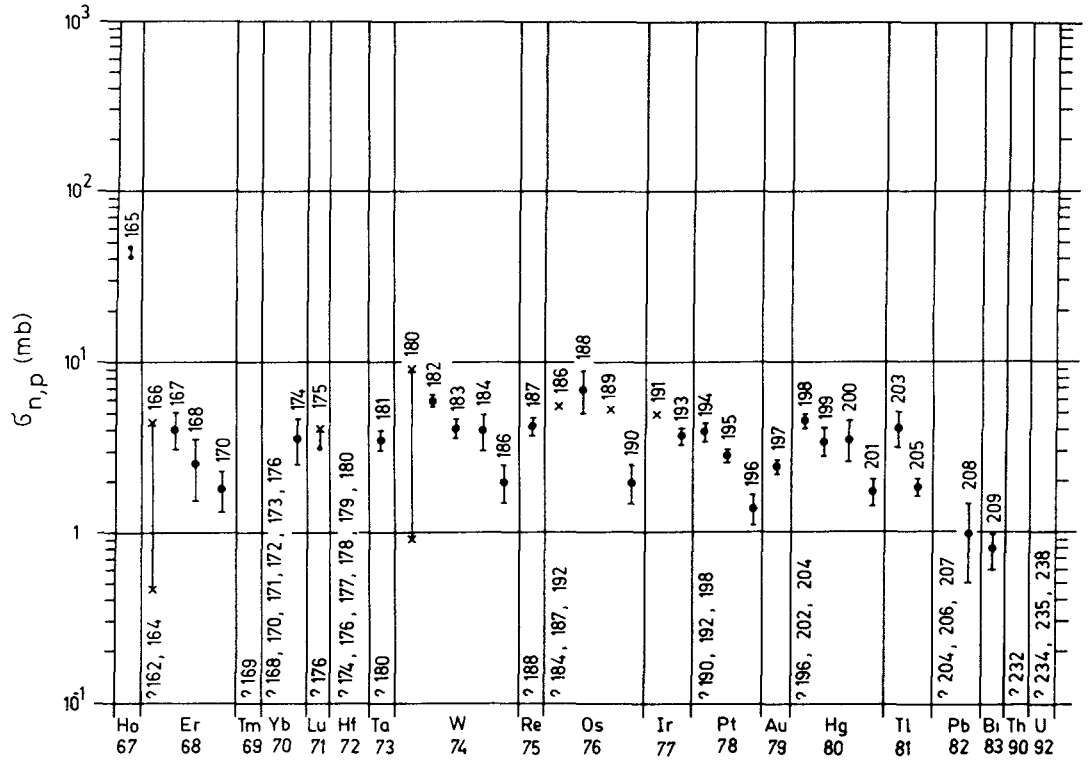
σn,p (mb)
Ho 67
Er 68
Tm 69
Yb 70
Lu 71
Hf 72
Ta 73
W 74
Re 75
Os 76
Ir 77
Pt 78
Au 79
Hg 80
Tl 81
Pb 82
Bi 83
Th 90
U 92

Fig. 2 e.

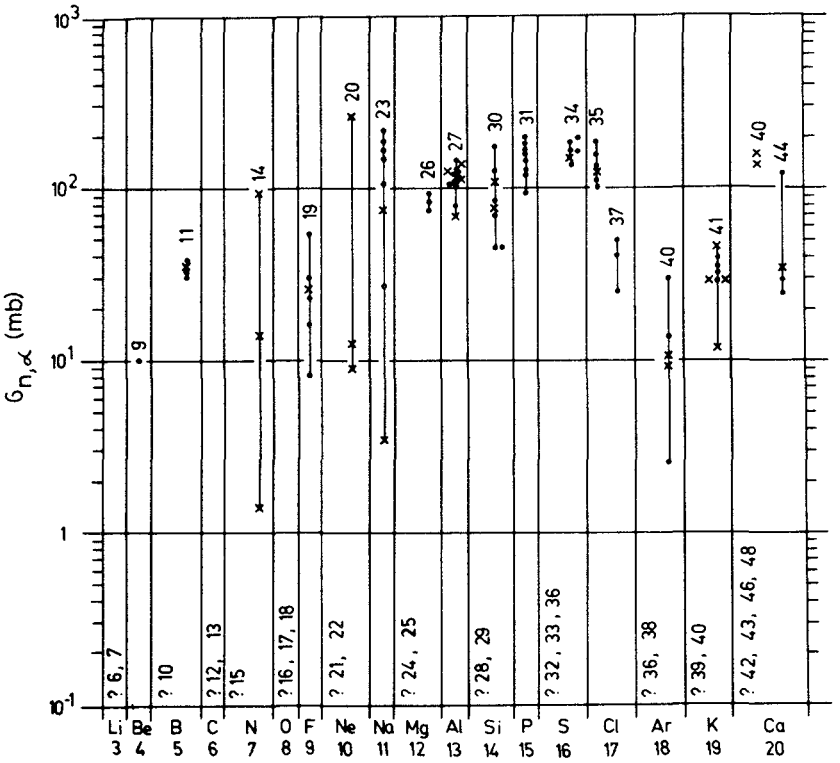

Fig. 3 a-d. Activation and helium production cross sections for (n,α) reactions at 14.5 MeV

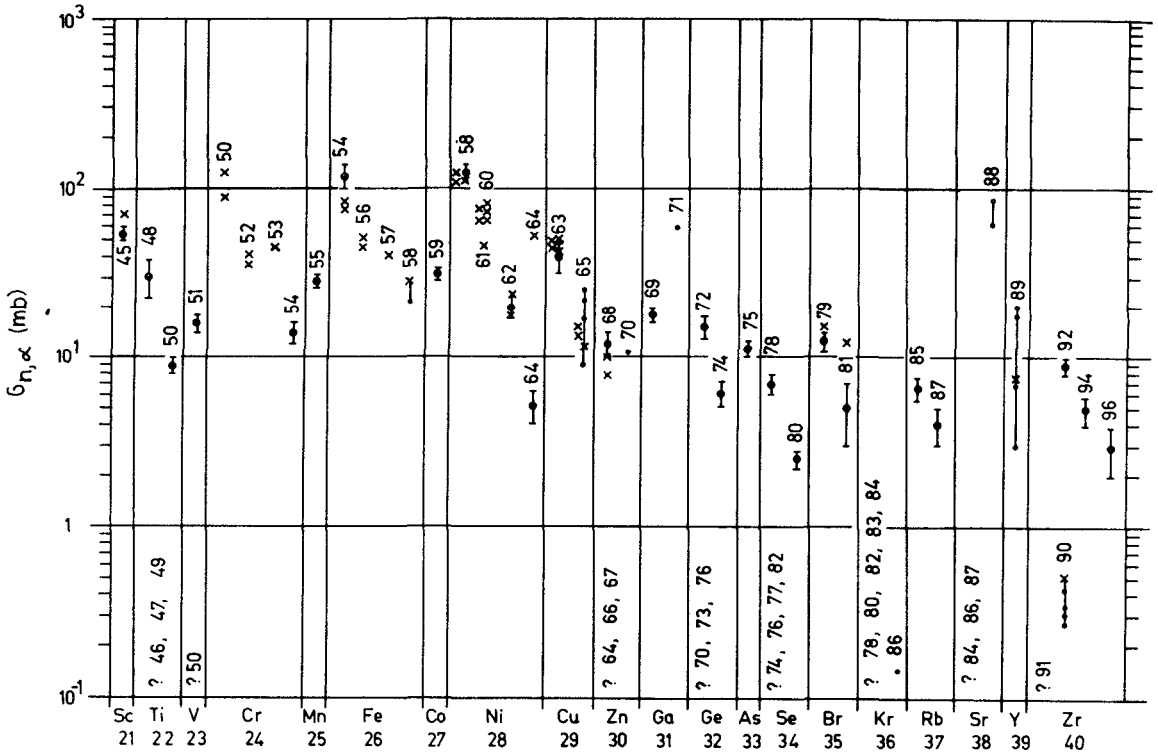

Fig. 3 b.

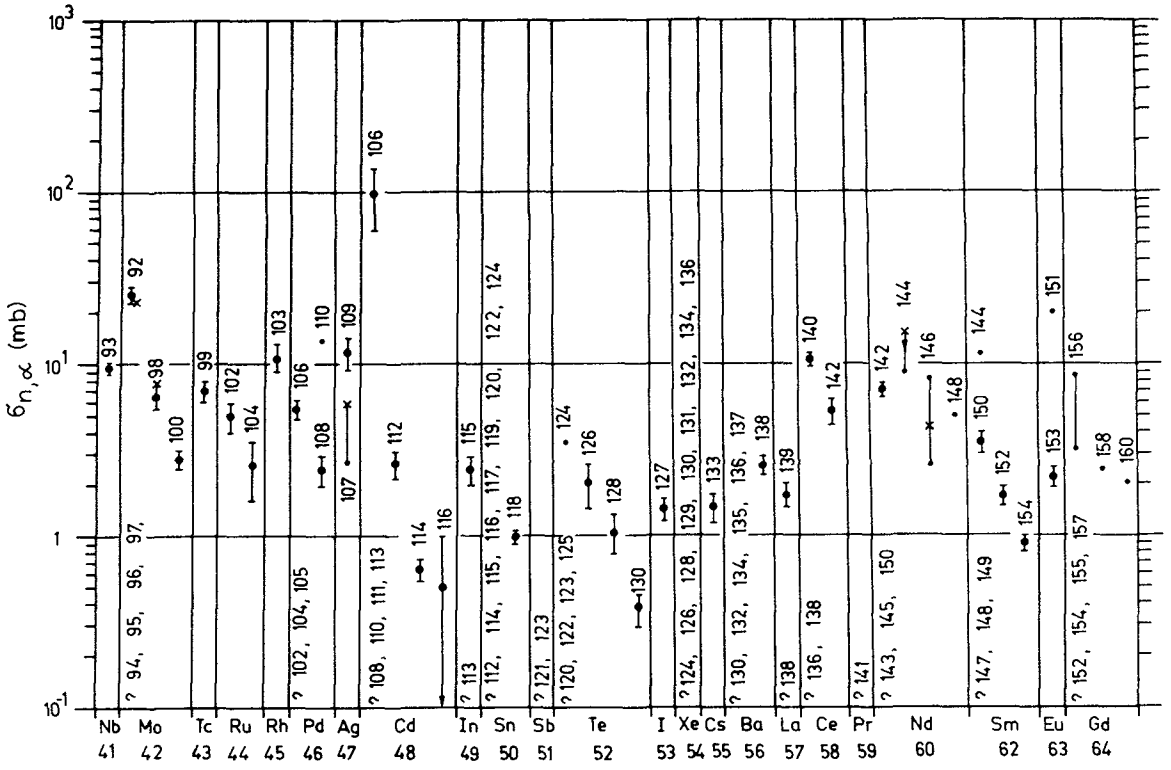
$\sigma_{n,\alpha}$ (mb)
Nb 41
Mo 42
Tc 43
Ru 44
Rh 45
Pd 46
Ag 47
Cd 48
In 49
Sn 50
Sb 51
Te 52
I 53
Xe 54
Cs 55
Ba 56
La 57
Ce 58
Pr 59
Nd 60
Sm 62
Eu 63
Gd 64

Fig. 3 c.

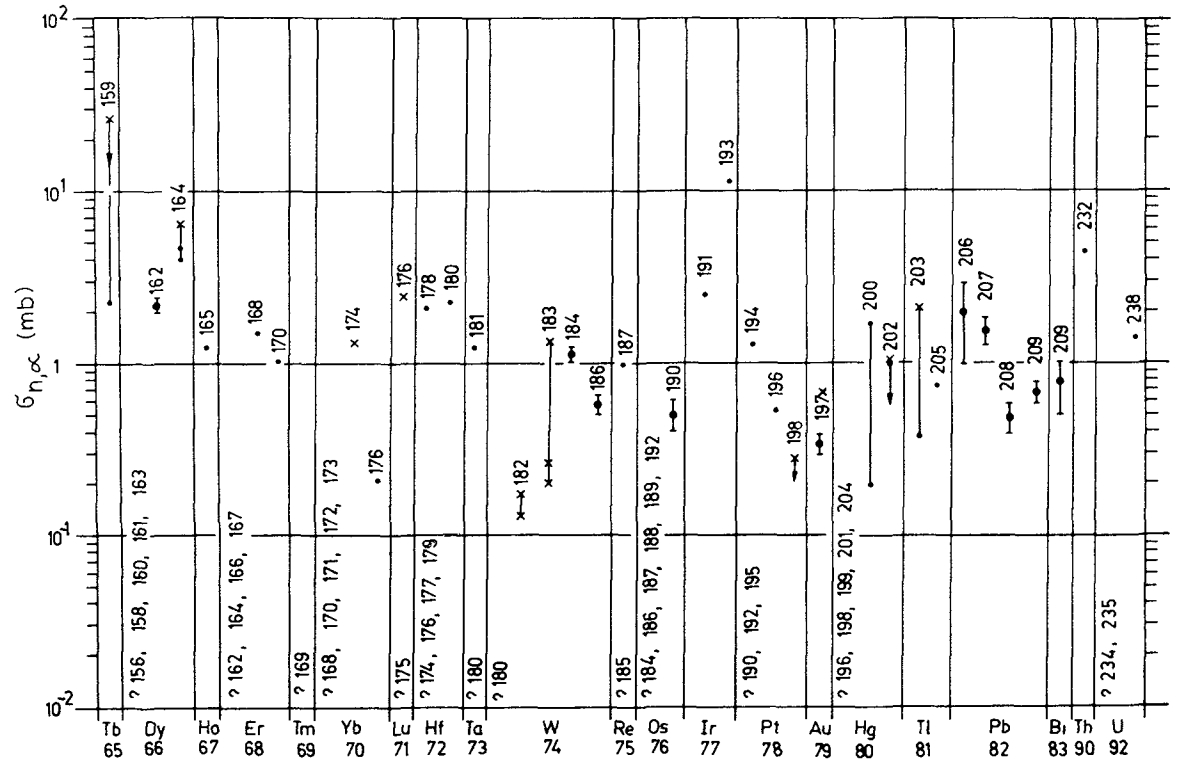
$\sigma_{n,\alpha}$ (mb)
Tb 65
Dy 66
Ho 67
Er 68
Tm 69
Yb 70
Lu 71
Hf 72
Ta 73
W 74
Re 75
Os 76
Ir 77
Pt 78
Au 79
Hg 80
Tl 81
Pb 82
Bi 83
Th 90
U 92

Fig. 3 d.

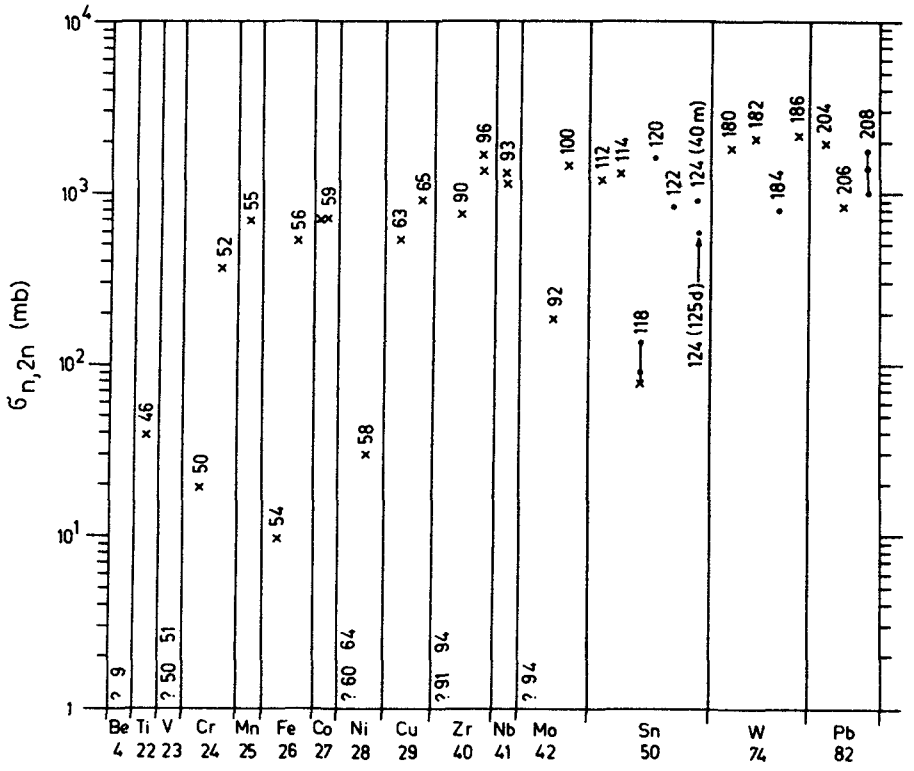

Fig. 4 Activation cross sections for (n,2n) reactions at 14.5 MeV

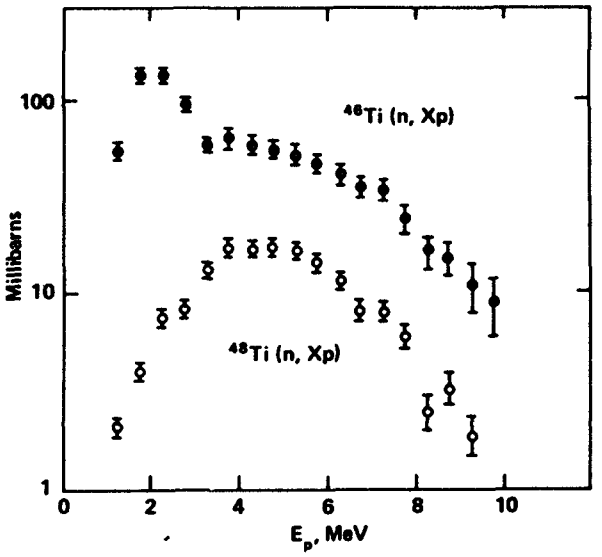

Fig. 5 Energy spectra of protons measured by MQS method [17]

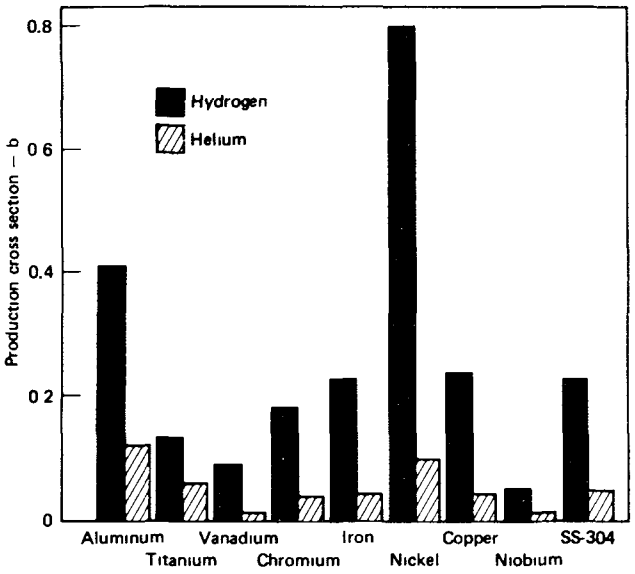

Fig.6 Total hydrogen and helium production cross sections for structural materials [17]

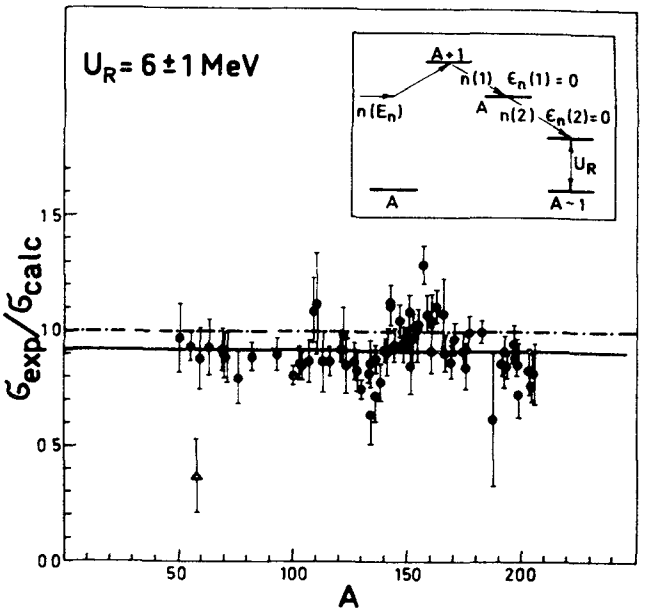

Fig.7 Ratios of measured and calculated (n,2n) cross sections for U_R=6 MeV using compound nucleus model

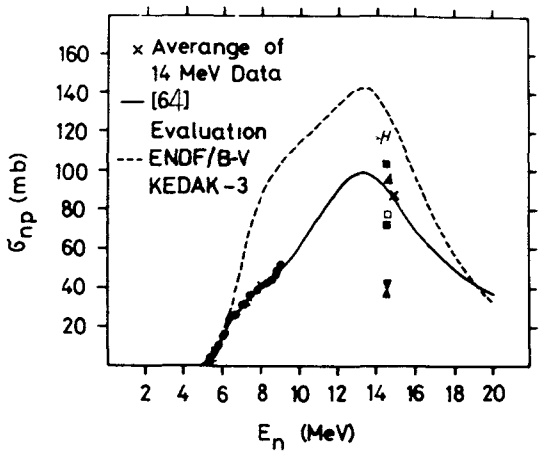

Fig.8 Comparision of selected experimental cross sections for the ^{52}Cr (n,p) ^{52}V reaction with three evaluation [64]

CORRELATION OF MACROSCOPIC MATERIAL PROPERTIES WITH MICROSCOPIC NUCLEAR DATA

R.L. SIMONS
Hanford Engineering Development Laboratory*,
Richland, Washington,
United States of America

ABSTRACT

This paper reviews the application of nuclear data to the correlation of neutron irradiation induced damage to materials. Two primary irradiation induced changes in the material occur during neutron irradiation [displacement of atoms forming crystal defects and the transmutation of atoms into gaseous or solid products]. The largest uncertainty in the calculation of crystal defects is due to the atomic model. Several alternate computer simulation or experimental based models are discussed. A review of recent experiments to validate the displacement cross section based on the modified Kinchen and Pease model is presented. The most notable problem in such experiments is the competing effects of damage rate or flux level. Recent experiments and calculations on the effect of transmutations on swelling and yield strength show that the buildup of selected transmutation products cannot be neglected. It is concluded that goal accuracies for nuclear data should be based on a need to determine integral damage parameters to within 10–20 percent (1 sigma).

Introduction

Radiation damage to structural materials is obviously an important aspect to consider when designing a fission or fusion device. It is well established that radiation damage is sensitive to the energy of the neutrons causing the damage. The energy dependence of damage has often been treated somewhat simplistically: only neutrons greater than a specific energy were assumed to cause the damage. The success of this method turned out to be reactor-specific, and the method worked only because the neutron spectra were similar. For application of radiation effects data to fusion reactor design problems, the use of fast-flux fraction to extrapolate to higher neutron energies is not successful. For this reason, the materials community studying radiation damage to fusion reactor materials has generally accepted the use of displacement per atom (dpa) to correlate irradiation effects to

*Operated by Westinghouse Hanford Company, a Subsidiary of Westinghouse Electric Corp. for the Department of Energy under Contract DE-AC14-76FF02170.

material properties. The United States light-water reactor surveillance program is preparing to switch from the use of fluence (E > 1.0 MeV) correlation to the use of dpa. An ASTM recommended practice for this switch has been completed.[1]

Two primary irradiation-induced changes occur during neutron irradiation: the displacement of atoms forming crystal defects and the transmutation of atoms into either gaseous or solid products. The material scientist studying irradiation damage to material by fusion-produced neutrons is faced with several questions:[2] Is the nature of high-energy (14-MeV) displacement damage the same as or different from that caused by fission neutrons (<2 MeV)? How do the high helium concentrations expected in a fusion environment affect the material properties? What effects do solid transmutation products have on the behavior of the irradiated materials? In the past few years, much work has been done to answer these questions. This paper will review recent work in this area.

Nuclear Data in Displacement Calculations

When the gross displacement of atoms is calculated, the material is generally assumed to be an amophorus solid. The Lindhard model[3] is then used to partition the energy dissipated in a collision cascade initiated by a primary recoil atom (PKA) between electronic and nuclear interactions. The integral equation that describes the calculation of the production rate of displaced atoms per atom is:

$$\dot{d} = \sum_j \int_{E=0}^{\infty} \int_{T=E_d}^{T_m} \phi(E)\ \sigma_j(E)\rho_j(E,T)\ \nu(T)\ dE\ dT \qquad (1)$$

where:

- $\phi(E)\ dE$ is the number of neutrons of energy E
- $\sigma_j(E)$ is the neutron-atom interaction cross section (i.e., elastic, in-elastic, or charged particle out-reaction) of the atom species j, and the summation is over all neutron reactions of energy E
- $\rho(E,T)$ is the probability that a neutron of energy E will produce a PKA of energy T
- $\nu(T)\ dT$ describes the number of secondary displaced atoms produced by the primary recoil atoms (modified for electronic losses)
- T_m is the maximum energy a neutron can impart to an atom
- E_d is the minimum energy required to displace an atom
- $\sum_j \phi(E)\ \sigma_j(E)\ \rho_j(E,T)$ is the primary recoil spectrum for atom struck by a neutron of energy E.

Figure 1 shows the displacement damage response as a function of neutron energy for three neutron spectra of interest. In all cases, 95% of the damage occurs above 0.1 MeV neutron energy and 1 keV recoil energy.

The application of nuclear data in a correlation of irradiation effects appears in two places in equation (1). First is the neutron spectrum $\phi(E)$. The neutron spectrum depends on nuclear data in two ways. (1) Neutron cross sections are used in the neutron physics calculation of the a priori spectrum. (2) Neutron dosimetry cross sections are used in the adjustment of the a priori neutron spectrum. The second place where nuclear data is used is the primary scattering cross section $\sigma_j(E)$. Thus the nuclear data are entirely contained in the primary recoil spectrum.

Nuclear data can also affect the correlation of irradiation-induced material property changes in displacement of atoms caused by recoil of atoms following prompt (n,γ) reactions. This is primarily a thermal neutron reaction and in most cases contributes only a few percent to the total displacement cross section. Exceptional cases involve highly thermalized spectra or highly moderated spectra in Fast Breeder Reactor (FBR) out-of-core structure components. For example, in the pressure vessel of a FBR the calculated (n,γ) contribution to total displacements may be about 30%. However, there is considerable uncertainty about the magnitude of the low energy recoil [including those from prompt (n,γ) reactions] contribution of the dpa exposure, as compared with the higher energy neutron elastic collision contribution, because of the relative survival efficiency in the displacement cascade. Measurements of electrical resistivity change (which is assumed to be proportional to the Frenkel pair defect population) at 4°K indicate that about one-third of the defects survive in the displacement cascades caused by high-energy recoils in fcc materials. About one-half of the defects survive in bcc materials.[4] However, up to 100% of the defects survive for low-recoil energies where (n,γ) damage occurs.[5] Figure 2 shows the number of Frenkel pairs produced by (n,γ) recoil in several materials vs the damage energy normalized to the minimum threshold energy for each material. The modified Kinchin and Pease displacement model corrected to a survival efficiency of 0.3 for high-energy ($T > 1$ keV) recoils is also shown. The upper curve results from a correlation of charged particle irradiation effects data, displacement cascade computer simulation data, and neutron irradiation effects data using primary recoil spectra.[6] It is apparent that the low-energy damage contribution relative to high energy (> 1 keV) damage can be more significant than indicated by the displacement cross section. However, the low-temperature resistivity data provide no information on how high-temperature irradiation affects the survivability of defects.

Assuming that the relative survivability of defects as a function of damage energy is not affected by temperature, a defect cross section for production of Frenkel pair was calculated for iron, and spectrum-averaged

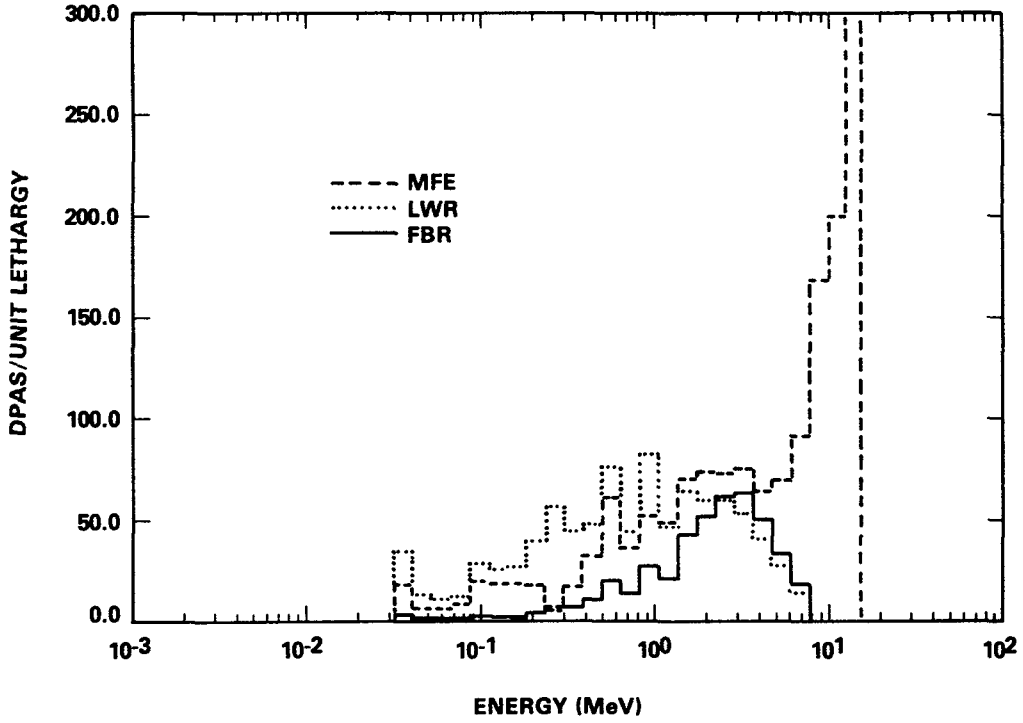

FIGURE 1. Neutron Energy Response of Displacement Damage.

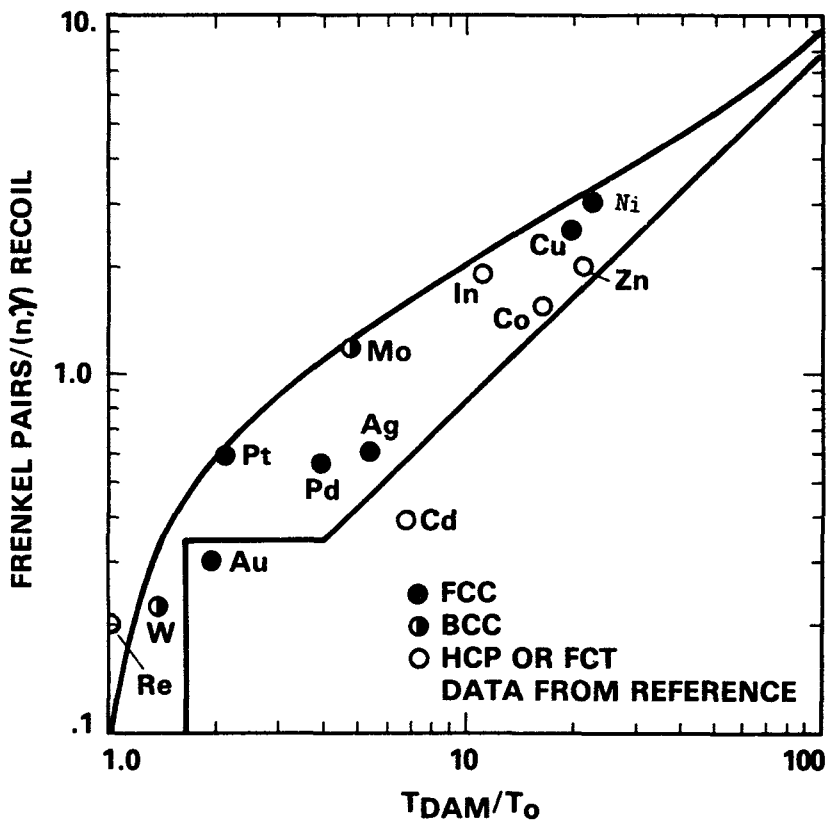

FIGURE 2. (n,γ) Recoil Damage in Metals.

cross sections were determined for a number of spectra. The results are shown in Table 1, along with the standard modified Kinchin and Pease model. It is apparent that for most test reactor spectra the enhanced low energy component of damage is only a small contribution to the total damage. However, in the softer Fast Breeder Reactor (FBR) spectra the effect can be as high as 44%. Even at this level of enhancement there are probably not any serious consequences because of the low level of exposure to most stainless steel components.

TABLE 1

SPECTRUM AVERAGED DISPLACEMENT CROSS SECTIONS FOR IRON IN SELECTED NEUTRON SPECTRA

Spectrum	Mean Neutron Energy (MeV)	Iron Cross Section (b) Frenkel Pairs	Displacements	Ratio* Pairs/Displ.
EBRII Z = 0.0 cm	0.83	167	448	1.00
EBRII Z = 18.3 cm	0.63	138	373	0.99
EBRII Z = 25 cm	0.48	114	312	0.98
EBRII Z = 50 cm	0.22	67.4	186	0.97
FBR Core	0.49	111	302	0.99
FBR Grid Plate	0.036	18.4	49.4	1.00
FBR Vessel Wall	0.0022	2.22	4.13	1.44
HFIR/PTP	0.42	76.0	186	1.10

*Normalized to 1.000 in EBRII Z=0.0cm

Energy Dependence of Displacement Damage

The energy dependence of damage in test reactor spectra has been assumed to be proportional to the damage energy. Experiments and computer simulation studies of defect survival can be used to test this assumption. If the shape of the energy dependence of damage is known, the magnitude can easily be established by a single experiment. However, confirming the shape of the function $\nu(T)$ is difficult at best. Experiments designed to measure variation in slope require irradiation in diverse spectra at constant flux magnitude. Usually a change in spectrum is accompanied by a change in flux. Thus flux level effects must be discerned from spectrum effects. Numerous simplifying assumptions are usually made when computer simulation studies are used to evaluate $\nu(T)$ because multi-atom crystals are large and hence require complex computer codes. The combination of experiments and computer simulation can produce boundaries on the extent of the variation of the slope of $\nu(T)$.

When macroscopic material properties are correlated with microscopic data, the primary recoil spectrum is assumed to be independent of time and temperature. It is assumed that the material remains homogeneous throughout the irradiation, that is, extended defects that existed prior to irradiation or evolve during the irradiation (such as grain boundaries, precipitates, voids, and loops) do not affect the PKA spectrum. The focal point of the correlation is on the secondary displacement function $\nu(T)$. The function $\nu(T)$ may represent the total defects produced (dpa), residual defects after short-term annealing, or other forms of residual damage (clusters). The Kinchin and Pease displacement function (modified by Lindhard's energy partition model) that is usually used to calculate the number of displaced atoms is linear in damage energy. The residual defects functions determined from computer simulation experiments are generally described by a small departure from linearity [(i.e., $(T_{dam}^{0.8})$], or at least the dpa function may be adjusted in magnitude by a multiplicative constant.[7] When other mechanisms (such as gaseous transmutations products) interact with displacive defects, the damage analysis becomes more complex.

Figure 3 shows two defect cross sections determined from computer simulation experiments and the standard displacement cross section. The mobile vacancy cross section counts only vacancies free to move in the crystal lattice after short-term annealing of the displacement spike has occurred.

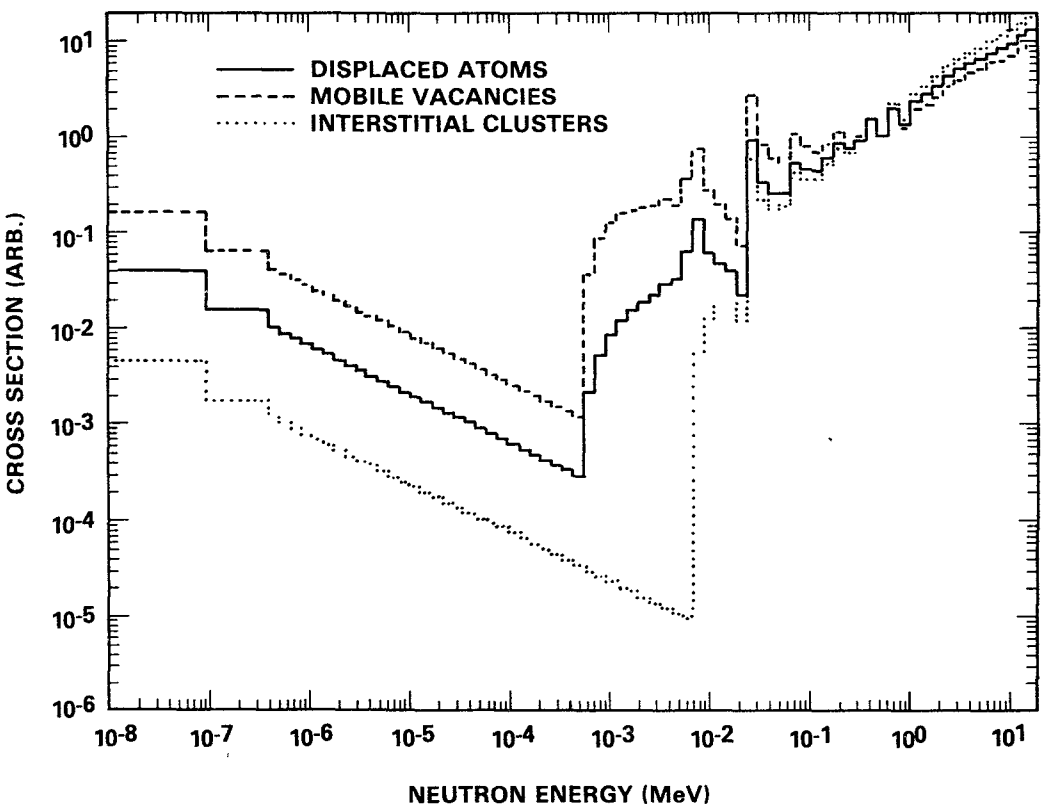

FIGURE 3. Normalized Defect Production Cross Sections.

Low-energy displacement cascades were found to be more efficient producers of free vacancies because the higher energy cascades produced more vacancy clusters while experiencing less defect annhilation. The interstitial cluster cross section emphasizes the high-energy damage because low-energy cascades did not produce sufficient densities of interstitial atoms for clustering to occur. In effect, the interstitial cross section exhibits a higher energy threshold than the other cross section. These are two examples of several potential defect types. An important outcome of simulation studies is that the maximum variation in the shape of $\nu(T)$ can be determined, and thus bounds can be placed on the neutron-energy-dependent damage cross sections.

Blackburn et al.[8] made careful measurements of tensile properties of annealed 304 and 316 stainless steel and of 308 stainless steel weld metal irradiated in EBR-II (385°C) at four axial locations, each with a specific neutron spectrum with mean neutron energies ranging from 0.2 to 0.8 MeV, as a function of neutron fluence. They found that dpa best characterized the energy dependence of irradiation damage experienced by the specimens. The mobile vacancy and interstitial cluster cross sections gave exposure parameters that bounded the variation in energy dependence. Figure 4 shows the empirically determined spectrum correlation factors vs displacement cross section (both parameters were normalized to unity at core center). Even though the dpa gave the best correlation, some systematic deviation from the dpa correlation remained -- deviation of 10-15% for hard in-core spectra and nearly 50% deviation in 304 SS irradiated in soft out-of-core spectra ($\overline{E} < 0.4$ MeV).

It is not clear how flux level effects might contribute to this descrepancy. However, if one assumes that the spectrum effect is separable from the flux level effect and that the spectral effect is proportional to a defect cross section, then the flux level function can be deduced from a plot of experimental spectrum correlation factor (K_s) divided by the defect cross section vs the flux level. Figure 5 suggests that a flux level effect could be linear until the flux reached 40-60% of the peak flux in EBRII; the flux level effect would be approximately constant for higher fluxes. Since the 304 SS shows a different function than the other steels, the flux level effect also appears to be a function of the chemistry of the material involved. To determine the exact form of this postulated flux level effect would require a larger range of fluxes. However, this data shows that flux effects could be substantial and can cause misinterpretation of spectral effects.

McVay et al.[9] studied the irradiation-induced swelling and creep behavior of solution annealed (SA) 304L stainless steel irradiated in EBRII at 385°C. They concluded that dpa was a good way to correlate the irradiation-induced strains. They also indicated that fast fluence (E >.1 MeV) gave

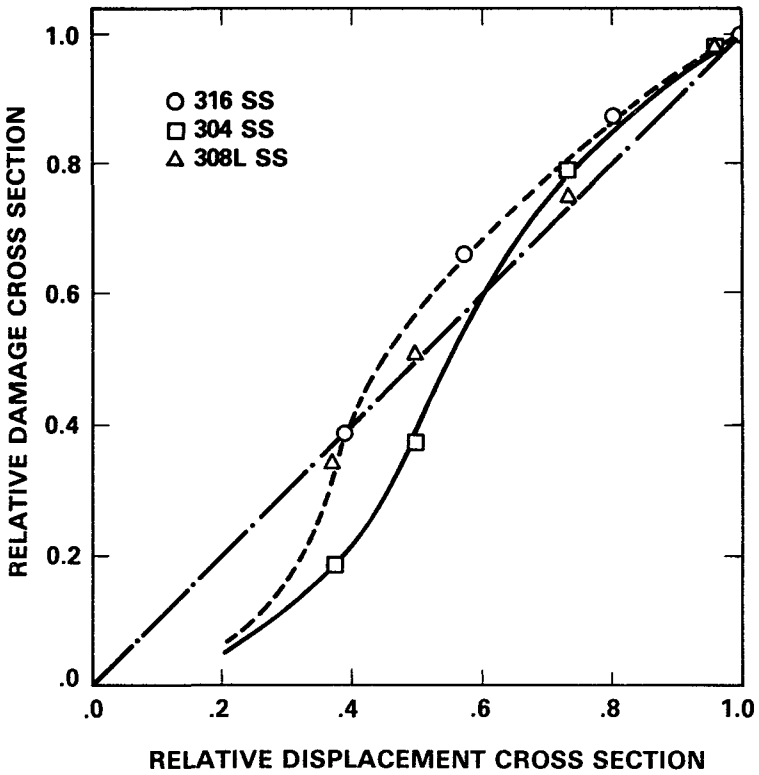

FIGURE 4. Measured versus Calculated Damage Parameter for Stainless Steel Irradiated at 385°C.

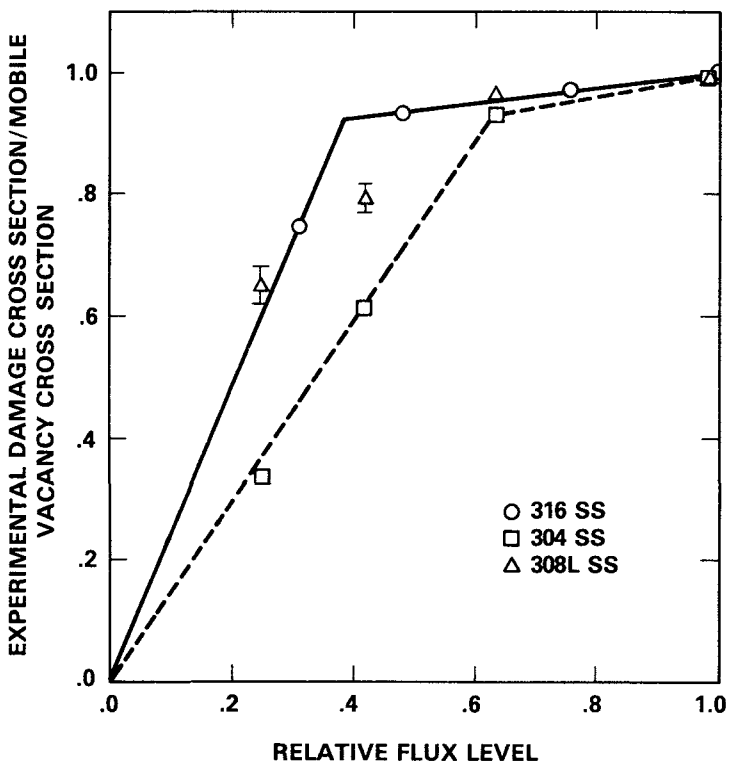

FIGURE 5. Empirical Flux Level Effect Function for Irradiation Induced Change in Yield Strength for Stainless Steel Irradiated at 385°C.

similar results. They did not separate out flux level and energy spectrum effect, since these parameters were varying simultaneously with axial location in the experiment.

ΔDBTT data used in damage function analyses for several ferritic steels irradiated in the temperature range 200-600°F were reevaluated.[10] The displacement, mobile vacancy, and interstitial cluster cross sections were used in this analysis. It was concluded that the displacement cross section gave the best correlation of the data. Figure 6 shows ΔDBTT data for A302B steel for four irradiation temperatures. A saturation function of exposure raised to the 0.5 power was fit to the data. In some cases the interstitial cluster cross section gave some improvement in the correlation; however, the amount of reduction in the variance over dpa was only 14%, which was not statistically significant.

Mas et al.[11] measured the ΔDBTT in a A508 ferritic steel irradiated at 235°C in different neutron spectra to the same fluence (E > 1 MeV). The harder neutron spectrum showed a ΔDBTT 40% higher than the softer spectrum. They tried several different energy dependent correlation factors and a 0.5 power law on damage exposure and found that fluence (E > 0.1 MeV) gave the least unfavorable correlation. The next best correlation of ΔDBTT was obtained with their "probable zones" model. Their probable zones model was similar in shape to the displacement cross section that is based on Lindhard's model of energy partition.

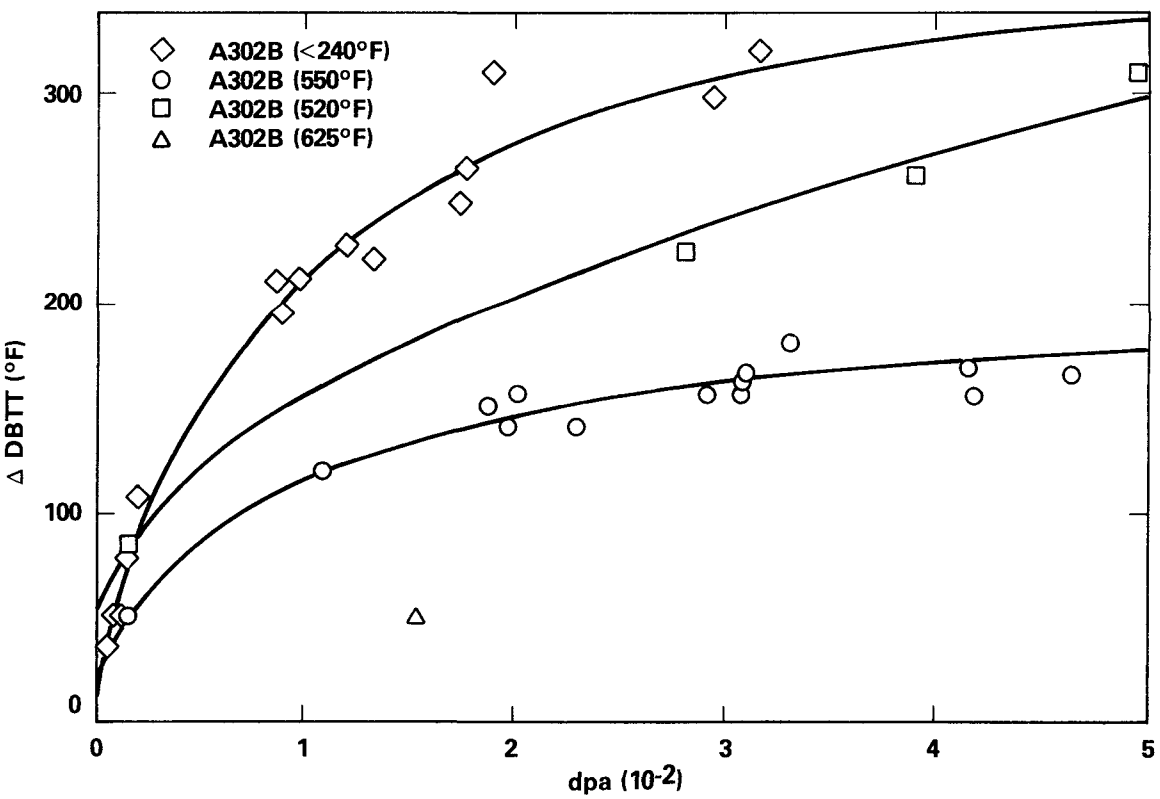

FIGURE 6. Shift in Ductile-Brittle Transition Temperature of A302B steel versus dpa for Several Irradiation Temperatures.

Odette[12] performed a systematic study of the effect of uncertainties on the predicted ΔDBTT. His physically based model contained spectral dependence, an aging contribution, temperature-dependent defect production, thermal self-annealing, saturation effects when there was defect overlap, and simple dislocation obstacle hardening. He looked at the effect of uncertainties in neutron exposure, irradiation temperature, and alloy chemistry. With an exposure uncertainty of a factor of two, which is typical of some older surveillance data, the corresponding uncertainty in the predicted ΔDBTT was 25%. With a smaller exposure uncertainty (±15%) the corresponding ΔDBTT uncertainty was small (∿5%). For past and projected irradiation temperature uncertainties, he found comparable effects on the ΔDBTT uncertainty. However, uncertainties in chemistry or effects of chemistry variation has an uncertainty two-to-three times larger than the uncertainty due to either dosimetry or irradiation temperature. It is apparent that other uncertainties than neutron dose can dominate the scatter in the data.

A projected uncertainty of 15% in the damage exposure is reasonable, relative to other uncertainties. Assuming that all of this uncertainty is from the primary recoil spectrum, this implies that the neutron interaction cross sections would have to be known to about 10%. The uncertainty due to the neutron spectrum would also be about 10%, which would give a root mean square combined uncertainty of ∿15%.

The relative uncertainty in the atomic displacement cross section due to variation in the electronic stopping power, nuclear models, and nuclear data sets, was studied by Doran et al.[13] They found that large variations in the electronic stopping power have only a minor effect on the relative spectrum-averaged displacement cross section among a wide range of fission reactor neutron spectra. The largest variation was found when fission neutrons were compared with 14 MeV neutrons. Even in this case, the relative uncertainty due to electronic stopping power was expected to be 12% or less. Damage energy was found to have only a small relative sensitivity (13% maximum) to variation in electronic stopping power over a widely varying range of atomic charge (Z). Similar results were found for the effects due to nuclear models and nuclear data set comparisons. The largest problem was due to systematic variations between nuclear data sets; this problem could be remedied by using a common nuclear data bank.

An accurate knowledge of the form of the displacement model has become increasingly important in recent years because of the large spectral differences known to exist between fission and fusion neutron spectra.[14] Several experiments have compared the effects on tensile properties after irradiation in the two type of spectra. Most experiments were conducted at room temperature. Jones et al.[15] irradiated Ni and Nb tensile specimens in (d,T) and (d,Be) neutron sources at room temperature and found that damage energy correlated the change in yield strength for Ni but not for Nb.

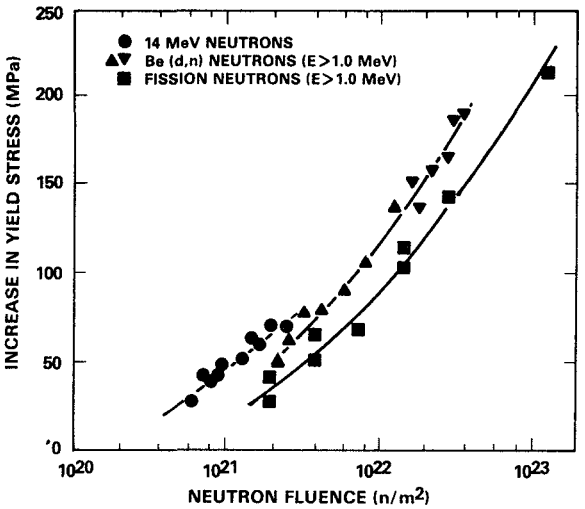

FIGURE 7a. Radiation strengthening in 316 stainless steel as a function of neutron fluence.

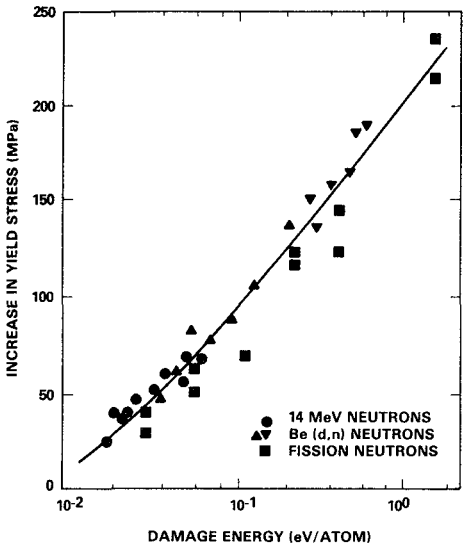

FIGURE 7b. Radiation strengthening in 316 stainless steel vs damage energy.

They attributed the lack of correlation in Nb to an interaction between point defects and impurity atoms. Similarly, Mitchell et al.[16] irradiated Cu, Nb, and V in a fission reactor spectrum and in (d,T) and (d,Be) sources; they also concluded that damage energy correlated yield strength satisfactorily for all but Cu. In this case the difference was attributed to differences in the form of high- and low-energy damage. Vandervoort et al.[17] irradiated solution-annealed 316 stainless steel in the same three spectra. They concluded that damage energy correlated the yield strength (Figure 7) and microstructural data better than fluence (E > 1 MeV). In all cases, the increase in yield strength correlated better with dpa than with fast fluence (E > 1 MeV) when fission and fusion spectra were compared.

Close examination of the various correlations shows reasonably good correlation of the data between fission reactor spectra with the dpa exposure parameter, and also good correlation of the data from irradiation in fusion neutron sources. However, the correlation of data from both fission and fusion neutron irradiations frequently shows a discrepancy. For example, in Figure 7b the spread in the increase in yield strength data is 10-30%, while the spread in the exposure parameter is up to a factor of two. The amount of strengthening perhaps is lower in the fission reactor case, suggesting that a cluster production cross section may be appropriate than a total displacement cross section.

Thus it appears that the dpa exposure parameter gives an adequate first-order correction for spectrum effects, but improved correlation of fission-fusion irradiation effects data (i.e., within 10-30%) will require improvements in the damage exposure index. The secondary displacement function $\nu(T)$ is the most likely place where improvements in the correlation can be made.

Transmutation Products

Helium is generally considered a detrimental element in a metal. When the irradiation temperature is high enough (>.5 T_m), the helium migrates to grain boundaries, where it causes premature failure at the grain boundaries under tensile loading. Helium has also been shown to be a source of void or bubble nucleation which can lead to swelling of the metal.

In a study of annealed 316 SS irradiated at 515 and 585°C, Blackburn et al.[18] found that helium affected ductility. By the time a few parts per million helium were produced, the ductility dropped to a fixed level of residual elongation. The same thing was found to occur in 20% CW 316.[19] In fact, the residual elongation remains fairly constant out to 50-100 appm helium before further loss in ductility occurs (Figure 8). It was also observed (Figure 9) that high neutron exposure softening of the strength of 20% CW 316 SS occurred in both fast and mixed spectrum reactors. The effect appears to be correlated with $\sqrt{\text{hpa} \cdot \text{dpa}}$ (where hpa is appm helium). However, the irradiation temperature for the HFIR data may be up to 100°C too low, thus precluding such a helium-dpa correlation. If synergistic helium-dpa interactions occur, a simple dpa correlation is inadequate for predicting the macroscopic response of metals in fusion neutron environments with data from fission reactor irradiations. In any event, the fact that helium affects the macroscopic properties of a material demonstrates the need for helium production cross sections which can be used to calculate helium concentrations in the metal for any neutron environment.

Solid transmutation products provide another important mechanism for changes in a material property. Bates et al.[20] showed (Figure 10) that

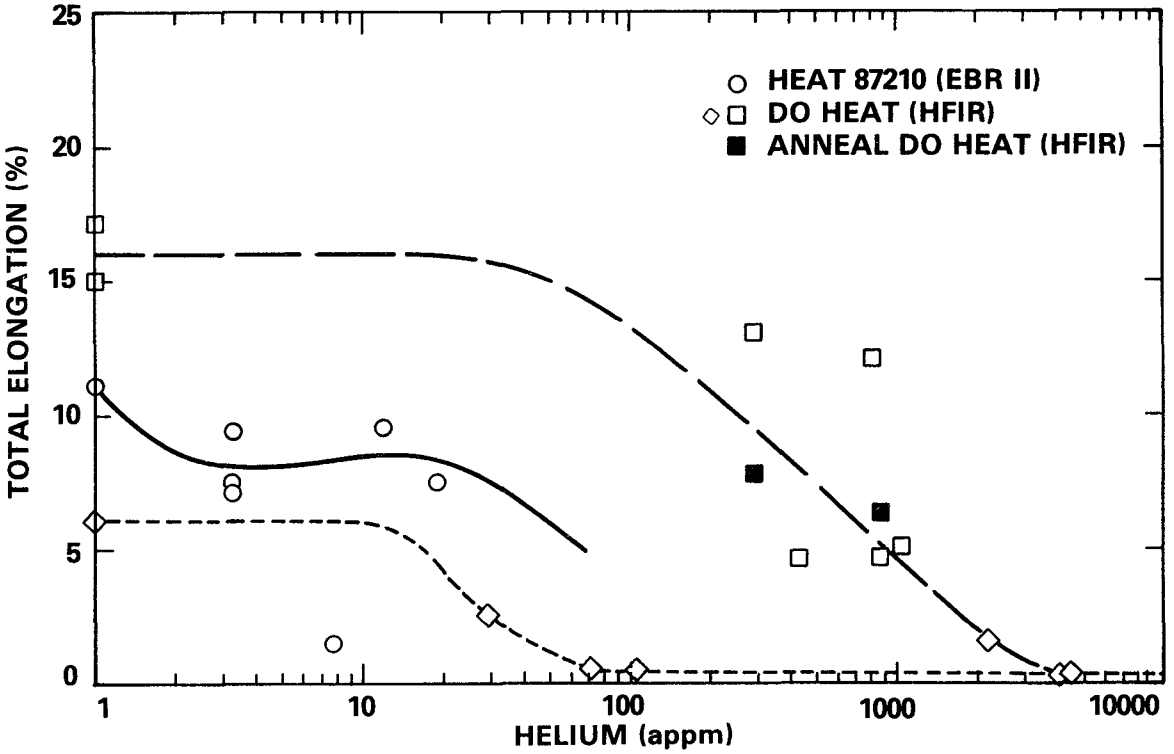

FIGURE 8. Total Elongations in 20% CW 316 SS vs Helium Constent.

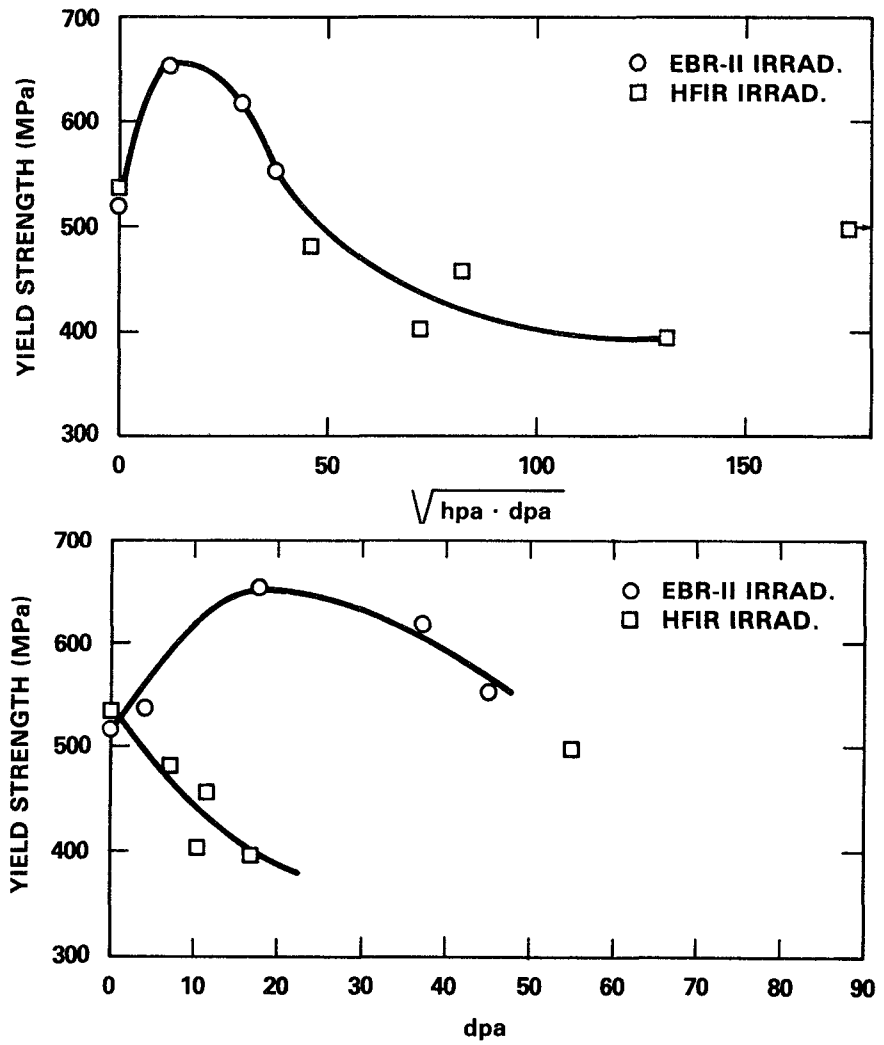

FIGURE 9. Correlation of Yield Strength in 20% Cold Worked 316 SS Irradiated at 470°C.

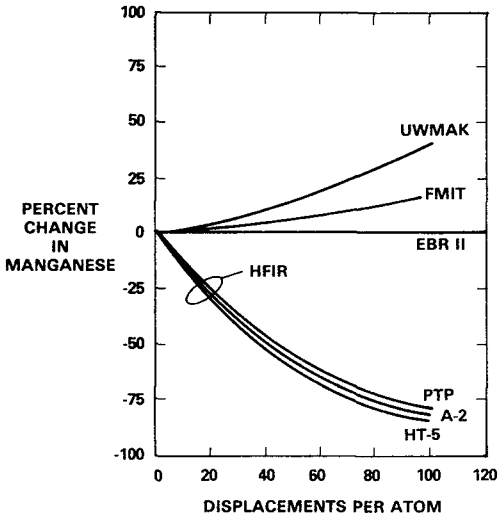

FIGURE 10. Change in Manganese Concentration as a Function of Exposure in Various Reactors. HT-5, A2 and PTP refer to different positions in HFIR.

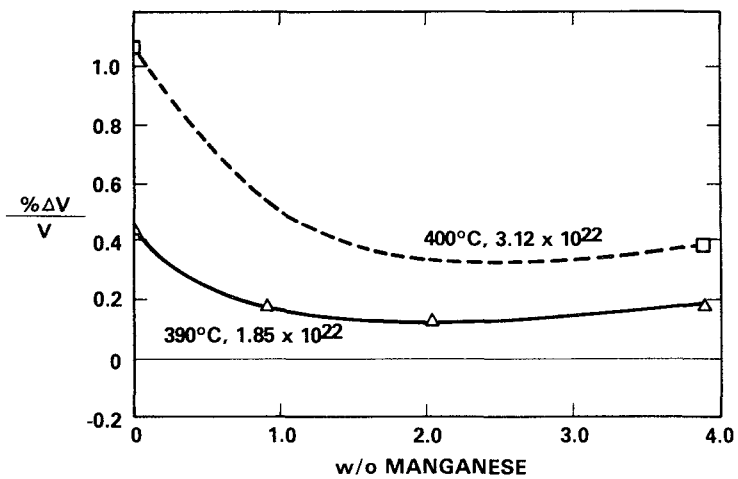

FIGURE 11. Effect of Manganese Content on Swelling of Annealed 316 at Low Temperatures and Low Fluence.

all the manganese can be burned out of stainless steel by irradiating it in a mixed spectrum reactor to a dose of ∿100 dpa. Swelling in stainless steel can be increased by up to a factor of two by removing the manganese (Figure 11). On the other hand, the manganese content can increase by 40% after irradiation in a fusion reactor spectrum to 100 dpa. The consequences of the variation in concentration of a chemical species depends on specific damage mechanisms. For example, if manganese content affected void swelling only during the nucleation phase early in the irradiation, the burn-out of manganese would have less effect than the absence of manganese from the start of the irradiation. The effect of burn-in and burn-out on the kinetics of microstructure evolution in a material needs to be studied in order to accurately evaluate the net effect on the material during the irradiation.

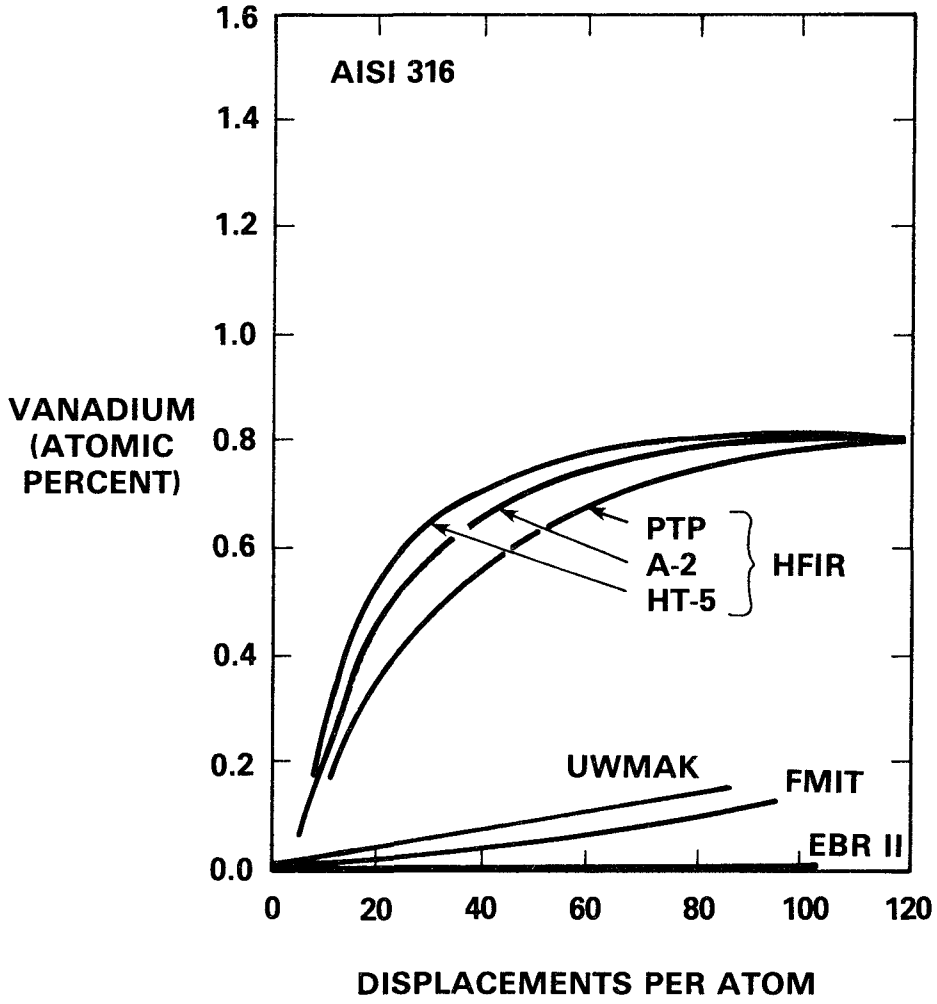

FIGURE 12. Vanadium Concentration as a Function of Exposure for Various Reactors. HT-5, A2 and PTP Refer to Different Positions in HFIR.

Similarly, vanadium is burned-in from chromium (Figure 12), and since vanadium readily combines with carbon, MC carbide precipitation would form. The precipitate may increase the strength of the steel by impeding the motion of dislocations.

A conclusion to be drawn from their study is that burn-in and burn-out effects need to be addressed in designing experiments or applying materials data to fission and fusion reactors. Consequently, this will require a survey and assembly of a library of appropriate nuclear cross sections for elements of importance to materials used in fission and fusion reactors. Bates et al[20] have calculated burn-in and burn-out of most important materials in stainless steel. It is also important to understand the effects of solid transmutation products, and to differentiate these effects from those due to helium.

Conclusions

The concern for the quality of nuclear data has become increasingly important in recent years because of the need to predict the behavior of materials in fusion environments or out-of-core structural components in fission reactors from data obtained from in-core irradiation of materials. Relative displacement cross sections used as an exposure index can be calculated fairly accurately (5-10% uncertainty) and are good for determining first-order corrections for spectral effects of irradiation damage. Larger uncertainties (30-50%) due to low energy recoils may be expected when extrapolating to well-moderated out-of-core fast breeder reactor spectra. However, this will probably not be a serious problem because of the extremely low total doses encountered. Generally speaking, first-order spectral correlations are satisfactory because other uncertainties (for example, temperature or chemistry) have overriding effects on most correlations.

Prediction of helium content in a metal is important for high temperature (> .5 T_m) application requiring a ductile material, and possibly for high doses (> 25 dpa) at lower temperatures where yield strength softening may occur. Predictions of both gaseous and solid transmutations are important in order to achieve an understanding of the damage mechanism at work.

Nuclear data needs for application to macroscopic data for structural materials are modest. Goal accuracies should be set at 10-20% (1σ) uncertainty in the integral damage parameter. Present data files for most materials of importance are adequate for correlating irradiation effects to materials for neutron energies up to 15 MeV. At present the greatest correlation problem is not in the PKA spectrum but is in the material property measurements, irradiation temperature, and the modeling of residual damage, that is $\nu(T)$. With the increased use of (d,Li) and (d,Be) neutron sources, the neutron cross-sections need to be extended up to 40 MeV. In this energy range, nuclear data are uncertain by 30-40% or do not exist. The most important materials to evaluate first are iron, chromium, and nickel. In the U.S.,-preliminary evalutions of iron and chromium have been completed, and nickel will be started next year. Other potential structural materials should be evaluated also.

References

1. ASTM Standard E-693-79, "Standard Practice for Characterizing Neutron Exposures in Ferritic Steels in Terms of Displacements per Atom (DPA)," ASTM Standards (1980), Part 45: Nuclear Standards, American Society for Testing and Materials, Philadelphia, PA, pp. 1204-1210, 1980.

2. R. E. Gold et al., "Materials Technology for Fusion: Current Status and Future Requirements," Nucl Tech./Fusion 1, pp. 169-237, April 1981.

3. J. Lindhard, M. Scharff, and H. E. Schiott, "Range Concepts and Heavy Ion Ranges (Notes on Atomic Collisions, II)," Mat. Fys. Medd. Dam. Vid. Selsk. 33 (14), 1963.

4. M. A. Kirk and L. R. Greenwood, "Determination of the Neutron Flux and Energy Spectrum in the Low-Temperature Fast-Neutron Facility in CP-5, Calculations of Primary-Recoil and Damage Energy Distributions, and Comparisons with Experiments," J. Nucl. Mat. 80, pp. 159-171, 1979.

5. M. W. Guinan, et at., "A Comparison of Experimental Defect Production Efficiency in Mo with Computer Simulation in W," DOE/ET-0065/6, Damage Analysis and Fundamental Studies Quarterly Progress Report, U.S. Department of Energy, Washington, DC, July 1979.

6. R. L. Simons, "The Correlation of Irradiation Effects Data Using Primary Recoil Data," DOE/ET-00463, Damage Analysis and Fundamental Studies Quarterly Progress Report, U.S. Department of Energy, Washington, DC, November 1980.

7. D. G. Doran, "The Conversion of Displacement Production to Defect Production in Stainless Steel through Computer Experiments," Nucl. Eng. and Design 33, pp. 55-62, 1975.

8. L. D. Blackburn, et al., "Strength and Ductility of Austentic Stainless Steels Irradiated in Various Fast Reactor Spectra," Proceedings of the Third ASTM-Euratom Symposium on Reactor Dosimetry, EUR 6813, pp. 326-333, 1980.

9. G. L. McVay, L. C. Walters, and G. D. Hudman, "Neutron Irradiation-Induced Creep of Helium-Pressurized 304L Stainless Steel Capsules," J. Nucl Mater. 79, pp. 395-405, 1979.

10. R. L. Simons, "Reevaluation of Ferritic Steel ΔDBTT Data Used in Damage Function Analysis," Proceedings of the Third ASTM-Euratom Symposium on Reactor Dosimetry, EUR 6813, pp. 178-185, 1980.

11. P. Mas, R. Perdreau, and P. Tran-Dai, "The Influence of the Neutron Spectrum on the Embrittlement of Steels for Reactor Vessels," Proceedings of an IAEA Technical Committee Meeting on Correlation Accuracy in Pressure Vessel Steel as Reactor Components Investigation of Change of Material Properties with Exposure Data, Jul-Conf-37, pp. 347-374, September 1979.

12. G. R. Odette, "A Quantitative Analysis of the Implications of the Accuracy of Dosimetry to Embrittlement Predictions: Past, Present, and Future," Proceedings of the Third ASTM-Euratom Symposium on Reactor Dosimetry, pp. 164-177, 1980.

13. D. G. Doran, D. M. Parkin, and M. T. Robinson, "Damage Energy and Displacement Cross Sections: Survey and Sensitivity," HEDL-SA 1161, Hanford Engineering Development Laboratory, Richland, WA, November 1976.

14. D. G. Doran and M. W. Guinan, "Fusion Materials High-Energy Neutron Studies -- A Status Report," Symposium on Neutron Cross-Sections from 10 to 50 MeV, Brookhaven National Laboratory, Upton, NY, BNL-NCS-51245, Vol. II, pp 459-493, July 1980.

15. R. H. Jones et al., "Microstructure and Tensile Properties of T(d,n) and Be(d,n) Neutron Irradiated Nickel, Niobium and 316SS," J. Nucl. Mater. 85 and 86, pp. 889-893, 1979.

16. J. B. Mitchell, "Exploratory Experiments Comparing Damage Effects of High-Energy Neutrons and Fission-Reactor Neutrons in Metals," UCRL 52388, Lawrence Livermore Laboratory, Livermore, CA, January 12, 1978.

17. R. R. Vandervoort, E. L. Raymond, and C. J. Echer, "High-Energy Neutron Irradiation Effects on the Tensile Properties and Microstructure of 316 Stainless Steel," Radiation Effects 45, pp. 191-198, 1980.

18. L. D. Blackburn, D. C. Greenslade, and A. L. Ward, Mechanical Properties of Type 316 Stainless Steel Materials After Irradiation at 515°and 585°C, HEDL-TME 81-4, Hanford Engineering Development Laboratory, Richland, WA, April 1981.

19. R. L. Simons, "Tensile Property Correlations for 20% CW 316 Stainless Steel," Proceedings of Meeting on Fusion Reactor Materials, Seattle, WA, August 9-12, 1981.

20. J. F. Bates, F. A. Garner, and F. M. Mann, "The Effect of Transmutation Products on Swelling in 316 Stainless Steel," Proceedings of the Meeting on Fusion Reactor Materials, Seattle, WA, August 9-12, 1981.

ACCURACY AND CONSISTENCY IN IRRADIATION TESTS OF LWR PRESSURE VESSEL STEELS

Review on Statements and Suggestions after CAPRICE-79 Meeting

W. SCHNEIDER
Kernforschungsanlage Jülich,
Jülich,
Federal Republic of Germany

Abstract:

The need for accuracy and consistency in the required life-time prediction and surveillance test results for pressure vessels as reactor components is summed up. Available recent uncertainty and variation statements to such results, mainly from CAPRICE-79 meeting, are reviewed. Possible requirements for a more thorough-going knowledge and a further reduction of the uncertainty contributions are considered, including possible demands in reporting nuclear data. Some suggestions are given for actions to come to a conclusion that a quantification of uncertainty limits within a stochastically based concept should be intended. Supporting this the preparation of a standard procedure is suggested for conducting tests of material damage under neutron exposure, for minimizing errors from lab to lab.

1. Introduction

It is well known that one of the causes limiting the lifetime of the light water reactor (LWR) is given by the neutron damage to which the material of the reactor pressure vessel is exposed during its service.
For making sure a proper and sufficiently reliable prediction for this lifetime limitation, the conditions in Table 1 have to be fulfilled.
Customarily this prediction is based on calculations and validated by accelerated irradiations of the pressure vessel material (s.e.g./I,411//I,439/). For these irradiations the reactor physical conditions for the accelerated position must be carefully selected with respect to the service location. Particularly the neutron spectrum in each of these locations must be known.
Several extended international and national attempts (s.e.g. /1//2//I,389//II,407//VI/)have been made with irradiation pro-

grammes to investigate the reliability of the lifetime prediction for reactor pressure vessels in the last years. Such programmes are directed to

- either (on the material testing side):
  a more perfect knowledge of the maximum permissible damage of a certain material, and to the most simple and reliable procedure in conducting tests to predetermine it,
- or (for studying the irradiation environment conditions):
  to erect for a certain time irradiation standards, for testing and intercomparing theoretical calculations and experimental methods.

From another point of view has been outgoing the IAEA Technical Committee Meeting /I/
C A P R I C E 79:
Correlation Accuracy in Pressure Vessel Steel as Reactor Component Investigation of Change of Material Properties with Exposure Date
Jülich, 24-27 September 1979

Table 1

DEMANDS to be Fulfilled
FOR an Adequate LIFETIME PREDETERMINATION
of Reactor Pressure Components in Service

I : The maximum permitted damage in service for the specific material must be known

II : The damaging capacity (or: effective damage cross-section density) distribution and its representative value for the component (in its location relatively to the neutron source distribution in the reactor) must be given

III: The neutron spectrum over the reactor component has to be determined and the (representative value of the) neutron fluence hitting the component during its lifetime has to be measured in an adequate way

---

Here the theme has been the discussion and comparison of all relevant uncertainties which may occur in the determination of the behaviour of that reactor structural material under neutron irradiation.

After a review of the statements (from /I/ and elsewhere) of those uncertainties, in the following requirements are discussed which appear useful for a more thorough knowledge and further reduction of them. Concluding some suggestions for further activities on an international scale are made, aiming mainly at a characterization of the radiation field of such material irradiations which should promise satisfyingly consistent comparisons between different positions and laboratories.

2. Necessary and available uncertainty information to irradiation tests

2.1 The correlation curve, its role and its uncertainties.

For demonstrating the influence of uncertainties and the importance of the consistency of test results from LWR pressure vessel steel irradiations, we have to realize the use of correlation curves for the predetermination of the material properties shift which is induced by fast neutron irradiation; we relate to Fig.1 and 2 (from /I,439/). For the conduction of surveillance tests in this frame one is referred to ASTM Standard E 185 /III/. If the damage of the material is exceeding the predicted value, the correlation is the basis for a new estimation of the material state for the pressure vessel End-of-Life.
The correlation curves require consistent experimental points if they claim to be generally valid. Uncertainties appear in these curves on the material side as well as on the side of the irradiation environment characterization, i.e., they combine to probability windows. An example of this for one correlation point is given in Fig. 3 (from /I,439/), using /3//V,1123/ surveillance irradiation results, estimates of fluence uncertainties and different error bounds.
Before entering the discussion of the results from CAPRICE 79 meeting, I want to recollect the principal types of uncertainty contributions to both sides or axes of the correlation curve.

2.2 Uncertainty types in the irradiation environment characterization.

Uncertainties in calculations of the neutron radiation field/IV,147//II,448//II,1275//V,1093/ can stem mainly from the neutron spectrum calculating procedure, from the location dependence including flux perturbation, and from time-dependent variations of the reactor power-to-local neutron flux density relation. On the other hand, in monitoring

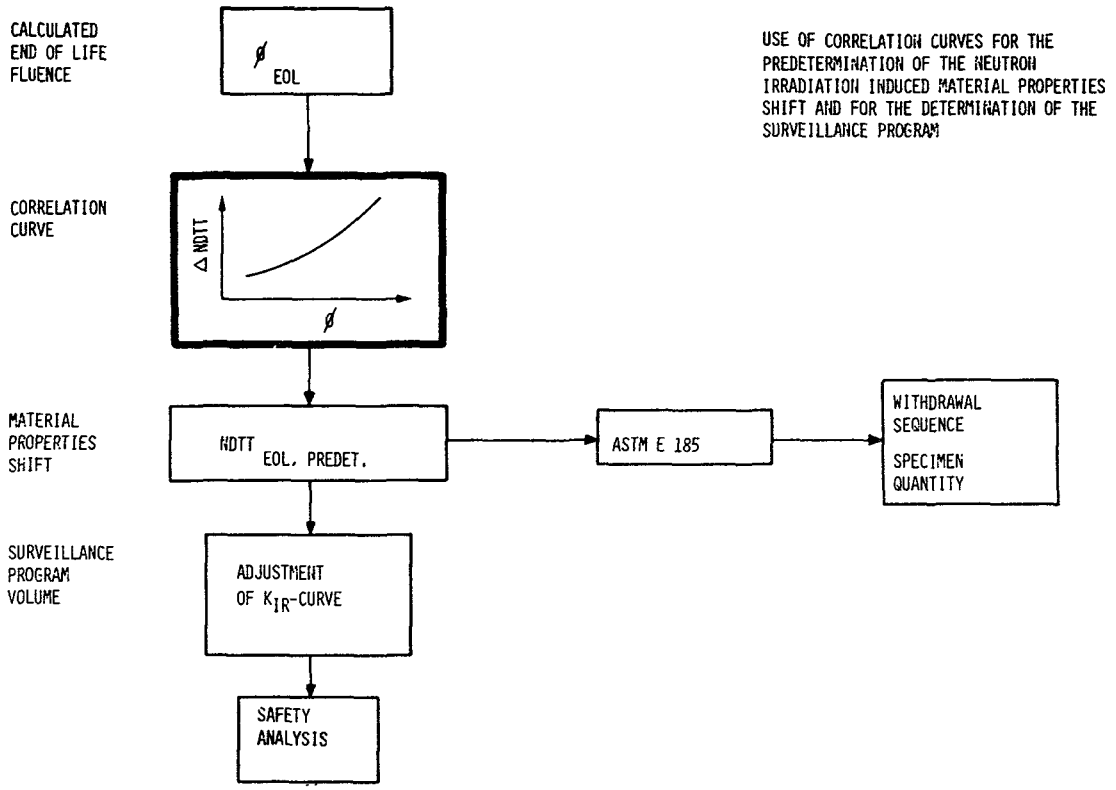
CALCULATED END OF LIFE FLUENCE
ϕ_{EOL}
USE OF CORRELATION CURVES FOR THE PREDETERMINATION OF THE NEUTRON IRRADIATION INDUCED MATERIAL PROPERTIES SHIFT AND FOR THE DETERMINATION OF THE SURVEILLANCE PROGRAM
CORRELATION CURVE
Δ NDTT
ϕ
MATERIAL PROPERTIES SHIFT
NDTT EOL, PREDET.
ASTM E 185
WITHDRAWAL SEQUENCE
SPECIMEN QUANTITY
SURVEILLANCE PROGRAM VOLUME
ADJUSTMENT OF K_{IR}-CURVE
SAFETY ANALYSIS

Fig. 1

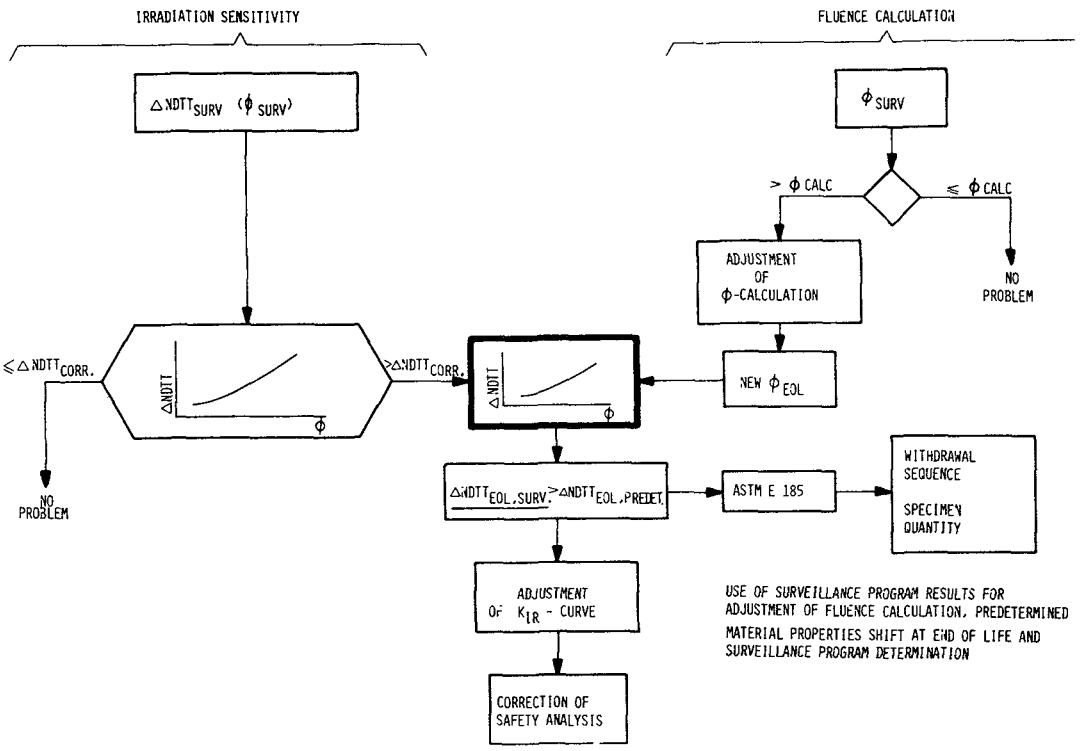
IRRADIATION SENSITIVITY
FLUENCE CALCULATION
$\Delta NDTT_{SURV}$ (ϕ_{SURV})
ϕ_{SURV}
$> \phi_{CALC}$
$\leq \phi_{CALC}$
ADJUSTMENT OF ϕ-CALCULATION
NO PROBLEM
$\leq \Delta NDTT_{CORR.}$
$> \Delta NDTT_{CORR.}$
ΔNDTT
ϕ
NEW ϕ_{EOL}
NO PROBLEM
$\Delta NDTT_{EOL,SURV.} \geq \Delta NDTT_{EOL,PREDET.}$
ASTM E 185
WITHDRAWAL SEQUENCE
SPECIMEN QUANTITY
ADJUSTMENT OF K_{IR} - CURVE
USE OF SURVEILLANCE PROGRAM RESULTS FOR ADJUSTMENT OF FLUENCE CALCULATION, PREDETERMINED MATERIAL PROPERTIES SHIFT AT END OF LIFE AND SURVEILLANCE PROGRAM DETERMINATION
CORRECTION OF SAFETY ANALYSIS

Fig. 2

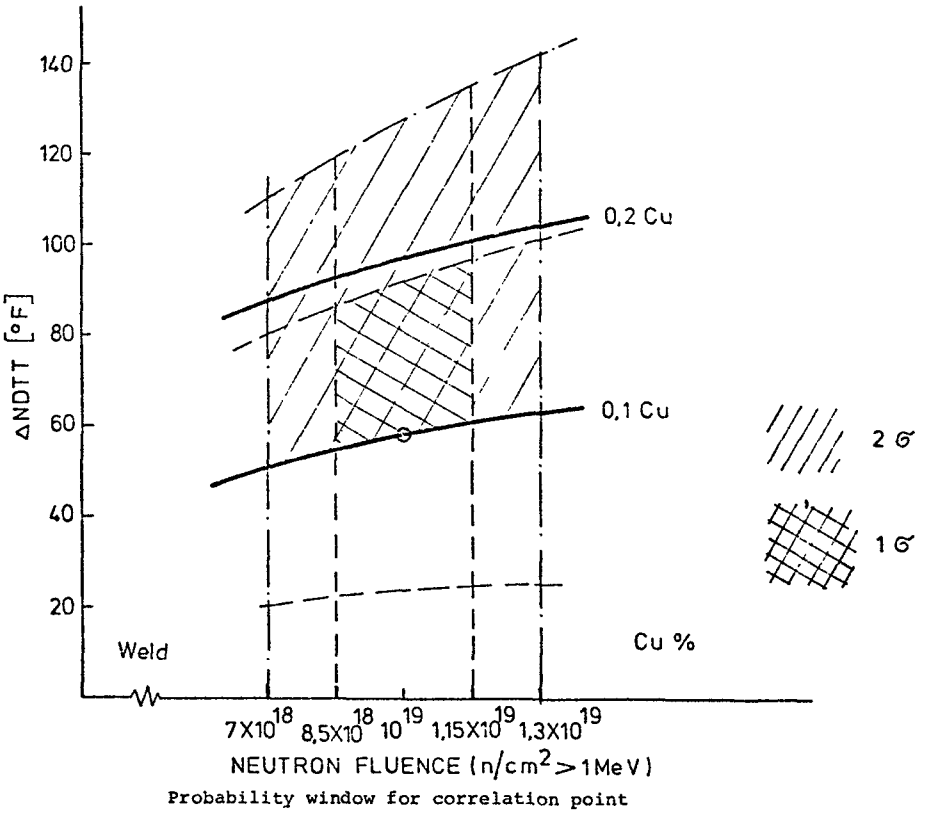

Fig. 3

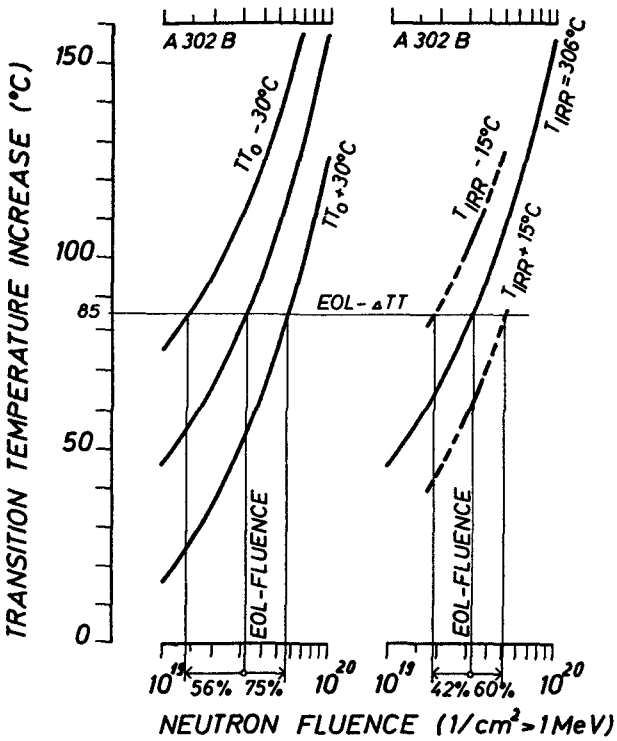

- LACKING CORRESPONDENCE OF THE COMPARED IRRADIATED AND UNIRRADIATED MATERIAL STATES IN THE UNIRRADIATED CONDITION (LEFT HAND FIGURE):

  INFLUENCE DEMONSTRATED ON THE BASIS OF A 30°C-TRANSITION TEMPERATURE DECREASE FROM THE MIDDLE TO THE OUTER EDGES OVER THE WIDTH OF THE PLATE, AS MEASURED ON HSST-PLATE 03 (CENTRAL AREA 1/4 THICKNESS)

- ERROR IN THE DETERMINATION OF THE IRRADIATION TEMPERATURE (RIGHT HAND FIGURE):

  INFLUENCE DEMONSTRATED ON THE BASIS OF A ±15°C IRRADIATION TEMPERATURE ERROR, USING A GRADIENT OF 1.4°C TRANSITION TEMPERATURE SHIFT DECREASE PER 1°C IRRADIATION TEMPERATURE INCREASE

- ERROR IN THE DETERMINATION OF FLUENCE:

  THE RELATIVE FLUENCE ERROR IS CAUSING AN DIRECTLY EQUIVALENT RELATIVE IRRADIATION TIME ERROR

Fig. 4

the irradiation fluence by neutron detectors, uncertainties arise mainly /II,493//II,623//IV,233//I,271/ by disturbing detector reactions, in the reaction cross-section averaged over the neutron spectrum in the irradiation position, and again in the time-dependent power-to-flux density variations. Furthermore one expects to have a better correlation in representing the neutron exposure by the number of displaced atoms in the material (in our case: steel) instead by the neutron fluence /4//I,310//V,1123/.

In Table 2 is presented the common neutron exposure evaluation by measurements, with uncertainty contributions roughly to be expected for the constituents of the reported formulae. For the conversion factor from "fluence" to "number of displaced atoms" uncertainty guess values according to /II,448/ have been assumed.

2.3. Uncertainty types in the material state determination.

The main origins of these uncertainties are shown in Table 3 (according to /5/). As prominent examples of a lack of correspondence between compared results can be mentioned the manufacturing history depending influence of a $\pm$30 K transition temperature variation of specimens taken from different locations in a steel plate /6/; and an error of $\pm$15 K in irradiation temperature determination /7/: in both cases an error in the fluence and so in the test exposure or lifetime determination will result, s. Fig. 4/V,285/. To the lack of correspondence cf also /8/.

2.4. Summary of uncertainty statements (from CAPRICE 79 and elsewhere).

Reviewing the single reports on uncertainties made at the CAPRICE 79 meeting /I/, on the materials side there has been found that more detailed evaluation is necessary because of the complexity of data. The need for applying standard procedures for the material selection as well as for the evaluation and for a comprehensive documentation has been stressed /I,4/. The problem in focus besides the usual variability of material properties and test procedures is the establishment of a measure for the accuracy needed applying safety analysis. Furtheron the importance of the single influences to the correlation of irradiation induced damage with neutron exposure is to investigate. The use of correlation mean curves is suggested, demanding an increased level in accuracy and documentation.

Under the uncertainties connected to the characterization of the irradiation environment, the lack of knowledge appeared more obvious in the results of calculations and in the technical conditions (local flux densities, temperatures) than in the methods of neutron metrology where the considerations show that a satisfyingly low uncertainty seems to be achievable.
The status and the aims in overall uncertainties in neutron metrology, radiation field calculation, and metallurgy, have been presented in Table 4 according to CAPRICE 79 meeting and as far as available /I,271/. For a more detailed review of these uncertainty statements the reader is referred to /5/.

Table 2

NEUTRON EXPOSURE DETERMINATION

by

Fluence Measurement $\Phi^I(T) = \frac{R^I}{\sigma^J} T \frac{f^{J\to I} H(T)}{K^I}$

DPA Evaluation $N_D^I(T) = \Phi^I(T) f_D^I$

with:

I Irradiation Test Field Characterization Index
J Reference Field Characterization Index
D Damage Index

Constituents		Uncertainty /1σ/ rel., ca.
T	Irradiation Time	(negl.)
R	Detector Reaction Rate [incl. photoreactions]	1-5 [≲40] %
σ^J	Reference Field Averaged Reaction Cross Section	2-10 %
$f^{J\to I}$	(Flux Density) Conversion Factor From Reference to Test Field	≲20 %
H	Irradiation Time Correction (for Flux Density)	10-20 %
K	Flux Perturbation Correction	≲10 %
f_D^I	Conversion Factor from Fluence to Number of Displaced Atoms in the Test Field	5-15 %

Table 3

ORIGINS OF UNCERTAINTIES

IN THE MATERIAL STATE DETERMINATION :

1. Materials property variation
   from chemical composition and from manufacturing history

2. Influence of (pre- and post-irradiation) material testing

3. Unsufficient physical correlation of the test results
   (e.g., of different provenance)

3. Discussion of Further Requirements

3.1 Inferences from CAPRICE 79. The central issue of the CAPRICE 79 meeting has been the following: If the overall uncertainty in the life-time assessment needs further reduction then, to attain this, (one or several) individual uncertainties should be found out which promise to act on the overall uncertainty particularly effectively in the sense of a reduction. It has been the more or less common opinion that the uncertainties connected to the lifetime assessment as looked at should further be more thoroughly estimated and reduced /I,140//I,210//I,271//I,439//II,397/. Current efforts are aimed at improvements in accuracy on the materials side as well as on the irradiation environmental side. The results of these efforts can take effect only in a probabilistic concept. Equally the estimation of the effect and of the accuracy possible or necessary will need correlation mean curves. The curves could easily be determined, if enough irradiation results favourably from surveillance irradiations and sufficient in accuracy and documentation would be available.

Because a requirement like "no uncertainty at all" can never be fulfilled, it should be said clearly and distinctly to which extent uncertainty limits should be required, i.e., what amount of uncertainties from a pragmatic standpoint should be even tolerated without accepting a too big safety margin which in turn would

lead to a too big sacrifice of lifetime of the reactor component. As far as we know, until now there does not exist a unique figure marking such an uncertainty limit requirement.
To the single values of the wanted uncertainty reduction reported at the CAPRICE 79 meeting /I,94/ (s. Table 4) there is to say that arguments for just this extent of reduction has not been given what indeed would be difficult because such a requirement as mentioned above must be seen in the context of the overall uncertainty with respect to the tolerable safety margin.
For our feeling a comprehensive uncertainty limit requirement in the mentioned pragmatic sense should be stated for a task like considered here. Having compiled and composed an overall uncertainty, reached values should be compared with the required limit for checking whether measures appear necessary to reduce them further or not.

3.2 Variations in approaches to characterize the damaging exposure.

For illustration, in Table 5 is shown variations of some approaches to characterize the damaging exposure in one experiment, given in several characterizing quantities and estimated by means of four different procedures, three of them using the same damage cross-section for steel $w_{St}(E)$ (a semiempirical one, according to Serpan /VIII-A,19/) but with different codes (DTF-IV; SAND-II; P1MG, all from /9/) to evaluate the neutron spectrum; the fourth using a theoretically derived function for pure iron /10/ applying again code P1MG /9/ for the spectrum calculation.
The characterizing quantities referred to in Table 5 are:

- The fraction of the damage (i.e., displacement) cross-section averaged over a certain part ($0<E_1<E_2<\infty$) of the spectrum of the irradiating neutrons:

$$W^{I}(E_1, E_2, \vec{r}) = \frac{\int_{E_1}^{E_2} w_{St}(E)\,\varphi_E(E,\vec{r})\,dE}{\int_{0}^{\infty} w_{St}(E)\,\varphi_E(E,\vec{r})\,dE} \qquad (1)$$

This quantity gives an indication how constant the contribution to the material damage from the spectral

Table 4

STATUS AND AIMS IN OVERALL UNCERTAINTIES

in Pressure Vessel Lifetime Assessment (after CAPRICE 79)

1σ - Uncertainty for the	Status % +	Main Sources	Aims % +
Metallurgical Variables	±45.. 90	Chemical Composition Microstructure	
Steel Irradiation Temperature	±20..40	Applied Measuring and Interpolating Methods	
Irradiation Exposure Parameters	±20.. 40	Lacking Corrections or Normalization, Resp.	± 10...15 for Neutron Metrology

+ incl. unknown systematic errors

Table 5

Maximum Variations (in Percents) of Characteristic Values, between Four Different Evaluations for the Same Irradiation[1]

Position[2]	Max. Percent Variations for: Damage % Fraction (>1MeV)	Damaging Capacity Barns	Lead Factor (LF)Φ	$\Delta\frac{LFd}{LF\Phi}$	Aver. Lead Factor Ratio $\frac{(LF)d}{(LF)\Phi}$	Applied Damage Funktion[3]
						A
AS	± 0	± 0,4				SERPAN's Semi-
AS:VW			± 10	±2,5	0,913	empirical Function
VW	±2,4	±2,6				G(E)
T/4	±8,2	±7,2				/VIII-A,19/
						B
AS	-30	+24				Theoret. Function
AS:VW			-4,3	-8,1	0,839	for Pure Fe
VW	-39	+35				w(E)
T/4	-45	+37				/10/

1 LWR PV steel in the IRL test reactor /9/

2 Reactor Positions:
A(ccelerated) S(urveillance); V(essel) W(all);
T/4: Quarter of Vessel Wall Thickness (from Reactor Core)

3 To A is given: maximum variation from the mean value
" B " " : deviation from the mean value to A

region between the neutron energies E_1 and E_2 is to be seen as a function of the material location $\vec{r}$.

- The damaging capacity (also to be called the effective /11/ damage cross-section) of a particular material, related to the neutron flux density above 1 MeV energy, in the irradiation position $\vec{r}$:

$$\frac{d}{\varphi_r}(\vec{r}) = \frac{\int_0^\infty w_{st}(E)\,\varphi_E(E,\vec{r})\,dE}{\int_{1\,MeV}^\infty \varphi_E(E,\vec{r})\,dE} \qquad (2)$$

While the well-known Damage-to-Activation Ratio (DAR) conversion factor (s.e. g./4/)

$$DAR = \frac{\sigma_i^f}{w_{St}^f} \cdot \frac{w_{St}^I}{\sigma_i^I} \qquad (3)$$

with:

σ_i, W_{St} cross section of the detector i, for steel damage, resp., averaged over:

f, I the fission, irradiation spectrum, resp.

has to be preferred for practical measurements while the damaging capacity as applied in the Irradiation Test Environmental Parameter Tables /I,271/ is advantageous for theoretical preassessments because it does need neither the knowledge of particular detector data nor that of absolute flux density values.

- The lead factor is correctly defined /II,397/ either by

$$(LF)_\Phi = \Phi(E_1, \vec{r}_A, t_I) : \Phi(E_1, \vec{r}_S, t_I) \qquad (4a)$$

i.e., as the lead factor for the neutron fluence Φ above energy E_1, for the accelerated ($\vec{r}_A$) and service ($\vec{r}_S$) locations, during the time t_I of the specimen irradiation in the $\vec{r}_A$ location,
or - what is to be preferred:

$$(LF)_D = N_D(\vec{r}_A, t_I) : N_D(\vec{r}_S, t_I) \qquad (4b)$$

i.e., as the lead factor for the number N_D of displaced atoms.

The presentation in Table 5 is taking into account only older but completed investigations, for avoiding to anticipate a review of the reliabilitytests for the irradiation environment characterization (mentioned in the Introduction) for which final reports not yet have been issued. Nevertheless, especially the strong deviation between the two different damage models can make obvious the need for a well-founded recommendation of a particular damage model and for further studies on (systematic)errors and uncertainties in this field.

3.3 Further measures and open questions for reliability tests and data inquiries.

In Table 6 are listed(from the statements in Table 2) certain points of view mainly to be considered for testing the reliability of the environment characterization to reactor structural material irradiations:

- The use of multiple reaction analysis in neutron metrology is adequate not only for a satisfying coverage of the damage response range of the material in question but also for some redundancy in the results. This facilitates cross-checking of the results, for ferreting errors and for adjusting calculated neutron spectra by measurement results.
- For proving the information on neutron spectra the benchmark field technique is in use, for calculations as well as for adjusting measurements (e.g./II,1275/ /IV,147//IV,233/). In this technique three classes of measurement uncertainties appear /II,623/:

    1. for cross section determination in the standard field,
    2. for transferability to (at least one of) reference fields adapted to the test region(s)
    3. for the assumption "the reference field is well adapted to the test region"

  In pure calculations, corresponding uncertainty classes may be expected. A certain restriction in applying the benchmark technique is that it can logically give only necessary but no sufficient validations.

- Irradiation time corrections (for the irradiation history as given in reactor power levels) should be carried out every time one is suspecting some error /II,1275/. This is done /12/ e.g. by multiplying the relative power by particular factors (obtained e.g. from power distribution measurements) for each re-

Table 6

RELIABILITY TEST CONSIDERATIONS

for Irradiation Environment Characterization to
Light-Water Reactor Pressure Vessel Surveillance

1. Multiple Reaction Analysis
   for mutual consistency check by different detector types and measurement methods, resp., after reaction corrections

2. Benchmark Neutron Fields
   for proving the results from calculations as well as from measurements

3. Irradiation Time Correction
   for irradiation history and flux-power relation variation

4. Flux Perturbation Correction
   for the presence of surveillance capsules

5. Correlation Studies
   of different damage exposure quantities with property shifts of materials under irradiation

6. Assessment of Uncertainties
   supporting the selection of the best suited measuring and evaluation methods

---

actor cycle. If possible, immediate neutron flux density measurements should be done in addition.

- Furthermore is to mention the flux perturbation correction /V,1093/ for the presence of surveillance capsules, leading to marked variations in azimuth-dependent neutron detector reaction rates.
- Correlation studies of different damage exposure quantities with shifts of single or several properties of materials under irradiation are made in various projects (e.g., /1//II, 208//II,334//II,407/).
- Point 6 in Table 6 refers to uncertainties while the points 1 to 5 refer to (also uncertainty affected) corrections to avoid errors. Clearly, the uncertainties

involved should be assessed as carefully as possible, but even more also their composition to the overall uncertainty, and it must be recognized that different approaches for measurements and calculations may result in different amounts for the overall uncertainty. One should avoid using too much information, e.g., including detector reactions showing too big errors or uncertainties in their nuclear data as known today /II,623/.

From these considerations, we have listed in Table 7 some measures or open questions which should be continued or should be taken into account more or less urgently, for reducing errors and uncertainties in the irradiation environment characterization.

4. Conclusions and Suggestions

Summarizing and concluding, some suggestions should be made in three areas (s. Sections 4.1,4.2,4.3) for international activities on the item discussed here.

4.1 Suggestion of a second CAPRICE meeting.

After the CAPRICE 79 meeting it has been the general opinion to have a follow-up meeting again on an international scale /I/. While it has been agreed at CAPRICE 79 that there is need for reduction in the uncertainties in the lifetime assessment for pressure vessel steels, no guide-line about the quantification of uncertainty limits has been given. So it is not possible to state whether the existing uncertainties are within or are not within uncertainty limits.

The quantification of uncertainty limits from the background of safety analysis which appears to be the only applicable measure should be part of the future task of the CAPRICE evaluation. This should result in a reasonable estimation of the efforts necessary to reduce the uncertainties further.

Furthermore, after having focused mainly on the uncertainties in the material state and in the test irradiation results in the CAPRICE 79 meeting, a second CAPRICE meeting should for my feeling be with priority devoted to a comprehensive discussion of the uncertainty in the steel lifetime predetermination itself.

4.2 Suggestion of an international status report (guidebook) of performing lifetime predetermination and surveillance of reactor pressure vessels.

While the CAPRICE activities are directed to a more fundamental and general discussion of the comprehension and

Table 7

SOME MEASURES FOR ENSURING ACCURACY

in the Environment Characterization
in Irradiation Tests of LWR Pressure Vessel Steels

Selection of Neutron Detector Reactions:

- Redundant equipment
- Cross-checking of results (affected with space, spectrum, and time dependent uncertainties)
- Optimal restriction, deciding according to:
  "coverage of damage response range"
  and " uncertainties sufficiently small"

Damage Model:

- Selection of sets to be recommended
  out of available displacement cross-sections
  (with fine and coarse energy grouping)
- To consider competing damage processes
  beside atomic displacements
- To pursue new developments in the mathematical
  theory of radiation damage in solids, and to
  discuss their possible applicability
- Reporting uncertainty amounts to the data sets

Covariances:

- Correlation tests for the uncertainty contributions

---

eventual reduction of all types of uncertainties and errors occuring in investigations of components designed for service under reactor neutron bombardment, questions of consistency in material irradiation tests are to be assigned more to the practical conduction of such tests.

For attaining the necessary consistent results in one correlation curve but from different origin, as discussed above, one promising precondition would be a generally adopted procedure. For this purpose and especially for the irradiation environment characterization, I have made

a suggestion to the International Working Group on Reliability of Reactor Pressure Components(IWG-RRPC)/13/, pointing out the following:
It has turned out from many investigations made during the last years (/I//II//III//V//VII/etc) that for performing such a characterization in an appropriate manner it is necessary to take into account not only the accumulated neutron fluence but also the neutron spectrum and the damage rate for the material in question, by reactor physics calculations as well as by neutron detector measurements, including also the influence of the technical and operational conditions in such a reactor irradiation. In pursuing this for the purpose of a sufficiently reliable lifetime assessment for reactor (pressure) components in the right manner, it appears advisable to convene a team of experts like, e. g., it has been existed in the former International Working Group on Reactor Radiation Measurements, having consisted of members delegated from the IAEA member countries.
My further suggestion made to the IWG-RRPC has been that such a team of experts should then in collaboration with the IWG-RRPC and the IAEA Nuclear Data Section submit proposals for procedures to perform neutron exposure determinations like indicated above which should be internationally adopted. One possible first approach to initiate such proposals could be to prepare a status report of requirements for and the ways of performing neutron exposure determinations. If accepted, such a status report could possibly later on be elaborated to an "(IAEA) Guidebook of performing lifetime predetermination and surveillance for reactor pressure components"as a tool presenting an agreed homogeneous method ensuring equivalent proceduring so that in the future correlation studies from different laboratories or countries of property changes with neutron exposure could be compared in an easy and non-ambiguous way.
The IWG-RRPC has decided /13/ to leave it to the Co-ordinated Research Programme on Irradiation Embrittlement of Pressure Vessel Steel to take any steps following to this suggestion. A suggested disposition for such a status report or guidebook has been attached here (Table 8); the questionnaire included there has been demanded at different occasions /I,474//II,397/.
A special point one should pay attention to which in this connection is the influence of the computer code selection and adaptation for calculation and measurement evaluation corrections.

Coming back to the demands in Table 1 to be fulfilled for an adequate reliable prediction for the reactor pressure vessel lifetime limitation, the establishment of a reference device seems to be an especially promising approach for fulfilling the conditions I and II. Different calculation and measuring methods may there be developed into perfect ones, for minimizing errors between different methods and laboratories. Pressure vessel models may be erected there, and their damaging capacity may be determined by calculation as well as by measurements. We remember that in the USA /1/II,334/ and in France /I,249/ /II,407/ such establishments have been in use already. Eventually it may appear feasible to use such an installation on an international scale as a permanent one, also for investigations of steel specimens under ideal monitoring conditions. This would open a permanent possibility for checking or replacing to a certain extent the common investigation procedure using accelerated irradiations of steel specimens in the reactor to be monitored itself. I would suggest to consider these questions also in the context of the status report to the IAEA, as suggested above (Table 8).

4.3 Suggestion for methodical and data inquiries.

Not anticipated - in my view even more encouraged - by the suggestions made even before, I want to submit still some special suggestions to the IAEA, aiming at inquiries on nuclear and other material specific data and associated methodical progress.

My suggestions here do not include questions on nuclear data for neutron detector reactions or for neutron spectrum calculation because this is supposed to belong to other Sessions of this Meeting. However, it has been demanded already /I,175/ to standardize damage cross sections for important materials like pressure vessel steels (cf. the older compilation /14/), obviously for better intercomparison between the laboratories and for reducing the errors. Supplementarily it should be studied whether and to which extent competing damage processes - beside the atomic displacement nowadays generally in use (s. /VIII-A,B//10//III-Standard E693-79/) - should eventually be prepared for an inclusion in such standardized damage cross section sets. A still more advanced consideration of this context would ask for the correctness of existing mathematical models for describing such damaging processes, and what influence from all this might be expected for damage cross section standard sets and for the en-

Table 8

Draft disposition to a

Status Report according to the suggestion made to the IWG-RRPC on Dec. 5,1980, tentatively preparing a Guidebook for Predetermination and Surveillance of the Lifetime for Reactor Pressure Components

---

Introduction

1. Material considerations
   Chemistry
   Microstructure
   Selection of material pieces and specimens
   Test results of non-irradiated specimens
   Test results of irradiated specimens
   Discussion of uncertainties

2. Irradiation environment considerations

   Technical conditions
   Reactor operation and the surveillance concept
   Irradiation parameter determination
   (Temperature and pressure; local neutron flux density)
   Calculational predetermination
   (Position and time dependent calculation of the neutron spectrum and of the damage-weighted damage exposure; with taking into account test specimen results)
   Surveillance results
   (With exposure formulation from neutron spectrum and fluence measurements, also taking into account the material damage)
   Discussion of uncertainties

3. Study of the need and benefit of the erection of a permament reference device,being available on an international scale for the investigation and intercomparison of reactor pressure components under irradiation

4. Summary and conclusions

Annex: Questionnaire accompanying every irradiation, for unified evaluation

---

vironment description we are speaking of here, including the involved uncertainties.
All the suggestions made here are listed in Table 9.

Table 9

SUGGESTED INTERNATIONAL ATTEMPTS

for Uncertainty and Error Studies and Reduction, in Future Irradiation Investigations of Reactor Structural Materials (like LWR Pressure Vessels)

1. Continuation of the International CAPRICE Discussion:
   Suggested is a second international specialists' meeting, for dealing with the question of a quantification of uncertainty limits and from this with the study of the appropriate further reduction of uncertainties in surveillance and lifetime prediction of LWR pressure vessels
2. Consultation of experts on an international scale
   - to prepare a Status Report (eventually a Guidebook)
   - including the question of a permanent Reference Device available for international (and national) purposes for presenting a homogeneous method and proceduring in conducting correlation tests of material behaviour under neutron exposure
3. Requests especially for international nuclear data projects:
   - Critical selection and recommendation of a standard set from available damage (i.e., d.p.a.) cross-sections
   - Study (and possibly improvement) of damage data sets, with inclusion of competing damage processes beside atomic displacements
   - Reference study of progress in the mathematical theory of radiation damage in solids
   - Uncertainty amounts to be reported or assessed on all stages of data preparation

References

Proceedings and Compilations

/I/ CAPRICE 79 -
Correlation Accuracy in Pressure Vessel Steel as Reactor Component Investigation of Change of Material Properties with Exposure Data.
Proc. IAEA Technical Committee Meeting, Jülich, Germany F.R., 24-27 September 1979
Editor W.Schneider. Jül-Conf-37 (1980)

/II/ Proc. 3rd ASTM-Euratom Symposium on Reactor Dosimetry
Ispra, Italy, 1-5 October 1979
Vols. 1,2. EUR 6813 (1980)

/III/ 1980 Annual Book of ASTM Standards
American Society for Testing and Materials, Philadelphia, Pa, USA

/IV/ Neutron Cross Sections for Reactor Dosimetry Vols. 1, 2. IAEA-208 (1978)

/V/ Proc. 2nd ASTM-EURATOM Symposium on Reactor Dosimetry
Palo Alto, Ca., USA, 3-7 Oct. 1977
Vols. 1 to 3, NUREG/CP-0004

/VI/ Co-ordinated Research Programme on Irradiation Embrittlement of Pressure Vessel Steels
Rep. IAEA Meeting, Vienna, 23-25 October 1974
IAEA-176 (1975)

/VII/ Proc. 1st ASTM-EURATOM Symposium on Reactor Dosimetry
Petten, The Netherlands, 22-26 September 1975 Parts 1,2 and Supplement. EUR 5667 (1977)

/VIII-A/ IAEA Specialists' Meetings on Radiation Damage Units in Graphite and Ferritic and Austenitic Steel. Seattle, WA, USA, 30 October - 1 November 1972 Nucl. Eng. Design 33 (1975), No.1

/VIII-B/ IAEA Specialists' Meeting on Radiation Damage Units Harwell, UK, 2-4 November 1976

Individual Papers

Papers taken from the Proceedings and Compilations quoted here (/I/ff) are referred to as /I, page no. in I/ff, other papers with single consecutive numbers /1/ff.

/I, 4/ Nagel,G., Chairman's Summary to Session 1 (on Determination of the Material State)

/I, 94/ Fabry,A., Chariman's Summary to Session 2 (on Irradiation Conditions)

/I, 140/ Alberman,A., J.P.Genthon, P.Mas. P.Perdreau, Précisions Requises et Obtenues dans la Dosimétrie des Aciers de Cuve des Réacteurs

/I, 175/ Zijp, W.L.,H.J.Nolthenius, Experience with Damage to Activation Ratios

/I, 210/ Fabry,A., F.B.K.Kam, Towards an Adequate Evaluation of LWR Pressure Vessel Steel Irradiation Exposures

/I, 249/ Alberman,A., Nimal,J.C., DOMPAC: Neutronic Model and Experimental Damage Characterization of a LWR Pressure Vessel

/I, 271/ McElroy, W.N., Chairman's Summary to Session 4 (on Correlations)

/I, 310/ Odette,G.R., Neutron Exposure Dependence of the Embrittlement of Reactor Pressure Vessel Steels

/I, 389/ Kodaira, T., S.Miyazono, et al., Behavior of Neutron Embrittlement of Mn-Mo-Ni Steels for LWR Pressure Vessel Ranging from Low to High Fluences.

/I, 411/ Marston, T.U., U.S. Nuclear Reactor Vessel Integrity Considerations.

/I, 439/ Nagel, G., Surveillance Irradiations and Reactor Pressure Vessel Safety.

/I, 474/ Report on the Discussion and on Its Results in Conclusions and Recommendations (Session 6)

/II,208/ Weise,L., H.Kuepper, The Damage Rate Correlation Programme

/II,334/ NcElroy,W.N., et al., LWR Pressure Vessel Surveillance Dosimetry Improvement Program

/II,397/ Norris,E.B., W.Schneider, Report on Workshop on LWR Pressure Vessel Surveillance in Practice and Irradiation Experiments

/II,407/ Alberman, A., M.Faure, et al., Expérience de dosimétrie 'DOMPAC'

/II,448/ Prillinger, G., K. Almalah, G.Hehn,G.Pfister, Assuracy of Neutron Spectrum Calculations for Prediction of Radiation Damage in PV Steel

/II,493/ Verbinski, V.V., et al., Effects of Photoreactions on Neutron Dosimetry for Reactor Pressure Vessel Lifetime Studies

/II,623/ Schneider,W., Remarks on Accuracies in Neutron Metrology

/II,1275/ Till, H., Neutron Radiometric and Calculation Benchmarking for LWR PV Radiation Effects

/IV,147/ McElroy,W.N., et. al., Spectral Characterization by Combining Neutron Spectroscopy, Analytical Calculations, and Integral Measurements

/IV,233/ Fabry, A., W.N.McElroy, et al., Review of Microscopic Integral Cross Section Data in Fundamental Reactor Dosimetry Benchmark Neutron Fields

/V, 285/ Bartholome,G., J.M.Cerles, Ch.Leitz, G.Nagel.W.Schneider, P.Soulat, Neutron Fluence Determination and Safety Analysis Aspects of Large Specimen Steel Irradiations

/V,1093/ Anderson, S.L. Characterization of the neutron environment

/V,1123/ Odette, R., Dudey, N., McElroy,W.N., Wullaert, R., Fabry,A., Application of Advanced Irradiation Analysis Methods to LWR Pressure Vessel Test and Surveillance Programs

/VIII-A,19/ Serpan, C.Z.Jr., Engineering damage cross sections

/1/ McElroy, W.N., et al., LWR Pressure Vessel Surveillance Dosimetry Improvement Programm - 1979 Annual Report NUREG/CR-1291 (1980)

/2/ Issler, L., Stand des Forschungsvorhabens Komponentensicherheit. Vortrag Nr. 9 im 5. MPA-Seminar 11./12.10.1979, Materialprüfanstalt Universität Stuttgart

/3/ Kass,J.N., et al., Radiation Effects in Boiling Reactor Pressure Vessel Steels. NEDO-21708, 77 NED 168 (1977)

/4/ Alberman, A., J.P. Genthon, et al., Introduction of Neutron Metrology for Reactor Radiation Damage. EUR 6182 (1978)

/5/ Nagel,G.,Schneider,W., Discussion of Uncertainty Statements after CAPRICE 79 Meeting. IAEA Specialists Meeting on Reliability Engineering and Lifetime Assessment of Primary System Components, Vienna, 1-3 Dec. 1980

/6/ Canonico, D.A., Transition Temperature Considerations for Thick-Wall Steel Nuclear Pressure Vessels Nucl.Eng.Design 17, 149-160 (1971)

/7/ Dorner, H., E.Sommer,Theoretische Grundlagen des Bruchverhaltens. 1.MPA-Seminar,Stuttgart,Germany F.R. (1975)

/8/ Nagel,G., Effect and possibilities of irradiation results error corection (demonstrated on the resutls of the IAEA Co-ordinate Programme) 9th ASTM Symposium on Effects of Radiation on Structural Materials, Richland, WA,USA, 11-13 July,1978

/9/ Serpan, C.Z.Jr., B.H. Menke, Nuclear Reactor Neutron Energy Spectra. ASTM Data Series Publications DS 52. ASTM, Philadelphia, Pa., USA (1974)

/10/ Genthon, J.P., B.Hasenclever, et al., Recommendations on the Measurement of Irradiation Received by the Structural Materials of Reactors.EUR 5274 d, e, f, n (1975)

/11/ Alberts, W.G., Various Concepts of Spectrum-Averaged Cross Sections for the Interpretation of Reaction Rates in Neutron Fields (in German), PTB-Mitteilungen 90 (1980), 265-268, Nr. 4.

/12/ Koban, J. (KWU Erlangen, Germany F.R.), personal communication (1980)

/13/ 4th Meeting of the International Working Group on Reliability of Reactor Pressure Components (IWG-RRPC). Vienna, 4-5 December 1980

/14/ Zijp,W.L., et al., Damage Cross Section Library (DAMSIG 77) ECN-36 (1978)

G.A.M.I.N. AND TUNGSTEN DAMAGE/ACTIVATION RATIO CORRELATIONS FOR IRRADIATION EFFECTS EVALUATION IN PRESSURE VESSEL STEELS

A. ALBERMAN, M. THIERRY
CEA, Centre d'études nucléaires de Saclay,
Service des piles,
Saclay

P. MAS, R. PERDREAU
CEA, Centre d'études nucléaires de Grenoble,
Service des piles,
Grenoble,
France

SUMMARY :

Computed iron and tungsten (W) d.p.a. damage cross-sections are very similar. Recently W detectors were implemented for direct damage fluence measurement in pressure vessels (P.V.) mock-ups : TRITON (Fontenay-aux-Roses) and OAK RIDGE reactors, as well as in dosimetry rigs for standard steel irradiations : MELUSINE (Grenoble).

The W detector response has been compared with calibrated graphite (G.A.M.I.N.) detectors or qualified spectrum computations. Fair agreement is obtained with d.p.a. model in standard locations. But this model must be adjusted for P.V. environment where higher damage/activation ratio are found. Consistency between both detectors shows that relative neutron damage effectiveness is enhanced below 1 MeV.

Metallurgical results on irradiated steels in MELUSINE confirm conservative damage analysis by these techniques.

I - INTRODUCTION.

For several years, the international dosimetry community has focused its efforts on damage analysis for pressure vessels steels. Two problems are of major importance from a dosimetry point of view. First, what is the best exposure parameter mainly for correlating irradiation results from different locations and also for safety reasons (evaluation of lead factors). Second, once the first step is achieved in cooperation with metallurgists [1], how this quantity can be measured with good accuracy. Apart from national programs in TRITON and MELUSINE, the Commissariat à l'Energie Atomique developed special devices in these two reactors respectively DOMPAC (P.V. simulator) [2] and PCBT (spectrum effects on impact tests) [3] and contributes [4] to the ORR-PSF surveillance dosimetry improvement program.

Tungsten (W) and graphite (GAMIN) / damage detectors feature in all these programs. Based upon electrical resistivity change after irradiation they provide experimental damage/activation ratios (DAR). This paper presents correlations obtained through the 2 techniques and derivation of effective damage energy threshold in tungsten which can be assumed representative for phenomena involved in irradiated metals [5]. Direct application is shown in available PCBT results.

II - DAMAGE DETECTORS.

Description of these detectors will not be mentioned here (see [5], [6]). We shall focus on DAR, directly proportional to their response (calibrated electrical resistivity change $\Delta R/R$ over $^{58}Ni(n,p)$ reactions per target atom) :

graphite DAR : $\phi_G^f / \phi_{Ni}^f = \alpha \cdot r$ $\qquad r = 10^{-7} \dfrac{\Delta R/R_{corr.}}{A_{Ni}}$

tungsten DAR : $\phi_{W_e}^f / \phi_{Ni}^f = \beta_e \cdot s$ $\qquad s = 10^{-5} \dfrac{\Delta R/R_{corr.}}{A_{Ni}}$

where ϕ_X^f is equivalent fission flux for reaction X [7] :

$$\phi_X^f = \frac{1}{\bar{X}^f} \int_0^\infty X(E)\, \varphi(E)\, dE$$

$\bar{X}^f$: averaged cross section over ^{235}U fission spectrum.

Definition worths for :

Nickel : ^{58}Ni (n,p) activation cross section

Graphite : d.p.a. damage function

Tungsten : d.p.a. damage function $W_e(E)$

Calibration factors (computed DAR/response) α and β_e must be constant in very different spectra in order to validate damage models. That is proved already for G.A.M.I.N. : best fit with THOMPSON-WRIGHT model [11] so $\alpha = 0.50 (\pm 0.01)$. Very recent results will now show how to derive β_e from $W_e(E)$ fitted to experiments.

III - CORRELATION BETWEEN GAMIN AND W RESPONSES.

Preliminary results presented [5] in customary spectra (ISIS, EL3, TRITON, FRJ2) have shown fair correlation between W response and computed d.p.a. model (UKNDL library), leading to calibration factor ($\beta = 0.247$). Latest results in steel environments are given in Table I. Relative error in measurements lies between 3-7% (1 σ).

Large steel volume environment increases tremendously damage responses of detectors. Remarkable consistency is found in "inside vessel" results (spectra 5,6,7,9,10) applying following law :

$$s = 1.69\ (r)^{0.88} \qquad \text{(Fig.1)}$$

Computed DAR rise exponential vs distance [2] and lead to such a "power law" correlation. Experimental W_e damage function should fit this law (0.88). Computed fit provides inferior values : UKNDL (0.75), ENDF IV (0.65) (Fig. 2). Therefore W damage efficiency is closer to graphite. Customary correlations are sufficient with W d.p.a. model for "hard" spectra ($s \lesssim 7$) but may underestimate damage up to 30 % in "softer" spectra.

Experimentally fitted W_e damage function is underway now but it appears already that on average

$$W_e \,/\, W_{d.p.a.} \begin{cases} \approx 2 & E < 1 \text{ MeV} \\ \approx 1 & E \geqslant 1 \text{ MeV} \end{cases}$$

leading to a constant calibration factor $\beta_e = 0.29$ ($1\,\sigma = 5.5\%$)

N°	Reactor	Spectrum	GAMIN : r	TUNGSTEN : s	Réf.
1	MELUSINE	Standard steel irradiation	-	5.39	[8]
2	"	PCBT - Special device	-	11.04	
3	TRITON	Standard steel irradiation	3.62	-	[9]
4	"	DOMPAC Surveillance pos.	3.40	6.29	[2]
5	"	" PV (1.5 cm depth)	3.86	5.53	
6	"	" 1/4 T	4.94	6.86	
7	"	" 1/2 T	6.81	9.84	
8	O.R.R.	P.S.F. Surveillance pos.	7.00	8.48	[4]
9	"	" 1/4 T	9.24	11.78	
10	"	" 3/4 T	24.16	27.60	

Table I - GAMIN and W responses in various PV-Steel environments

For steel DAR :

$$\phi^f_{Fe} / \phi^f_{Ni} = 0.96 \, (\phi^f_{W_e} / \phi^f_{Ni})^{0.77} = 0.37(S)^{0.77}$$

best fit for all spectra.

Effective damage thresholds : $\phi^f_{W_e}$ $\begin{cases} \approx \phi \ (E > 0.27 \text{ MeV}) & \text{PV mock-ups} \\ \approx \phi \ (E > 0.20 \text{ MeV}) & \text{else} \end{cases}$

when $\phi^f_G \approx \phi \ (E > 0.075 \text{ MeV})$ all spectra

IV - INTERPRETATION OF STEEL IRRADIATIONS IN MELUSINE.

Embrittlement studies were performed [3], on A 508 class 3 PV steel with high Cu contents and at 235°C. This choice was made to increase radiation effects and avoid excessive in-pile time. Sets of 27 Charpy V specimen were irradiated in each of 2 differents positions (Fig.3) :

. standard reflector rig,

. PCBT special inside a steel block.

Computed spectra (Fig.4) show enhanced contribution below 1 MeV in PCBT device - Fluences ($E > 1$ MeV) attained were fairly close : 7.6 and $9.1.10^{18}$ $n.cm^{-2}$ (measurements through Cu and Fe monitors).

Spectrum indices were studied [8], implementing threshold reactions on ^{115}In, ^{47}Ti, ^{58}Ni, ^{54}Fe, ^{63}Cu, ^{27}Al, ^{48}Ti, ^{93}Nb, ^{237}Np, ^{238}U as well as W detectors. Consistency with computed DOT 3.5 code indices was proved. Neutron and damage fluences respective to transition temperature shifts are given in Table 2.

	ϕ_{Fe} ($\bar{\sigma}$ = 79,7 b) $10^{18} n.cm^{-2}$	ϕ (>1 MeV) $10^{18} n.cm^{-2}$	ϕ (>0,1 MeV) $10^{18} n.cm^{-2}$	$\phi^f_{W_e}$ $10^{18} n.cm^{-2}$	D.P.A. (STEEL)	PROBABLE ZONES MODEL	ΔTT
STANDARD POSITION	9.35	7.6	16.3	15.8	$1.025\ 10^{-2}$	$1.16\ 10^{-4}$	83,5°C
PCBT SPECIAL	5.9	9.1	39.2	22.6	$1.57\ 10^{-2}$	$1.96\ 10^{-4}$	119°C
SPECIAL / STANDARD		1.2	2.41	1.423	1.532	1.682	1.425

Table 2 - MELUSINE irradiation effects and fluences

Special / standard ratio show good agreement with W exposure parameter assuming linear dependance of ΔTT with fluence. Though generally expected effects should vary as $(\phi)^{1/n}$ with $2 < n < 3$ [10] (in this case ϕ (>0.1 MeV) is the best fit), one can but call for more metallurgical tests in broader fluence ranges.

V - CONCLUSION.

Presented results call attention on 3 points :

1) Damage detectors are consistent in PV steel dosimetry.

2) Determination of the best exposure parameters : in what extent theoretical d.p.a. model for steel is reliable when both damage detectors (light and heavy metals) show lower effective damage threshold ?

3) What amount of work still need to be made in order to deliver a consistent set of experimental damage cross sections (for all available detectors) ?

R E F E R E N C E S

[1] CAPRICE 79 - IAEA Technical Meeting, Julich, September 1979
Ed. by W. SCHNEIDER - Julich Conf.37 (1980)

[2] A. ALBERMAN, J.C. NIMAL "DOMPAC Experiment"
in CAPRICE 79 (Ibid)

[3] P. MAS, R. PERDREAU, P. TRAN DAI "Influcence of neutron embrittlement ...
in CAPRICE 79 (Ibid)

[4] A. ALBERMAN, M. BENOIST, M. THIERRY "Mesure des flux de dommages dans le simulateur de cuve PWR d'OAK RIDGE (ORR-PSF)"
to be presented in 4th ASTM-EURATOM Symposium on reactor dosimetry
Washington, March 1982

[5] A. ALBERMAN, J.P. GENTHON and coll. "Le détecteur miniaturisé au tungstène" CEA.CONF.4734
in Proc. 3rd ASTM-EURATOM Symposium on reactor dosimetry, Ispra, 1979

[6] J.P.GENTHON, B.T. KELLY, S.B. WRIGHT "Irradiation flux characteristics in DIDO type reactors"
Nucl. Inst. and Methods 131, 1 (1975)

[7] J.P. GENTHON, B.W. HASENCLEVER and coll. "Recommandations on measurements ..." EUR.5274 (1974)

[8] P. MARCONE "Caractérisation d'emplacements d'irradiation en reacteur d'essais au moyen de détecteurs fissiles et de détecteurs de dommages"
Thèse de 3ème cycle - Octobre 1980

[9] P. PETREQUIN, P. SOULAT "Etude de la fragilisation des aciers de cuve ..." in Reliability problems on reactor pressure components 10-14 Oct. 1977, Vienne IAEA SM 218/21 (1978)

[10] A.D. AMAYEV, N.F. PRADYUK "The effect of neutron irradiation on the embrittlement on reactors vessels steels" Atomizdat p. 241 (1968)

[11] J.P. GENTHON, J.C. NIMAL, F. VERGNAUD "Détermination des flux de dommages... in Proc. 1st ASTM-EURATOM on reactor dosimetry PETTEN (1975)

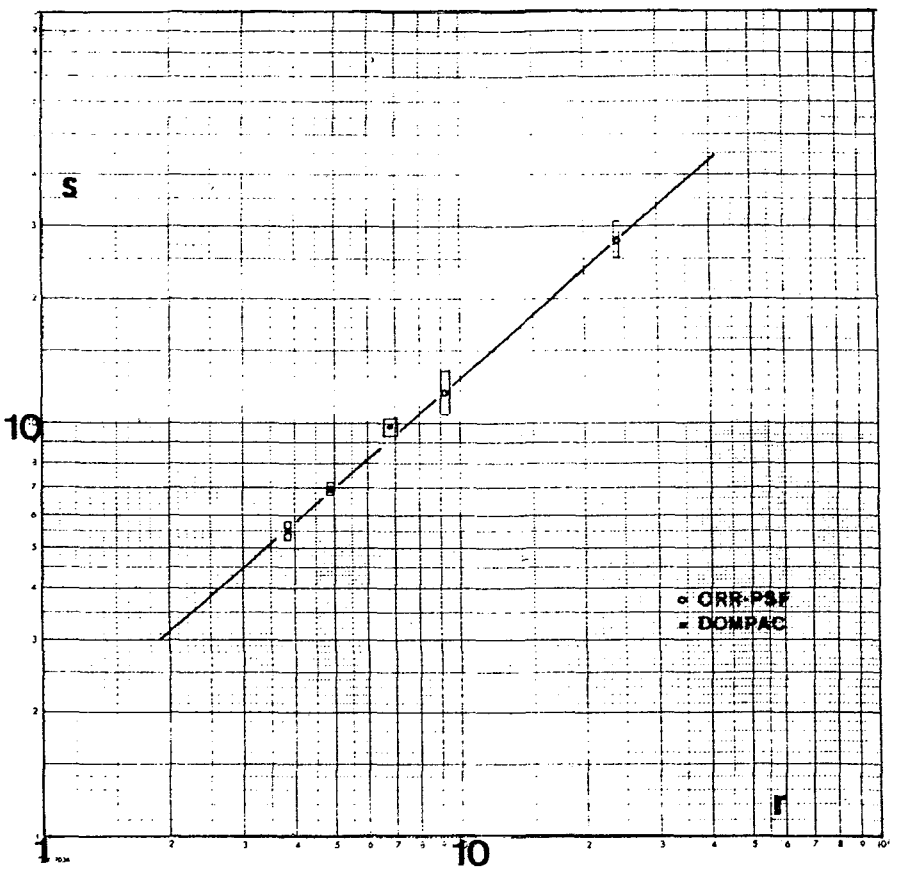

Fig. 1 - Tungsten / GAMIN responses in P.V. mock-ups

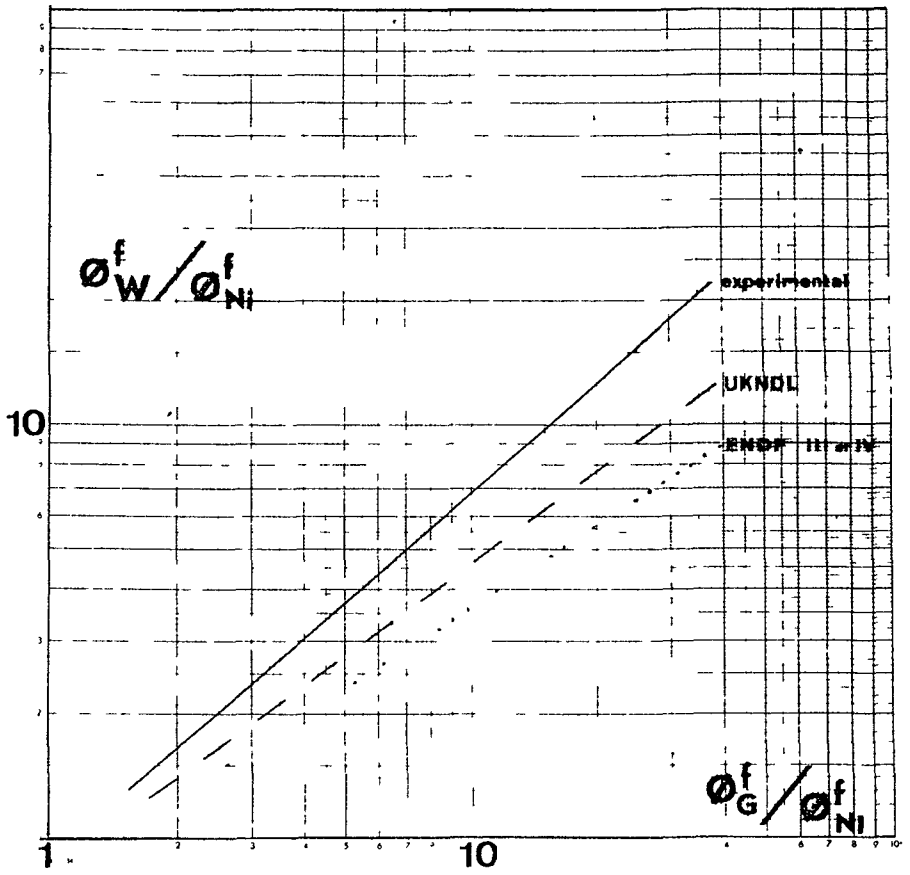

Fig. 2 - Tungsten DAR / Graphite DAR correlation in P.V. mock-ups

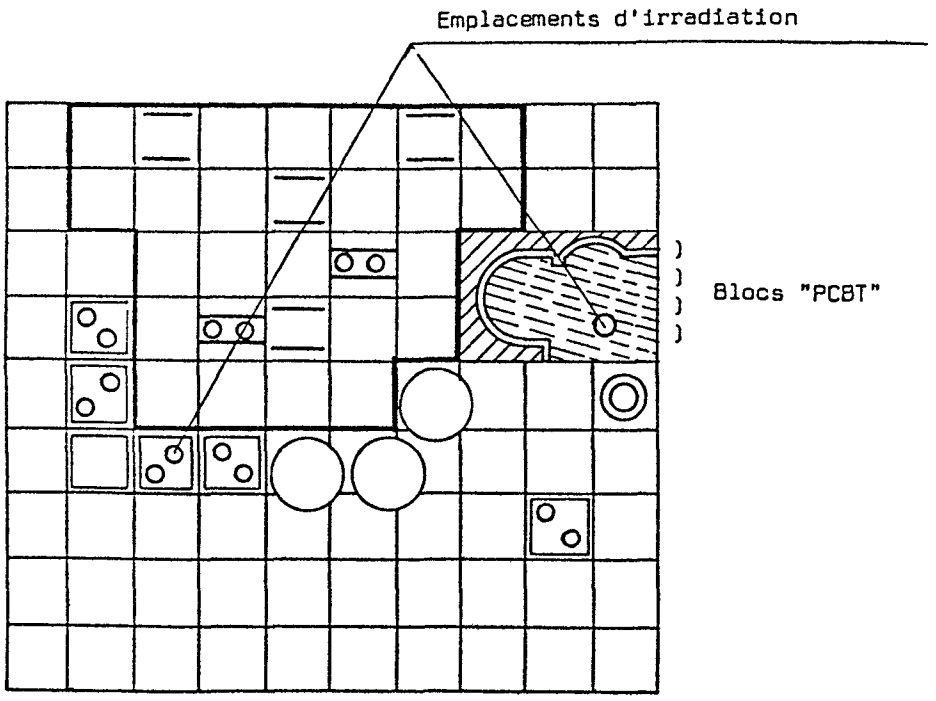

Fig. 3 - MELUSINE steel positions

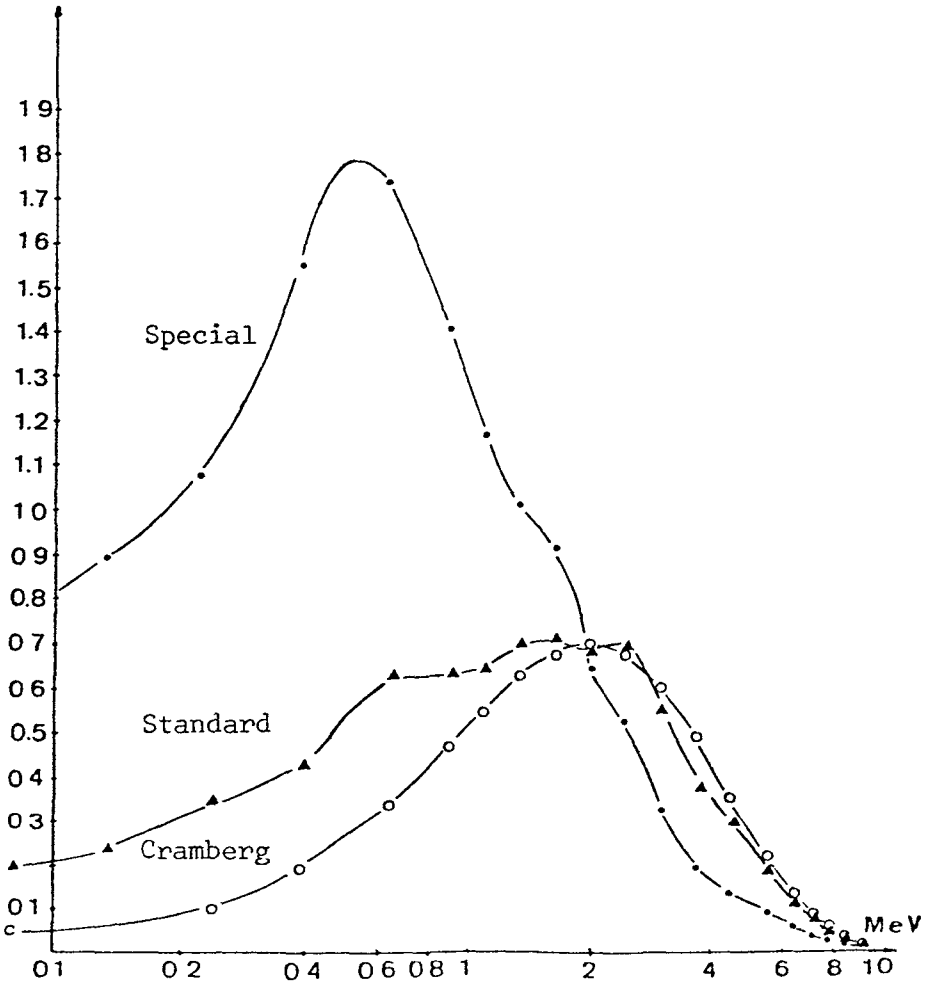

Fig. 4 - Computed spectra in standard and PCBT positions

FIRST RESULTS OF THE REAL-80 EXERCISE

W.L. ZIJP*, C. ERTEK†, É.M. ZSOLNAY+,
E.J. SZONDI+, H.J. NOLTHENIUS*, D.E. CULLEN†
*Netherlands Energy Research Foundation ECN,
Petten,
Netherlands

†International Atomic Energy Agency,
Vienna

+Nuclear Reactor of the Technical University,
Central Research Institute of Physics,
Budapest,
Hungary

SUMMARY

This report presents some preliminary results of the first phase of the interlaboratory exercise REAL80 to study uncertainties in integral parameters (such as displacement rate per atom steel, activation rate per atom nickel), derived from spectrum information obtained by means of activation spectrometry of well defined test cases.
More balanced and extended results will be presented at the 4th ASTM-Euratom Symposium on Reactor Dosimetry, Washington, D.C., 22-26 March 1982.
In this first report attention has also been given to the nuclear data aspects of the exercise.

1. BACKGROUND

In the concluding session of the third ASTM-Euratom Symposium on Reactor Dosimetry (held at Ispra, 1-5 October 1979) there was warm support for the suggestion to organize a follow-up of the previous international activities on the intercomparison of unfolding codes. It was felt that such a study should pay particular attention to the uncertainty of integral parameters (displacement rates and activation rates), derived from neutron flux density spectrum information (based on experimental activation rates) by an unfolding procedure.
The IAEA was invited to organize the action and to complete it in a very tight time schedule.

2. PROJECT NAME

The exercise has received the code name REAL-80 (Reaction Rate Estimates, Evaluated by Adjustment Analysis in Leading Laboratories).

3. AIM

The aim of the REAL-80 exercise is to arrive at a realistic value for the uncertainty in integral radiation damage parameters (like the displacement rate), when such a value is derived by means of existing unfolding procedures. The conditions should be well defined and well chosen with respect to input values (comprising values, variances and covariances for the flux densities, activation and damage cross-section data, and experimental activation rates). For instance, the exercise should give answers to questions like:

1. What is the quality of the neutron spectrum derived by different existing unfolding/adjustment procedures?
2. What is the quality of an integral damage parameter, like the number of displacements per atom (dpa), derived with aid of the adjusted spectrum?
3. What is the quality of a predicted activation rate?

The exercise should be performed within a period of two years, so that the results will be available for discussion at the 4th ASTM-Euratom Symposium (to be held at Washington, D.C., 22-26 March 1982).

It is emphasized that the outcome of the exercise will reflect the state-of-the-art in 1980 of the capabilities of laboratories, in deriving values and uncertainties for the predicted number of displacements. All participating laboratories should use their own existing practices.

4. ORGANIZATION

The REAL-80 exercise is organized by the IAEA in Vienna, under the joint responsibility of the IAEA Seibersdorf laboratory (responsible officer Dr. C. Ertek) and the IAEA Nuclear Data Section (responsible officer Dr. J.J. Schmidt). W.L. Zijp (ECN, Petten) acted as consultant.
The analysis of the numerical results of this exercise is performed by the IAEA Nuclear Data Section with the collaboration of the Budapest Technical University and the Petten research centre.

5. CONTENTS OF THE FIRST PHASE OF REAL-80

Since the time schedule was too tight to prepare the required covariance information for the cross-section data and the envisaged reactor neutron spectra, it was decided mid 1980 to start with a first phase, dealing with only two neutron spectra, for which detailed information became available in time.
Input information for the ORR spectrum comprising 19 reaction rates (12 reaction rates without cover and 7 reaction rates inside a cadmium cover) was kindly supplied by Dr. L.R. Greenwood (ANL).
Input information for the YAYOI spectrum, comprising 12 reaction rates, was kindly supplied by Dr. M. Nagazawa (Tokyo), supplemented with information from Dr. Greenwood.

In February 1981 the IAEA distributed magnetic tapes with input data required in the exercise together with an information sheet to some prospective 30 participants all over the world.
The participating laboratories were asked to perform the following actions:

- adjust (unfold) the two reactor neutron spectra for the ORR and the YAYOI reactors and make statements, if possible, on the uncertainties and the correlations for the group flux densities;
- calculate the activation rate of nickel, using the cross sections of $^{58}Ni(n,p)^{58}Co$, and also the standard deviation in this value;
- calculate the damage rate in iron, using the damage cross-section data supplied (based on an ASTM-standard), and also the standard deviation in this value;
- report to the IAEA in a prescribed format, preferably within two months after receipt of the IAEA tape.

6. REVIEW OF THE RESPONSES

At the end of August 1981 35 solutions were received from 8 different laboratories. The names of the participants and the adjustment codes used are listed in appendix 1. Solutions received after 15 August 1981 could not yet be taken into account during the preparation of this document.
The IAEA assigned a code number and checked the formats on transmission errors etc.
Then the information was passed to the other two analysing laboratories (Budapest and Petten).
These laboratories had the following tasks for a brief survey of the first results:

- The Budapest Technical University for compiling information on participants answers and for checking the information from a physics point of view, such as
  - number of SAND-II, STAY'SL, etc. responses;
  - completeness of data and error information;
  - group structure;
  - adjustment conditions (convergence criteria, etc.);
  - quality of covariance information.
- The ECN for preparing a survey on the comparison, comprising
  - characteristic values such as the ϕ_{total}, $\phi_{>1MeV}$, $\phi_{>0,1MeV}$;
  - DAR values for aluminium and steel with nickel as activation reaction;
  - values of the average relative deviations;
  - comparison of output spectra;
  - preparation of relevant tables and figures.

In the tables in this report only the IAEA code will be applied to denote the separate solutions.

The deviations from the output format prescribed by the IAEA have been corrected where necessary, and are not mentioned here. Some mistakes have been detected, and most of them could be corrected easily. In general the format for the transmission of the output data worked quite well, so that computer treatment of the results was rather easy.
From the first results it became clear, that a more stringent description of the format is useful, when the second phase of the exercise is started.
The analysis of the data received is not yet finished. Moreover it is expected that the IAEA will receive some more solution spectra.
Some groupings of the 35 solutions are listed in table 1.
Some characteristics of the solutions received from the various laboratories are given in table 2.

7. THE INPUT SETS FOR THE FIRST EXERCISE

The input neutron spectrum, the group cross-section and the input reaction rates with their uncertainties in the form of variance-covariance matrices were completely described for the three input contributions.
One input set was derived for the Oak Ridge Research Reactor. The spectrum is a typical thermal spectrum with a predominant 1/E part.
The other set was derived for the central region of the YAYOI reactor. This is a fast reactor with a relatively hard neutron spectrum.
For the latter spectrum 12 reaction rates could be applied in the input set, and for the ORR set 19 reaction rates were available.
The input neutron spectrum for the ORR was calculated with a transport theory code.
The thermal part was derived with an extrapolation procedure.
The calculation was performed using 100 groups and a cross-section library mainly based on the ENDF/B-V file.
The input spectrum for the YAYOI reactor was calculated with the one-dimensional ANISN code, with 39 groups. In this code the cross-section library ENDF/B-III was applied.
The quality of the neutron spectra is to be considered as reasonable because of the assumptions made in both calculations (model, homogenization, groups, etc.).
The codes didn't yield directly the variance-covariance matrices.
For this reason Dr. L.R. Greenwood developed correlation matrices which are suitable for this exercise.
The cross-section data as well as the neutron spectra were converted to a 100-groups structure. This 100-groups structure is suited for most of the adjustment codes.
The primary source of the input cross-section data was the ENDF/B-V dosimetry file. The group cross-sections had to be corrected in a number of cases for neutron selfshielding and for the cadmium cover.

For this reason fine structure cross-sections were corrected and then collapsed to the 100-groups structure.
A variant of the input set for both spectra consists of the same information except that a cross-section library in 620 groups is applied. However for the cross-section data in 620 groups the relevant information on necessary corrections is lacking.

8. PROBLEMS WITH INPUT DATA

The following problems encountered in preparing and gathering the input data for the REAL-80 exercise are worthwhile to be mentioned here.

8.1. Consistency of ORR input data

During the preparation of the ORR input data it turned out, that the values for input activities, the input cross-sections, and the input spectrum as a whole are not in accordance with their stated variances and covariances. This inconsistency can be detected by a message from the STAY'SL code that the relevant chi-square value is unlikely small. At present it is not clear to which extent this situation has influenced the results of the intercomparison.

8.2. Choice between two cross-section sets

The participants had the freedom to use either the 620 groups data, or the 100 groups data. Unfortunately the information sheets on the exercise were not clear enough on the point that substantial differences might be present between the two input cross-section sets provided on the tape. As stated before, only the 100 groups data contained corrections for selfshielding and for the cadmium cover.

8.3. The 620 group cross-section data

During the preparatory phase it was discovered that there were some non-negligible discrepancies between two sets of 620 group cross-section data, derived from the ENDF/B-V dosimetry file by two different laboratories using quite different computer codes for this conversion. At the end of August 1981 an advance copy was made available of the modified ENDF/B-V dosimetry file. The 620 group cross-section data set derived from this file was also made available by BNL. A quick comparison between this data set from BNL and a data set derived from the modified file by another computer program showed that if the numerical accuracy is taken into account, no discrepancies remain.

8.4. Absence of covariance data

It has to be noted, that physical information on the covariances between activation rates, between group flux densities and between group cross-

section data was practically completely absent; only the covariance data for the input reaction rates for YAYOI was based on experimental information. Since correlation matrices had to be specified in the exercise, some data had to be generated by careful consideration. In some cases the correlation between group values was described with aid of a gaussian function.
One should realize that there is an interconnection between the element values in the covariance matrices and the (in)consistency of the whole set of input data.

8.5. The displacement cross-section data

The ASTM standard procedure E693-79 refers to the calculation of displacement in ferritic steel (iron). The values of the displacement cross-section are based on ENDF/B-IV cross-sections, the Lindhard model of energy partition between atoms and electrons, and the IAEA recommended conversion of damage energy to displacements. In the ASTM model it is assumed that the displacement cross-section for iron is an adequate approximation for ferritic steel.
In the REAL-80 input data set these cross-section values in the 620 groups structure have been coded as ASTM-DISPL-STEEL.
In the Euratom Working Group on Reactor Dosimetry values have been derived for the displacement cross-sections in stainless steel (with the following composition in mass per cent: 74% Fe, 18% Cr, and 8% Ni), based on elastic and inelastic cross-section values published by M. Lott et al. in 1973. In the REAL-80 input data set these data have been coded as EUR-DISPL-STEEL.
Some small differences may be expected between the values according to the ASTM standard and the Euratom practice, due to different compositions of the steel, due to different origins for the cross-section data set, and the different group structures (in combination with conversion procedures for group values).
A rough quantitative comparison of both cross-section curves showed appreciable local differences. The spectrum averaged cross-sections differ however less than 2,5 per cent. The uncertainties of the displacement cross-section values were arbitrarily chosen to be equal to 15 per cent. It was proposed to use a Gaussian approximation with a fixed width for the correlations between group values.

9. GENERAL OBSERVATIONS ON ADJUSTMENT CONDITIONS

On the basis of the solutions which could be considered up till now we came to the following findings.

9.1. Unfolding codes

A relatively large number of solutions is based on an adjustment code of the SAND-II type. Four distinct versions of this code have been

identified: SAND-II, SANDBP, SANDMX, and SANDPET. Literature references for a few codes (two SAND-IL versions, NEUPAC and LSL) were not available. Only a few laboratories have prepared solutions with more than one code. Results with NEUPAC seem to be very similar to the results of STAY'SL.

9.2. Number of groups

The number of energy groups used in the adjustment procedure was 100 in about half of the cases, while only some results were presented in the 620 groups structure. This situation is probably due to the advice given by the IAEA to the participants. This advice was based on the fact that the 100 groups cross-section data set was already modified to take into account the effect of selfshielding of the foils and the presence of cadmium cover. The 620 groups cross-section data had not been modified, and were not accompanied by the necessary correction factors.

9.3. Number of solutions

The definition of the exercise allowed the participants to prepare more than one solution for the same problem. As a result in some cases several solutions were given, either with more than one adjustment code, or with the same code under different conditions (deletion of one or more reaction rates; use of more than one group structure).

9.4. Special group structures

Sometimes solutions were based on a group structure different from the 620 groups or the 100 groups of the input specification. In these cases the conversion procedure (with interpolation and extrapolation schemes) were not specified by the participants. This means that the input data for these special group structures may not have unambiguous values. This implies that systematic effects and deviations might have been introduced by the participants choice of an own group structure.

9.5. Effect of group structure

One participant gave for one code three solutions for three different group structures (50, 20, and 10 groups). It was observed that these three solutions gave slightly different numerical results.

9.6. Convergence criteria

The convergence criteria are not the same for the different adjustment codes. And for the same type of codes the numerical values are in general different.

As common convergence parameter in the analysis of the participants data the so called Average Relative Deviation (ARD) seems best suited.

This parameter is defined as

$$ARD = \left\{ \sum_{i=1}^{n} \left[(\alpha_i^m - \alpha_i^c) / s_i^m \right]^2 / n \right\}^{\frac{1}{2}}$$

where n = number of input reaction rates;

α_i^m = measured (input) reaction rate;

α_m^c = calculated reaction rate, using the solution spectrum;

s_i^m = estimated uncertainty of the difference between α_i^m and α_i^c.

The numerical values are given in table 4. This table shows also values for the standard deviation of the reaction rates, called DEV

$$DEV = \left\{ \sum_{i=1}^{n} \left[(\alpha_i^m - \alpha_i^c) / \alpha_i^c \right]^2 / (n-1) \right\}^{\frac{1}{2}} .$$

9.7. Standard deviation

The standard deviation was suggested to the participants as measure for the uncertainty to be reported.
At least one case was identified where the participant did not report the standard deviation of individual observations, but the standard deviation of the mean value (which is a factor $\sqrt{n}$ smaller). In many cases uncertainty information given by the participants was very poor.

9.8. Correlation data

Not always information was supplied on the calculation procedure for the covariance data (or the related correlation matrices). The information originated sometimes from the properties of the least squares principle, and sometimes from Monte Carlo variations applied in accordance with the input standard deviations.
It turned out that the patterns of the correlation matrices based on the STAY'SL least squares approach and based on Monte Carlo variations using the SAND-II approach were significantly different (see figures 6 and 7). This finding is not yet completely understood and requires further study.

10. NUMERICAL COMPARISON OF OUTPUT DATA

10.1. Rough comparison of output spectrum shapes

The information contained in the output spectra was converted to group fluence rate values in 12 energy decade regions, and compared with the corresponding information for the two input spectra. In this way a rough comparison was made.

The numerical data are given in table 4. A few discrepant solutions inflated the coefficients of variation for some group flux densities in an appreciable way (see also fig. 5).
The choice of 12 decade groups was rather arbitrary and was based on available software features. Probably this choice is not an optimal one.
It is to be noted that the two groups 0 ... 1 MeV and 1 ... 10 MeV had the smallest coefficients of variation. This is of course the region where one has the responses from all threshold reactions.

10.2. Output covariance information

Only three of the adjustment codes used by the participating laboratories (i.e. STAY'SL, NEUPAC, and SANDBP) provided information on the correlation between the output group flux densities. The covariance information was made available in the form of correlation matrices.
The covariance data supplied by the codes STAY'SL and NEUPAC indicate a close similarity in the algorithm of these programs.
Appreciable differences were observed in the correlation matrices obtained by means of the codes STAY'SL and SANDBP. The correlation data were derived in a deterministic way by the program STAY'SL, while in case of SANDBP a Monte Carlo variation method was used.
The perspective plots of the correlation matrices for the STAY'SL output spectra (see figures 6 and 7) show no correlation for energy groups far from each other. On the other hand, the program SANDBP gives solutions with very strong correlations in the resonance energy region. This effect is clearly observed for the YAYOI spectrum, where the 90% response regionsof the detectors in the set always cover partly or wholly the energy region above 0,1 MeV. (See figure 1).

10.3. Fluence rate values

Of interest are the following fluence rate values: ϕ_{tot}, $\phi_{>1MeV}$, and $\phi_{>0,1MeV}$, which can be derived from the input data. A summary of the data based on the information supplied by the participants is given in table 3, where absolute values are given for the two input spectra, and values for the output spectra, relative to the corresponding input spectrum.
At present it is not clear whether the choice between the 100 and 620 groups input cross-section data sets has influence on the results. Neglecting a possible effect in this sense, we calculated coefficients of variation: the numerical values are listed at the bottom of the lists in table 3. Remarkable is that some values show an appreciable discrepancy. The origin of the discrepancies has not yet been studied.
A check showed that the fluence rate values supplied by the participants are generally in accordance with the data for the output spectra.

10.4. Activation rates in nickel

The values as derived by the participants are also shown in table 3. Noteworthy is that two values derived by means of one particular code are nearly twice the value found with all other codes; this applies however only for the ORR spectrum case.

10.5. Displacement rates in steel

No large discrepancies have been observed. The values calculated for the YAYOI output spectra are roughly 20% higher than for the input spectrum.

11. GENERAL CONCLUSIONS AND RECOMMENDATIONS

Although not all responses from the participating laboratories could yet be taken into account, and although the analysis of the numerical data has only just started, we have tried to formulate, tentatively, some preliminary conclusions and recommendations.

11.1. With respect to the interpretation of the results for the ORR spectrum, one should bear in mind that the whole set of input data was not optimal with respect to the consistency of the data. A study of the effect of (in)consistency of the input data on the output has still to be made.

11.2. The spectral shapes of the output spectra show considerable spread, both for the thermal ORR spectrum and for the fast YAYOI spectrum. The integral spectrum parameters, such as $\phi_{>1MeV}$ and $\phi_{>0,1MeV}$, show much less variation.

11.3. The predicted displacement rates in steel show more convergence than the predicted activation rates in nickel. This may suggest that one has to be very careful in deriving calculated displacement rates from the experimental response from only one (nickel) threshold activation detector and supplementary spectrum information.

11.4. With respect to the predicted activation rate in nickel we arrived, when taking into account all responses, at a coefficient of variation of 25 per cent for the ORR spectrum and of 10 per cent for the YAYOI spectrum. When the outlying values for one code for the ORR spectrum are deleted, one obtains a coefficient of variation of about 2 per cent.

11.5. For the predicted displacement rate in steel we observed a coefficient of variation of 7% for the ORR spectrum and of 2,5% for the YAYOI spectrum.

11.6. The coefficient of variation for the activation rates in nickel and the displacement rate in steel derived from the sets of responses were of the same order of magnitude as the largest uncertainties quoted by some participants.

11.7. The pattern of the correlation matrix for the output spectrum derived in a deterministic way with the STAY'SL code is clearly different from the patterns of the correlation matrix derived in a stochastic way with Monte Carlo variations using the SAND-II algorithm, without making strict assumptions for the covariance matrix of the input spectrum. Further study is required to have a good understanding of the background for these different patterns.

11.8. The input cross-section data for the ORR in 100 groups were already corrected for selfshielding and the presence of a cadmium cover. The input cross-section data in 620 groups were not corrected for these effects. For this reason it was recommended to use preferably the 100 group cross-section data set.
In the near future the problems of selfshielding and the influence of cadmium covers have to be considered in detail. The IAEA is advised to promote such a study.

11.9. An intercomparison should be made on conversion procedures for processing of evaluated data to multigroup forms. The IAEA is advised to organize such an intercomparison.

11.10. The second phase of REAL-80 will be discussed with experts during the 4th ASTM-Euratom Symposium on Reactor Dosimetry, to be held at Washington D.C., March 1982.
Tentatively the authors recommend that a second phase should be started in 1982, and should comprise adjustment of the ^{252}Cf fission neutron spectrum and of a CTR type neutron spectrum.
The conditions for the second phase should be similar to those for the first phase.
If the experts consider such a second phase highly desirable, then it seems necessary that the IAEA gives support in organizing the follow-up of REAL-80, in order to have a good implementation of the ideas.

12. ACKNOWLEDGEMENTS

The cooperative contributions from Dr. L.R. Greenwood (ANL), G.C.H.M. Verhaag (ECN), and K. Lewis (IAEA) are gratefully acknowledged.

Table 1. Groupings of REAL-80 solutions.

viewpoint	ORR spectrum	YAYOI spectrum
number of solutions considered	18	17
. in 100 groups	7	9
. in 620 groups	4	1
. in other structure	7	7
. without uncertainties	10	8
. with uncertainties only for spectrum	4	4
. with uncertainties for spectrum and reaction rates	4	5
. without correlations	13	10
. with correlations only for spectrum	4	6
. with correlations for spectrum and reaction rates	1	1
. SAND-II, SANDBP, SANDPET, SANDMX	7	5
. STAY'SL	2	2
. CRYSTAL BALL	1	1
. WINDOWS	2	2
. LOUHI-78	2	1
. NEUPAC	1	3
. LSL	3	4

Table 2. Information on the solutions.

	IAEA code	no.	presentation neutron spectrum: number of groups or points	presentation neutron spectrum: form	presentation neutron spectrum: interp. data a)	st.dev.spec	st.dev.char	cor.matrix spectrum	remarks
ORR spectrum	001BB	1	620	$\phi_E(E)$	1	Y	Y	-	40 iterations
	003EB	2	40	$\phi_E(E)$	2	Y	-	-	-
	005EB	3	40	$\phi_E(E)$	2	Y	-	-	smoothing?
	006AB	4	100	$\phi_E(E)$	1	Y	-	Y	-
	008FB	5	100	$\phi_u(E)$	-	Y	Y	Y	-
	011AA	6	100	$\phi_g(E)$	-	Y	-	Y	cor. matrix of integral data
	013BA	7	100	$\phi_E(E)$	-	-	-	-	-
	015BC	8	100	$\phi_E(E)$	-	Y	Y	Y	FE58GC deleted, 5 iterations
	018BD	9	621	$\phi_E(E)$	5	-	-	-	AU1972N deleted, 4 iterations
	019BD	10	100	$\phi_E(E)$	5	-	-	-	AU1972N deleted, 12 iterations
	020BD	11	621	$\phi_E(E)$	5	-	-	-	AU1972N deleted, 6 iterations
	021BD	12	621	$\phi_E(E)$	5	-	-	-	AU1972N deleted, 6 iterations
	023CA	13	100	$\phi_E(E)$	-	-	-	-	3 iterations
	031HA	14	20	$\phi_g(E)$	-	Y	Y	Y	-
	032HA	15	10	$\phi_g(E)$	-	-	-	-	-
	033HA	16	50	$\phi_g(E)$	-	-	-	-	-
	034GA	17	20	$\phi_g(E)$	-	-	-	-	AU1972N deleted
	035GA	18	20	$\phi_g(E)$	-	-	-	-	AU1972N, U238G, U235F, FE58G deleted

	IAEA code	no.	presentation neutron spectrum: number of groups or points	presentation neutron spectrum: form	presentation neutron spectrum: interp data	st.dev.spect.	st.dev.char.	cor. matrix spectrum	remarks
YAYOI spectrum	Y02BB	1	620	$\phi_E(E)$	1	Y	Y	-	40 iterations
	Y04EB	2	40	$\phi_E(E)$	2	Y	-	-	-
	Y07AB	3	100	$\phi_E(E)$	1	Y	-	Y	-
	Y09FB	4	100	$\phi_u(E)$	-	Y	Y	Y	NI58P used
	Y10FB	5	100	$\phi_u(E)$	-	Y	Y	Y	NI58P used
	Y12AA	6	100	$\phi_g(E)$	-	Y	-	Y	cor. matrix of integral data
	Y14BA	7	100	$\phi_E(E)$	-	-	-	-	-
	Y16BC	8	100	$\phi_E(E)$	-	Y	Y	Y	4 iterations, TI47P deleted
	Y17BC	9	100	$\phi_E(E)$	-	Y	Y	Y	6 iterations, TI47P deleted, 5 points smoothing
	Y22BD	10	100	$\phi_E(E)$	5	-	-	-	12 iterations
	Y24CA	11	100	$\phi_E(E)$	-	-	-	-	4 iterations
	Y25HA	12	20	$\phi_g(E)$	-	Y	-	Y	-
	Y26HA	13	20	$\phi_g(E)$	-	-	-	-	reduced weight for TI47P
	Y27HA	14	10	$\phi_g(E)$	-	-	-	-	-
	Y28GA	15	50	$\phi_g(E)$	-	-	-	-	-
	Y29GA	16	20	$\phi_g(E)$	-	-	-	-	W186G deleted
	Y30GA	17	20	$\phi_g(E)$	-	-	-	-	W186G, TI47P deleted

a) 1 denotes $\phi_E(E)$ is constant.
2 denotes $\phi_E(E)$ is linear in E.
3 denotes $\ln\phi_E(E)$ is linear in lnE.

Table 3. Integral parameters as supplied by participants.

Reference values for input spectrum:

	ϕtot	$\phi > 1$ MeV	$\phi > 0{,}1$ MeV	R_{Ni}	R_{dpa}
ORR	$1{,}932\times10^{17}$	$3{,}808\times10^{16}$	$8{,}127\times10^{16}$	$5{,}142\times10^{-13}$	$5{,}450\times10^{-9}$
YAYOI	$1{,}614\times10^{15}$	$7{,}473\times10^{14}$	$1{,}548\times10^{15}$	$9{,}632\times10^{-15}$	$1{,}031\times10^{-10}$

	IAEA code	no.	relative values for: ϕtot	$\phi > 1$ MeV	$\phi > 0{,}1$ MeV	R_{Ni}	R_{dpa}
ORR spectrum	001BB	1	1,06	1,04	1,03	1,04	1,06
	003EB	2	1,10	0,981	1,02	1,88	1,06
	005EB	3	1,01	0,992	0,896	1,91	1,01
	006AB	4	1,03	1,06	1,01	1,03	1,04
	008FB	5	1,03	1,06	1,01	1,03	1,04
	011AA	6	1,04	1,06	1,04	1,03	1,05
	013BA	7	1,04	1,04	1,04	1,00	1,03
	015BC	8	1,00	1,07	1,01	1,03	1,04
	018BD	9	-	-	-	-	-
	019BD	10	-	-	-	-	-
	020BD	11	-	-	-	-	-
	021BD	12	-	-	-	-	-
	023CA	13	1,02	1,02	1,02	1,01	1,02
	031HA	14	1,02	1,06	1,02	1,02	1,04
	032HA	15	1,04	1,08	1,03	1,00	1,04
	033HA	16	1,03	1,06	1,03	1,02	1,04
	034GA	17	1,67	1,07	1,51	1,06	1,30
	035GA	18	1,07	1,06	1,16	1,05	1,12
average *			1,08	1,05	1,06	1,15	1,06
coefficient of variation *			0,158	0,029	0,132	0,275	0,068

	IAEA code	no.	relative values for: ϕtot	$\phi > 1$ MeV	$\phi > 0{,}1$ MeV	R_{Ni}	R_{dpa}
YAYOI spectrum	Y02BB	1	1,34	1,22	1,32	0,870	1,18
	Y04EB	2	1,28	1,10	1,27	0,903	1,16
	Y07AB	3	1,27	1,18	1,26	0,933	1,16
	Y09FB	4	1,26	1,18	1,26	1,05	1,18
	Y10FB	5	1,26	1,19	1,26	1,04	1,18
	Y12AA	6	1,25	1,15	1,25	0,948	1,15
	Y14BA	7	1,24	1,13	1,23	0,997	1,15
	Y16BC	8	1,29	1,21	1,28	1,09	1,21
	Y17BC	9	1,28	1,21	1,28	1,09	1,21
	Y22BD	10	-	-	-	-	-
	Y24CA	11	1,26	1,19	1,27	1,06	1,19
	Y25HA	12	1,28	1,20	1,28	0,998	1,18
	Y26HA	13	1,28	1,21	1,28	1,08	1,21
	Y27HA	14	1,24	1,10	1,23	1,03	1,15
	Y28HA	15	1,28	1,16	1,29	0,955	1,17
	Y29GA	16	1,32	1,43	1,38	0,869	1,23
	Y30GA	17	1,24	1,08	1,29	1,23	1,21
average *			1,27	1,18	1,28	1,01	1,18
coefficient of variation *			0,022	0,067	0,028	0,094	0,022

*typical outliers have not yet been discarded.

Table 4. Convergence parameters.

$$ARD = \left\{ \sum_{i=1}^{n} \left[(\alpha_i^m - \alpha_i^c) / s_i^m \right]^2 / n \right\}^{\frac{1}{2}}$$

$$DEV = \left\{ \sum_{i=1}^{n} \left[(\alpha_i^m - \alpha_i^c) / \alpha_i^c \right]^2 / (n-1) \right\}^{\frac{1}{2}}$$

	IAEA code	no.	ARD	DEV		IAEA code	no.	ARD	DEV
ORR spectrum	001BB	1	0,37	3,24	YAYOI spectrum	Y02BB	1	0,47	5,13
	003EB	2	0,42	3,88		Y04EB	2	0,79	7,68
	005EB	3	0,36	3,20		Y07AB	3	0,72	7,92
	006AB	4	0,29	3,43		Y09FB	4	1,48	25,23
	008FB	5	0,29	3,39		Y10FB	5	0,86	10,23
	011AA	6	0,31	3,64		Y12AA	6	0,78	8,52
	013BA	7	0,75	6,79		Y14BA	7	0,92	9,92
	015BC	8	0,38	4,69		Y16BC	8	0,68	5,61
	018BD	9	2,31	23,01		Y17BC	9	0,72	5,60
	019BD	10	0,33	3,06		Y22BD	10	0,73	7,81
	020BD	11	1,13	6,65		Y24CA	11	0,99	11,37
	021BD	12	1,13	6,66		Y25HA	12	0,48	6,01
	023CA	13	1,00	9,73		Y26HA	13	0,71	9,88
	031HA	14	0,31	2,12		Y27HA	14	0,57	7,17
	032HA	15	0,54	4,07		Y28HA	15	0,36	4,70
	033HA	16	0,15	1,24		Y29GA	16	0,38	4,34
	034GA	17	0,77	4,63		Y30GA	17	0,32	2,63
	035GA	18	17,28	198,86					

Input spectrum

ARD value for ORR : 1,12.
ARD value for YAYOI: 2,34.

Remark: Where reactions have been deleted, a zero contribution to the summation in ARD and DEV has been introduced. An improved calculation is envisaged.

Table 5. Group fluence rates in decade structure.

group	decade (in MeV)	ORR spectrum			YAYOI spectrum			
		absolute input value (in $m^{-2}.s^{-1}$)	average relative output value	coefficient of variation for 18 solutions (in %)	absolute input value (in $m^{-2}.s^{-1}$)	average relative output value (17 sol.)	coefficient of variation for * 17 solutions (in %)	10 solutions (in %)
1	10^{-10}... 10^{-9}	$3,45\times10^{17}$	4,73	84,5	$2,57\times10^{3}$	5,99	324	42
2	10^{-9} ... 10^{-8}	$2,61\times10^{19}$	1,34	37,2	$1,11\times10^{5}$	2,45	176	12
3	10^{-8} ... 10^{-7}	$3,60\times10^{20}$	0,88	25,4	$5,62\times10^{6}$	1,23	65	11
4	10^{-7} ... 10^{-6}	$1,33\times10^{20}$	1,36	67,8	$4,28\times10^{8}$	1,34	62	10
5	10^{-6} ... 10^{-5}	$1,31\times10^{20}$	0,92	15,2	$1,96\times10^{10}$	1,13	44	26
6	10^{-5} ... 10^{-4}	$1,61\times10^{20}$	0,77	26,5	$6,84\times10^{11}$	1,28	66	14
7	10^{-4} ... 10^{-3}	$7,87\times10^{19}$	1,23	27,3	$6,26\times10^{13}$	1,32	78	19
8	10^{-3} ... 10^{-2}	$7,12\times10^{19}$	1,18	54,3	$9,22\times10^{15}$	1,28	58	14
9	10^{-2} ... 10^{-1}	$1,59\times10^{20}$	1,22	60,9	$6,46\times10^{17}$	1,19	39	13
10	10^{-1} ... 10^{0}	$4,32\times10^{20}$	1,07	22,3	$8,02\times10^{18}$	1,36	3	2
11	10^{0} ... 10^{1}	$3,80\times10^{20}$	1,06	3,0	$7,46\times10^{18}$	1,18	7	2
12	10^{1} ... 18	$6,88\times10^{17}$	1,28	43,6	$1,68\times10^{16}$	0,93	36	22

*The reduced set of 10 solutions does not comprise some clearly deviating solutions, and the solutions with only 10 or 20 groups.

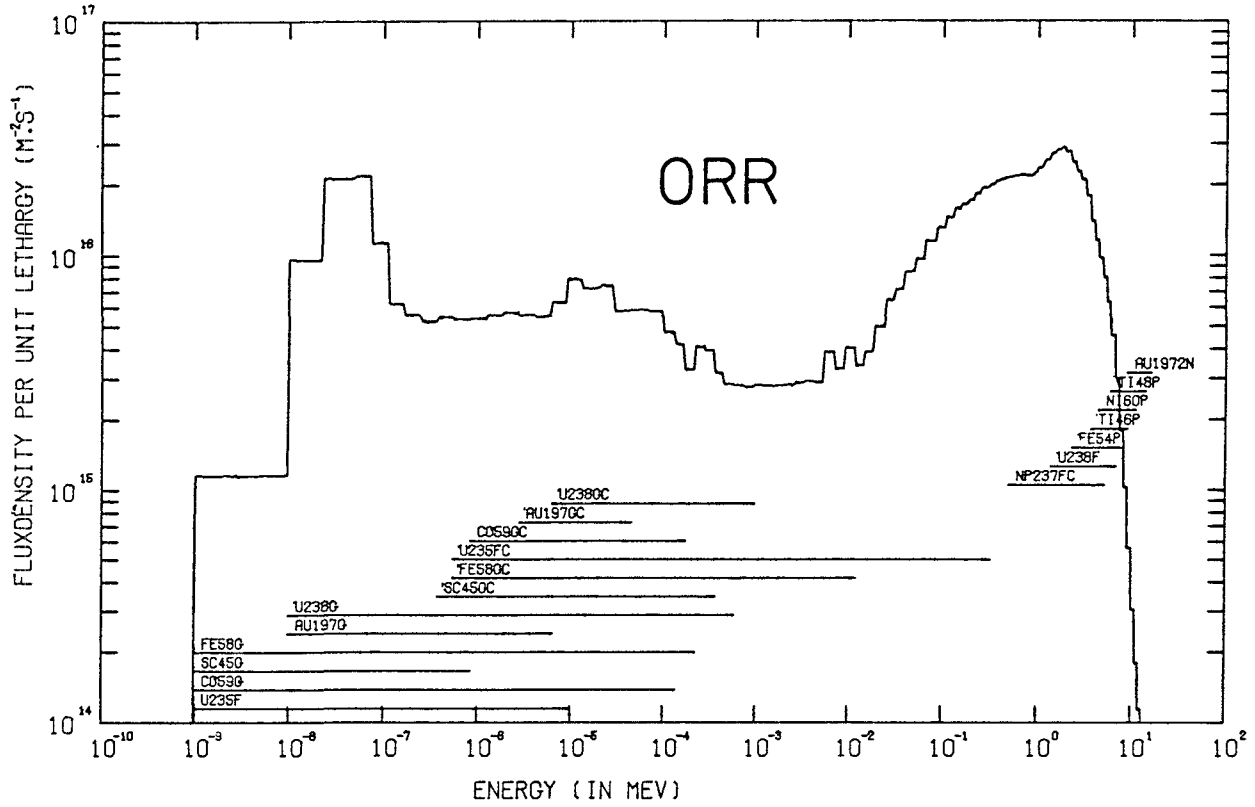

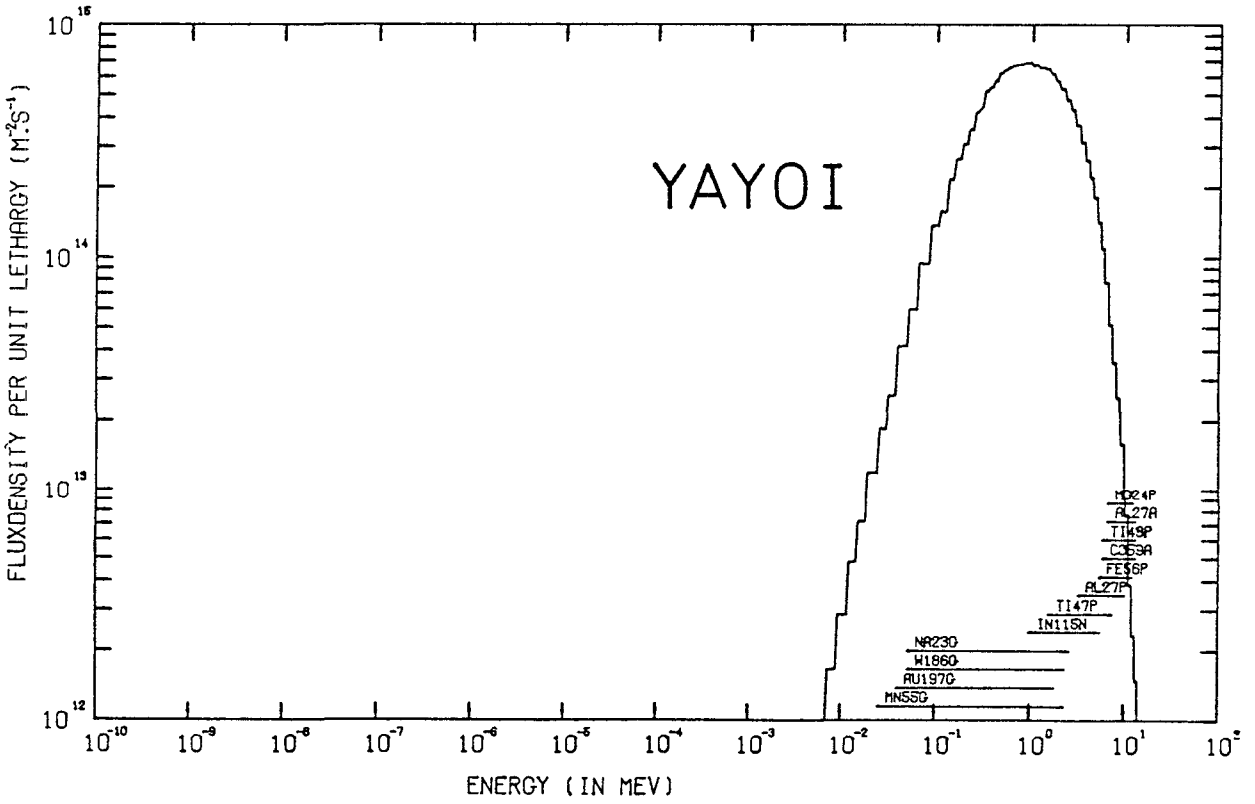

FIG.1 TYPICAL OUTPUT SPECTRA WITH 90% RESPONSE REGIONS

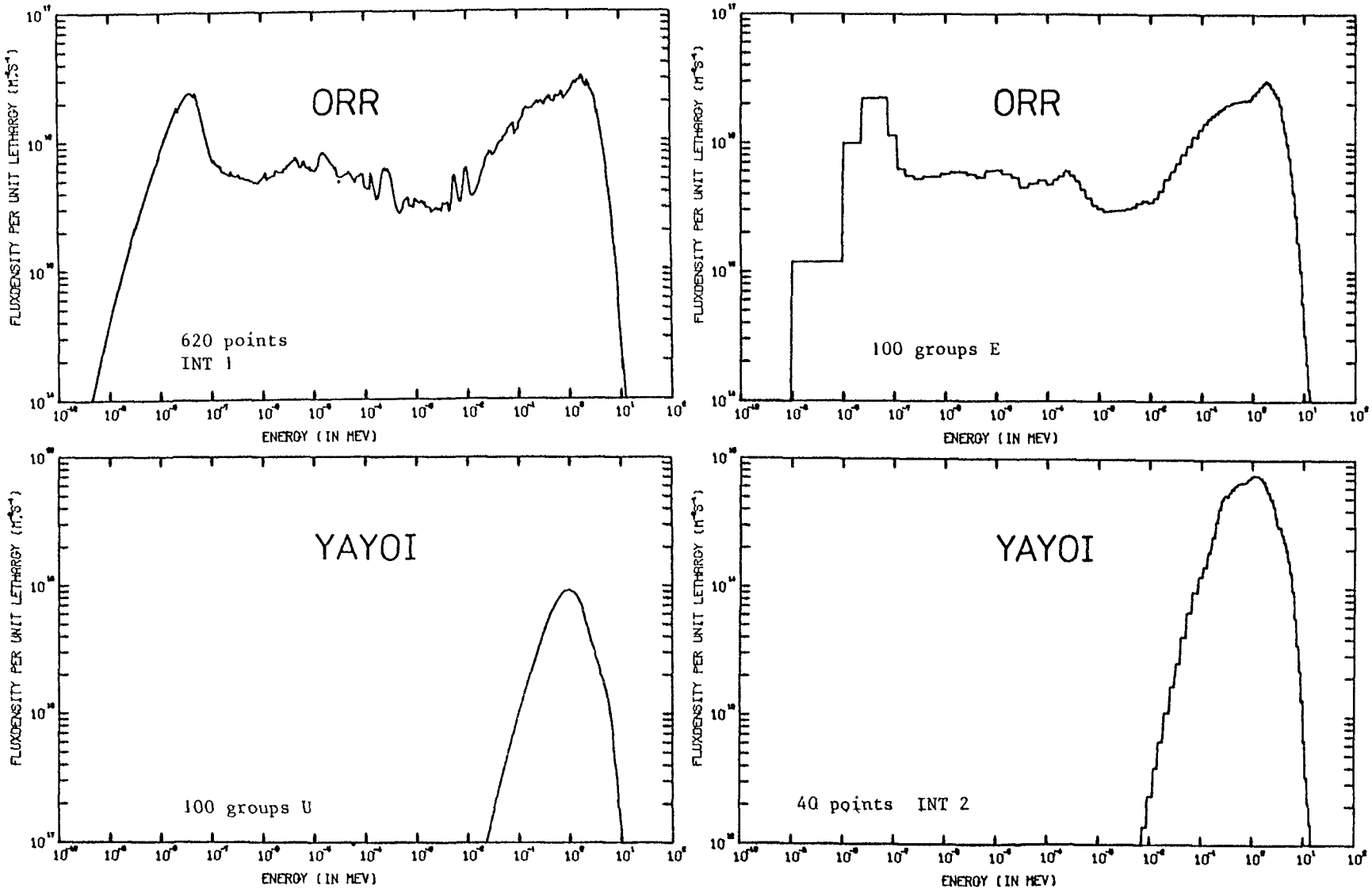

Fig. 2. SOME OUTPUT SPECTRA IN DIFFERENT ENERGY GROUPINGS.

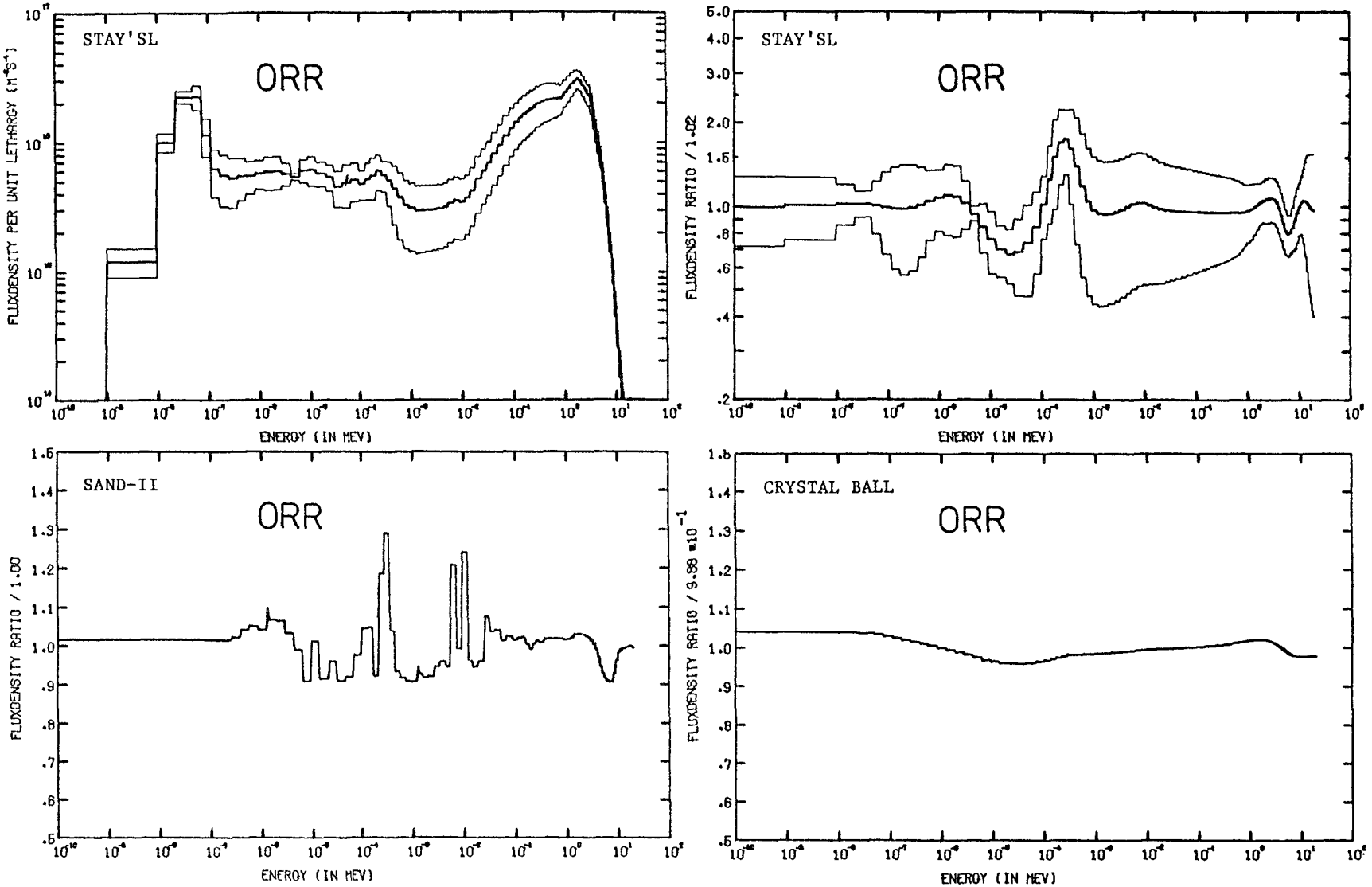

Fig. 3. OUTPUT ORR SPECTRUM AND RATIO OF OUTPUT AND INPUT FOR THREE CODES.

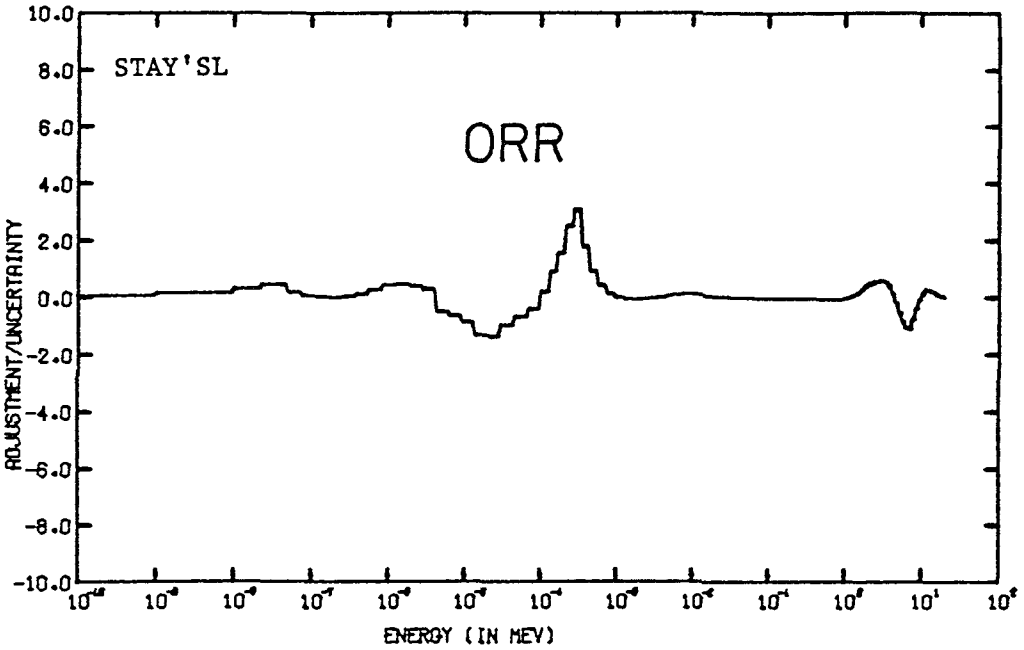

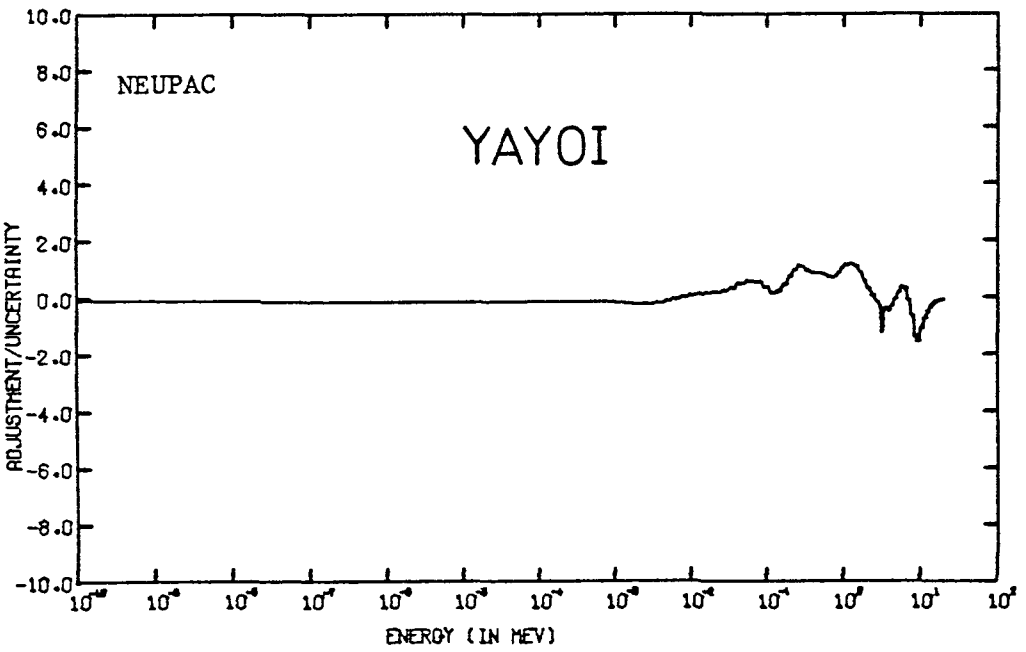

Fig. 4. TWO ADJUSTMENT/UNCERTAINTY CURVES.

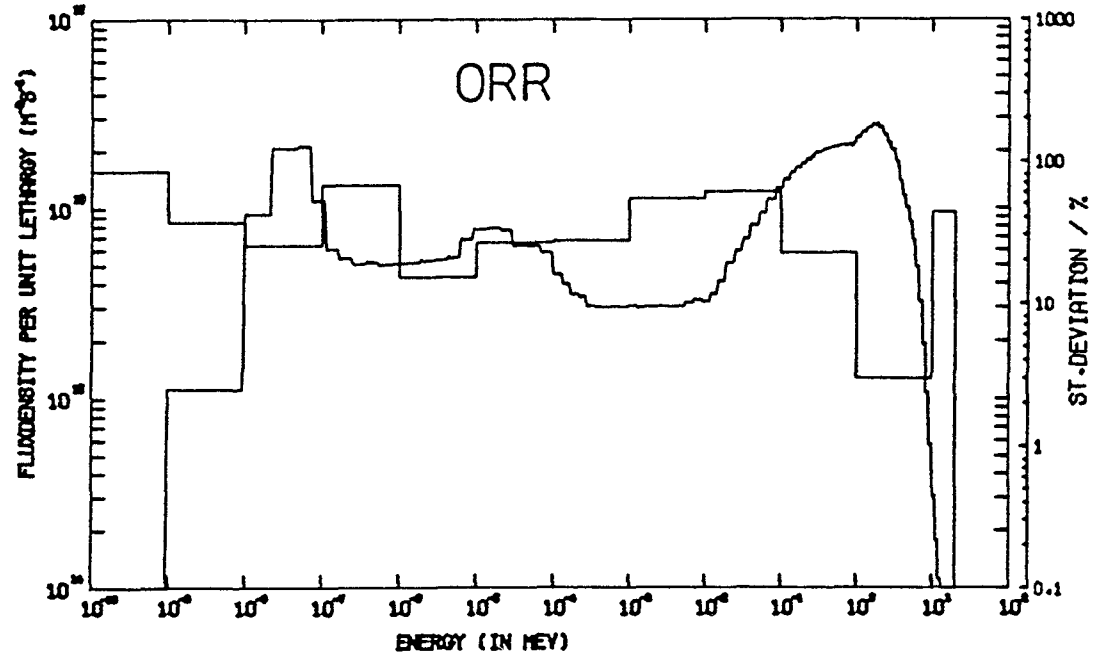

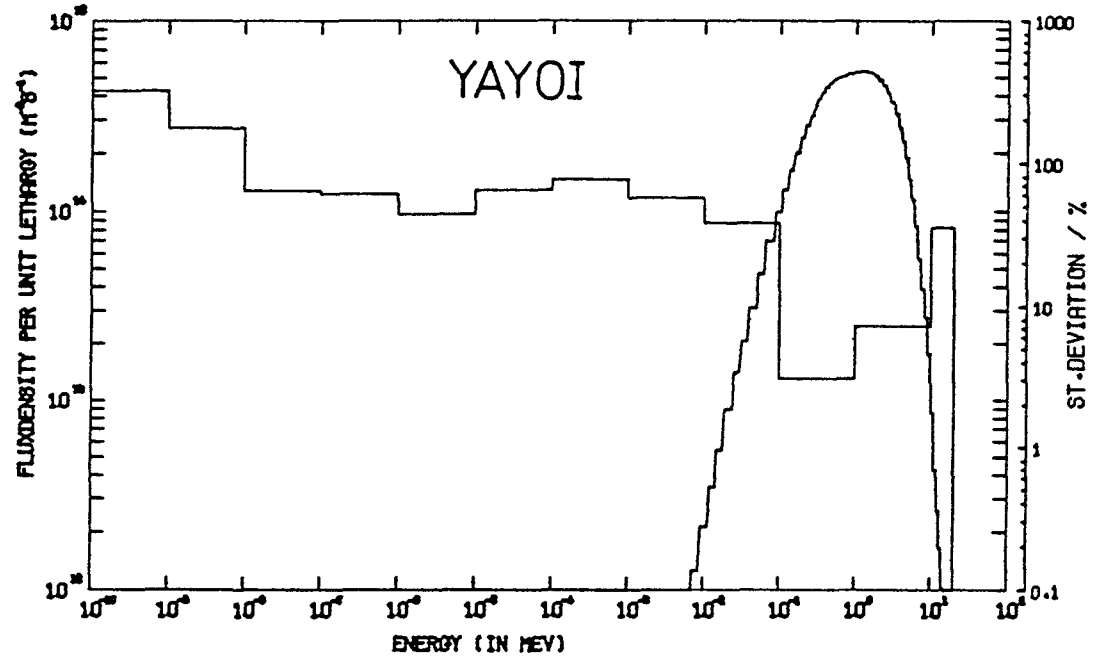

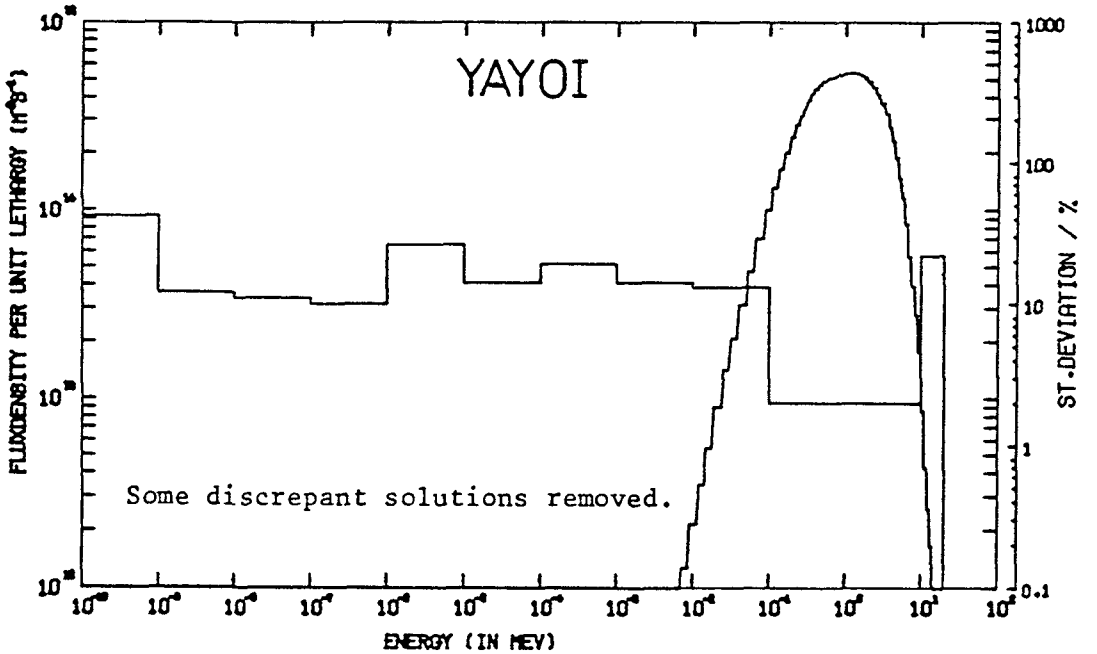

Fig. 5. Rough comparison of output spectrum shapes.

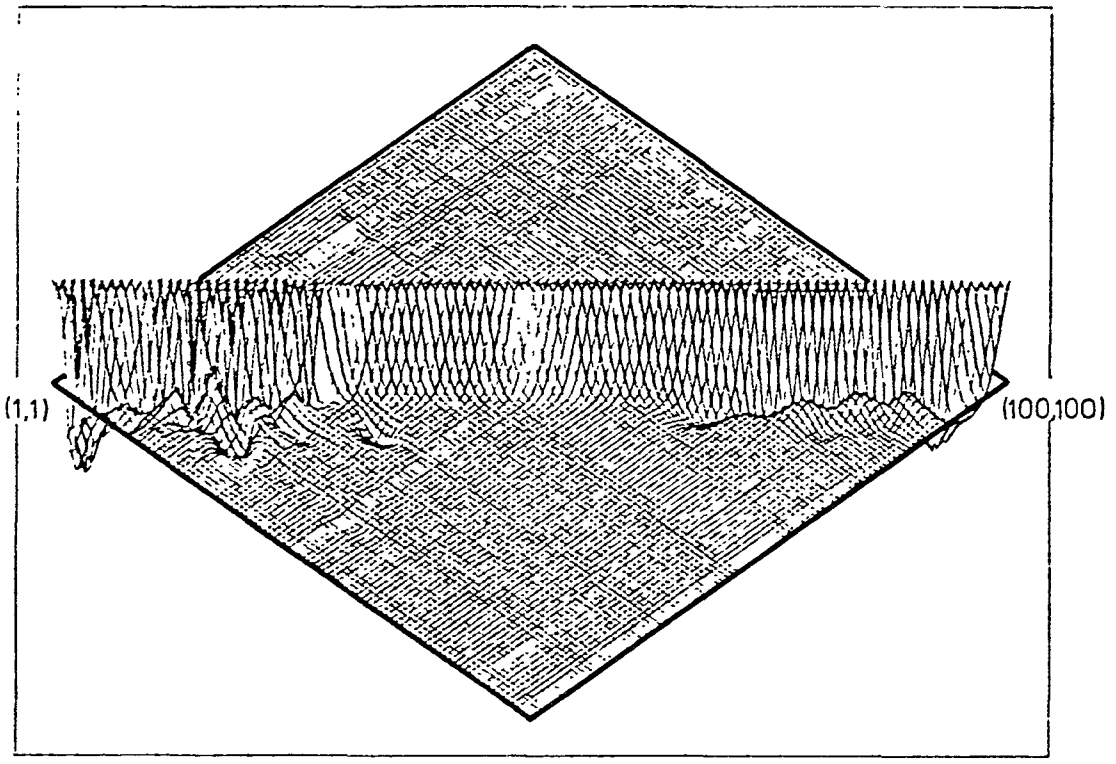

REAL-80 G06AB
Correlation function of group flux densities for ORR (STAY'SL).

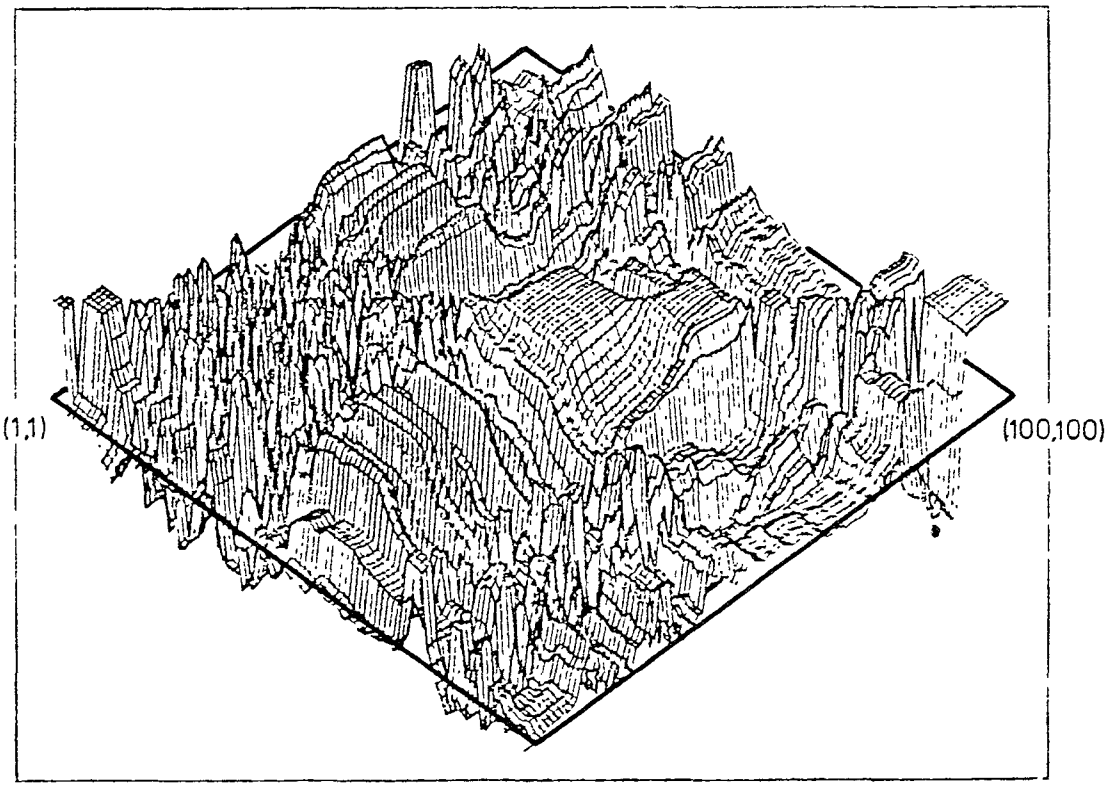

REAL-80 G15BC
Correlation function of group flux densities for ORR (SAND-II).

Fig. 6.

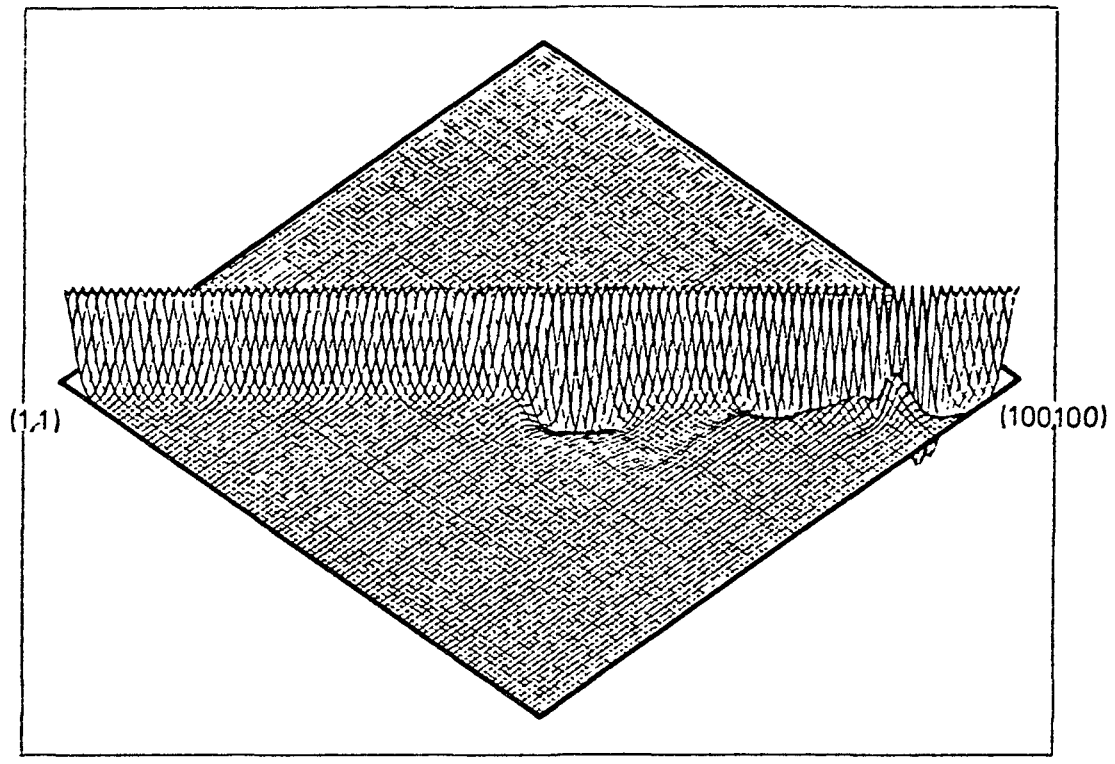

REAL-80 Y07AB

Correlation function of group flux densities for YAYOI (STAY'SL).

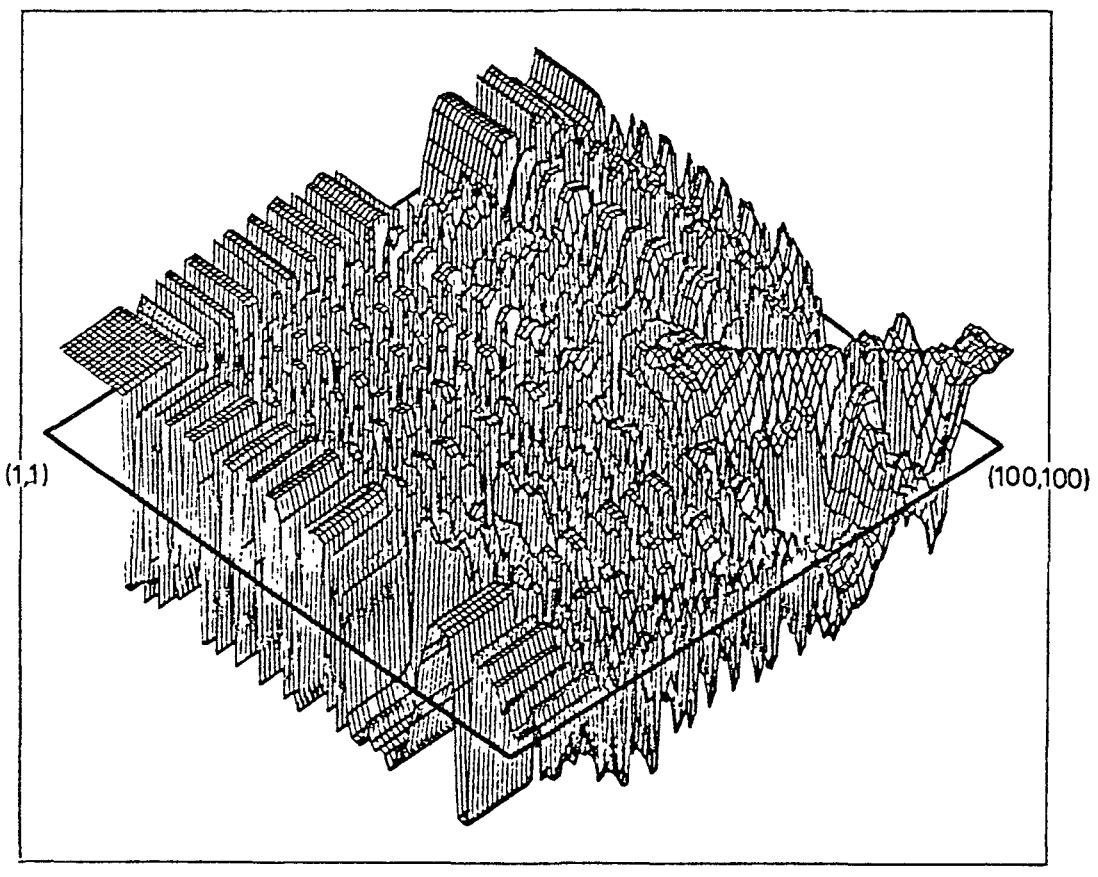

REAL-80 Y16BC

Correlation function of group flux densities for YAYOI (SAND-II).

Fig. 7.

LIST OF PARTICIPANTS

GER JUL L. Weise
Kernforschungsanlage Jülich GmbH
Zentralabteilung für Brennelemente und Bestrahlungstechnologie
Postfach 1913
D-5170 Jülich
Federal Republic of Germany.

GER PTB M. Matzke
Physikalisch-Technische Bundesanstalt
Abteilung 7, Bundesallee 100
Postfach 3345
D-3300 Braunschweig
Federal Republic of Germany.

HUN BME É.M. Zsolnay, E.J. Szondi
Nuclear Reactor of the Technical University
H-1521 Budapest
Hungary.

JAP TOK T. Taniguchi
Faculty of Engineering
University of Tokyo
7-3-1; Hongo, Bunkyo-ku
Tokyo
Japan.

NED ECN W.L. Zijp, H.J. Nolthenius, et al.
Netherlands Energy Research Foundation ECN
Postbus 1
1755 ZG Petten
The Netherlands.

SF HLS J. Sandberg, J. Routti
Helsinki University of Technology
Department of Technical Physics
Otaniemi
SF-02150 Espoo 15
Finland.

UK RRA M. Austin
Rolls Royce and Associates Limited
P.O. Box No. 31
Derby, DE2 8BJ
United Kingdom.

UNO IAE C. Ertek
IAEA Seibersdorf laboratory
Wagramerstrasse 5
P.O. Box 100
A-1400 Vienna
Austria.

USA ANL L.R. Greenwood
Chemical Engineering Division
Argonne National Laboratory
9700 South Cass Avenue
Argonne, Ill. 60439
USA.

USA GEV G.C. Martin Jr.
G.E. Vallecitos Nuclear Center
Nuclear Engineering Division
P.O. Box 460
Pleasanton, CA 94566
USA.

USA HED E.P. Lippincott
Hanford Engineering Development Laboratory
P.O. Box 1970
Richland, WA 99352
USA.

USA ORL F.W. Stallmann
Oak Ridge National Laboratory
Building 3001
P.O. Box X
Oak Ridge, TN 37830
USA.

YUG IJS M. Najzer
Institut Josef Stefan
Jamova 39
P.O.B. 199-4
YU-61001 Ljubljana
Yúgoslavia.

LIST OF ADJUSTMENT CODES

CRYSTAL BALL
FERRET
GERDM02
ITER
LOUHI-78
LSL
NEUPAC
SAND-II
SANDBP
SANDMX
SANDPET
STAY'SL
WINDOWS

Remark:
Some of the solutions have been received after 15 August 1981;
these results could not yet be included in this report.

RESULTS OF HEDL CALCULATIONS ON THE REAL-80 PROJECT

E.P. LIPPINCOTT, D.L. OBERG
Westinghouse Hanford Company,
Hanford Engineering Development Laboratory,
Richland, Washington,
United States of America

Abstract

Calculations for the YAYOI and ORR spectra have been performed using the FERRET least squares adjustment code. Results indicate one reaction rate to be discrepant for the YAYOI case and excellent agreement for all reactions in the ORR case. Predictions of damage rates and uncertainties were made for each spectrum.

Calculations have been performed at the Hanford Engineering Development Laboratory (HEDL) on the two cases presented by the REAL-80 project for an interlaboratory comparison. For the HEDL calculations the FERRET code[1] was used.

The FERRET code uses both integral and differential data to adjust a priori fluxes Φ_0, which are typically obtained from calculations. A log-normal least-squares algorithm weights both the a priori values and the measured data in accordance with assigned uncertainties and correlations. In general, the measured values f are linearly related to the flux Φ by some response matrix A:

$$f_i^{(s,\alpha)} = \sum_g A_{ig}^{(s)} \Phi_g^{(\alpha)} \qquad (1)$$

where i indexes the measured values belonging to a single data set s, g designates the energy group, and α delineates separate spectra that may be simultaneously adjusted. For example,

$$R_i = \Sigma_g \sigma_{ig} \Phi_g \qquad (2)$$

relates a set of measured reaction rates R_i to a single spectrum Φ_g by the multigroup cross sections σ_{ig}. (In this case, FERRET also adjusts the cross sections.) Differential flux measurements have the particularly simple response, $A_{gg'} = \delta_{gg'}$, where $\delta_{gg'}$ is the Kronecker delta. The log-normal approach automatically accounts for the physical constraint of positive fluxes, even with large assigned uncertainties.

Results

The results for the YAYOI spectrum are presented in Tables 1 and 2 and Figure 1. In Table 1 the case is run without the $^{58}Ni(n,p)^{58}Co$ reaction and the reaction rate for this reaction is calculated. In Table 2 the calculation is performed with the ^{58}Ni reaction included. In the latter case the ^{58}Ni reaction rate calculated for the adjusted spectrum agrees with the measured value within 1%.* For the case without ^{58}Ni included the calculated value is 14% low which is almost twice the 1σ calculated uncertainty. This difference is due to the $^{47}Ti(n,p)$ reaction which was found to be more than 1σ inconsistent with the other reaction rates. In a third case which included neither the ^{58}Ni or the ^{47}Ti reaction, the calculated ^{58}Ni reaction rate agrees with the measured value within 7% with a 1σ of 12%.

The ^{47}Ti result is much more consistent, however, if the $^{47}Ti(n,p)$ cross section is renormalized to agree with measurements in the CFRMF, BIG 10, and ^{235}U fission spectrum. The data from these fields indicate the cross section should be lowered 17 $\pm$ 3%.

The results for the ORR spectrum are given in Table 3. Good agreement was obtained for all the given reaction rates.

Conclusions

The two REAL-80 cases should provide a basis for preliminary intercomparison of results from unfolding codes. The ORR case should present no difficulties whereas the YAYOI case, because of the discrepancy of the ^{47}Ti, will likely get different results depending on code treatment. It is recommended that further REAL-80 exercises be conducted on other spectra with not only investigation of unfolding codes but also data sets and procedures.

References

1. F. A. Schmittroth, "FERRET Data Analysis Code," HEDL-TME 79-40, Hanford Engineering Development Laboratory, Richland, WA, 1979.

* This agreement is in part due to adjustment of the $^{58}Ni(n,p)$ cross section. The value in Table 2 is calculated with the unadjusted cross section and thus shows a calculated value almost 5% below the measured value (1.07×10^{-14}).

TABLE 1

REAL-80 PROJECT

YAYOI SPECTRUM - CASE 1

FERRET UNFOLDING CODE — 100 GROUPS

ALL REACTIONS EXCEPT $^{58}Ni(n,p)^{58}Co$ INCLUDED

Total Flux	$2.07 \times 10^{11} \pm 5.1\%$	n/cm^2-sec
Flux Greater Than 0.1 MeV	$1.99 \times 10^{11} \pm 6.0\%$	n/cm^2-sec
Flux Greater Than 1 MeV	$9.05 \times 10^{10} \pm 10.3\%$	n/cm^2-sec
Damage Rate for Iron	$1.21 \times 10^{-10} \pm 6.1\%$*	displacements/atom-sec
$^{58}Ni(n,p)^{58}Co$ Reaction Rate	$9.20 \times 10^{-15} \pm 8.9\%$*	reactions/atom-sec

*Uncertainty in cross section not included.

TABLE 2

REAL-80 PROJECT

YAYOI SPECTRUM - CASE 2

FERRET UNFOLDING CODE — 100 GROUPS

ALL REACTIONS INCLUDED

Total Flux	$2.08 \times 10^{11} \pm 5.0\%$	n/cm^2-sec
Flux Greater Than 0.1 MeV	$2.00 \times 10^{11} \pm 5.9\%$	n/cm^2-sec
Flux Greater Than 1 MeV	$9.08 \times 10^{10} \pm 10.0\%$	n/cm^2-sec
Damage Rate for Iron	$1.24 \times 10^{-10} \pm 5.6\%$*	displacements/atom-sec
$^{58}Ni(n,p)^{58}Co$ Reaction Rate	$1.02 \times 10^{-14} \pm 5.1\%$*	reactions/atom-sec

*Uncertainty in cross section not included.

TABLE 3

REAL-80 PROJECT

ORR SPECTRUM

FERRET UNFOLDING CODE — 100 GROUPS

ALL REACTIONS INCLUDED

Total Flux	$1.99 \times 10^{13} \pm 5.5\%$	n/cm^2-sec
Flux Greater Than 0.1 MeV	$8.34 \times 10^{12} \pm 9.0\%$	n/cm^2-sec
Flux Greater Than 1 MeV	$4.03 \times 10^{12} \pm 6.3\%$	n/cm^2-sec
Damage Rate for Iron	$5.68 \times 10^{-9} \pm 4.6\%$*	displacements/atom-sec
$^{58}Ni(n,p)^{58}Co$ Reaction Rate	$5.28 \times 10^{-13} \pm 4.7\%$*	reactions/atom-sec

*Uncertainty in cross section not included.

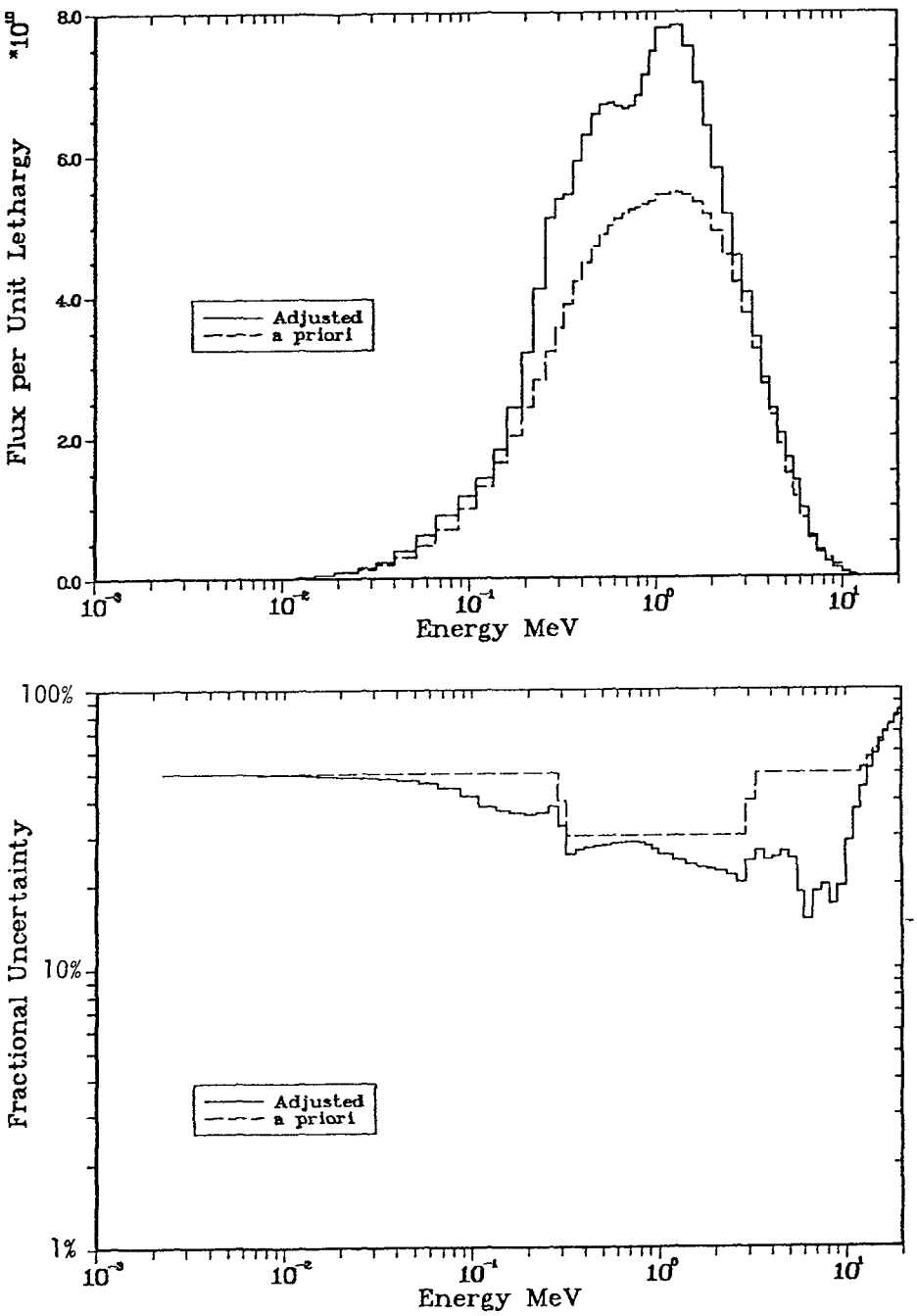

FIGURE 1 YAYOI SPECTRUM

UNFOLDING OF REAL 80 SAMPLE DATA BY ITER AND STAYSL CODES

B. GLUMAC, M. NAJŽER
E. Kardelj University,
J. Štefan Institute,
Ljubljana,
Yugoslavia

Abstract

REAL 80 sample data are unfolded by ITER-2, ITER-3 and STAYSL codes. ITER-3 which is an extension of ITER-2 is briefly described. Besides solution spectra the total fluence, fluence above 0,1 and 1 MeV, displacement per atom, $^{60}Ni(n,p)$ reaction rate and damage to activation ratio are given. Derived are explicit expressions for standard deviation of the above integral data.

1. Introduction

The REAL 80 international project gives an opportunity to compare different unfolding codes on a full size real problem including the complete covariance analysis. In this contribution three codes ITER-2, ITER-3 and STAYSL were investigated. ITER-2 and STAYSL are well documented in ref.1 and 2 respectively. ITER-3 is an extension of ITER-2 and is briefly described in section 2. Though ITER-2 is able to handle only the variances of data and not the whole covariance matrix, it was included into the analysis to compare it with more sophisticated codes. Besides spectra the following integral quantities were calculated: total fluence, fluence above 0,1 and 1 MeV, displacement per atom, $^{60}Ni(n,p)$ reaction rate and damage to activation ratio. Explicit expressions for the standard deviation of all integral quantities were derived and are given in section 3.

2. Description of ITER unfolding codes

2.1. ITER-2

The iterative algorithm of the unfolding code ITER-2 is thoroughly described in reference (1). This routine can not take into account the covariances of the input spectrum but only the variances of the reaction rates and the diagonal covariance submatrices of the crossections. ITER-2, as applied in REAL-80 is additionally limited in such a way that it takes into account only the variances of the reaction rates and treats the crossections as fully correlated.

2.2. ITER-3

Algorithm of ITER-3 is basically similar to ITER-2 i.e. it applies the same iteration procedure. The program has been expanded so that it can give an estimation of the output spectrum covariance matrix. The ITER-3 code is also partially documented in ref. (1). The difference between ITER-2 and ITER-3 is that ITER-3 takes into account the diagonal correlation submatrices of the crossections when calculating the adjustment operator for each iterative step. The elements of the relative covariance matrix M of the solution spectrum are calculated in the same way as that of the STAYSL code (2).

3. Results

3.1. Input data

REAL-80 input data set provides reaction rates and their covariance matrices, input spectra in 100 energy groups with the associated covariance matrices and 100-group crossections with their standard deviations. The covariance matrix of the crossections was calculated following reference (3). Correlations between groups of a certain crossection (diagonal correlation submatrices) are assumed to be gaussian with FWHM=10, the correlations between groups of different crossections (nondiagonal correlation submatrices) are fixed to be 0.01.

3.2. Neutron spectra

Unfolding was made with three codes (ITER-2, ITER-3 and STAYSL) on the three sets of input data: ORR data set with 19 measured reaction rates, YAYOI data set with 13 measured reaction rates and YAYOI data set with 12 measured reaction rates. This last data set is nothing but the original YAYOI data set from which the reaction ^{47}Ti(n,p) was omitted. It can be seen from Tab. 1 that this reaction could not be properly fitted with any of the three codes applied.

Fig. 1 presents ratios of initial spectrum approximations towards solution spectra for ORR and YAYOI (12 reaction rates) data sets for STAYSL and ITER-3 unfolding codes. ITER-2 gives almost exactly the same ratio as ITER-3.

All unfoldings were done by the use of our PDP 11/34 minicomputer. It is interesting to compare computing time of different unfolding codes: ITER-3 and STAYSL were running some 5 hours on the ORR input data (the two routines handle complete crossection covariance matrix, i.e. appx. 10^6 numbers) while ITER-2 ran only appx. one minute.

3.3. Integral quantities

We applied three unfolding codes on three input data sets thus obtaining nine solution spectra. For each of the solution spectra we have calculated the following integral quantities together with their standard

deviations: total integral, integral above 0.1 MeV, integral above 1 MeV, reaction rate for the ^{60}Ni(n,p) reaction, displacement per atom and damage - to - activation ratio. We feel it is convenient to summarize in an easy-to-program form how the estimations of standard deviations were done for the spectrum integrals, reaction rate of ^{60}Ni(n,p) or DPA and the DAR calculation. The theory behind the above expressions is evident from the works pf F.Perey (4).

3.3.1. Standard deviation od the spectrum integral:

let vector $\emptyset = (\emptyset_1,\ldots,\emptyset_n)$ represent group solution spectrum, let vector $Z = (z_1,\ldots,z_n)$ contain relative standard deviationsof the group spectrum and let $C_\emptyset = (c^\emptyset_{ij})$ be solution vector's correlation matrix. Integral of the spectrum between groups k and l is:

$$I = \sum_{i=k}^{l} \emptyset_i \qquad /3.1/$$

and the relative standard deviation of this integral is:

$$\sigma_I = \sqrt{\sum_{i=k}^{l} \sum_{j=k}^{l} \emptyset_i \emptyset_j z_i z_j c^\emptyset_{ij} / I^2} \qquad /3.2/$$

3.3.2. Standard deviation of the ^{60}Ni(n,p) reaction rate or DPA:

let vector $R = (r_1,\ldots,r_n)$ contain crossection and vector $S = (s_1,\ldots,s_n)$ contain relative standard deviations of this crossection and let $C_R = (c^R_{ij})$ be the crossections correlation matrix. The reaction rate is:

$$m = \sum_{i=1}^{n} \emptyset_i r_i \qquad /3.3/$$

and the relative standard deviation of the reaction rate is:

$$\sigma_m = \sqrt{\sum_{i=1}^{n} \sum_{j=1}^{n} \emptyset_i \emptyset_j r_i r_j s_i s_j c^R_{ij} + \sum_{i=1}^{n} \sum_{j=1}^{n} r_i r_j \emptyset_i \emptyset_j z_i z_j c^\emptyset_{ij}} / m^2 \qquad /3.4/$$

3.3.3. Standard deviation of the damage-to-activation ratio

let $\emptyset_r$ be the spectrum we investigate and $M_{\emptyset r}$ its covariance matrix, let $\emptyset_f$ be a standard fission spectrum and $M_{\emptyset f}$ its covariance matrix, let Σ_a be a certain activation crossection (^{60}Ni(n,p)) and $M_{\Sigma a}$ its covariance matrix and let Σ_d be the damage function with its covariance matrix $M_{\Sigma d}$. Damage-to-activation ratio is given by:

$$d = (\varkappa_r/\varkappa_f)/(y_r/y_f) \qquad /3.5/$$

where $\varkappa_r = \emptyset^t_r \Sigma_d$, $\varkappa_f = \emptyset^t_f \Sigma_d$, $y_r = \emptyset^t_r \Sigma_a$ and $y_f = \emptyset^t_f \Sigma_a$. We define

vector $Q = (q_1, q_2, q_3, q_4) = (\varkappa_r, \varkappa_f, y_r, y_f)$. By making the Taylor expansion and retaining only the first term of the series we obtain:

$$|\delta d\rangle \sim \frac{\partial d}{\partial Q} |(\delta Q)^t\rangle = S\,|(\delta 0)^t\rangle \qquad /3.6/$$

Expression /3.6/ defines vector S as:

$$S = (\partial d/\partial \varkappa_r,\ \partial d/\partial \varkappa_f,\ \partial d/\partial y_r,\ \partial d/\partial y_f) \qquad /3.7/$$

Standard deviation of DAR is given by:

$$\langle \delta d\,|(\delta d)^t\rangle = S^t \langle \delta Q|(\delta Q)^t\rangle S = S^t.M.S \qquad /3.8/$$

where $\langle \delta Q|(\delta Q)^t\rangle$ is a 4x4 covariance matrix. Let us calculate for example matrix element M_{11}. We again apply the Taylor expansion of integral quantities defined in /3.5/ and retain only the leading term:

$$M_{11} = \langle \delta \varkappa_r\,|(\delta \varkappa_r)^t\rangle \qquad /3.9/$$

$$\langle (\phi_r^t \delta\Sigma_d + \Sigma_d^t \delta\phi_r)\ \ (\phi_r(\delta\Sigma_d)^t + \Sigma_d(\delta\phi_r)^t)\rangle \sim \phi_r^t M_{\Sigma_d} \phi_r + \Sigma_d^t M_{\phi_r} \Sigma_d$$

We have assumed that no correlations exist between ϕ_r and Σ_d. Using expression /3.9/ we can now calculate all other elements of the matrix M defined in /3.8/. Note that the correlations of all "mixed" components $\langle q_i\,|(q_j)^t\rangle$ if $i \neq j$ have been set to zero, which is not always the case for the correlations between ϕ_r and ϕ_f. Complete matrix M is given below:

$$\begin{array}{cccc}
\phi_r^t M_{\Sigma d} \phi_r + \Sigma_d^t M_{\phi r} \Sigma_d & \phi_r^t M_{\Sigma d} \phi_f & \Sigma_d^t M_{\phi r} \Sigma_a & 0 \\
\phi_f^t M_{\Sigma d} \phi_r & \phi_f^t M_{\Sigma d} \phi_f + \Sigma_d^t M_{\phi f} \Sigma_d & 0 & \Sigma_d^t M_{\phi f} \Sigma_a \\
\Sigma_a^t M_{\phi r} \Sigma_d & 0 & \phi_r^t M_{\Sigma a} \phi_r + \Sigma_a^t M_{\phi r} \Sigma_a & \phi_r^t M_{\Sigma a} \phi_f \\
0 & \Sigma_a^t M_{\phi f} \Sigma_d & \phi_r^t M_{\Sigma a} \phi_r & \phi_f^t M_{\Sigma a} \phi_f + \Sigma_a^t M_{\phi f} \Sigma_a
\end{array}$$

All integral quantities described in this section have been calculated using our program named DART and are presented in Tab. II for all nine REAL-80 solution spectra.

4. Comparison of ITER and STAYSL results

Calculated reaction rates given in Table I and chisquare data in Table II show no appreciable difference in fit quality between the codes. In the case of YAYOI data the same large discrepancy for $^{47}Ti(n,p)$ reaction rate was found. This reaction was then skipped. The fit was improved but no large effect on the solution spectra was observed. A too low value of chisquare was found in the case of ORR data. This indicates that the input variances may not properly reflect the actual spread in these data.

Solution spectra obtained by the three codes do not deviate appreciably as can be seen from Figs. 1a and b. In ITER spectra a fine structure is found which is inherent to this method. A more detailed comparison of spectra can be made by help of Figs. 1a and b where ratio of input to output spactra is plotted. It is clear that STAYSL solution is more similar to the initial spectrum and the deviations are also more smooth. In the case of ORR spectrum the mean deviation from the guess spectrum seems to be equal for ITER and STAYSL while in the case of YAYOI spectrum the ITER curve is systematically lower than the STAYSL curve at energies below about 1 KeV. These differences however do not reflect appreciably in integral data which do not deviate more than 2% as can be seen from data in Table II.

Most difference between codes is found, as expected, in the estimation of error bands. It is interesting to note that ITER-2 behaves differently in the case of ORR and YAYOI data with respect to the other two codes.

STAYSL and ITER-3 requires more than two orders of magnitude more computer time as ITER-2. Most of it is used on handling very large matrices. By far the largest dimension is due group energy structure which is much finer than the actual resolving power. This may be required to obtain spectra because the fine structure of the cross section must be properly represented. It may be questionable if the same approach is needed for error and correlation analysis and if it is justified by the quality of covariance matrix data.

5. Conclusions

Results of the present investigation show that all three codes give similar solution spectra and almost identical integral quantities in spite of basically different algorithms. This fact supports the conclusion that the solution is mainly influenced by the quality of input data and not so much by the unfolding code.

It is clear that the STAYSL solution as well as its deviation from input spectrum are much more smooth in comparison with ITER results.

There is more difference in error bands. It is worth to note the reduction of error band by STAYSL and ITER-3 codes in the case of ORR spectrum.

To speed up the computation by ITER-3 code we are investigating the possibility to split the unfolding process into two parts. First, the solution spectrum will be found by less demanding approach similar to ITER-2. Later the covariance matrix and error bands will be calculated by a condensed input covariance matrix.

References:

1) M.Najžer et al., Many Channel Spectrum Unfolding 3rd ASTM - Euratom Symposium, Ispra, Italy, Oct. 1979.

2) F.Perey, STAYSL - Least Squares Dosimetry Unfolding Code, RSIC-PSR-113.

3) C.Ertek, Report on REAL-80 Project, INDC/P(80) - 17, June 1980.

4) F.Perey, unpublished works.

Tab 1 : Reaction rates for REAL-80

ORR(19)	input	Staysl	Iter-3	Iter-2
AU197(N,G)	0.954E-09	0.946E-09	0.946E-09	0.943E-09
AU197(N,G)CADM	0.511E-09	0.514E-09	0.513E-09	0.513E-09
AU197(N,2N)	0.160E-13	0.161E-13	0.160E-13	0.160E-13
SC45(N,G)	0.114E-09	0.120E-09	0.120E-09	0.119E-09
SC45(N,G)CADM	0.629E-11	0.628E-11	0.648E-11	0.638E-11
U238(N,G)	0.550E-10	0.561E-10	0.562E-10	0.563E-10
U238(N,G)CADM	0.440E-10	0.430E-10	0.431E-10	0.431E-10
U238(N,F)	0.170E-11	0.169E-11	0.169E-11	0.169E-11
U235(N,F)	0.198E-08	0.197E-08	0.197E-08	0.196E-08
U235(N,F)CADM	0.143E-09	0.145E-09	0.149E-09	0.148E-09
NP237F(N,F)	0.854E-11	0.855E-11	0.861E-11	0.862E-11
CO59(N,G)	0.194E-09	0.201E-09	0.201E-09	0.200E-09
CO59(N,G)CADM	0.367E-10	0.362E-10	0.362E-10	0.362E-10
FE58(N,G)	0.595E-11	0.561E-11	0.562E-11	0.559E-11
FE58(N,G)CADM	0.647E-12	0.632E-12	0.631E-12	0.632E-12
FE54(N,P)	0.401E-12	0.400E-12	0.394E-12	0.395E-12
TI46(N,P)	0.502E-13	0.487E-13	0.487E-13	0.490E-13
TI48(N,P)	0.134E-14	0.128E-14	0.127E-14	0.129E-14
NI60(N,P)	0.105E-13	0.112E-13	0.113E-13	0.114E-13

YAYOI(13)	input	Staysl	Iter-3	Iter-2
CO59(N,A)	0.147E-16	0.143E-16	0.143E-16	0.143E-16
MN55(N,G)	0.848E-15	0.867E-15	0.895E-15	0.903E-15
FE56(N,P)	0.100E-15	0.994E-16	0.950E-16	0.950E-16
AL27(N,P)	0.387E-15	0.404E-15	0.382E-15	0.383E-15
AL27(N,A)	0.674E-16	0.677E-16	0.697E-16	0.696E-16
MG24(N,P)	0.147E-15	0.149E-15	0.149E-15	0.149E-15
NA23(N,G)	0.785E-16	0.847E-16	0.840E-16	0.843E-16
TI47(N,P)	0.168E-14	0.223E-14	0.221E-14	0.223E-14
TI48(N,P)	0.257E-16	0.271E-16	0.272E-16	0.271E-16
NI58(N,P)	0.107E-13	0.104E-13	0.102E-13	0.103E-13
IN115(N,N)	0.212E-13	0.211E-13	0.210E-13	0.211E-13
W186(N,G)	0.116E-13	0.103E-13	0.106E-13	0.106E-13
AU197(N,G)	0.282E-13	0.253E-13	0.260E-13	0.262E-13

YAYOI(19)	input	Staysl	Iter-3	Iter-2
CO59(N,A)	0.147E-16	0.143E-16	0.143E-16	0.143E-16
MN55(N,G)	0.848E-15	0.867E-15	0.897E-15	0.902E-15
FE56(N,P)	0.100E-15	0.993E-16	0.951E-16	0.951E-16
AL27(N,P)	0.387E-15	0.405E-15	0.390E-15	0.390E-15
AL27(N,A)	0.674E-16	0.678E-16	0.696E-16	0.696E-16
MG24(N,P)	0.147E-15	0.149E-15	0.149E-15	0.149E-15
NA23(N,G)	0.785E-16	0.848E-16	0.842E-16	0.843E-16
TI48(N,P)	0.257E-16	0.271E-16	0.271E-16	0.271E-16
NI58(N,P)	0.107E-13	0.106E-13	0.106E-13	0.106E-13
IN115(N,N)	0.212E-13	0.215E-13	0.216E-13	0.216E-13
W186(N,G)	0.116E-13	0.103E-13	0.106E-13	0.106E-13
AU197(N,G)	0.282E-13	0.253E-13	0.260E-13	0.261E-13

Tab. 2 : REAL - 80 integral parameters

Spect	prog	de	chisq	integral						dar	sd	dpa	sd	actni	sd
				total	sd	gt 1	sd	gt .1	sd						
Yayoi	Stayst	13	1.818	.2074+12	.052	.9049+11	.085	.1978+12	.063	1.522	.108	.1246-09	.102	.1037-13	.076
Yayoi	Iter-3	13	1.726	.2070+12	.047	.8828+11	.080	.1960+12	.060	1.527	.106	.1232-09	.101	.1023-13	.078
Yayoi	Iter-2	13		.2086+12		.8877+11		.1973+12		1.528		.1239-09		.1028-13	
Yayoi	Stayst	12	1.321	.2074+12	.051	.9082+11	.081	.1978+12	.062	1.502	.104	.1256-09	.102	.1059-13	.077
Yayoi	Iter-3	12	1.197	.2089+12	.046	.9034+11	.078	.1978+12	.059	1.502	.103	.1258-09	.101	.1061-13	.079
Yayoi	Iter-2	12		.2095+12		.9033+11		.1983+12		1.503		.1259-09		.1061-13	
Orr	Stayst	19	.242	.1989+14	.052	.4032+13	.054	.8222+13	.082	1.361	.087	.5681-08	.100	.5290-12	.086
Orr	Iter-3	19	.266	.1999+14	.052	.4045+13	.057	.8337+13	.083	1.389	.090	.5711-08	.100	.5209-12	.085
Orr	Iter-2	19		.1992+14		.4051+13		.8314+13		1.387		.5712-08		.5220-12	

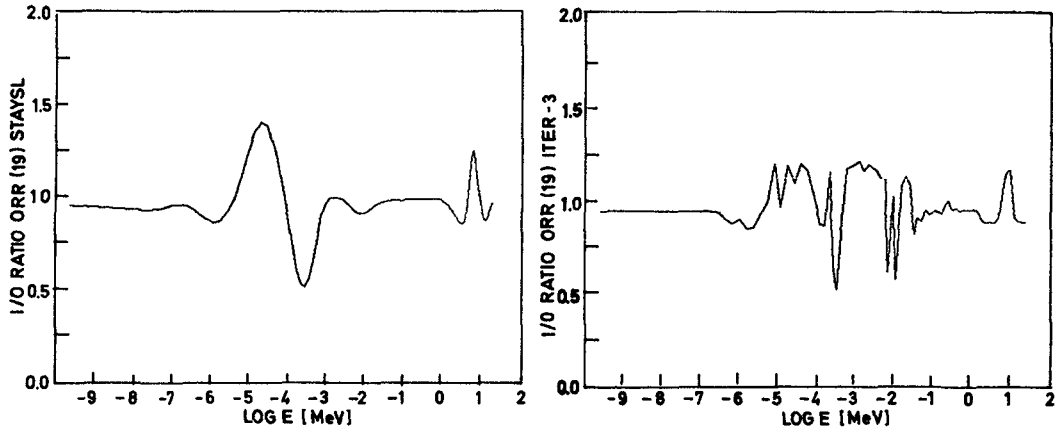

a.) ORR spectrum (19 reaction rates)

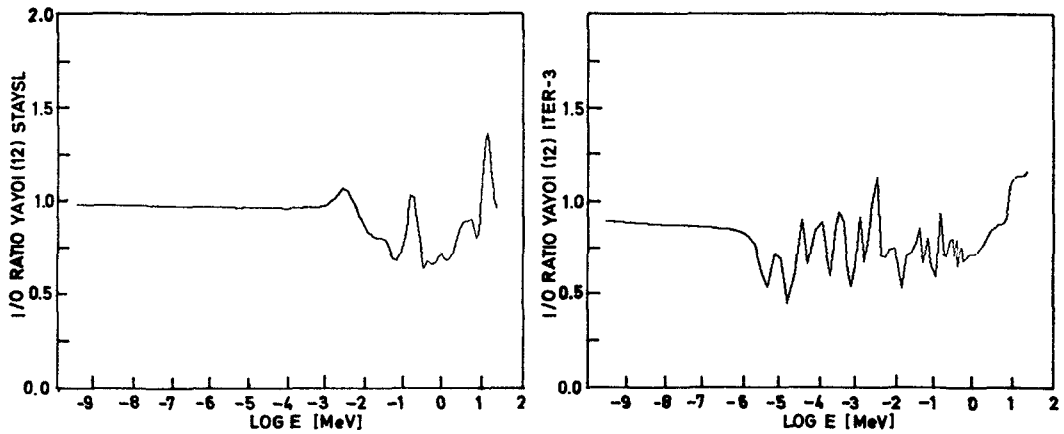

b.) YAYOI spectrum (12 reaction rates)

Fig. 1 : Input/Output ratios for REAL - 80 spectra

CONCLUSIONS AND RECOMMENDATIONS OF THE IAEA ADVISORY GROUP MEETING ON NUCLEAR DATA FOR RADIATION DAMAGE ASSESSMENT AND SAFETY ASPECTS

The conclusions and recommendations of the IAEA AGM on Nuclear Data for Radiation Damage Assessment and Safety Aspects consist of three separate reports developed by the participants of the three workshops which took place during the meeting on 15 and 16 October 1981.

1. Workshop on Nuclear Data for Environment Characterization.

2. Workshop on Status of Nuclear Data for Radiation Damage calculations (in terms of d.p.a.) and Damage Correlation Estimates.

3. Workshop on Evaluation of Preliminary Results of the REAL-80 (Reaction Rate Estimates, Evaluated by Adjustment Analysis in Leading Laboratories) International Exercise.

Conclusions and recommendations

Workshop 1. Nuclear Data for Environment Characterization

Chairman L.R. Greenwood

1. Requests for dosimetry cross section measurements have been made to the U.S. Evaluation Working Group on Cross-Sections (CSWEG) and to the World Request List for Nuclear Data of the IAEA (WRENDA). However, there are also discrepant reaction cross sections in ENDF/B-V, such as $^{47}Ti(n,p)$, $^{60}Ni(n,p)$, and $^{63}Cu(n,\alpha)$. It is recommended that IAEA prepare a file of all significant discrepancies in the ENDF/B-V Dosimetry and IRDF data files and stimulate reevaluation of these discrepant cross-sections.

2. The time interval between ENDF/B-V and IRDF data evaluations is too long and some files are already outdated. These dosimetry files should thus be reviewed more frequently with respect to the most discrepant reactions or significant new data, perhaps by IAEA; also this may be done with the new ENDF-A data file of integrally adjusted dosimetry cross-sections.

3. Integral cross section measurements for dosimetry reactions in well-known neutron fields should be considered during the evaluation of neutron cross sections. These data should then be included in the data files.

4. In order to insure the consistency of evaluated neutron cross sections and activity measurements, essential nuclear decay data, isotopic abundances, and fission yields should be included in evaluated dosimetry nuclear data files.

5. The particularly important Rh(n,n') and Nb(n,n') dosimetry reactions should be included in the ENDF/B-V and IRDF data files.

6. It is recommended that IAEA circulate a ^{93m}Nb(16 y) standard for calibration purposes, similar to the previous effort with Rhodium. Guidelines for self-absorption corrections should be included with the standard.

7. The critical reviews of nuclear data by IAEA-INDC are particularly useful to the international community and this work should be encouraged.

8. It is recommended that IAEA promote sensitivity studies of covariance matrices for neutron dosimetry cross sections and neutron input flux spectra. IAEA should also summarize and distribute available covariance information in an easily readable and condensed form, such as the recent work by D. Muir. The variances in this ENDF/B-V-based file should be adopted for unfolding; however, the covariance files must be tested. It is also recommended that IAEA support the generation of computer codes designed to construct covariance matrices, especially for resonance parameter data contained in ENDF formated files, and to transform covariance matrices between different group structures.

9. At present it is often very difficult to construct covariance matrices from available documentation. The Nuclear Data Section of the IAEA should advertise the necessity of proper documentation of experimental nuclear data measurements so that covariance information can be obtained. It is especially important that the correlations between different sources of uncertainty are clearly stated.

10. Covariance uncertainty matrices should be generated for all benchmark, standard, reference, or controlled environment neutron fields to allow the proper propagation of uncertainties in nuclear data measured in these spectra.

11. The ^{252}Cf neutron spectrum should be remeasured above 7 MeV with a goal accuracy better than 10 %.

Workshop 2. Status of Nuclear Data for Radiation Damage Calculations and Damage Correlation Estimates

Chairman W. Schneider

The participants have discussed the quality and availability of displacement cross-section data. The following conclusions and recommendations were made.

1. It is recommended, for the time being, to use the following sets of displacement cross sections: ASTM and Euratom (for 640 neutron energy groups and for neutron energies up to 20 MeV). The data sets are based on ENDF/B-IV (ASTM) and ENDF/B-III (Euratom) libraries. These sets have been published in: ASTM Standard E 693-79 and included in EUR 5274 (in 50 energy groups); the Euratom set will be published in the DAMSIG-81 data library (in 640 groups) *). These recommended sets should be applied particularly for damage evaluation for pressure vessel steels in light-water reactors.

2. It is recommended to develop a new Reactor Radiation Damage Nuclear Data File of an international reference status within the next three years. This file should incorporate the file being prepared now in the U.S.A. which is based on ENDF data and which is expected to be issued in 1982 and made available internationally through the four nuclear data centers. It is understood that the released US-file will include data for Fe, Cr and Ni up to 20 Mev.

   It is recommended to supplement the future International Reactor Radiation Damage File, for Fe, Cr and Ni up to 40 MeV, and to include the data for Al up to 40 MeV with the first priority.
   The data for Graphite, O, Ti, V, Mn, Cu, Zr, Mo, W up to 40 Mev and for Nb, Sn up to 20 Mev should be included in the file with second priority.

---

*) available as report ECN-104 (Petten, November 1981)

Few experimental data above 20 MeV exist. More experimental data are wanted, but in their absence one has to recur to theoretical calculations. Theoretical calculations of H and He production cross-sections show that at higher incident energies the contributions of reactions of the type (n,pp) and (n,pα) cannot be neglected for target nuclei with small neutron excess. Evaluations of needed changes in the energy dependence of the damage function should be considered in future theoretical and experimental research. For special purposes and environments (like e.g. D_2O reactors, strong γ-ray fields) the file should include the damage cross sections for (n,γ), (γ,n), and (γ,γ') reactions.

3. The Working Group recognizes the importance of neutron and gamma-ray kerma as a damage mechanism in organic materials such as fiberglass-reinforced epoxy. Some nuclear data for separate isotopes are required along with Q-values, nuclear decay data and spectra of emitted particles. The data for the following elements are essential in this context: Be, C, N, O, F, Na, Al, Si, Ca. The Working Group strongly supports the recommendations of the IAEA Advisory Group Meeting on Nuclear Data for Fusion Reactor Technology, Dec. 1978 (Ref. INDC(NDS)-101/LF, p. 14, 15) to create a kerma factor library with covariance information.

4. It is recommended to report uncertainties in the displacement or damage energy cross sections due to uncertainties in the nuclear data. The uncertainties should be reported in the form of a variance-covariance matrix. The uncertainty in the nuclear data should be based, if possible, on uncertainty information contained in the ENDF/B-V cross section library.

5. It is recommended that damage detectors are further developed and that the relationship between measured damage and displacement cross sections (as d.p.a.) is studied.

6. It is recommended to continue the study of competing damage processes (besides d.p.a.) in light water reactors, in fast breeder reactors and in fusion reactor investigations.

   For the calculations of gas production and solid transmutation accurate excitation functions would be necessary from threshold up to about 30 Mev for (n,γ); (n,xn); (n,tot.H) and (n, tot.He) mostly between 9 and 15 Mev. The list of important materials (e.g. Li, C, N, O, Al, Si, Ti, V, Cr, Mn, Fe, Ni, Cu, Zr, Nb, Mo, Pb) can be found in the IAEA biennual publication WRENDA.

   The two step process $^{58}Ni(n,\gamma)^{59}Ni(n,\alpha)^{56}Fe$ contributes considerably to the total helium production in stainless steels at high neutron fluences even in the fast neutron fields. It is recommended that in future work the contribution of this process should be duly accounted for.

   It is further recommended that the Nuclear Data Section encourage measurements of total cross-sections up to 40 MeV for the above mentioned reactions. Such measurements are extremely useful for parametrization of nuclear model calculations.

7. The Advisory Group Meeting has noticed that the International Working Group for Reliability of Reactor Pressure Components has (in its Session in Vienna, 4-5 December 1980) agreed to the suggestion of preparing a Status Report of lifetime prediction and surveillance procedures for LWR pressure vessels, for studying the comparability and homogeneity of the procedures (and eventually for making recommendations for improving the homogeneity, by means of a Guidebook).

   This plan has found the support of the Advisory Group Meeting.

   It is recommended for this purpose to convene a small group of experts of reactor physicists, dosimetrists and metallurgists.

8. The Advisory Group Meeting urges the Nuclear Data Section to persuade the contrbutors of WRENDA to realistically redefine the accuracy requirements of their nuclear data needs pertinent to the scope of this meeting.

Workshop 3. Evaluation of Preliminary Results of the REAL-80 International Exercise

Chairman W.L. Zijp

The preliminary results obtained thus far were discussed in some detail, and some useful suggestions were made for the preparation of the final report of the REAL-80 project. Some particular problems mentioned in the preliminary REAL-80 report presented at this meeting received full attention.

1. It was felt that a separate and detailed study should be made on the effect of neutron self-shielding in activation detectors, and on the influence of cadmium, gadolinium and boron covers.

2. The occurrence of clearly different patterns of correlation matrices mentioned in the report was also discussed. It was noted that a study of this topic had already started in Budapest within the framework of REAL-80. Such a study is extremely useful for getting a better idea of the origin of different patterns of correlation matrices.

3. Also the problem of unlikely small values of the generalised chi-square parameter for the set of input data for the O.R.R. (Oak Ridge Research Reactor) received full attention. Often one might assume that the experimental values for reaction rates, cross sections and group flux densities are much better known than their uncertainties and correlation coefficients. One should always try to start the adjustment procedure with an input data set with a more likely value of chi-square. It is recognized that the consistency of all data used in an adjustment procedure plays an essential role. If the adjustment procedure leads to an unlikely value of chi-space, then the set of input data is inconsistent and the results of the adjustment algorithm are questionable. In this case the input data should be carefully examined in an attempt to improve its consistency. Any changes (which need not be equal for the different parameters) should be based on a good knowledge of the physics aspects of the adjustment problem.

   In general the internal consistency of the input data was considered to be more important than the particular algorithm of the adjustment code.

   With respect to actions in the future it was realised that one has a severe problem due to the fact that hardly any experimental correlation information is available for neutron spectra of interest. This may lead to a delay in any follow-up of the REAL-80 project.

   When a follow-up of REAL-80 is being organised, then one should include also a neutron spectrum representative for a reactor pressure vessel.

   It is expected that probably sufficient correlation data will be available within a short time for the benchmark fields of ISNF[1] and CFRMF[2] (based on sensitivity studies). With respect to the PCA[3] in the ORR poolside facility it was expected that in 1982 valuable covariance information on the neutron spectrum might become available. There was no strong support to include in a future exercise the ^{252}Cf fission neutron spectrum, since it was too well known by other techniques to expect improvement by adjustment procedures.

4. The following recommendations are based on the REAL-80 report, and the subsequent discussions in the workshop.

   a) The IAEA is advised to promote a detailed study of the problems of selfshielding and the influence of cadmium, gadolinium and boron covers.

   b) The IAEA is advised to organize an intercomparison on conversion procedures for processing of evaluated data to multigroup form.

   c) The IAEA should give support to studies for comparing the merits of several adjustment codes.

   d) The IAEA should take into account the study of differences observed in the structure of correlation matrices, when preparing the final report on the REAL-80 exercise, and give the necessary support to the work already started at Budapest.

   e) A possible follow-up of the REAL-80 project should be considered, when the final results of the present exercise have been communicated, and when more experimental information on correlation matrices for neutron spectra becomes available. The following spectra were in particular suggested for consideration in a future exercise: ISNF[1]; CFRMF[2] and PCA[3].

   1) ISNF = Intermediate Spectrum Neutron Facility

   2) CFRMF = Coupled Fast Reactivity Measurements Facility

   3) PCA = Pool critical assembly

LIST OF PARTICIPANTS

AUSTRIA

Strohmaier, B.	Institut für Radiumforschung und Kernphysik der Universität Wien, Boltzmanngasse 3, A-1090 Wien
Uhl, M.	Institut für Radiumforschung und Kernphysik der Universität Wien, Boltzmanngasse 3, A-1090 Wien

BRAZIL

Auler, L.T.	Instituto de Engenharia Nuclear, Cidade Universitaria, Ilha do Fundao, 21910 Rio de Janeiro

CZECHOSLOVAKIA

Brumovský, M.	Škoda Concern, Plzeň
Ošmera, B.	Nuclear Research Institute, CS-250 68 Řež

FRANCE

Alberman, A.	CEA, Centre d'études nucléaires de Saclay, Service des Piles, F-91190 Gif-sur-Yvette
Gonnord, J.	CEA, Centre d'études nucléaires de Saclay, Service d'études des réacteurs et de mathématiques appliquées, B.P. 2, F-91190 Gif-sur-Yvette
Mas, P.	CEA, Centre d'études nucléaires de Grenoble, Service des piles/Groupe dosimétrie, 85X, avenue des Martyrs, F-38041 Grenoble Cedex

GERMAN DEMOCRATIC REPUBLIC

Seeliger, D.	Technische Universität Dresden, Sektion Physik, Mommsenstrasse 13, DDR-8027 Dresden

GERMANY, FEDERAL REPUBLIC OF

Goel, B.	Institut für Neutronenphysik und Reaktortechnik, Postfach 3640, D-7500 Karlsruhe
Mannhart, W.	Physikalisch Technische Bundesanstalt, Bundesallee 100, D-3300 Braunschweig
Mattes, M.	Institut für Kernenergetik der Universität Stuttgart, Postfach 80, 1140, Pfaffenwaldring 31, D-7000 Stuttgart 80
Schneider, W.	Kernforschungsanlage Jülich GmbH, Postfach 1913, D-5170 Jülich 1

HUNGARY

Csikai, J.	Institute of Experimental Physics, Kossuth Lajos University, P.O. Box 105, H-4001 Debrecen

ISRAEL

Yiftah, S.	Soreq Nuclear Research Centre, Atomic Energy Commission, Yavne 70600

ITALY

d'Angelo, A.	CNEN, CSN-Casaccia, Santa Maria di Galeria, C.P. 2400, I-00100 Rome
Petilli M.	CNEN, CSN-Casaccia, Santa Maria di Galeria, C.P. 2400, I-00100 Rome
Sandrelli, G.	Via Armando Diaz 10, Saronno (Varese)
Sangiust, V.	CESNEF, Politecnico di Milano, Instituto di Ingegneria Nucleare, Via Ponzio 34/3, I-20133 Milan

JAPAN

Iwata, T.	Tokai Research Establishment, Japan Atomic Energy Research Institute, Tokai-mura, Naka-gun, Ibaraki-ken 319-11

NETHERLANDS

Zijp, W.L.	Netherlands Energy Research Foundation ECN, Postbus 1, NL-1755 ZG, Petten

POLAND

Morstin, K.	Institute of Nuclear Physics and Techniques, Akademia Gorniczo-Hutnicza, Al. Mickiewicza 30, Krakow

SWITZERLAND

Stiller, P.	Swiss Federal Institute for Reactor Research, CH-5303 Würenlingen

UNITED STATES OF AMERICA

Dudziak, D.	Los Alamos National Laboratory, Los Alamos, N.M.87545
Greenwood, L.R.	Chemical Engineering Division, Argonne National Laboratory, 9700 South Cass Avenue, Argonne, IL. 60439

Lippincott, E.P. — Westinghouse Hanford Company,
Hanford Engineering Development Laboratory,
P.O. Box 1970,
Richland, WA 99352

McGarry, E.D. — National Bureau of Standards,
Washington, DC 20234

Simons, R.L. — Westinghouse Hanford Company,
Hanford Engineering Development Laboratory,
P.O. Box 1970, Richland, WA 99352

YUGOSLAVIA

Najžer, M. — E. Kardelj University,
Jožef Stefan Institute,
P.O.Box 199-4, YU-61001 Ljubljana

ORGANIZATIONS

COMMISSION OF THE EUROPEAN COMMUNITIES

Dierckx, R. — Joint Research Centre,
I-21020 Ispra (Varese), Italy

IAEA

Ertek, C. — Department of Safeguards,
Division of Operation A,
Wagramerstrasse 5, P.O.Box 100,
A-1400 Vienna, Austria

Kocherov, N. — Nuclear Data Section
Wagramerstrasse 5, P.O.Box 100,
A-1400 Vienna, Austria